# BOSQUE

## CONTENIDO

# BOSQUE

## CONTENTS

REVISIONES

# Endemic *Juniperus gracilior* varieties of the Hispaniola island, tree taxa of environmental and economic relevance and a valuable phytochemical source

Variedades de *Juniperus gracilior* endémicas de la Hispaniola, taxones con relevancia económica y ambiental y valiosas fuentes de fitoquímicos

**Carolina Juncá Morales [a]\*, Luis Enrique Rodríguez de Francisco [a], Cristina López-Hidalgo [b], Rafael M Navarro Cerrillo [c], Omar Paíno Perdomo [a], Jesús Valentín Jorrín Novo [d]**

\*Corresponding author: [a] Instituto Tecnólogico de Santo Domingo, Basic and Environmental Sciences Area, Santo Domingo, Dominican Republic, tel.: 809-567-9271 ext.: 608, 1074736@est.intec.edu.do, luis.defrancisco@intec.edu.do, omar.perdomo@intec.edu.do, carolinajuncam@yahoo.com

[b] Universidad de Oviedo, Faculty of Biology, Department of Organisms and Systems Biology, Oviedo, Spain, lopezhcristina@uniovi.es

[c] Universidad de Córdoba, Department of Forestry Engineering, Córdoba, Spain, rmnavarro@uco.es

[d] Universidad de Córdoba, Department of Biochemistry and Molecular Biology, Córdoba, Spain, bf1jonoj@uco.es

SUMMARY

The *Juniperus* genus has long been used and studied for the chemical components of its aerial parts (leaves, bark, twigs) and their bioactivity. Nevertheless, these studies and their compilation have been primarily focused on Europe and North America distributed taxa, leaving the knowledge and economic potential of the endangered Caribbean taxa highly underrepresented in the literature. Although, these conifers have been barely investigated for their bioactive compounds, bibliography does indicate the presence of potent antitumoral, anti-inflammatory and antimicrobial molecules such as deoxypodophyllotoxin, podophyllotoxin, amentoflavone and widdrol. Additional phytochemical potential can also be inferred from the systematical essential oil studies of the taxa, the only source of chemical composition information on most of them. These investigations can aid in the narrowing down of the possible bioactivities their lipidic extracts may possess, while also providing clues for the bioassays necessary to confirm them. This review aims to compile the known information on the usage, bioactivity and chemical composition of the Hispaniolian *J. gracilior* varieties and their phylogenetically proximal taxa (*J. gracilior* var. *saxicola*, *J. barbadensis* and *J. bermudiana*), to propitiate more holistic and in depth chemical studies on these potential phytochemical sources, in turn providing an economical incentive for their conservation.

*Key words:* bioactive compounds, conservation, metabolomics, Caribbean.

RESUMEN

El género *Juniperus* ha sido utilizado y estudiado a lo largo de los años por la bioactividad de los compuestos fitoquímicos encontrados en sus tejidos (hojas, corteza, ramas). Mayoritariamente, dichas investigaciones y las recopilaciones de estas se han centrado en taxones distribuidos en Europa y América del Norte, dejando de lado la investigación y potencial económico de otros, como los caribeños, que actualmente se encuentran en peligro de extinción. Aunque los compuestos bioactivos de los últimos apenas han sido estudiados, en la literatura se reportan potentes moléculas antitumorales, antiinflamatorias y antimicrobianas como la desoxipodofilotoxina, podofilotoxina, amentoflavona y el widdrol en su composición. De igual manera, investigaciones fitoquímicas realizadas a sus aceites esenciales con objetivo taxonómico, que en muchos casos representan la única fuente de información química de estos *Juniperus* del Caribe, permiten inferir propiedades bioactivas adicionales de los mismos, lo que resalta su posible potencial. Este trabajo tuvo como objetivo recopilar la información conocida sobre el uso, la bioactividad y la composición química de las variedades de *J. gracilior* endémicas de la Hispaniola y sus taxones filogenéticamente cercanos (*J. gracilior* var. *saxicola*, *J. barbadensis* y *J. bermudiana*), para propiciar futuros estudios holísticos y exhaustivos de los metabolitos encontrados en estas posibles fuentes de compuestos fitoquímicos, proporcionando así un incentivo económico para su conservación.

*Palabras clave:* compuestos bioactivos, conservación, metabolómica, Caribe.

## INTRODUCTION

The *Juniperus* genus, commonly referred to as "cedars" in English and "enebro" or "sabina" in Spanish, comprises 67 species and 37 varieties (Adams 2014). From Tibetan mountains to tropical islands, juniper trees and shrubs are distributed in all continents except Antarctica. Of the 114 taxa, seven are localized in the Caribbean archipelago: *J. gracilior* var. *gracilior* (Pilger), *J. gracilior* var. *ekmanii* (Florin) R. P. Adams and *J. gracilior* var. *urbaniana* (Pilger *et* Ekman), endemic to Hispaniola island, *J. gracilior* var. *saxicola* (Britton *et* P. Wilson), endemic to Cuba, *J. barbadensis* var. *barbadensis* (Linnaeus), endemic to St. Lucia, *J. barbadensis* var. *lucayana* (Britton) R. P. Adams, found in Cuba, Bahamas and Jamaica, and *J. bermudiana* (Linnaeus), endemic to Bermuda (Adams 2014).

Species within the *Juniperus* genus have long been used for therapeutic purposes and known for their pharmacological properties (Seca *et al*. 2015). Their chemical components have also been utilized in food production as flavoring (Falasca *et al.* 2013) and could be used as food preservatives (Lesjak *et al.* 2017). Additionally, polyphenols and other compounds of the genre provide an essence potentially used in the cosmetic (Rangel *et al.* 2018), while also being interesting for pharmaceutical industries, with individual bioactive compounds being potential leads for new drug development (Kwon *et al.* 2010, Tavares and Seca 2018). Although these investigations have been gathered by review articles such as those written by Seca and Silva (2006), Seca and collaborators (2015) and Tavares and Seca (2018), the economic value and potential of the critically endangered *J. gracilior* (Pilger) Hispaniolan varieties have not been described (García *et al*. 2016). This review aims to emphasize the current and potential use of bioactive chemical components from *J. gracilior* by compiling pertinent information of phylogenetically proximal taxa (*J. gracilior* var. *saxicola*, *J. barbadensis* var. *barbadensis*, *J. barbadensis* var. *lucayana* and *J. bermudiana*). Information available in Dominican governmental reports and overall bibliography was consulted to provide a comprehensive review for *J. gracilior* chemical components and to highlight its economic potential as a way of guaranteeing this species conservation (Newton 2008).

## JUNIPERS IN THE HISPANIOLA ISLAND, ENVIRONMENTAL SITUATION AND ECONOMIC IMPORTANCE

The Hispaniola is a Caribbean island comprised of two countries, the Dominican Republic and Haiti. The forest cover of the island is reported to be ~2 % on the west side (Haiti) and ~ 41 % on the east (Dominican Republic) (Posner *et al*. 2010, MIMARENA 2019). These habitats have a biodiverse flora with an array of endemic species, being especially true in the mountainous territory, which holds pine forests and hundreds of endemic species, including its most representative conifer species *Pinus occidentalis* (Swartz)*, Podocarpus hispaniolensis* (Laubenfels) and *J. gracilior* (Posner *et al*. 2010, Cano-Ortiz *et al.* 2016, MIMARENA 2019). The islands' juniper (*Juniperus*) varieties (figure 1) inhabit elevations between 1,000 and 2,550 meters above sea level, with locations (figure 2) differing among varieties. *J. gracilior* var. *gracilior* inhabits Dominican mountainous ranges such as Sierra Martín García, Cordillera Central, Sierra de Bahoruco (Zanoni and Mejia 1986) and Sierra de Neiba (Familia *et al.* 2019), while *J. gracilior* var. *ekmanii* is found in the Haitian Massif de la Selle, Massif du Nord (Adams 1983) and the Dominican Sierra de Bahoruco (Adams 2014), and *J. gracilior* var. *urbaniana* occupies Haitian Massif de la Selle and Dominican Sierra de Bahoruco (Adams 2014).

Although these forests represent an environmental and economic benefit for the island, since colonial times, unsustainable depletion of their vegetation has resulted in significant forest reduction and in the critical endangerment of many endemic taxa (Posner *et al.* 2010, García *et al.* 2016). The three *J. gracilior* varieties have been jeopardized due to this anthropic intervention. Mainly, as a result of continuous community and farmland establishment in and tree logging, which locals undertake to economically sustain themselves and supply the demand of the fragrant *ekmanii* and *gracilior* wood, coveted in the territory (Adams 1983, Peguero and Clase 2015). Since in the 1980s, reforestation efforts have been made on the island, however, the endemic junipers have not taken a significant role in this rehabilitation (Williams 2011, MIMARENA 2019). Two organizations, Dominican National Botanical Garden [2007 - ongoing] and Arche aux Plantes [2013 - 2018], have in recent times, undertaken projects which aim to conserve and propagate seeds of the species (Conservatoire Botanique National de Brest 2017, Mattana *et al.* 2017). Nevertheless, these have not sufficed to augment populations enough to reduce extinction risk.

## BIOACTIVE PREPARATIONS AND EXTRACTS FROM CARIBBEAN JUNIPERS

*Juniperus* species have been used in traditional or folk medicine even when the scientific bases of their mode of action and the chemicals behind their bioactivity are unknown. Within the genus*, J. oxycedrus* and *J. communis* are the most studied in terms of their pharmacological and therapeutic effects (Tavares and Seca 2018). The list of referenced properties pertaining the extracts of their aerial parts is ample, including antifungal (Ortiz *et al.* 2004), insect repellent (Jacobson 2018), antitussive (Carpenter *et al.* 2012), antihypertensive (Usmanghani *et al.* 1997), diuretic (Öztürk *et al.* 2011), antiseptic (Khare 2007)**,** anti-inflammatory (Khare 2007, Jazayeri *et al.* 2014), carminative (Usmanghani *et al.* 1997, Khan *et al.* 2012) hypoglycemic (Orhan *et al.* 2012), antioxidant (Jazayeri *et al.* 2014) and abortive (Öztürk *et al.* 2011), while also being

**Figure 1**. Morphology of the three endemic *J. gracilior* varieties. A) Leaves and berry (purple structure), *gracilior* variety; B) *gracilior* variety tree; C) Leaves and cones (yellow structures), *ekmanii* variety; D) Trunk, *ekmanii* variety; E) Leaves and cones (yellowish structures) *urbaniana* variety; F) *urbaniana* variety shrub. Photo credits: Carolina Juncá (A, B) and Amelia Mateo (C, D, E, F).

Morfología de las tres variedades endémicas de *J. gracilior*. A) Hojas y fruto (estructura morada), variedad *gracilior*; B) Árbol, variedad *gracilior*; C) Hojas y conos (estructuras amarillas), variedad *ekmanii*; D) Tronco, variedad *ekmanii*; E) Hojas y conos (estructuras amarillas), variedad *urbaniana*; F) Arbusto, variedad *urbaniana*. Fotografías tomadas por Carolina Juncá (A, B) y Amelia Mateo (C, D, E, F).
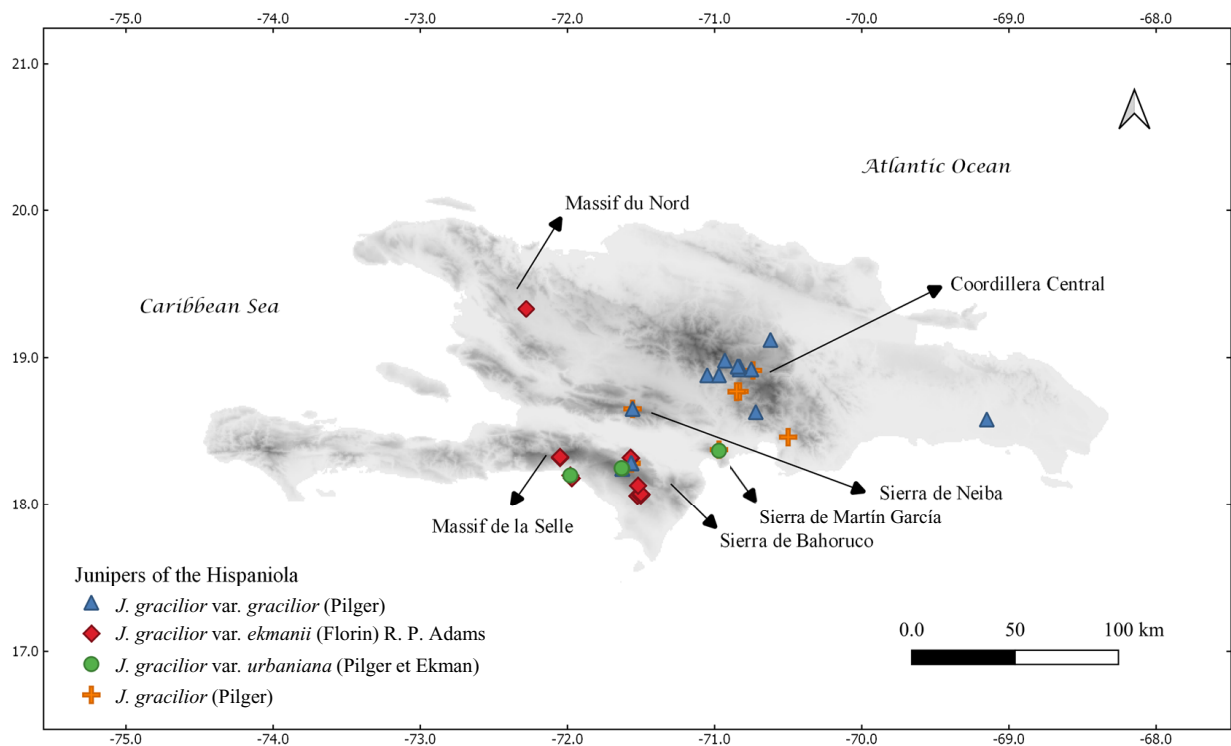


**Figure 2**. Distribution of *J. gracilior* in Hispaniola Island. Sightings obtained from GBIF (GBIFab) and field trips organized by the Instituto Tecnológico de Santo Domingo (INTEC) between 2018 and 2019 (unpublished data).

Distribución de las variedades de *J. gracilior* en la isla de la Hispaniola. Avistamientos obtenidos de GBIF (GBIFab) y de viajes de campo organizados por el Instituto Tecnológico de Santo Domingo (INTEC) entre 2018 y 2019 (datos no publicados).

used as remedies for urinary infection (Grosourdy 1864), cold, bronchitis (Öztürk *et al.* 2011) diabetes (Orhan *et al.* 2012, Carpenter *et al.* 2012), asthma (Khan *et al.* 2012), urticaria, dysentery, leucorrhea (But *et al.* 1997), haemorrhoids (Öztürk *et al.* 2011) and tuberculosis (Omari *et al.* 2019).

Although a vast array of information can be found for taxa in territories outside the Caribbean, for the four species that do inhabit these islands, historical uses bibliography is scarce. Only *J. bermudiana* preparations have been reported to be utilized in precolonial times for medicinal and culinary purposes (Wolsak 2017). Nevertheless, studies have reported that Caribbean junipers have been employed in treating urinary infections and have also presented cytotoxic, antioxidant, antibacterial and pest repellency properties (Fitzgerald *et al.* 1957, Grosourdy 1864, Martínez *et al.* 1996, Jacobson 2018). A list of the bioactivities attributed to Caribbean juniper preparations can be found in table 1.

## JUNIPERS AS A SOURCE OF PHYTOCHEMICALS AND BIOACTIVE COMPOUNDS

Besides the interest shown for its bioactive preparations, *Juniperus* genus has been investigated for phytochemicals such as abietatriene derivatives, widdrol, deoxypodophyllotoxin, amentoflavone, dehydroabietic acid and limonene, whose properties could aid in new drug and product development (Kwon *et al.* 2010, Seca *et al.* 2015, Tavares and Seca 2018, Mukhtar *et al.* 2018). Among these taxa, those form the Caribbean are known to possess potent antitumor molecules against human cancer cell lines. For instance, in these taxa, researchers have been able to identify deoxypodophyllotoxin (Tammami *et al.* 1977), considered to be one of the most cytotoxic metabolites in the genus (Tavares and Seca 2018), and its biosynthetic product podophyllotoxin (Renouard *et al.* 2011), whose

concentrations in Caribbean taxa have made *J. bermudiana* its second most important producer (Bazaldúa *et al.* 2019). Chemical studies have also led to the detection of other useful compounds such as amentoflavone (Gadek and Quinn 1985), a flavonoid with properties such as antitumoral (Chen *et al.* 2015) antimicrobial (Coulerie *et al.* 2013), antioxidant (Li *et al.* 2014), anti-inflammatory (Abdallah *et al.* 2015), antidiabetic (Laishram *et al.* 2015) and diuretic (Aguilar *et al.* 2015, Tavares and Seca 2018). Additionally, widdrol has been found, a lignin reported to be antiproliferative against adenocarcinoma HT29 cells (Kwon *et al.* 2010), lipolysis inducer in mice adipocytes (Jeong *et al.* 2015) and inhibitor of *B. cinerea* growth (Ortiz *et al.* 2005). Moreover, other compounds with antifungal activity against *B. cinerea* have been identified and evaluated, including 15-hidroxy-α-pseudowiddrene, cedrol, 3-hydroxypseudowiddran-6(7)-en-4-ol, 12-hydroxywiddrol, sandaracopimaric acid and α-bisabolol (Ortiz *et al.* 2004, 2005).

Besides the aforementioned compounds, which have been uncovered and bioassayed, other molecules have been reported as part of the essential oil characterization of Caribbean junipers. A list summarizing reported compounds can be found in table 2. Said characterization of foliar terpenes was used to determine the systematic relationship among the taxa utilizing gas chromatography coupled with mass spectrometry (GC-MS) (Adams 1983, 2000). These studies revealed that in Hispaniolan varieties, bornyl acetate accounts for more than 30 % of their essential oil terpene content, followed by terpinen-4-ol, sabinene, limonene in *J. gracilior* var. *gracilior*, limonene and sabinene in *J. gracilior* var. *ekmanii,* and sabinene, limonene and terpinen-4-ol in *J. gracilior* var. *urbaniana* (Adams 1983, 2000). Junipers found in Caribbean territories other than this island do not possess bornyl acetate as their major essential oil component. Perhaps the best example is the Cuban *J. gracilior* variety, *saxicola*, which

**Table 1.** Reported bioactivities of Caribbean taxa extracts.

Bioactividades reportadas para los extractos de los taxones caribeños.

| Taxa | Extract (organ) | Bioactivity | Reference |
|---|---|---|---|
| *J. bermudiana* | Ethanolic extract (twigs and leaves) | Inhibitory activity toward the P-388 lymphocytic leukemia (PS) cell line and cytotoxic activity toward human epidermoid carcinoma of the nasopharynx (KB) | Tammami *et al.* 1977 |
| *J. barbadensis* var. *lucayana* | Acetone extract (wood) | Inhibition of the fungus *Botrytis cinerea* growth | Ortiz *et al.* 2004 |
| *J. barbadensis* var. *lucayana* | Ethanolic extract (wood) | Inhibition of the fungus *B. cinerea* growth | Ortiz *et al.* 2004 |
| *J. barbadensis* var. *lucayana* | Aqueous extract (stem) | Antimicrobial activity against *Staphylococcus aureus* | Martínez *et al.* 1996 |
| *J. barbadensis* var. *barbadensis* | Aqueous extract (shoots) | Treats urinary system pathologies | Grosourdy 1864 |

**Table 2.** Summary of identified metabolites in Caribbean taxa.
Resumen de los metabolitos identificados en taxones caribeños.
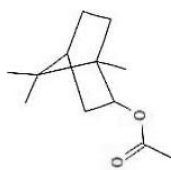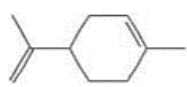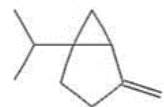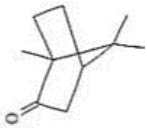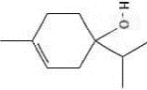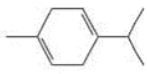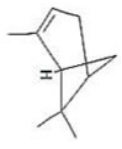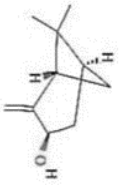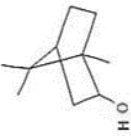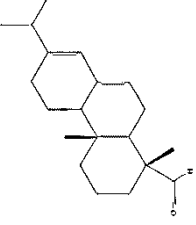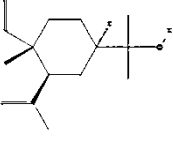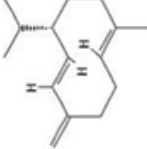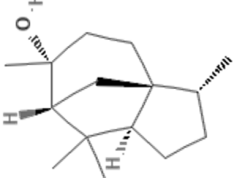
| Compound (PubChem ID) method | Structure | Chemical Type | Taxa | Organ (solvent) | Identification | References |
|---|---|---|---|---|---|---|
| Bornyl acetate (6448) |  | Monoterpene | *J. gracilior* var. *gracilior* | Leaves (water) | GC-MS | Adams 1983 |
| | | | *J. gracilior* var. *ekmanii* | Leaves (water) | GC-MS | Adams 1983 |
| | | | *J. gracilior* var. *urbaniana* | Leaves (water) | GC-MS | Adams 2000 |
| | | | *J. gracilior* var. *saxicola* | Leaves (water) | GC-MS | Adams 2000 |
| | | | *J. barbadensis* var. *barbadensis* | Leaves (water) | GC-MS | Adams 2000 |
| | | | *J. barbadensis* var. *lucayana* | Leaves (water) | GC-MS | Adams 1983 |
| | | | *J. bermudiana* | Leaves (water) | GC-MS | Adams 1983 |
| Limonene (22311) |  | Monoterpene | *J. gracilior* var. *gracilior* | Leaves (water) | GC-MS | Adams 1983 |
| | | | *J. gracilior* var. *ekmanii* | Leaves (water) | GC-MS | Adams 1983 |
| | | | *J. gracilior* var. *urbaniana* | Leaves (water) | GC-MS | Adams 2000 |
| | | | *J. gracilior* var. *saxicola* | Leaves (water) | GC-MS | Adams 2000 |
| | | | *J. barbadensis* var. *barbadensis* | Leaves (water) | GC-MS | Adams 2000 |
| | | | *J. barbadensis* var. *lucayana* | Leaves (water) | GC-MS | Adams 2000 |
| | | | *J. bermudiana* | Leaves (water) | GC-MS | Adams 1983 |
| Sabinene (18818) |  | Monoterpene | *J. gracilior* var. *gracilior* | Leaves (water) | GC-MS | Adams 1983 |
| | | | *J. gracilior* var. *ekmanii* | Leaves (water) | GC-MS | Adams 1983 |
| | | | *J. gracilior* var. *urbaniana* | Leaves (water) | GC-MS | Adams 2000 |
| | | | *J. gracilior* var. *saxicola* | Leaves (water) | GC-MS | Adams 2000 |
| | | | *J. barbadensis* var. *barbadensis* | Leaves (water) | GC-MS | Adams 2000 |
| | | | *J. barbadensis* var. *lucayana* | Leaves (water) | GC-MS | Adams 2000 |
| | | | *J. bermudiana* | Leaves (water) | GC-MS | Adams 1983 |
| Myrcene (31253) |  | Monoterpene | *J. gracilior* var. *gracilior* | Leaves (water) | GC-MS | Adams 2000 |
| | | | *J. gracilior* var. *ekmanii* | Leaves (water) | GC-MS | Adams 2000 |
| | | | *J. gracilior* var. *urbaniana* | Leaves (water) | GC-MS | Adams 2000 |
| | | | *J. gracilior* var. *saxicola* | Leaves (water) | GC-MS | Adams 2000 |
| | | | *J. bermudiana* | Leaves (water) | GC-MS | Adams 2000 |

**Table 2** Continued

| Compound | Class | Species | Part | Method | Reference |
|---|---|---|---|---|---|
| Camphor (2537) | Monoterpene | J. gracilior var. gracilior | Leaves (water) | GC-MS | Adams 2000 |
| | | J. gracilior var. ekmanii | Leaves (water) | GC-MS | Adams 2000 |
| | | J. gracilior var. urbaniana | Leaves (water) | GC-MS | Adams 2000 |
| | | J. gracilior var. saxicola | Leaves (water) | GC-MS | Adams 2000 |
| | | J. bermudiana | Leaves (water) | GC-MS | Adams 2000 |
| Terpene-4-ol (11230) | Monoterpenol | J. gracilior var. gracilior | Leaves (water) | GC-MS | Adams 1983 |
| | | J. gracilior var. ekmanii | Leaves (water) | GC-MS | Adams 1983 |
| | | J. gracilior var. urbaniana | Leaves (water) | GC-MS | Adams 2000 |
| | | J. gracilior var. saxicola | Leaves (water) | GC-MS | Adams 2000 |
| | | J. barbadensis var. barbadensis | Leaves (water) | GC-MS | Adams 2000 |
| | | J. barbadensis var. lucayana | Leaves (water) | GC-MS | Adams 2000 |
| | | J. bermudiana | Leaves (water) | GC-MS | Adams 2000 |
| γ-Terpinene (7461) | Monoterpene | J. gracilior var. gracilior | Leaves (water) | GC-MS | Adams 1983 |
| | | J. gracilior var. ekmanii | Leaves (water) | GC-MS | Adams 1983 |
| | | J. gracilior var. urbaniana | Leaves (water) | GC-MS | Adams 2000 |
| | | J. gracilior var. saxicola | Leaves (water) | GC-MS | Adams 2000 |
| | | J. barbadensis var. barbadensis | Leaves (water) | GC-MS | Adams 2000 |
| | | J. barbadensis var. lucayana | Leaves (water) | GC-MS | Adams 2000 |
| | | J. bermudiana | Leaves (water) | GC-MS | Adams 2000 |
| α-Pinene (6654) | Monoterpene | J. gracilior var. gracilior | Leaves (water) | GC-MS | Adams 1983 |
| | | J. gracilior var. ekmanii | Leaves (water) | GC-MS | Adams 1983 |
| | | J. gracilior var. urbaniana | Leaves (water) | GC-MS | Adams 2000 |
| | | J. gracilior var. saxicola | Leaves (water) | GC-MS | Adams 2000 |
| | | J. barbadensis var. barbadensis | Leaves (water) | GC-MS | Adams 2000 |
| | | J. barbadensis var. lucayana | Leaves (water) | GC-MS | Adams 2000 |
| | | J. bermudiana | Leaves (water) | GC-MS | Adams 1983 |
| Trans-pinocarveol (1201530) | Monoterpene | J. bermudiana | Leaves (water) | GC-MS | Adams 2000 |

**Table 2** Continued

| Compound | Type | Species | Tissue | Method | Reference |
|---|---|---|---|---|---|
| Borneol (64685) | Monoterpene | *J. gracilior* var. *ekmanii* | Leaves (water) | GC-MS | Adams 1983 |
| | | *J. gracilior* var. *urbaniana* | Leaves (water) | GC-MS | Adams 1983 |
| | | *J. barbadensis* var. *lucayana* | Leaves (water) | GC-MS | Adams 2000 |
| | | *J. bermudiana* | Leaves (water) | GC-MS | Adams 2000 |
| δ-2-Carene (78249) | Monoterpene | *J. gracilior* var. *gracilior* | Leaves (water) | GC-MS | Adams 1983 |
| | | *J. gracilior* var. *ekmanii* | Leaves (water) | GC-MS | Adams 2000 |
| | | *J. gracilior* var. *urbaniana* | Leaves (water) | GC-MS | Adams 2000 |
| | | *J. barbadensis* var. *lucayana* | Leaves (water) | GC-MS | Adams 2000 |
| | | *J. gracilior* var. *gracilior* | Leaves (water) | GC-MS | Adams 2000 |
| 4-Epi-Abietal (6427962) | Diterpene | *J. gracilior* var. *saxicola* | Leaves (water) | GC-MS | Adams 2000 |
| Elemol (92138) | Sesquiterpene | *J. barbadensis* var. *barbadensis* | Leaves (water) | GC-MS | Adams 2000 |
| | | *J. gracilior* var. *urbaniana* | Leaves (water) | GC-MS | Adams 2000 |
| | | *J. gracilior* var. *saxicola* | Leaves (water) | GC-MS | Adams 2000 |
| | | *J. barbadensis* var. *lucayana* | Leaves (water) | GC-MS | Adams 2000 |
| Germacrene D (5317570) | Sesquiterpene | *J. gracilior* var. *gracilior* | Leaves (water) | GC-MS | Adams 2000 |
| | | *J. gracilior* var. *ekmanii* | Leaves (water) | GC-MS | Adams 2000 |
| | | *J. gracilior* var. *urbaniana* | Leaves (water) | GC-MS | Adams 2000 |
| Cubebol (11276107) | Sesquiterpene | *J. gracilior* var. *gracilior* | Leaves (water) | GC-MS | Adams 2000 |
| | | *J. gracilior* var. *ekmanii* | Leaves (water) | GC-MS | Adams 2000 |
| | | *J. gracilior* var. *urbaniana* | Leaves (water) | GC-MS | Adams 2000 |
| | | *J. gracilior* var. *saxicola* | Leaves (water) | GC-MS | Adams 2000 |
| | | *J. barbadensis* var. *barbadensis* | Leaves (water) | GC-MS | Adams 2000 |
| | | *J. barbadensis* var. *lucayana* | Leaves (water) | GC-MS | Adams 2000 |
| | | *J. bermudiana* | Leaves (water) | GC-MS | Adams 2000 |

Table 2 Continued
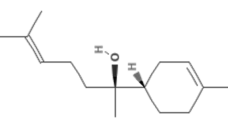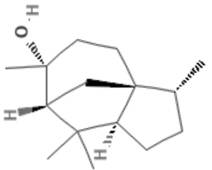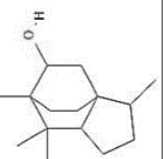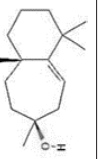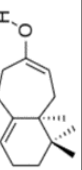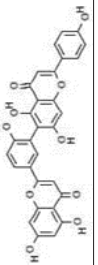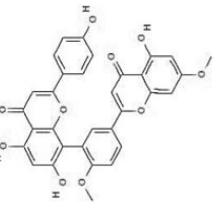
| Compound | Type | Species | Part (extract) | Methods | Reference |
|---|---|---|---|---|---|
| β-Eudesmol (91457) | Sesquiterpene | J. gracilior var. gracilior | Leaves (water) | GC-MS | Adams 2000 |
|  |  | J. gracilior var. ekmanii | Leaves (water) | GC-MS | Adams 2000 |
|  |  | J. gracilior var. urbaniana | Leaves (water) | GC-MS | Adams 2000 |
|  |  | J. gracilior var. saxicola | Leaves (water) | GC-MS | Adams 2000 |
| α-Eudesmol (92762) | Sesquiterpene | J. gracilior var. gracilior | Leaves (water) | GC-MS | Adams 2000 |
|  |  | J. gracilior var. ekmanii | Leaves (water) | GC-MS | Adams 2000 |
|  |  | J. gracilior var. urbaniana | Leaves (water) | GC-MS | Adams 2000 |
|  |  | J. gracilior var. saxicola | Leaves (water) | GC-MS | Adams 2000 |
| Methyl eugenol (7127) | Cinnamate | J. gracilior var. gracilior | Leaves (water) | GC-MS | Adams 2000 |
|  |  | J. gracilior var. ekmanii | Leaves (water) | GC-MS | Adams 2000 |
|  |  | J. gracilior var. urbaniana | Leaves (water) | GC-MS | Adams 2000 |
|  |  | J. bermudiana | Leaves (water) | GC-MS | Adams 2000 |
| Sandaracopimaric acid (221580) | Diterpene | J. bermudiana | Leaves (*) | CC, TLC, IR, H-NMR | Khan 1989 |
| Hydroxypseudowiddran-6(7)-en-4-ol** (+) | Sesquiterpene | J. barbadensis var. lucayana | Wood (ethanol) | CC, TLC, HPLC, H NMR, C NMR, 2D NMR, MS, IR | Nuñez et al. 2007 |
| 15-Hydroxyallocedrol** (+) | Sesquiterpene | J. barbadensis var. lucayana | Wood (ethanol) | CC, TLC, HPLC, H NMR, C NMR, 2D NMR, MS, IR | Nuñez et al. 2007 |
| 12-Hydroxywiddrol** (+) | Sesquiterpene | J. barbadensis var. lucayana | Wood (ethanol) | CC, TLC, HPLC, H NMR, C NMR, 2D NMR, MS, IR | Nuñez et al. 2007 |
| β-Chamigrenic acid (13648247) | Sesquiterpene | J. barbadensis var. lucayana | Wood (ethanol) | CC, TLC, HPLC, H NMR, C NMR, 2D NMR, MS, IR | Nuñez et al. 2007 |

14

**Table 2** Continued

| Compound | Structure | Class | Species | Part (solvent) | Method | Reference |
|---|---|---|---|---|---|---|
| α-Bisabolol (442343) |  | Sesquiterpene | *J. barbadensis* var. *lucayana* | Wood (ethanol) | CC, HPLC, spectroscopy | Ortiz *et al.* 2005 |
| Cedrol (65575) |  | Sesquiterpene | *J. barbadensis* var. *lucayana* | Wood (ethanol) | CC, HPLC, spectroscopy | Ortiz *et al.* 2005 |
| allo-Cedrol (527227) |  | Sesquiterpene | *J. barbadensis* var. *lucayana* | Wood (ethanol) | CC, HPLC, spectroscopy | Ortiz *et al.* 2005 |
| Widdrol (94334) |  | Sesquiterpene | *J. barbadensis* var. *lucayana* | Wood (ethanol) | CC, HPLC, spectroscopy | Ortiz *et al.* 2005 |
| 15-Hidroxy-α-pseudowiddrene** (+) |  | Sesquiterpene | *J. barbadensis* var. *lucayana* | Wood (ethanol) | CC, HPLC, spectroscopy | Ortiz *et al.* 2005 |
| Robustaflavone (5281694) |  | Flavonoid | *J. bermudiana* | Leaves and small branchlets (70 % etanol and petrol) | HPLC-UV | Gadek and Quinn 1985 |
| 7,4-dimethylamentoflavone (5271805) |  | Flavonoid | *J. bermudiana* | Leaves and small branchlets (70 % etanol and petrol) | HPLC-UV | Gadek and Quinn 1985 |

**Table 2** Continued

| Compound | | Type | Species | Part (extraction) | Method | Reference |
|---|---|---|---|---|---|---|
| Amentoflavone (5281600) |  | Flavonoid | *J. bermudiana* | Leaves and small branchlets (70 % etanol and petrol) | HPLC-UV | Gadek and Quinn 1985 |
| Quercetin-3-O-a-L-rhamnopyranoside (4046293) |  | Flavonoid | *J. bermudiana* | Leaves (water and then ethyl acetate) | CC, TLC, IR, H-NMR | Khan 1989 |
| Cupressuflavone (5281609) |  | Flavonoid | *J. bermudiana* | Leaves and small branchlets (70 % etanol and petrol) | HPLC-UV | Gadek and Quinn 1985 |
| Hinokiflavone (5281627) |  | Flavonoid | *J. bermudiana* | Leaves and small branchlets (70 % etanol and petrol) | HPLC-UV | Gadek and Quinn 1985 |
| Naringenine (932) |  | Flavonoid | *J. barbadensis* var. *lucayana* | Wood (ethanol) | CC, TLC, HPLC, H NMR, C NMR, 2D NMR, MS, IR | Nuñez *et al.* 2007 |
| Aromadendrin (122850) |  | Flavonoid | *J. barbadensis* var. *lucayana* | Wood (ethanol) | CC, TLC, HPLC, H NMR, C NMR, 2D NMR, MS, IR | Nuñez *et al.* 2007 |

Continue

**Table 2** Continued

| Compound | Structure | Type | Species | Source | Methods | Reference |
|---|---|---|---|---|---|---|
| 1-Nonacosanol (243696) |  | Fatty alcohol | *J. bermudiana* | Leaves (*) | CC, TLC, IR, H-NMR | Khan 1989 |
| Nonacosane (12409) |  | Hydrocarbon | *J. bermudiana* | Leaves (*) | CC, TLC, IR, H-NMR | Khan 1989 |
| Podophyllotoxin (10607) |  | Lignan | *J. barbadensis* var. *lucayana* | Leaves (water) | CC, IR, NMR | Fitzgerald *et al.* 1957 |
| Deoxypodophyllotoxin (345501) |  | Lignan | *J. bermudiana* | Twigs and leaves (ethanol) | CC, TLC, IR, NMR | Tammami *et al.* 1977 |

+: compound not found in PubChem, structure taken from reference; x: unspecified; *: acetone extraction treated with petroleum ether and benzene; **: a novel compound found in the taxa; CC: column chromatography; TLC: thin layer chromatography; IR: infrared spectroscopy; H-NMR: proton nuclear magnetic resonance; GC: gas chromatography coupled to mass spectrometry; HPLC: high-performance liquid chromatography; MS: mass spectrometry; C-NMR: carbon nuclear magnetic resonance; UV: ultraviolet spectroscopy; 2D NMR: two-dimensional nuclear magnetic resonance spectroscopy.

has 4-epi-abietal, elemol and sabinene as its majoritary terpenes, only having 0.3 % bornyl acetate in its oil (Adams 2000). As for the remaining Caribbean junipers: *J. barbadensis* var. *barbadensis* has limonene, sabinene, terpinen-4-ol, and α-pinene, while *J. bermudiana,* has limonene, α-pinene and camphor, and *Juniperus barbadensis* var. *lucayana* α-pinene, limonene and sabinene as their major essential oil terpenes (Adams 2000). The bioactive potential of the pure form of some of these majority essential oil compounds can be consulted in table 3.

In general, literature describing the chemical composition and usage of the Caribbean taxa is concentrated on *J. bermudiana* and *J. barbadensis* var. *lucayana* (Fitzgerald *et al.* 1957, Tammami *et al.* 1977, Gadek and Quinn 1985, Khan 1989, Martínez 1996, Ortiz *et al.* 2004, 2005, Nuñez *et al.* 2007, Renouard *et al.* 2011, Wolsak 2017). The other taxa are only mentioned in studies about insect repellency and are not reported their traditional usage and medicine bibliography in their respective countries (Jacobson 2018). Studies involving a holistic chemical characterization of these taxa with subsequent bioactivity assays need to be conducted to elucidate the phytochemical composition and potential usage of these conifers. The mentioned pure form bioactivities of these essential oil terpenes, although not accounting for their synergistic or antagonistic interactions with other compounds, might present a lead for future bioactivity assays of the taxa.

## FUTURE DIRECTION IN INVESTIGATING JUNIPERS PHYTOCHEMICALS, THE METABOLOMICS APPROACH

As mentioned above, the full phytochemical composition of endemic Caribbean *Juniperus* spp. is widely understudied. This information, being of pivotal importance for botanical, conservation, and pharmacological purposes, is crucial for bioprospecting studies of the species to increase its protection locally. Currently, among the characterization of living organisms, metabolomics is playing a key role, either alone or in combination with guided biological activity assays (Wishart 2016). Metabolomics is the systematic study, identification and quantification, of the metabolites in an organism at a specific moment in time (metabolome) (Tugizimana *et al.* 2013). And while phylogenetic lineages can help select new taxon targets for bioactivity studies, metabolomics can help identify structurally related metabolites conserved throughout evolution that might be of interest to the investigator (Mawalagedera *et al.* 2019).

In a broad sense, the steps of a metabolomics study (figure 3) are as follows: material sampling and extraction, extract analyses or data acquisition, statistical analyses and metabolite identification (Choi and Verpoorte 2014). How these steps are performed ultimately depends on the investigator's objective and approach (targeted or untargeted). A targeted approach identifies and quantifies a few known and predetermined metabolites, while an untargeted one aims to study all the known and unknown metabolites present in a sample (Tugizimana *et al.* 2013).

For metabolite identification and quantification, different extraction solvents and methodologies can be employed. According to the analytical platform used, metabolomic studies mainly belong to two groups, MS- and RMN- based. These can be utilized in parallel or combination to other classic protocols of thin layer, liquid or gas chromatography, spectrometry and spectroscopy (Nuñez *et al.* 2007). The platforms employed in the identification of chemical components of the *Juniperus* Caribbean clade can be found in table 2. As a whole, this genus has had compounds from leaf, wood and berry extract characterized, with most of these investigations being designed with

**Table 3.** Essential oil majority terpenes of Hispaniolian junipers and their pure form bioactivities.

Bioactividades de las formas puras de los terpenoides mayoritarios en el aceite esencial de los *Juniperus* de la Hispaniola.

| Terpene | Bioactivities | References |
|---|---|---|
| Bornyl acetate | Antioxidant and anti-inflammatory. Acaricidal against *Dermatophagoides farinae, D. pteronyssinus* and *Tyrophagus putrescentiae*. Strong fumigant with contact toxicity against *Liposcelis bostrychophila* and *Tribolium castaneum*. | Lee *et al.* 2009, Chen *et al.* 2014, Yang *et al.* 2014, Feng *et al.* 2019 |
| Terpinen-4-ol | Anti-demodectic and antimicrobial against *Streptococcus mutans* and *Lactobacillus acidophilus*. Significant growth inhibitor of colorectal, pancreatic, prostate and gastric cancer cells. | Shapira *et al.* 2016, Bordini *et al.* 2018, Cheung *et al.* 2018 |
| Sabinene | Strong antioxidant activity and antibacterial activity against *Escherichia coli*. | Sharma *et al.* 2019 |
| Limonene | Antiviral, anti-inflammatory, and antibacterial. Antitumor capabilities for gastric lung, pancreatic, mammary, liver and colon tumor models. | Stayrook *et al.* 1997, Yoon *et al.* 2010, Jia *et al.* 2013, Astani and Schnitzler 2014, Zhang *et al.* 2014, Miller *et al.* 2015, Yu *et al.* 2018, Hafidh *et al.* 2018, Han *et al.* 2019 |
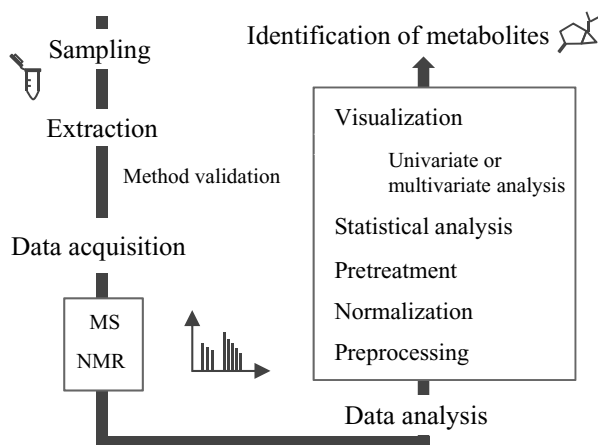
**Figure 3**. General metabolomics workflow.

Flujo de trabajo general para un experimento de metabolómica.

a targeted approach to specific chemical groups (Adams 2000, Renouard *et al*. 2011, Falasca *et al*. 2013, Rangel *et al*. 2018). For the identification of novel and/or useful bioactive compounds of *J. gracilior* and other Caribbean junipers, an untargeted approach focused on a larger range of metabolites including uninvestigated chemical groups such as polyphenols, known antioxidants, anti-mutagenic and antitumor compounds (Rangel *et al*. 2018), might need to be used.

ACKNOWLEDGEMENTS

REFERENCES

Abdallah HM, FM Almowallad, A Esmat, IA Shehata, EA Abdel-Sattar. 2015. Anti-inflammatory activity of flavonoids from *Chrozophora tinctoria*. *Phytochemistry Letters* 13: 74-80. DOI: https://doi.org/10.1016/j.phytol.2015.05.008

Adams RP. 1983. The Junipers (*Juniperus*, *Cupressaceae*) of Hispaniola Comparison with other Caribbean species and among collections from Hispaniola. *Moscosoa* 2(1): 77-89.

Adams RP. 2000. Systematics of smooth leaf margin *Juniperus* of the Western hemisphere based on leaf essential oils and RAPD DNA fingerprinting. *Biochemical Systematics and Ecology* 28(2): 149-162. DOI: https://doi.org/10.1016/S0305-1978(99)00047-2

Adams RP. 2014. Junipers of the world: The genus *Juniperus*. Indiana, United States of America. Trafford Publishing. 422 p.

Aguilar MI, WV Benítez, A Colín, R Bye, R Ríos-Gómez, F Calzada. 2015. Evaluation of the diuretic activity in two Mexican medicinal species: *Selaginella nothohybrida* and *Selaginella lepidophylla* and its effects with ciclooxigenases inhibitors. *Journal of Ethnopharmacology* 163: 167-

172. DOI: https://doi.org/10.1016/j.jep.2015.01.031

Astani A, P Schnitzler. 2014. Antiviral activity of monoterpenes beta-pinene and limonene against herpes simplex virus in vitro. *Iranian Journal of Microbiology* 6(3): 149-155.

Bazaldúa C, A Cardoso-Taketa, G Trejo-Tapia, B Camacho-Diaz, J Arellano, E Ventura-Zapata, ML Villarreal. 2019. Improving the production of podophyllotoxin in hairy roots of *Hyptis suaveolens* induced from regenerated plantlets. *PloS One* 14(9): e0222464. DOI: https://doi.org/10.1371/journal.pone.0222464

Bordini E, CC Tonon, RS Francisconi, F Magalhães, P Huacho, TL Bedran, S Pratavieira, LC Spolidorio, DP Spolidorio. 2018. Antimicrobial effects of terpinen-4-ol against oral pathogens and its capacity for the modulation of gene expression. *Biofouling* 34(7): 815-825. DOI: https://doi.org/10.1080/08927014.2018.1504926

But PPH, T Kimura, JX Gue, CK Sung. 1997. International collation of traditional and folk medicine: Northeast Asia Part II. Singapore, Singapore. World Scientific Publishing. 248 p.

Cano-Ortiz A, C Musarella, J Fuentes, C Gomes, E Cano. 2016. Distribution patterns of endemic flora to define hotspots on Hispaniola. *Systematics and Biodiversity* 14(3): 261-275. DOI: https://doi.org/10.1080/14772000.2015.1135195

Carpenter CD, T O'Neill, N Picot, JA Johnson, GA Robichaud, D Webster, CA Gray. 2012. Anti-mycobacterial natural products from the Canadian medicinal plant *Juniperus communis*. *Journal of Ethnopharmacology* 143(2): 695-700. DOI: https://doi.org/10.1016/j.jep.2012.07.035

Chen JH, WL Chen, YC Liu. 2015. Amentoflavone Induces Anti-angiogenic and Anti-metastatic Effects Through Suppression of NF-κB Activation in MCF-7 cells. *Anticancer Research* 35(12): 6685-6693.

Chen N, G Sun, X Yuan, J Hou, Q Wu, LW Soromou, H Feng. 2014. Inhibition of lung inflammatory responses by bornyl acetate is correlated with regulation of myeloperoxidase activity. *Journal of Surgical Research* 186(1): 436-445. DOI: https://doi.org/10.1016/j.jss.2013.09.003

Cheung I, AL Xue, A Kim, K Ammundsen, M Wang, JP Craig. 2018. In vitro anti-demodectic effects and terpinen-4-ol content of commercial eyelid cleansers. *Contactlens & Anterior Eye* 41(6): 513-517. DOI: https://doi.org/10.1016/j.clae.2018.08.003

Choi Y, R Verpoorte. 2014. Metabolomics: What You See is What You Extract. *Phytochemical Analysis* 25(4): 289-290. DOI: https://doi.org/10.1002/pca.2513

Conservatoire Botanique National de Brest. 2017. Sauvetage du Genévrier d'Ekman et préservation de la flore de la Forêt des Pins à Haïti. Consulted Jun. 15 2020. Available in http://www.cbnbrest.fr/nos-actions-phares/107

Coulerie P, M Nour, A Maciuk, C Eydoux, JC Guillemot, N Lebouvier, E Hnawia, K Leblanc, G Lewin, B Canard, B Figadère. 2013. Structure-activity relationship study of biflavonoids on the Dengue virus polymerase DENV-NS5 RdRp. *Planta Medica* 79(14): 1313-1318. DOI: https://doi.org/10.1055/s-0033-1350672

Estévez A. 2019. Memoria Institucional: Ano 2019. Consulted Apr. 25 2020. Available in https://ambiente.gob.do/wp-content/uploads/2020/01/Memoria-Institucional-2019.pdf

Falasca A, D Melck, D Paris, G Saviano, A Motta, M Iorizzi. 2013. Seasonal changes in the metabolic fingerprint of *Juniperus communis* L. berry extracts by 1H NMR-based

metabolomics. *Metabolomics* 10(1): 165-174. DOI: https://doi.org/10.1007/s11306-013-0566-1

Familia L, T Montilla, T Clase, G Santana, A Guerrero. 2019. Cambios en la cobertura boscosa del bosque nublado en la sierra de Neiba, República Dominicana. *Ciencia, Ambiente y Clima* 2(1): 7-22. DOI: https://doi.org/10.22206/cac.2019.v2i1.pp7-22

Feng YX, Y Wang, ZY Chen, SS Guo, CX You, SS Du. 2019. Efficacy of bornyl acetate and camphene from *Valeriana officinalis* essential oil against two storage insects. *Environmental Science and Pollution Research* 26(16): 16157-16165. DOI: https://doi.org/10.1007/s11356-019-05035-y

Fitzgerald DB, JL Hartwell, J Leiter. 1957. Distribution of the Tumor-Damaging Lignans among Conifers. *Journal of the National Cancer Institute* 18(1): 83-99. DOI: https://doi.org/10.1093/jnci/18.1.83

Gadek P, C Quinn. 1985. Biflavones of the subfamily *Cupressoideae*, *Cupressaceae*. *Phytochemistry* 24(2): 267-272. DOI: https://doi.org/10.1016/S0031-9422(00)83535-9

García R, B Peguero, F Jiménez, A Veloz, T Clase. 2016. Lista Roja de la Flora Vascular en República Dominicana. Jardín Botánico Nacional Dr. Rafael Ma. Moscoso. Consulted May 14 2020. Available in http://www.jbn.gob.do/transparencia/index.php/publicaciones-t?start=20

GBIF (Global Biodiversity Information Facility, DK). 1887-2020a. GBIF Occurrence Database (online). Consulted Apr. 21 2020. Available in https://doi.org/10.15468/dl.4mv9mb

GBIF (Global Biodiversity Information Facility, DK). 1887-2020b. GBIF Occurrence Database (online). Consulted Apr. 21 2020. Available in https://doi.org/10.15468/dl.r8bn5a

Grosourdy R. 1864. El médico botánico criollo: Tomo 3. Paris, France. Francisco Brachet. 416 p.

Hafidh RR, SZ Hussein, MQ MalAllah, AS Abdulamir, F Abu Bakar. 2018. A High-throughput Quantitative Expression Analysis of Cancer-related Genes in Human HepG2 Cells in Response to Limonene, a Potential Anticancer Agent. *Current Cancer Drug Targets* 18(8): 807-815. DOI: https://doi.org/10.2174/1568009617666171114144236

Han Y, Z Sun, W Chen. 2019. Antimicrobial Susceptibility and Antibacterial Mechanism of Limonene against *Listeria monocytogenes*. *Molecules* 25(1): 33. DOI: https://doi.org/10.3390/molecules25010033

Jacobson M. 2018. Glossary Of Plant Derived Insect Deterrents. Florida, United States of America. CRC Press. 219 p.

Jazayeri SB, A Amanlou, N Ghanadian, P Pasalar, M Amanlou. 2014. Apreliminary investigation of anticholinesterase activity of some Iranian medicinal plants commonly used in traditional medicine. *DARU Journal of Pharmaceutical Sciences* 22(1): 17. DOI: https://doi.org/10.1186/2008-2231-22-17

Jeong HY, HJ Yun, BW Kim, EW Lee, HJ Kwon. 2015. Widdrol-induced lipolysis is mediated by PKC and MEK/ERK in 3T3-L1 adipocytes. *Molecular and Cellular Biochemistry* 410(1-2): 247-257. DOI: https://doi.org/10.1007/s11010-015-2558-0

Jia SS, GP Xi, M Zhang, YB Chen, B Lei, XS Dong, YM Yang. 2013. Induction of apoptosis by D-limonene is mediated by inactivation of Akt in LS174T human colon cancer cells. *Oncology Reports* 29(1): 349-354. DOI: https://doi.org/10.3892/or.2012.2093

Khan I. 1989. Chemistry of Natural Products. PhD Thesis. Aligarh, India. Department of Chemistry, Aligarh Muslim University. 450 p.

Khan M. A Khan, A Najeeb-ur-Rehman, A Gilani. 2012. Pharmacological explanation for the medicinal use of *Juniperus excelsa* in hyperactive gastrointestinal and respiratory disorders. *Journal of Natural Medicines* 66(2): 292-301. DOI: https://doi.org/10.1007/s11418-011-0605-z

Khare CP. 2007. Indian medicinal plants: An illustrated dictionary. Berlin/Heidelberg, Germany. Springer Verlag. 900 p.

Kim S, J Chen, T Cheng, A Gindulyte, J He, S He, Q Li, BA Shoemaker, P Thiessen, B Yu, L Zaslavsky, J Zhang, EE Bolton. 2019. PubChem 2019 update: improved access to chemical data. *Nucleic Acids Research* 47(D1): D1102–D1109. DOI: https://doi.org/10.1093/nar/gky1033

Kwon HJ, EW Lee, YK Hong, HJ Yun, BW Kim. 2010. Widdrol from *Juniperus chinensis* induces apoptosis in human colon adenocarcinoma HT29 cells. *Biotechnology and Bioprocess Engineering* 15(1): 167-172. DOI: https://doi.org/10.1007/s12257-009-0154-4

Laishram S, Y Sheikh, D Moirangthem, L Deb, B Pal, N Talukdar, J Borah. 2015. Anti-diabetic molecules from *Cycas pectinata* Griff. traditionally used by the Maiba-Maibi. *Phytomedicine* 22(1): 23-26. DOI: https://doi.org/10.1016/j.phymed.2014.10.007

Lee CH, JM Park, HY Song, EY Jeong, HS Lee. 2009. Acaricidal activities of major constituents of essential oil of *Juniperus chinensis* leaves against house dust and stored food mites. *Journal of Food Protection* 72(8): 1686-1691. DOI: https://doi.org/10.4315/0362-028X-72.8.1686

Lesjak M, I Beara, D Orčić, G Anačkov, P Knežević, Z Mrkonjić N Mimica–Dukić. 2017. Bioactivity and chemical profiling of the *Juniperus excelsa*, which support its usage as a food preservative and nutraceutical. *International Journal of Food Properties* 20(S2): 1652-1663. DOI: https://doi.org/10.1080/10942912.2017.1352598

Li X, L Wang, W Han, W Mai, L Han, D Chen. 2014. Amentoflavone Protects against Hydroxyl Radical-induced DNA Damage via Antioxidant Mechanism. *Turkish Journal of Biochemistry* 39(1): 30-36. DOI: https://doi.org/10.5505/tjb.2014.65882

Martínez M, J Betancourt, N Alonso-González, A Jauregui. 1996. Screening of some Cuban medicinal plants for antimicrobial activity. *Journal of Ethnopharmacology* 52(3): 171-174. DOI: https://doi.org/10.1016/0378-8741(96)01405-5

Mattana E, K Manger, M Way, T Ulian, R García, W Encarnacion, T Clase, B Peguero, F Jimenez. 2017. A new seed bank for Hispaniola to support the conservation and sustainable use of the Caribbean native flora. *Oryx* 51(3): 394-395. DOI: https://doi.org/10.1017/s0030605317000692

Mawalagedera S, D Callahan, A Gaskett, N Rønsted, M Symonds. 2019. Combining Evolutionary Inference and Metabolomics to Identify Plants with Medicinal Potential. *Frontiers In Ecology And Evolution* 7: 267. DOI: https://doi.org/10.3389/fevo.2019.00267

Miller JA, K Pappan, PA Thompson, EJ Want, AP Siskos, HC Keun, J Wulff, C Hu, JE Lang, HH Chow. 2015. Plasma metabolomic profiles of breast cancer patients after short-term limonene intervention. *Cancer Prevention Research* 8(1): 86-93. DOI: https://doi.org/10.1158/1940-6207.CAPR-14-0100

MIMARENA (Ministerio de Medio Ambiente y Recursos Naturales, DO). 2019. Sexto Informe Nacional de Biodiver-

sidad de la República Dominicana. Ministerio de Medio Ambiente y Recursos Naturales. Consulted Mar. 30 2020. Available in https://ambiente.gob.do/download/382/sexto-informe-de-biodiversidad/18975/sexto-informe-nacional-sobre-biodiversidad-chm.pdf

Mukhtar Y, M Adu-Frimpong, X Xu, J Yu. 2018. Biochemical significance of limonene and its metabolites: future prospects for designing and developing highly potent anti-cancer drugs. *Bioscience Reports* 38(6): BSR20181253. DOI: https://doi.org/10.1042/BSR20181253

Newton A. 2008. Conservation of tree species through sustainable use: How can it be achieved in practice? *Oryx* 42(2): 195-205. DOI: https://doi.org/10.1017/S003060530800759X

Nuñez YO, IS Salabarria, IG Collado, R Hernández-Galán. 2007. Sesquiterpenes from the wood of *Juniperus lucayana*. *Phytochemistry* 68(19): 2409-2414. DOI: https://doi.org/10.1016/j.phytochem.2007.05.030

Omari KE, M Hamze, S Alwan, M Osman, C Jama, NE Chihib. 2019. In-vitro evaluation of the antibacterial activity of the essential oils of *Micromeria barbata*, *Eucalyptus globulus* and *Juniperus excelsa* against strains of *Mycobacterium tuberculosis* (including MDR), *Mycobacterium kansasii* and *Mycobacterium gordonae*. *Journal of Infection and Public Health* 12(5): 615-618. DOI: https://doi.org/10.1016/j.jiph.2019.01.058

Orhan N, M Aslan, M Pekcan, DD Orhan, Bedir E, Ergun F. 2012. Identification of hypoglycaemic compounds from berries of *Juniperus oxycedrus subsp. oxycedrus* through bioactivity guided isolation technique. *Journal of Ethnopharmacology* 139(1): 110-118. DOI: https://doi.org/10.1016/j.jep.2011.10.027

Ortiz Núñez Y, I González Collado, R Hernández-Galán, IS Salabarría, Y Rodríguez, MA Alvarez, Y Lorenzo. 2004. Actividad fungicida de cuatro especies Cubanas de plantas sobre *Botrytis cinerea* Pers. Estudio Fitoquímico. *Revista Cubana de Química* 16: 204-206.

Ortiz Y, R Hernández-Galán, I Spengler, Y Rodríguez, R Sánchez, IG Collado. 2005. Studies on fungicides constituents of *Juniperus lucayana* Britton. Biotransformation by *Botrytis cinerea* and C*olletotrichum gloeosporioides*. *Revista Cubana de Quimica* 17(3): 225.

Öztürk M, İ Tümen, A Uğur, F Aydoğmuş-Öztürk, G Topçu. 2011. Evaluation of fruit extracts of six Turkish *Juniperus* species for their antioxidant, anticholinesterase and antimicrobial activities. *Journal of the Science of Food and Agriculture* 91(5): 867-876. DOI: https://doi.org/10.1002/jsfa.4258

Peguero B, T Clase. 2015. Composición y estructura de la vegetación en Cerro Angola, San José de las Matas, provincia Santiago, República Dominicana. *Moscosoa* 19: 37-69.

Posner S, GA Michel, JR Toussaint. 2010. Haiti Biodiversity and Tropical Forest Assessment. USDA Forest Service. Consulted Apr. 25 2020. Available in https://usaidgems.org/Documents/FAA&Regs/FAA118119LAC/Haiti_FAA_118-119_Dec_2010%20(1).pdf

Rangel ML, JA Guerrero-Analco, JL Monribot-Villanueva, AL Kiel-Martínez, S Avendaño-Reyes, JPD Abad, I Bonilla-Landa, R Dávalos-Sotelo, JL Olivares-Romero, G Angeles. 2018. Anatomical and chemical characteristics of leaves and branches of *Juniperus deppeana* var. *deppeana* (*Cupressaceae*): A potential source of raw materials for the perfume and sweet candies industries. *Industrial Crops and Products* 113: 50-54. DOI: https://doi.org/10.1016/j.indcrop.2017.12.046

Renouard S, T Lopez, O Hendrawati, P Dupre, J Doussot, A Falguieres, C Ferroud, D Hagege, F Lamblin, E Laine, C Hano. 2011. Podophyllotoxin and deoxypodophyllotoxin in *Juniperus bermudiana* and 12 other *Juniperus* species: Optimization of extraction, method validation, and quantification. *Journal of Agricultural and Food Chemistry* 59(15): 8101-8107. DOI: https://doi.org/10.1021/jf201410p

Seca A, A Silva. 2006. The chemical composition of the *Juniperus* Genus (1970–2004). *In* Govil JN, VK Singh, R Bhardwaj eds. Recent Progress in Medicinal Plants. Texas, United States of America. Studium Press LLC. p. 401-522.

Seca A, PC Pinto, A Silva. 2015. The Current Status of Bioactive Metabolites from the Genus *Juniperus*. *In* Gupta VK ed. Bioactive Phytochemicals: Perspectives for Modern Medicine. Jammu, India. Daya Publishing House. p. 365-408.

Shapira S, S Pleban, D Kazanov, P Tirosh, N Arber. 2016. Terpinen-4-ol: A Novel and Promising Therapeutic Agent for Human Gastrointestinal Cancers. *PloS One* 11(6): e0156540. DOI: https://doi.org/10.1371/journal.pone.0156540

Sharma S, J Gupta, PK Prabhakar, P Gupta, P Solanki, A Rajput. 2019. Phytochemical Repurposing of Natural Molecule: Sabinene for Identification of Novel Therapeutic Benefits Using in Silico and in Vitro Approaches. *Assay and Drug Development Technologies* 17(8): 339-351. DOI: https://doi.org/10.1089/adt.2019.939

Stayrook KR, JH McKinzie, YD Burke, YA Burke, PL Crowell. 1997. Induction of the apoptosis-promoting protein Bak by perillyl alcohol in pancreatic ductal adenocarcinoma relative to untransformed ductal epithelial cells. *Carcinogenesis* 18(8): 1655-1658. DOI: https://doi.org/10.1093/carcin/18.8.1655

Tammami B, SJ Torrance, JR Cole. 1977. Antitumor agent from *Juniperus bermudiana* (*Pinaceae*): Deoxypodophyllotoxin. *Phytochemistry* 16(7): 1100-1101. DOI: https://doi.org/10.1016/S0031-9422(00)86752-7

Tavares W, A Seca. 2018. The Current Status of the Pharmaceutical Potential of *Juniperus* L. Metabolites. *Medicines* 5(3): 81. DOI: https://doi.org/10.3390/medicines5030081

Tugizimana F, L Piater, I Dubery. 2013. Plant metabolomics: A new frontier in phytochemical analysis. *South African Journal of Science* 109(5-6): 1-11. DOI: https://doi.org/10.1590/sajs.2013/20120005

Usmanghani K, A Saeed, MT Alam. 1997. Indusyunic medicine: Traditional medicine of herbal animal and mineral origin in Pakistan. Karachi, Pakistán. University of Karachi Press. 591 p.

Williams V. 2011. A Case Study of the Desertification of Haiti. *Journal Of Sustainable Development* 4(3): 20-31. DOI: https://doi.org/10.5539/jsd.v4n3p20

Wishart DS. 2016. Emerging applications of metabolomics in drug discovery and precision medicine. *Nature Reviews Drug Discovery* 15(7): 473-484. DOI: https://doi.org/10.1038/nrd.2016.32

Wolsak AS. 2017. Of fishpots, bonnets, and wine: the cultural history of the Bermuda palmetto. Master's Thesis. Vancouver, United States of America. Faculty of Graduate and Postdoctoral Studies, University of British Columbia. 245 p. DOI: https://doi.org/10.14288/1.0362882

Yang H, R Zhao, H Chen, P Jia, L Bao, H Tang. 2014. Bornyl

acetate has an anti-inflammatory effect in human chondrocytes via induction of IL-11. *IUBMB Life* 66(12): 854-859. https://doi.org/10.1002/iub.1338

Yoon WJ, NH Lee, CG Hyun. 2010. Limonene suppresses lipopolysaccharide induced production of nitric oxide, prostaglandin E2, and pro-inflammatory cytokines in RAW 264.7 macrophages. *Journal of Oleo Science* 59(8): 415-421. DOI: https://doi.org/10.5650/jos.59.415

Yu X, H Lin, Y Wang, W Lv, S Zhang, Y Qian, X Deng, N Feng, H Yu, B. 2018. Qian. d-limonene exhibits antitumor activity by inducing autophagy and apoptosis in lung cancer. *Onco Targets Ther* 4(11): 1833-1847. DOI: https://doi.org/10.2147/OTT.S155716

Zanoni TA, M Mejia. 1986. Notas sobre la flora de la isla Española II. *Moscosoa* 4: 105-132

Zhang XZ, L Wang, DW Liu, GY Tang, HY Zhang. 2014. Synergistic inhibitory effect of berberine and d-limonene on human gastric carcinoma cell line MGC803. *Journal of Medicinal Food* 17(9): 955-962. DOI: https://doi.org/10.1089/jmf.2013.2967

ARTÍCULOS

# Aportes en la toma de decisiones para el manejo forestal con ganadería integrada del bosque de *Prosopis caldenia* del centro de Argentina

Contributions in decision-making for forest management with integrated livestock in the *Prosopis caldenia* forest of central Argentina

**Marco Jesús Utello** [a]*, **Santiago Ignacio Fiandino** [a], **Juan Carlos Tarico** [a],
**Marcela Alejandra Demaestri** [a], **José Omar Plevich** [a]

*Autor de correspondencia: [a] Universidad Nacional de Río Cuarto, Facultad de Agronomía y Veterinaria,
Departamento de Producción Vegetal, Ruta Nacional 36, km 601, Río Cuarto (5800), Córdoba, Argentina, tel.: 54-358-4676509,
mutello@ayv.unrc.edu.ar

## SUMMARY

In *Prosopis caldenia* forests, currently, the main activity is cattle rearing. Almost all research focuses on the herbaceous component, losing sight of the value of the forest resource and the implications of its management on the forage resource. The objective of this work is to evaluate forage availability based on forest cover, apply a model of diameter classes that allows predicting the evolution of forest mass and establish the relationship between the evolution of forest cover and forage availability. For this, forage availability was measured under and outside the projection of woody canopies, in two covers: open (10-15 $m^2$ $ha^{-1}$) and closed (25-30 $m^2$ $ha^{-1}$). Afterwards, through a model of diameter classes, it was sought to predict how the parameters of forest mass would evolve. The results of the herbaceous component showed that, up to 15 $m^2$ $ha^{-1}$ of basal area (BA), there is no significant decrease in forage availability (approximately 2,700 kg $ha^{-1}$). Regarding the forestry component, in a projected period of 10 years, 6.68 $m^3$ $ha^{-1}$ would be obtained, representing 9.61 % of total standing volume. The relationship between canopy coverage and BA showed increase of 3.18 % per BA unit ($R^2$ = 0.96). This would allow projecting their participation by diameter class to propose improvement cuts that allow conducting these systems at coverage levels that do not significantly affect forage yield.

*Key words:* irregular structure, simulation, modeling, forage, pasture.

## RESUMEN

En los bosques de *Prosopis caldenia,* actualmente, la principal actividad es la cría de ganado bovino. Casi la totalidad de las investigaciones se centran en el componente herbáceo perdiendo de vista el valor del recurso forestal y las implicancias de su manejo en el recurso forrajero. Este trabajo tiene como objetivos evaluar la disponibilidad forrajera en función de la cobertura boscosa, aplicar un modelo de clases diamétricas que permita predecir la evolución de la masa boscosa y establecer la relación entre la evolución del vuelo forestal y la disponibilidad forrajera. Para ello, se midió la disponibilidad forrajera bajo y fuera la proyección de copas de la leñosa, en dos coberturas: abierto (10-15 $m^2$ $ha^{-1}$) y cerrado (25-30 $m^2$ $ha^{-1}$). Luego mediante un modelo de clases diamétricas se buscó predecir cómo evolucionarían los parámetros de la masa forestal. Los resultados del componente herbáceo demostraron que, hasta 15 $m^2$ $ha^{-1}$ de área basal (AB), no se producen disminuciones significativas en la disponibilidad forrajera (aproximadamente 2.700 kg $ha^{-1}$). En cuanto al componente forestal, en un lapso proyectado de 10 años, se obtendría 6,68 $m^3$ $ha^{-1}$ y representa el 9,61 % del volumen total en pie. La relación entre la cobertura de copas y el AB, mostró un incremento de 3,18 % por unidad de AB ($R^2$ = 0,96). Esto permitiría proyectar su participación por clase diamétrica con el fin de proponer las cortas de mejoramientos que permitan conducir estos sistemas en niveles de cobertura que no afecten significativamente el rendimiento forrajero.

*Palabras clave:* estructura irregular, simulación, modelado, forraje, pastura.

## INTRODUCCIÓN

La región Espinal abarca una superficie de 329.395 km² bordeando la pampa argentina. Las tierras forestales cubren el 7,5 % del territorio y se concentran en el distrito del caldén (*Prosopis caldenia* Burk.) (SAyDS, 2007). El aprovechamiento forestal se desarrolló fuertemente durante la primera mitad del siglo XX. Sin embargo, en la actualidad la actividad forestal es marginal y la principal actividad económica desarrollada en los bosques es la cría de ganado va-

cuno, que utiliza en forma casi exclusiva el forraje que crece en el sotobosque (SAyDS 2007). Por lo general, el manejo ganadero en la región es extensivo, con cargas animales inadecuadas, poca división de potreros y sin descansos estacionales (Dussart *et al*. 1998). Este tipo de manejo favorece la invasión de leñosas, que se ve potenciada por el efecto del bovino como agente dispersante (Pelaez *et al*. 1992).

Casi la totalidad de las investigaciones en bosque de *P. caldenia* se centran en el componente herbáceo (Gabutti *et al*. 1999, Esterlich *et al*. 2005, Morici *et al*. 2009) perdiendo de vista el valor del recurso forestal y las implicancias del manejo de este en el recurso forrajero. Tal es el caso del estudio realizado por Roman *et al.* (2015) en el noroeste de la ecorregión del espinal, quienes encontraron que la tasa de crecimiento de las especies herbáceas bajo la copa del estrato leñoso, fue superior a aquella medida en posiciones de cielo abierto. Sin embargo, la producción de biomasa herbácea no fue asociada a variables de densidad del estrato arbóreo y, en consecuencia, no se puede predecir qué efectos tendrían diferentes técnicas de manejo forestal sobre la misma, lo cual limita fuertemente la toma de decisiones.

Conocer la dinámica del crecimiento del vuelo forestal y su efecto sobre el estrato herbáceo resulta indispensable para mejorar la toma de decisiones a la hora de conducir este tipo de sistemas mixtos. Si bien existen estudios que involucran la dinámica de crecimiento y las tasas de regeneración del bosque de *P. caldenia* (Dussart *et al*. 1998, Bogino y Villalba 2008), los mismos no tuvieron como fin generar modelos de ordenación que proyecten la evolución del vuelo forestal para su manejo y aprovechamiento. La falta de modelos de ordenación es una limitante para la promoción del aprovechamiento y conservación del bosque, ya que los usuarios de los recursos requieren bases técnicas antes de implementar actividades económicas de aprovechamiento (Coirini 2013).

En masas irregulares en equilibrio el mismo número de pies que abandonan una clase diamétrica debido a la mortalidad, crecimiento o entresaca, son sustituidos por un número equivalente procedente de la clase diamétrica inferior en el período correspondiente entre dos intervenciones. La curva de equilibrio o distribución diamétrica ideal ha sido uno de los modelos biométricos más estudiados en el campo de las ciencias forestales (Madrigal 1994). Es por ello, que el diámetro del fuste es la variable más usada en las decisiones de manejo de bosques irregulares (Iturre *et al*. 2017). A su vez, los modelos de distribuciones diamétricas pueden resultar muy útiles en la proyección del cambio de frecuencia por categorías. Constituye un método relativamente simple para estimar el crecimiento y producción utilizando el incremento en diámetro de los árboles y otras variables referidas a la masa. Existe un gran número de antecedentes en modelos y propuestas de aprovechamiento del bosque nativo para diferentes regiones (Beltrán *et al*. 2018, Urbano *et al*. 2018). Para citar algunos ejemplos, está el sistema STAND aplicado por Vargas *et al*. (2008) en rodales irregulares y mixtos de la región

de El Salto, Durango, México. También el *Forest Vegetation Simulator* (FVS), ampliamente aplicado en Estados Unidos. Se cuenta en bosques del chaco semiárido con la experiencia de la aplicación del simulador MOSIMAFO (Iturre *et al*. 2017).

En la ecorregión del Espinal, al presente no se citan experiencias en simulaciones del crecimiento del vuelo forestal y, menos aún, el empleo de modelos de clases diamétricas, como en el caso de la región chaqueña (Sanquetta *et al*. 1999, Araujo e Iturre 2014, Iturre *et al*. 2017). La principal causa radica en la dificultad de obtener los incrementos diamétricos en pies de diferentes edades, debido a la falta de inventarios forestales continuos en parcelas permanentes.

El siguiente trabajo tiene como objetivo general el de abordar en forma integral el estudio del componente forestal y herbáceo para aportar elementos en la toma de decisiones en el manejo del bosque de *P. caldenia*. Como objetivos específicos se considera: (a) evaluar la disponibilidad forrajera en términos de cantidad y calidad en función de la cobertura boscosa, (b) la aplicación de un modelo de clases diamétricas que permita predecir cómo evolucionarían los parámetros de la masa en un bosque de *P. caldenia* en relación a una distribución diamétrica ideal y (c) establecer la relación entre la evolución del vuelo forestal y la disponibilidad forrajera. Para tal fin, se realizaron inventarios de los recursos forestales y forrajeros.

MÉTODOS

*Descripción y ubicación de la zona de estudio.* El caldenal es un bosque xerófilo dominado por *P. caldenia* y es la formación arbórea predominante del distrito del caldenal dentro de la región fitogeográfica del Espinal. Su estructura, generalmente se presenta asociado con otras leñosas arbóreas como algarrobo (*Prosopis flexuosa* DC), chañar (*Geoffroea decorticans* Burkart) y sombra de toro (*Jodina rhombifolia* Hook. *et* Arn. Reissek) que es acompañado por un estrato arbustivo donde se destacan *Schinus fasciculata* (Griseb.), *Celtis ehrenbergiana* (Klotzsch) Liebm. y *Condalia microphylla* Cav. Presenta un estrato herbáceo denso compuestos por gramíneas perennes mixtas (Anderson *et al*. 1970).

La región de estudio se localiza 30 kilómetros al oeste de la localidad de Villa Huidobro, en el sudoeste de la provincia de Córdoba, Argentina. Se caracteriza climáticamente como semiárida en transición a subhúmeda de régimen monzónico. La temperatura media anual es de 16,6 °C. Enero es el mes más cálido con una media de 24 °C, y julio el más frío con una temperatura media de 9 °C. La precipitación media anual es de 893 mm, aunque presenta gran variabilidad interanual (valores climatológicos medios 1981-2010 de las estadísticas del Servicio Meteorológico Nacional).

*Definición del módulo silvopastoril.* El estudio se realizó en el establecimiento "Estancia Ralicó" (34°54'25" S; 64°50'03" O) que posee una superficie de 15.300 ha, de la cuales 9.000 ha corresponden a bosque de *P. caldenia* en

distinto grado de cobertura y conservación. Históricamente el establecimiento estuvo dividido en potreros de aproximadamente 600 ha. A partir del año 2016, se implementó un sistema de pastoreo rotativo de alta carga instantánea. Para ello, se dividió un lote de 600 ha en 30 parcelas de 20 ha. Las divisiones se realizaron mediante alambre eléctrico buscando espacios dentro del monte sin abrir picadas. El pastoreo se lleva a cabo introduciendo altas cargas, de entre 900 y 1.200 animales por parcela, en lapsos de 3 a 4 días, una vez al año. La cantidad de animales y la duración del tiempo se ajusta en función de la disponibilidad forrajera. Esta alta carga instantánea obliga a que animal no seleccione y consuma por completo la biomasa herbácea, lo que se verificó por la observación de un escaso o nulo remanente de pastoreo. Al comienzo de los ensayos fue necesario suplementar con rollos de heno de alfalfa para estimular a que los animales aprovechen el forraje de escasa calidad como resultados del subpastoreo del manejo anterior.

*Inventario forestal.* Para la caracterización del bosque se realizó un inventario forestal siguiendo los lineamientos del Primer Inventario Forestal Nacional (PIFN) (SAyDS 2007). Se establecieron 43 parcelas circulares de 500 m², con un radio de 12,62 m, donde se midieron los diámetros a altura de pecho (dap), el reclutamiento, la altura total y la cobertura de copa.

Dentro de cada parcela se contemplaron todos los árboles que al menos poseían uno de sus fustes con un dap igual o mayor a 10 cm; todos aquellos individuos con dap inferiores a ese valor fueron considerados parte del reclutamiento o regeneración del bosque. Los individuos con dap ≥ 10 cm fueron ordenados en clases diamétricas cuyo intervalo de clase fue de 5 cm y, a partir de ellos, se calculó el área basal (AB) en m² ha⁻¹ y se realizó una zonificación del bosque en dos estructuras: 1. Bosque cerrado y 2. Bosque abierto. A faltas de investigaciones locales que definan con precisión la densidad de un bosque abierto o cerrado, se estableció el límite de 15 m² ha⁻¹ de AB. Por debajo se consideró bosque abierto y, por encima bosque cerrado. La definición de dicho valor se hizo a partir de lo propuesto por SAyDS (2007) donde establece valores de área basal promedios para bosque abierto y cerrado en el distrito del caldenal.

La regeneración se clasificó según tres clases de la siguiente manera: clase 1: renovales menores de 1,30 m de altura; clase 2: renovales mayores de 1,30 m de altura y menores de 5 cm de dap y; clase 3: renovales mayores de 1,30 m de altura y con dap entre 5 y 10 cm.

Para la obtención de la altura total (h), que corresponde a la distancia desde el suelo hasta el extremo superior del árbol, se utilizó hipsómetro de Suunto. Para la medición de los diámetros de copas (DC) se proyectaron sus límites utilizando una regla telescópica de 4 m. Luego con cinta métrica se midieron los radios hacia los cuatro puntos cardinales. En la medición de estas dos variables (h y DC) se incluyeron individuos de todas las clases diamétricas en cada parcela.

La composición específica a nivel de rodal fue evaluada definiendo los valores relativos en número de pies (densidad) y área basal (AB). Se pudo determinar una marcada dominancia de *P. caldenia* (cuadro 1) sobre el resto de las

**Cuadro 1.** Variables descriptivas medias y desvíos estándar en dos coberturas boscosas: abierto (AB ≤ 15 m² ha⁻¹) y cerrado (AB ≥ 15 m² ha⁻¹), de la estancia Ralicó (Provincia de Córdoba, Argentina). D: densidad (árboles ha⁻¹), AB: área basal (m² ha⁻¹), % D: valor relativo del número de pies ocupado por cada especie, y % AB: valor relativo de área basal ocupado por cada especie. x̄: media y S: desvío estándar.

Mean descriptive variables and standard deviations in two forest coverings: open (AB ≤ 15 m² ha⁻¹) and closed (AB ≥ 15 m² ha⁻¹), from Ralicó Farm (Córdoba Province, Argentina). Where: D: density (trees ha⁻¹), AB: basal area (m² ha⁻¹), % D: relative value of the number of feet occupied by each species, and % AB: relative value of basal area occupied by each species. x̄: mean and S: standard deviation.

| Tipo de bosque | Variable | Especie | | | | |
|---|---|---|---|---|---|---|
| | | *P. caldenia* | *P. flexuosa* | *G. descorticans* | *S. fasciculata* | *J. rhombifolia* |
| | | x̄ ± S | x̄ ± S | x̄ ± S | x̄ ± S | x̄ ± S |
| Abierto | D | 165 ± 147,67 | 16 ± 41,85 | 6 ± 14,65 | 9 ± 16,51 | 3 ± 7,33 |
| | AB | 7,68 ± 4,05 | 0,41 ± 0,82 | 0,17 ± 0,57 | 0,23 ± 0,45 | 0,06 ± 0,21 |
| | % D | 83,57 ± 16,76 | 5,83 ± 12,59 | 3,58 ± 8,05 | 5,86 ± 10,15 | 1,16 ± 2,84 |
| | % AB | 89,95 ± 11,46 | 4,56 ± 9,63 | 1,69 ± 4,88 | 3,2 ± 6,78 | 0,6 ± 2,03 |
| Cerrado | D | 312,38 ± 147,44 | 15,24 ± 38,94 | 20,95 ± 41,22 | 27,62 ± 64,34 | 0,95 ± 4,36 |
| | AB | 21,47 ± 8,52 | 0,54 ± 1,33 | 0,36 ± 0,71 | 0,67 ± 1,36 | 0,01 ± 0,05 |
| | % D | 84,75 ± 21,07 | 3,11 ± 6,81 | 5,14 ± 10,61 | 7,01 ± 14,44 | 0,3 ± 1,36 |
| | % AB | 91,37 ± 14,4 | 3,25 ± 8,09 | 1,73 ± 4,1 | 3,63 ± 6,99 | 0,03 ± 0,13 |

especies donde, el porcentaje relativo de ocupación promedio fue de 90 % del área basal. El resto de la composición relativa se repartió entre *P. flexuosa, G. descorticans, S. fasciculata* y en menor proporción por *J. rhombifolia*, la cual suele aparecer como individuos dispersos. Por consiguiente, la modelación y el análisis de la cobertura se abordó desde la especie principal (*P. caldenia*) por ser la que mayor impacto tendría en el recurso forrajero y en el aprovechamiento forestal.

El estrato arbustivo estuvo integrado mayoritariamente por *S. fasciculata, C. ehrenbergiana* y *C. microphylla*. La aparición de estas especies no es continua. Existen zonas de considerable abundancia y otras relativamente escasas.

*Medición de la biomasa herbácea.* Establecida la estratificación del bosque en abiertos (AB ≤ 15 m² ha$^{-1}$) y cerrados (AB ≥ 15 m² ha$^{-1}$), la disponibilidad del estrato herbáceo se determinó por medio de muestreos completamente aleatorizados en las siguientes condiciones: 1. bajo copa en bosque cerrado, 2. entre copas en bosque cerrado, 3. bajo copa en bosque abierto y 4. entre copas en bosque abierto. Se tomaron 16 repeticiones por condición. Los muestreos se realizaron previo a la entrada de los animales y el material recolectado comprende al acumulado entre dos pastoreos, de acuerdo al sistema de pastoreo expuesto anteriormente, corresponde a un año de crecimiento.

Las situaciones de bosque cerrado alcanzaron en promedio 27,5 m² ha$^{-1}$ de AB y se encontraron pocos intersticios de espacio sin proyección de copas. Los bosques abiertos presentaron en promedio 12,5 m² ha$^{-1}$ de AB. El tamaño de muestreo para el estrato herbáceo fue de 0,25 m². En laboratorio se identificaron las especies que integraban las muestras y se determinó los porcentajes en término de ocupación. Luego se llevaron a estufa (60 °C) de aire forzado hasta peso constante. Posteriormente se realizó un análisis de calidad por condición, donde se terminó: proteína cruda, digestibilidad de la fibra en detergente neutro (FDN), total de nutrientes digestibles (TND), carbohidratos no fibrosos (CNF) y valor relativo del forraje (VRF). El análisis de calidad no tuvo como fin encontrar diferencias estadísticas entre condiciones, ya que es conocida la gran variación temporal del pastizal, además de la selección por parte de los animales. Lo que se persiguió fue determinar dentro de qué valores se encontraba en relación al aprovechamiento nutricional de la biomasa.

*Obtención de un modelo de distribución diamétrica.* Para establecer el modelo de distribución diamétrica del componente leñoso bajo estudio, se siguieron los lineamientos propuestos en el modelo, o Ley de De Liocourt (Madrigal 1994):

$$N_i = N_{max}(1 + a)^{(D_{max} - D_i)/d} \quad [1]$$

Donde, Ni: N° de pies de la clase i; Di: Diámetro medio de la clase i; Nmax: N° de pies de la clase de diámetro máximo; Dmax: Diámetro medio de la clase de diámetro máximo; d: Intervalo de clases diamétricas; y a: constante de modelo.

El modelo exponencial puede formularse también con la expresión [2]:

$$Ni = k. e^{-q*Di} \quad [2]$$

Donde k y q son constantes, siendo q = 1/d * ln (1+a).

La función exponencial [2] se transformó en una función lineal aplicando logaritmos [3]:

$$\ln y = \ln k - q * \ln e \, Di \quad [3]$$

Para luego expresarse como:

$$Z = \beta_0 + \beta_1 * X_i \quad [4]$$

Donde: *Z* = número de pies para un valor área basimétrica (AB), el diámetro máximo (Dmax) y el cociente de De Liocourt "q". El termino Xi reemplaza a Di.

Esta función transformada permitió establecer relaciones que posibilitaron calcular el coeficiente $\beta_1$ para un valor de "q" elegido y de $\beta_0$ para una determinada área basal (Araujo 2014).

El cociente entre el número de individuos de clases diamétricas consecutivas es igual a la constante "q", por lo tanto, se puede expresar como:

$$\frac{Ni}{Ni + 1} = \frac{e^{(\beta 0 + \beta 1 * Xi)}}{e^{(\beta 0 + \beta 1 * Xi + 1)}} = q \quad [5]$$

Multiplicando los términos de la ecuación, se obtiene:

$$q * e^{(\beta 0 + \beta 1 * Xi + 1)} = e^{(\beta 0 + \beta 1 * Xi)} \quad [6]$$

Aplicando logaritmos y simplificando:

$$\ln q + (\beta 0 + \beta 1 * Xi + 1) \ln e = (\beta 0 + \beta 1 * Xi) \ln e \quad [7]$$

$$\ln q = \beta 0 + \beta 1 * Xi - \beta 0 - \beta 1 * Xi + 1 \quad [8]$$

$$\ln q = \beta 1 * Xi - \beta 1 * Xi + 1 \quad [9]$$

$$\ln q = \beta 1 (Xi - Xi + 1) \quad [10]$$

Despejando β1:

$$\beta 1 = \frac{\text{Ln } q}{Xi - Xi + 1} \quad [11]$$

Con esta expresión se calculó el nuevo valor de β1 para un determinado valor de "q". De la misma manera, el área basal (AB), expresada en m² ha$^{-1}$, se define por:

$$AB = \frac{\pi * D_1^2}{40.000} * f_1 + \frac{\pi * D_2^2}{40.000} * f_2 + \cdots \frac{\pi * Dn^2}{40.000} * fn \quad [12]$$

En que $D_1^2$,.., $Dn^2$ representan el menor y mayor diámetro de la distribución y $f_1$,.., $fn$ son las frecuencias respectivas.

Despejando el término (p / 40.000), el factor común $e^{\beta 0}$ y reemplazando las frecuencias f por su valor $[e^{(b0 + b1\ Xi)}]$ se obtuvo:

$$AB = \frac{\pi}{40.000} * [e^{\beta 0}(D_1^2 * e^{(\beta 1 * D_1)} + D_2^2 * e^{(\beta 1 * D_2)} + \cdots Dn^2 * e^{(\beta 1 * Dn)})]\ [13]$$

Donde:

$$e^{\beta 0} = \frac{AB * 40.000}{\pi * (D_1^2 * e^{(\beta 1 * D1)} + D_2^2 * e^{(\beta 1 * D2)} + \cdots + Dn^2 * e^{(\beta 1 * Dn)})}\ [14]$$

Finalmente, aplicando logaritmo neperiano se llegó a la expresión que relaciona el coeficiente β0 con el área basal AB:

$$\beta 0 = Ln * [\frac{AB * 40.000}{\pi * (\Sigma Di^2 * e^{(\beta 1 * Di)})}]\qquad [15]$$

La base del método es la determinación de partes proporcionales de área basal para las diferentes clases, que luego se usan para calcular un área basal correcta, distribuyendo el nivel deseado de área basal en las respectivas clases. Luego, el área basal elegida es transformada en número de árboles para construir la distribución diamétrica.

Por consiguiente, para definir la distribución equilibrada se seleccionaron los valores de q, AB y diámetro máximo (Dmax). El valor de q = 1,46, empleado para la construcción de la curva de equilibrio, se obtuvo de ajustes previos en bosque de buen estado de cobertura. El AB, se fijó en 15 m² ha⁻¹, esto guarda relación con los resultados del apartado de la biomasa forrajera.

Se utilizó un Dmax de 50 cm, establecido a partir de que, bajo el régimen de aprovechamiento de entresaca, se corta la última clase llegando a un diámetro mínimo de corta de 45 cm. En la gran mayoría de los *Prosopis* spp., cuando el individuo alcanza ese dap garantiza un buen desarrollo, capaz de producir abundantes semillas y un buen rendimiento en aserradero. Además, como lo plantea Bogino y Villalba (2008), entorno a ese diámetro el incremento corriente se cruza con el incremento medio estableciendo el momento óptimo de aprovechamiento desde el punto de vista forestal.

*Proyección del crecimiento forestal.* La modelación del crecimiento fue realizada a través de un modelo de clases diamétricas, utilizando como base la distribución diamétrica inicial obtenida del inventario. El modelo permitió proyectar la evolución del número de pies por clase diamétrica. Dado el corto período de tiempo de la modelación (10 años) se asumió que todos los árboles sobrevivirían al período considerado.

Asumiendo la propuesta de Silva (1989), la fracción de árboles que se mueve anualmente a lo largo de todo el intervalo de clases, debido al crecimiento diametral, fue estimada por un índice de crecimiento (IC), calculado por la siguiente fórmula:

$$IC = Ic * P/a \qquad [16]$$

Donde, *IC*: Índice de crecimiento. *Ic*: Incrementos corriente en diámetro de la clase. *P*: Número de años del período considerado. *a*: Amplitud de la clase de diámetro.

Para el cálculo del *Ic* se emplearon los datos obtenidos en el trabajo de Bogino y Villalba (2008), donde se establece el crecimiento radial y tiempos de rotación de *P. caldenia* en el centro de la Argentina. Con los datos dendrocronológicos del sitio "El Liebral", próximo al estudiado, a partir del ajuste de una función de tres tramos, ecuación [17], se obtuvieron los incrementos corrientes (*Ic*) por clase diamétricas:

Conociendo las existencias medias anuales en número de individuos por clase diamétrica y el IC, fue posible calcular el número de años necesarios para que todos los pies de una clase pasen a la siguiente y proyectar la distribución diamétrica.

Otro punto importante a considerar en el modelado fue el ingreso o reclutamiento que se introducirían a la primera clase diamétrica. A falta de experiencias locales, las cantidades mínimas y las cantidades ideales de árboles que deben permanecer en la regeneración por hectárea se determinaron a base de experiencias hechas en bosques de estructura similar del Chaco semiárido (Coirini 2013). En el caso de bosques de *P. caldenia*, la cantidad mínima debería estar entorno a los 150 a 200 árboles de futura cosecha por hectárea (Coirini 2013). La cantidad de ejemplares inventariados en la regeneración fue de 234 individuos ha⁻¹. A esos 234 pies se los multiplicó por el IC de la clase y arrojó un valor de 23,4 pies ha⁻¹ año⁻¹. En relación con esto, se formuló la hipótesis de que ingresarán 23,4 individuos por

$$Ic = 2,92 + \begin{cases} (0,87 * dap) & dap \leq 4,44\ cm \\ ((0,87 * 4,44) + (dap - 4,44) * -0,07) & 4,44\ cm < dap \leq 32,89\ cm \\ ((0,87 * 4,44) + (32,89 - 4,44) * -0,07 - 0,05 * (dap - 32,89)) & dap > 32,89\ cm \end{cases} \quad [17]$$

Donde, Ic: incremento corriente anual (mm). dap: diámetro a altura de pecho (cm).

año (tasa de reclutamiento). En el Chaco semiárido Iturre *et al*. (2017) en simulaciones de *Aspidosperma quebracho-blanco* utilizaron valores de 16,8 pies ha^{-1} año[-1].

*Crecimiento del volumen.* Para la estimación de volumen y su distribución por clase, se recurrió a la función desarrollada por Chauchard (2009) en *P. caldenia* durante el último Inventario Forestal Nacional:

$$Va = 2,89421 * ga - 6,306998 * ga^{1,5} + 0,588971 * ga * h \quad [18]$$

Donde, Va*: volumen con corteza hasta punta fina de 5 cm (m$^3$). ga*: área basal acumulada de todos los fustes del árbol (m$^2$). h*: altura total (m).

La determinación de altura se realizó mediante el ajuste de la ecuación [19]:

$$h = 12,59 * (1 - 0,8^{(-2,05 * dap)}) \quad [19]$$

Donde, h: altura total del árbol (m). dap: diámetro altura de pecho (m).

*Determinación de la cobertura arbórea.* Para la determinación de la cobertura del estrato superior se ajustó la ecuación [20]:

$$dc = \frac{11,92}{(1 + 5,36^{(-6,44 * dap)})} \quad [20]$$

Donde, dc: diámetro de copa del árbol (m). dap: diámetro altura de pecho (m).

La ecuación [20] se aplicó a todos los pies de las parcelas para conseguir los diámetros de copas que luego se emplearon en la determinación de sus respectivas áreas, a fin de obtener el porcentaje de cobertura de la leñosa.

La ecuación [19] y [20] presentan un coeficiente de determinación R$^2$: 0,86 y 0,65, respectivamente. En ambas ecuaciones todos sus parámetros fueron altamente significativos ($P < 0,0001$) y sus respectivos coeficientes estimados se mostraron altamente correlacionados.

*Análisis estadísticos.* Los datos de biomasa herbácea fueron analizados mediante análisis de la varianza (ANOVA) y test LSD de Fisher para la comparación de medias, utilizando el software estadístico Infostat (Di Rienzo 2018). Se utilizó el mismo *software* para los análisis de regresión donde emplea el método de mínimos cuadrados en modelos lineales y el método *Nelder-Mead simplex algorithm* para las no lineales (Nelder y Mead 1965). La selección de los modelos se realizó comparando el coeficiente de determinación (R$^2$), el cuadrado medio del error (CMerror), el nivel de significancia de los parámetros, y los valores del criterio de información de Akaike (AIK) y el criterio de información bayesiano (BIC).

RESULTADOS

En cuanto a la disponibilidad de la biomasa herbáceas, de las cuatro situaciones evaluadas (cuadro 2), solo en la posición bajo copa en bosque cerrado se observó una disponibilidad significativamente inferior ($P < 0,05$). Es importante resaltar que en bosque abierto la cobertura de copas no superó el 50 % de la superficie de suelo, esto puede apreciarse en la línea de corte en la figura 2.

**Cuadro 2.** Biomasa herbácea en kilogramos de materia seca (MS) área total y resumen de los principales indicadores de calidad de las pasturas en las cuatro situaciones estudiadas.

Herbaceous biomass in kg of dry matter (DM) total area and summary of the main indicators of pasture quality in the four situations studied.

| Muestra | | Biomasa de herbáceas | Indicadores de calidad del Forraje | | | | |
|---------|---|---------------------|------------------------------------|---|---|---|---|
| Tipo de bosque | Posición respecto de la copa | MS kg ha^{-1} | Proteína cruda (%) | Digest. FDN (%) | TND (%MS) | CNF (%MS) | VRF |
| Abierto | Bajo copas | 2.923 a | 13,3 | 38,2 | 52,7 | 18,3 | 88 |
| Abierto | Entre copas | 2.732 a | 11,3 | 32,2 | 52,0 | 17,7 | 79 |
| Cerrado | Entre copas | 2.436 a | 13,5 | 44,2 | 53,5 | 10,1 | 83 |
| Cerrado | Bajo copas | 1.666 b | 14,5 | 48,5 | 55,3 | 17,1 | 91 |
| Bosque (*P*) | | 0,0019* | - | - | - | - | - |
| Posición (*P*) | | 0,2286 ns | - | - | - | - | - |
| Bosque x Posición (*P*) | | 0,0484* | - | - | - | - | - |

Análisis NIRS CV. Laboratorio certificado por National Forage Testing Association. VRF: valor relativo de forraje. CFN: carbohidratos no fibrosos. TND: total de nutrientes digestibles.
*P*: probabilidades límites en ANOVA. *: $P < 0,05$; ns: $P > 0,05$. Letras diferentes indican diferencias significativas (LSD Fisher, $P < 0,05$).

En relación a la composición del pastizal, bajo copa en bosque cerrado, las muestras se integraban por un 40 % de *Setaria leucopila* (Scribn. *et* Merr.) K.Schum, un 50 % de *Bromus catharticus* Vahl y menos del 10 % de *Stipa hyalina* Nees. En bosque cerrado, fuera de la proyección de copas, las muestras estuvieron integradas por un 50 % de *S. leucopila* y un 50 % de *S. hyalina*; no se encontró *B. catharticus*. En el bosque abierto, bajo la proyección de copas, las muestras estuvieron integradas por un 10 % de *S. leucopila*, un 10 % de *B. catharticus*, un 10 % de *Nassella tenuissima* Barkworth y un 70 % de *Carex sororia* Kunth. En la posi-

ción de bosque abierto entre copas, las muestras presentaron un 10 % de *Stipa brachychaeta* Godron, un 20 % de *S. leucopila* y un 80 % de *Cyperus cayennensis* Britton.

Los resultados del componente leñoso muestran que al comparar la distribución de AB actual versus ideal, por clase diamétrica, se observa ciertos baches que podrían comprometer la producción sostenida en el tiempo (figura 1). La distribución ideal planteada buscó la recuperación de la estructura irregular con una mayor participación de pies jóvenes en la distribución de pies por clase diamétrica (cuadro 3).
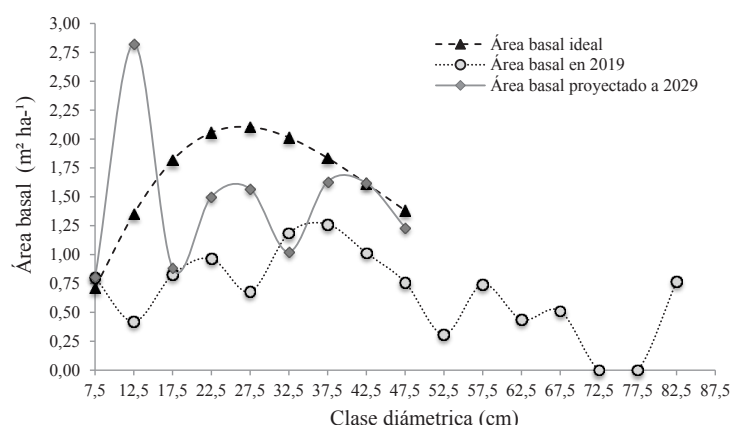


**Figura 1**. Distribución del área basal (m² ha⁻¹): actual, ideal y proyectada en función de la clase diamétrica (cm).

Distribution of the basal area (m² ha⁻¹): current, ideal and projected according to the diametric class (cm).

**Cuadro 3.** Proyección del número de pies, área basal y volumen total por clase diamétrica para un periodo de 10 años.

Projection of the number of feet, basal area and total volume by diameter class for a period of 10 years.

| Clase (cm) | *Incremento Corriente (mm año⁻¹) | Frecuencia (N pies ha⁻¹) | | | Área basimétrica (m² ha⁻¹) | | | Volumen (m³ ha⁻¹) | | |
|---|---|---|---|---|---|---|---|---|---|---|
| | | Año 2029 | Ideal | Diferencia | 2029 | Año Ideal | Diferencia | Año 2029 | Ideal | Diferencia |
| 2,5 | 5,1 | 234,0 | 235,0 | -1,0 | 0,11 | 0,12 | 0,00 | 0,52 | 0,52 | 0,00 |
| 7,5 | 6,6 | 181,5 | 161,0 | 20,6 | 0,80 | 0,71 | 0,09 | 3,85 | 3,42 | 0,44 |
| 12,5 | 6,2 | 230,0 | 110,2 | 119,7 | 2,82 | 1,35 | 1,47 | 14,17 | 6,79 | 7,38 |
| 17,5 | 5,9 | 36,7 | 75,5 | -38,8 | 0,88 | 1,82 | -0,93 | 4,58 | 9,42 | -4,84 |
| 22,5 | 5,5 | 37,7 | 51,7 | -14,0 | 1,50 | 2,06 | -0,56 | 7,97 | 10,92 | -2,96 |
| 27,5 | 5,2 | 26,4 | 35,4 | -9,0 | 1,57 | 2,10 | -0,53 | 8,47 | 11,35 | -2,89 |
| 32,5 | 4,8 | 12,3 | 24,3 | -11,9 | 1,02 | 2,01 | -0,99 | 5,57 | 10,96 | -5,39 |
| 37,5 | 4,6 | 14,8 | 16,6 | -1,8 | 1,63 | 1,84 | -0,20 | 8,91 | 10,03 | -1,11 |
| 42,5 | 4,3 | 11,4 | 11,4 | 0,0 | 1,62 | 1,61 | 0,00 | 8,82 | 8,80 | 0,02 |
| 47,5 | 4,1 | 7,0 | 7,8 | -0,8 | 1,23 | 1,38 | -0,15 | 6,68 | 7,48 | -0,80 |
| | Total ha⁻¹ | 792 | 729 | 63 | 13,2 | 15,0 | -1,8 | 69,5 | 79,7 | -10,2 |

Los cálculos de la distribución ideal de pies, AB y volumen, son en base a un valor de q: 1,46, un AB total de 15 m² ha⁻¹ y un diámetro máximo de corta de 50 cm. El número de pies, AB y volumen proyectados para el año 2029 resulta de la aplicación del IC calculado por clase y la tasa de reclutamiento. Los valores negativos en la columna "diferencia", indican un déficit y los valores positivos el exceso con respecto a la curva balanceada que se ha determinado.

Por otro lado, la proyección del crecimiento a partir de la distribución diamétrica del bosque abierto, permite observar un aumento considerable de densidad en la clase diamétrica de 12,5 cm. Este aumento representaría el 108 % en el número de pies y área basal (cuadro 3) con respecto a la distribución ideal o de equilibrio establecida como distribución óptima de manejo. Es importante remarcar que se habla de un aumento fuera del óptimo, porque según lo establecido, con 110 pies en la clase 12,5 cm para el año 2029, sería suficiente para asegurar la reserva de la clase siguiente de 17,5 cm.

La relación entre la cobertura copas y el área basal mostró una alta asociación (figura 2) expresado en un coeficiente de determinación $R^2 = 0,96$. El aumento en la cobertura de copas fue de 3,18 % por unidad de incremento de AB (m² ha⁻¹) (EE = 0,10; min. 2,96 (95 %) y máx. 3,39 (95 %); n = 39). Este resultado permite transformar las magnitudes de densidad en área basal a porcentaje de cobertura. Esto toma gran relevancia ya que, el tratamiento de la densidad en la bibliografía aparece expresada en área basal, desde un abordaje netamente forestal, y en términos cualitativos desde un punto de vista ganadero o del manejo del pastizal.

Si asociamos los resultados de la simulación del vuelo forestal con la relación de cobertura de copas y área basal (figura 2), el incremento en densidad de 1,47 m² ha⁻¹ en la clase de 12,5 cm, se traduciría en un 5 % de cobertura arbórea excedente al óptimo para mantener una estructura exponencial negativa o en forma de J invertida. Además, la
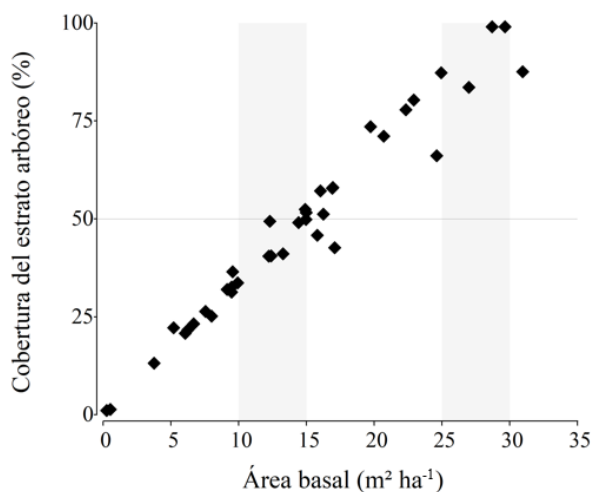


**Figura 2.** Relación entre la cobertura del estrato arbóreo y el área basal para cada parcela de muestreo. Bandas grises corresponden a las densidades en términos de área basal arbórea donde se realizaron los muestreos de biomasa herbácea.

Relationship between the coverage of the tree stratum and the basal area for each sample plot. Gray bands correspond to the densities in terms of the tree basal area where herbaceous biomass samplings were carried out.

relación mencionada (figura 2), permite estimar que, con un aprovechamiento por diámetro mínimo de corta, si se remueve la última clase diamétrica (7 pies), que equivale a 1,23 m² ha⁻¹, se liberarían un 4 % de la superficie del suelo.

DISCUSIÓN

Los resultados del componente herbáceo hacen suponer que, para mantener los niveles de producción de biomasa forrajera al máximo, debería manejarse el estrato arbóreo en niveles de 10 a 15 m² ha⁻¹ de AB, que fue el rango en el que se inventarió la biomasa herbácea en bosque abierto (figura 2) ya que, en la condición bajo las copas en el bosque cerrado la disponibilidad de biomasa herbácea es significativamente menor ($P < 0,05$), respecto al resto de las posiciones. Esto indicaría que, en el bosque abierto los niveles de sombra o competencia por agua no son tan marcados (relación entre el AB acumulada y la cobertura de copas, figura 2) y, por lo tanto, la disponibilidad de biomasa herbácea no difiere bajo o fuera de la proyección de copas.

Un aspecto a tener en cuenta es que, la inclinación de los rayos solares genera que las sombras proyectadas por la mañana temprana, y a medida que avanza la tarde, sean más largas que las proyectadas al mediodía. Debido a esto, en esos momentos del día, bajo la copa de los árboles no se proyecta la sombra producida por el propio árbol, aunque si pueden proyectarse sombras de algún otro árbol adyacente. Esta última situación es más probable a medida que aumenta el AB (Fiandino 2019). Por otro lado, si bien la radiación fotosintéticamente activa bajo el dosel de la leñosa no se midió, muchos autores y para diferentes especies, encuentran que el límite para la producción de forraje ronda entre el 70 % (Fernández *et al*. 2002) y el 50 % (Fiandino 2019) de la interceptación de la radiación. Esto permite deducir que, bajo copas en bosque abierto, la disminución de la radiación no supera dicho umbral (observar línea de corte en 50 % de cobertura en la figura 2).

En cuanto a la calidad del forraje, si bien no se analizó estadísticamente, los valores alcanzados en las situaciones evaluadas (cuadro 2) puede atribuirse a las diferentes comunidades vegetales que allí crecen. La posición bajo copa en bosque cerrado, las muestras estaban integradas principalmente por especies citadas como de mayor calidad forrajera. Gaggiotti *et al*. (1996) determinaron que *B. catharticus* alcanza una digestibilidad máxima de 77 %. Por ende, la presencia de *B. catharticus* bajo el dosel de los árboles, tendería a mejorar la calidad de la base forrajera.

La mayor proporción de *S. leucopila* y *B. catharticus* en bosque cerrado, coincide con lo encontrado por Gabutti *et al.* (1999), donde reporta un aumento de estas especies en el sotobosque en pastizales bajo caldenales en la provincia de San Luis, Argentina. En el mismo sentido, el aumento de estas especies bajo la proyección de copas de *P. caldenia*, tienden a mejorar la calidad del pastizal.

En bosque abierto, bajo la proyección de copas, también aparece *B. catharticus* aunque en muy baja propor-

ción. Se observa un 70 % de *C. sororia,* de una digestibilidad máxima de 58 % (Hidalgo *et al.* 1998) que hace que la calidad de la muestra sea superior a la situación de bosque abierto donde comienza a aparecer especies como *S. brachychaeta,* de escaso valor forrajero.

En cuanto al componente leñoso, la distribución diamétrica desequilibrada que caracteriza al bosque en la actualidad es, probablemente, el resultado de regímenes de aprovechamiento que fueron implementados en el pasado sin un criterio silvícola claro. La proyección de su crecimiento en los próximos 10 años, representan un amento en la densidad en términos de AB que, a su vez, se traduce en un amento en la cobertura de copas. Esto significa que, de no considerar el manejo de estos excedentes, llevaría a un cierre del dosel, una disminución de los incrementos diamétricos y a una menor producción de pasto cuando se exceda el 50 % de cobertura arbórea.

El modelado de crecimiento forestal permite anticiparse y visualizar como se incrementará el número de pies en las sucesivas clases diamétricas, lo que posibilitaría planificar cortas de mejoramiento como: clareos, raleos, cortas de liberación, limpieza o sanitarias, que permitan hacer una selección de los individuos de futura cosecha y, proyectar el número de pies y volumen de madera a obtener en un determinado periodo.

Los resultados de volumen total proyectados a 2029 (69,5 m$^3$ ha$^{-1}$) concuerda con los datos proporcionados por el último inventario forestal nacional (SAyDS 2007), donde en bosques de *P. caldenia* de 15 m$^2$ ha$^{-1}$ de AB, se reportó un volumen medio total de 62,3 m$^3$ ha$^{-1}$. Estos valores de producción se encuentran en concomitancia con los reportados por Coirini *et al.* (2013), donde en el distrito del *P. caldenia* es posible obtener entre 0,5 y 0,8 m$^3$ ha$^{-1}$ de incremento anual. Si multiplicamos estos valores por el periodo proyectado tenemos entre 5 y 8 m$^3$ ha$^{-1}$, lo que significa que los resultados de la simulación están dentro de los encontrado por otros autores en bosques de *P. caldenia*. En síntesis, para la estructura bajo estudio, si el silvicultor opta por cortar la última clase, en el año 2029, obtendrían siete pies maduros que se encuentran en la clase de 47,5 cm, lo que equivale a 6,68 m$^3$ ha$^{-1}$. El volumen acumulado por todas las clases diamétricas será de 69,5 m$^3$ ha$^{-1}$, lo que significaría remover tan solo el 9,61 % del volumen total en pie. En masas irregulares es recomendable no remover más del 20 % (Araujo 2014) para no tender a su regularidad y mantener la estructura de equilibrio.

Por último, en términos de cobertura de copas, la remoción de la última clase liberaría un 4 % de la superficie, mientras que aplicar un raleo con una intensidad del 50 % de los pies en la clase de 12,5 cm, establecido de acuerdo a la distribución ideal, permitiría liberar un 5 % de la superficie. Por lo tanto, la experiencia de este análisis nos pone de manifiesto en términos relativos los impactos que tendrían las prácticas silvícolas de mejoramiento y aprovechamiento sobre la apertura del vuelo forestal. La cual, a su vez, impactará en el desempeño de la herbácea.

## CONCLUSIONES

En relación al componente herbáceo se concluye que, hasta ciertos niveles de área basal acumulada, no se producen disminuciones significativas en la disponibilidad de biomasa forrajera bajo la proyección de copas, respecto la posición a cielo abierto, lo que permitiría manejar el dosel de la leñosa en los niveles indicados. Además, bajo la proyección de las copas, se observó un cambio en la composición del pastizal a favor de especies de mayor valor forrajero y que sería interesante de indagar en profundidad en futuras investigaciones ya que, hasta aquí, no se puedo concluir con evidencia suficiente.

En cuanto al componente forestal, la experiencia de este trabajo indica que el empleo de un modelo de clases diamétricas arroja resultados satisfactorios en cuanto a la proyección de los parámetros forestales, contrastados a valores reportados en bosque de similares características, lo que permitirían planificar las cortas de mejoramientos y conducir estos bosques en niveles de cobertura que no afecten significativamente el rendimiento del recurso forrajero.

La estrecha relación entre la cobertura de copas y el área basal permite transformar los valores normalmente expresados en área basal a porcentaje de cobertura. Además, dicha relación apoyada mediante un método de simulación, como el aquí desarrollado, pueden predecir cómo evolucionaría la cobertura arbórea en el tiempo y el impacto de las prácticas silvícolas para mantener una estructura diamétrica objetivo y que, a su vez, maximice el rendimiento del componente herbáceo.

Las limitantes de este trabajo están relacionadas a la modelación en dos aspectos. Uno tiene que ver con la tasa de mortalidad y, el otro, con la tasa de reclutamiento. Si bien, en un principio, se estimó mediante la construcción de índices por información recabada de los inventarios, luego se decidió no implementarlos y se optó por no extender el periodo de simulación más allá de 10 años, como lo sugieren los autores de estos modelos. La tarea que resta hacia adelante es, a través de parcelas permanentes, medir tasas de mortalidad, reclutamientos e incrementos diamétricos asociados a variables de sitio para validar y mejorar la capacidad de predicción de los modelos.

regeneración del estrato arbóreo, lo que posibilitaría avanzar con la metodología de ordenación de bosque irregular propuesta en este trabajo.

## REFERENCIAS

Anderson DL, JA Del Águila, AE Bernardón. 1970. Las formaciones vegetales en la provincia de San Luis. *Revista de Investigaciones Agropecuarias. Serie 2. Biología y Producción Vegetal* 2(3): 153-183.

Araujo PA, MC Iturre. 2014. Ordenamiento de Masas Irregulares. Facultad de Ciencias Forestales. Universidad Nacional de Santiago del Estero. E-Book ISBN 978-987-1676-39-2. Consultado 10 jul. 2018. Disponible en: https://fcf.unse.edu.ar/archivos/series-didacticas/SD-28-Ordenacion-bosques-irregulares-ARAUJO.pdf

Beltrán HA, L Chauchard, A Dezzotti, GM Pastur. 2018. Modelo de crecimiento diamétrico de *Nothofagus alpina* y su relación con el de *Nothofagus obliqua* y *Nothofagus dombeyi* en los bosques naturales de la Patagonia argentina. *Bosque* 39(1): 107-117. http://dx.doi.org/10.4067/S0717-92002018000100107.

Bogino S, R Villalba. 2008. Radial growth and biological rotation age of *Prosopis caldenia* Burkart in Central Argentina. *Journal of Arid Environments* 72: 16-23. https://doi.org/10.1016/j.jaridenv.2007.04.008.

Chauchard L, R Sbrancia, A Medina, A Rabino. 2009. Funciones de Volumen Total para *Prosopis caldenia* Burk, Argentina. *Quebracho* 17(1,2): 41-51.

Coirini R, M Karlin, M Brassiolo. 2013. Prácticas forestales en los bosques nativos de la República Argentina Ecorregión Forestal Espinal. Buenos Aires, Argentina. Secretaría de Ambiente y Desarrollo Sustentable de la Nación Argentina. 175p.

Di Rienzo JA, F Casanoves, MG Balzarini, L Gonzalez, M Tablada, CW Robledo. 2018. Grupo InfoStat, FCA, Universidad Nacional de Córdoba, Argentina. http://www.infostat.com.ar

Dussart E, Lerner P, Peinetti R. 1998. Long term dynamics or two populations on *Prosopis caldenia* Burkart. *Journal of Range Management* 51: 685-691.

Estelrich HD, CC Chirino, EF Morici, B Fernández. 2005. Dinámica de áreas naturales cubiertas por bosque y pastizal en la Región semiárida central de la Argentina. Modelo conceptual. Heterogeneidad de la Vegetación. Santa Rosa, La Pampa, Argentina. Facultad de Agronomía UNLPam. p. 351-364.

Fernández ME, JE Gyenge, G Dalla-Salda, T Schlichter. 2002. Silvopastoral systems in NW Patagonia: I. Growth and photosynthesis of *Stipa speciosa* under different levels of *Pinus ponderosa* cover. *Agroforestry Systems* 55: 27-35.

Fiandino SI, 2019. Efecto de los recursos agua y radiación sobre la productividad del pastizal natural en sistemas silvopastoriles de la Sierra de Comechingones. Tesis Doctoral. Universidad Nacional de Río Cuarto. 246 p.

Gabutti EG, Privitello MJL, Maidana MA, Harrison RU. 1999. Producción anual del pastizal natural del bosque de caldén (*Prosopis caldenia* burk.) de la provincia de San Luis, Argentina. *Archivo Latinoamericano Producción Animal* 7(1): 1-8.

Gaggiotti MdelC, LA Romero, OA Bruno, EA Comeron, OR Quaino. 1996. Tabla de composición química de alimentos. II - Forrajes verdes. INTA. Rafaela, Santa Fe, Argentina.

Hidalgo LG, MA Cauhépé, AN Erni. 1998. Digestibilidad y contenido de proteína bruta en especies de pastizal de la Pampa Deprimida. Argentina. R*evista de Investigación Agraria: Producción y Sanidad Animales* 13: 165-177.

Iturre MC, PA Araujo, CJ Trejo. 2017. Simulación del crecimiento de bosques nativos del Chaco Semiarido. Aplicación del sistema informático MOSIMAFO. *Quebracho* 25(1,2): 54-62.

Madrigal CA. 1994. Ordenación de montes arbolados. Madrid, Esàña. ICONA. 375 p.

Morici E, V Doménech-García, G Gómez-Castro, A Kin, A Saenz, C Rabotnikof. 2009. Diferencias estructurales entre parches de pastizal del caldenal y su influencia sobre el banco de semillas, en la provincia de la pampa, argentina. *Agrociencia* 43: 529-537.

Nelder JA, R Mead. 1965. A simplex method for function minimization. *The computer journal* 7(4): 308-313.

Pelaez D, RM Boo, OR Elia. 1992. Emergence and seedling survival of caldén in the semiarid region of Argentina. *Journal of Range Management* 45: 564-568. http://hdl.handle.net/10150/644555

Roman L, C Fuser, M Cocco, M Flores Palenzona, C Percara, C de la Peña. 2015. Evaluación del componente herbáceo en el espinal del noroeste del departamento Concordia, Entre Ríos. *In* 3° Congreso Nacional de Sistemas Silvopastoriles: VIII Congreso Internacional Sistemas Agroforestales. Iguazú, Argentina. Ediciones INTA. p. 37-38.

Sanquetta CR, JE Arce, F dos Santos Gomes, E Coutinho da Cruz. 1999. Evaluación y simulación precoces del crecimiento de rodales de *Pinus taeda* L. con matrices de transición. *Quebracho* 7: 31-42.

SAyDS (Secretaría de Ambiente y Desarrollo Sustentable de la Nación Argentina, AR). 2007. Primer inventario nacional de bosques nativos: informe regional espinal, segunda parte. Buenos Aires, Argentina. Secretaría de Ambiente y Desarrollo Sustentable de la Nación Argentina. 154 p.

Silva JNM. 1989. The behaviour of the tropical rain forest of the brasilian amazon after logging. Tesis Ph.D. Oxford, Inglaterra. Oxford Forestry Institute, University of Oxford. 119 p.

Urbano E, S do Amaral Machado, AF Filho, CR Sanquetta, JD Zea-Camaño. 2018. Modelación del volumen de rodal para especies secundarias en bosques nativos de *Mimosa scabrella* en la región metropolitana de Curitiba, Paraná, Brasil. *Bosque* 39(2): 227-237. http://dx.doi.org/10.4067/S0717-92002018000200227

Vargas BL, JR Corral, FC Cruz, OC Aguirre, J Nagel. 2008. Uso y aplicación de los simuladores de crecimiento forestal en la toma de decisiones silviculturales. *Revista Forestal Latinoamericana* 23(2): 33-52. http://www.saber.ula.ve/handle/123456789/33374

# Effect of carbonization on wood anatomy of three Fabaceae species from an Araucaria forest stand in Southern Brazil

Efecto de la carbonización en la anatomía de la madera de tres especies de Fabaceae del Bosque de Araucaria, sur de Brasil

**Ângela Maria Stüpp [a], Helena Cristina Vieira [a], Polliana D'Angelo Rios [b], Graciela Inés Bolzon de Muñiz [c], Silvana Nisgoski [c]\***

[a] Federal University of Paraná, Av. Pref. Lothário Meissner, 632, Jardim Botânico, 80.210-170, Curitiba, PR, Brazil, angela.stupp@ufpr.br, helenavieira@ufpr.br

[b] University of Santa Catarina State, Forest Engineering Course, Av. Luiz de Camões, 2090, bairro Conta Dinheiro, 88520-000 Lages, SC, Brazil, a2pdr@cav.udesc.br

\*Corresponding author: [c] Federal University of Paraná, Forest Engineering and Technology Department, Laboratory of Wood Anatomy and Quality, Av. Pref. Lothário Meissner, 632, Jardim Botânico, 80.210-170, Curitiba, PR, Brazil, graciela.ufpr@gmail.com, silvana.ufpr@gmail.com

SUMMARY

The aim of this study was to measure and compare some anatomical elements of wood and charcoal of *Inga vera*, *Machaerium paraguariense* and *Muellera campestris* to support identification of the materials seized by regulatory authorities. For each species, three trees were analyzed. After wood evaluation, all samples (moisture content of $12 \pm 1$ %) were wrapped in aluminum foil and carbonized in a muffle furnace for 8 hours with final temperature of 450 °C and a heating rate of 1.66 °C/min. The number of measurements was based on 30 readings regarding tangential diameter and vessel density, along with frequency, height and width of rays (in micrometers). After carbonization, changes in cell dimensions and different behavior were observed in the Fabaceae species evaluated. In all species, vessel diameter declined; vessel density decreased in *Inga vera* and increased in the other species; ray height decreased in *Inga vera* and *Muellera campestris*, and increased in *Machaerium paraguariense*; and ray width and frequency increased in all species. We concluded that due to the conservation of wood anatomical structures after carbonization, the inclusion of this species in a database would be effective to support efforts to control deforestation in the south of Brazil.

*Key words: Inga vera*, *Machaerium paraguariense*, *Muellera campestris*, anatomical characteristics, charcoal.

RESUMEN

El objetivo de este estudio fue medir y comparar algunos elementos anatómicos de madera y carbón vegetal de *Inga vera*, *Machaerium paraguariense* y *Muellera campestris* con el fin de apoyar la identificación de los materiales incautados por las autoridades reguladoras. Para cada especie, se analizaron tres árboles. Después de la evaluación de la madera, todas las muestras (contenido de humedad de $12 \pm 1$ %) se envolvieron en papel de aluminio y se carbonizaron en un horno de mufla durante 8 horas con una temperatura final de 450 °C y una velocidad de calentamiento de 1,66 °C/min. El número de mediciones se basó en 30 lecturas con respecto al diámetro tangencial y densidad de los vasos, junto con frecuencia, altura y ancho de los radios (en micrómetros). Después de la carbonización, se observaron cambios en las dimensiones celulares y diferentes comportamientos en las especies de Fabaceae evaluadas. En todas las especies, el diámetro del vaso disminuyó; la frecuencia de los vasos disminuyó en *Inga vera* y aumentó en otras especies; la altura de los radios disminuyó en *Inga vera* y *Muellera campestris*, y aumentó en *Machaerium paraguariense*; y el ancho y la frecuencia de los radios aumentaron en todas las especies. Concluimos que debido a la conservación de las estructuras anatómicas de la madera después de la carbonización, la inclusión de esta especie en una base de datos sería efectiva para apoyar los esfuerzos para controlar la deforestación en el sur de Brasil.

*Palabras clave: Inga vera*, *Machaerium paraguariense*, *Muellera campestris*, características anatómicas, carbón vegetal.

INTRODUCTION

Charcoal is an important raw material for iron and steel making. A potential problem is identification of its origin, which can be from planted forests or illegal wood from native forests (Gonçalves and Schell-Ybert 2012). Sometimes illegal logging is hidden by making charcoal because carbonization makes it harder to identify species. Additiona-

lly, charcoal from native wood is often mixed, for example, with charcoal from *Eucalyptus* L'Hér., a species planted for charcoal production. On this basis, it is necessary to know which anatomical changes that occur during carbonization are related to each species. In general, qualitative characteristics remain unchanged, while some variations occur in dimensions and frequency of vessels and rays (Gonçalves *et al*. 2012, Gonçalves and Scheel-Ybert 2016). Similarly, Osterkamp *et al*. (2018) reported that during carbonization, chemical and physical processes occur that result in changes in wood cell dimensions, although general anatomical characteristics remain without major alterations. Therefore, based on wood anatomy, it is possible to distinguish most species after burning (Muñiz *et al*. 2012b).

Literature reports wood and charcoal anatomy for some species in Brazil, such as macro or microscopic description of *Copaifera* cf. *langsdorfii* Desf. and *Dipteryx odorata* (Aubl.) Willd (Nisgoski *et al*. 2012); *Cedrelinga cateniformis* (Ducke) Ducke and *Enterolobium schomburgkii* (Benth.) Benth. (Muñiz *et al*. 2012a); *Pouteria macrophylla* (Lam.) Eyma and *Micropholis guianensis* (A.DC.) Pierre (Muñiz *et al*. 2013); *Byrsonima spicata* (Cav.) DC., *Calophyllum brasiliense* Cambess., *Cecropia sciadophylla* Mart., *Cochlospermum orinocense* (Kunth) Steud. and *Schefflera morototoni* (Aubl.) Maguire *et al.* (Nisgoski *et al*. 2014); *Brosimum acutifolium* Huber, *Ficus citrifolia* Mill., *Hyeronima laxiflora* (Tul.) Müll. Arg. and *Sapium glandulatum* (Vell.) Pax. (Nisgoski *et al*. 2015); Anacardiaceae species (Gonçalves and Scheel-Ybert 2016); *Mimosa scabrella* Benth., *Miconia cinnamomifolia* (DC.) Naudin, *Cecropia glaziovii* Snethl, *Hyeronima alchorneoides* Allemão and *Pera glabrata* (Schott) Baill. (Carvalho *et al*. 2017); and angelim species (Muñiz *et al*. 2016); besides 80 species described in an anthracology atlas (Scheel-Ybert and Gonçalves 2017).

The Araucaria forest stands in Santa Catarina State, Brazil, are composed of approximately 925 species, from 439 genera in 116 botanical families (Gasper *et al*. 2013). One of the most important is the Fabaceae family, with 58 species recorded (Gasper *et al*. 2013), some with high commercial importance, such as *Inga vera* Willd. and *Muellera campestris* (Mart. ex Benth) M. J. Silva *et* A. M. G. Azevedo (Richter and Dallwitz 2000), while others are listed by the Environmental Ministry as endangered in Brazil, such as 12 species from the genus *Inga* Mill. and one from *Machaerium* Pers. (MMA 2014).

Considering the extraordinary biological diversity in Brazil, as well as the difficulties related to the inspection of environmental crimes, a reference collection and database with a large number of samples is necessary to facilitate efficient identification of wood and charcoal by regulatory authorities. The aim of this study was to verify wood and charcoal anatomical characteristics in different radial positions of three Fabaceae species (*Inga vera*, *Machaerium paraguariense* Hassl and *Muellera campestris*) to contribute with information to a database for these species evaluation.

## METHODS

Wood samples from *Inga vera*, *Machaerium paraguariense* and *Muellera campestris* were obtained from trees cut by Brazilian Institute of Environment and Renewable Natural Resources (IBAMA) in a region that is now inundated by a reservoir (San Roque hydroelectric plant) in Santa Catarina State. For each species, three trees were collected. Specimens of the botanical material were deposited at Lages Herbarium of Santa Catarina State University – LUSC (table 1). The access to the botanical material was registered under the code AF3EDDC with the Genetic Heritage Management Council (CGEN/SISGEN).

For each tree, we selected a disc with no defects at breast height (DBH) for evaluation and wedge obtainability. The material was divided into three samples oriented in anatomical sections (transversal, longitudinal radial, longitudinal tangential), with dimensions of 2 x 2 x 2 cm, codified as near pith (next to the pith, though not including it), intermediate (exactly halfway between near bark and near pith) and near bark (in the outermost part of the disc) (figure 1). Radial sampling was done to cover most anatomical variation that can interfere in wood identification, since results will be added to a database for posterior practical application in forest supervision. Samples were from heartwood, transition and sapwood, varying depending on tree diameter. For characterization, samples were smoothed with #1200 sandpaper.

Wood and charcoal analyses were performed on the same samples. After wood evaluation, all samples (moisture content of 12 ± 1 %) were wrapped in aluminum foil and carbonized in a muffle furnace, as described by Muñiz *et al*. (2012b), with final temperature of 450 °C (two hours at final temperature) and a heating rate of 1.66 °C min$^{-1}$, totaling eight hours. Description of wood and charcoal was based on images obtained with a Discovery V12 stereomicroscope (Zeiss) with the Axio Vision Rel. 4.7 software. Charcoal details were observed with a Hitachi
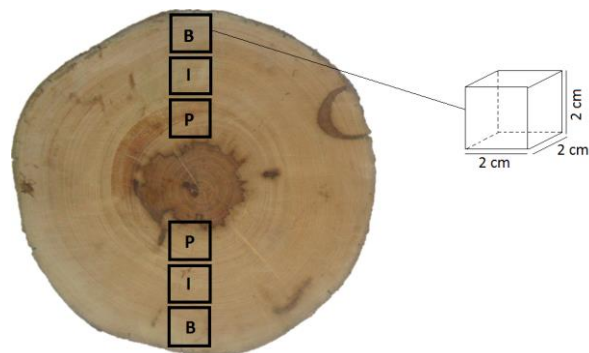


**Figure 1.** Illustration of sampling disk diagram of *Muellera campestris,* where B: near bark, I: intermediate, P: near pith.

Diagrama de muestreo en disco de *Muellera campestris,* donde: B: próximo a la corteza; I: intermedio; P: próximo a la médula.

**Table 1.** Species and record numbers.

Especies y números de registro.

| Species/Record number | DBH (cm) | Coordinates (WGS84) | Altitude (m) |
|---|---|---|---|
| *Inga vera* | | | |
| LUSC 6225 | 26.0 | lat: -27.484728 long: -50.805003 | 701 |
| LUSC 6226 | 18.0 | lat: -27.484378 long: -50.805603 | 851 |
| LUSC 6227 | 17.5 | lat: -27.484228 long: -50.805753 | 731 |
| *Machaerium paraguariense* | | | |
| LUSC 6243 | 18.3 | lat: -27.489997 long: -50.805392 | 734 |
| LUSC 6244 | 12.9 | lat: -27.489997 long: -50.805417 | 734 |
| LUSC 6245 | 11.0 | lat: -27.490006 long: -50.805433 | 734 |
| *Muellera campestris* | | | |
| LUSC 6237 | 31.2 | lat: -27.496892 long: -50.810606 | 692 |
| LUSC 6238 | 25.1 | lat: -27.497081 long: -50.810536 | 696 |
| LUSC 6239 | 15.0 | lat: -27.483572 long: -50.808342 | 740 |

TM-1000 tabletop scanning electron microscope (SEM) directly from the material, without coating. The description of the anatomical elements of wood and charcoal samples followed procedures from International Association of Wood Anatomists (IAWA, 1989) and 30 measurements were made for tangential diameter and vessel density, as well as frequency, height and width of rays (dimensions in micrometers).

A statistical analysis was performed considering the kind of material (wood or charcoal) and different positions in the disk (near bark, intermediate, near pith), resulting in a 2 x 3 factorial analysis. Differences in data between wood and charcoal were evaluated by the Scott-Knott test at 95% probability, using the Sisvar software.

RESULTS

*Qualitative characteristics*. <u>*Inga vera*</u>. In wood samples, growth ring boundaries were distinguished by differences in fiber zones. Vessels: diffuse porosity, solitary vessels (68 %) and in radial multiples 2-5 (14 %, 9 %, 2 %, 7 %, respectively for multiples of 2, 3, 4 and more than 4) (figure 2A), simple perforate plates (figure 2H), intervessel pits alternate, gums and other deposits present (figure 2A). Axial parenchyma: lozenge-aliform and confluent (figure 2A). Rays homogeneous, all ray cells procumbent, 1-3 cells wide, not storied (figure 2B). After carbonization, most qualitative characteristics remained intact (figure 2C) and it was also possible to observe not storied rays (figure 2D), some ray cells with ruptures (figure 2E) and cells in uniseriate and multiseriate rays (figure 2F). The presence of crystals in axial parenchyma cells was verified (figure 2G, H).

*Machaerium paraguariense*. In wood samples, growth ring boundaries were little distinguished by fiber zones (figure 3A). Vessels: diffuse porous, mostly solitary vessels (84 %) (figure 3A), in radial multiples 2-4 present, simple perforate plate (figure 3H), alternate intervessel pits. Axial parenchyma: winged-aliform and confluent; diffuse-in-aggregates. Rays: heterogeneous, with procumbent body ray cell and 1-2 rows of square marginal cells, 1-3 cells wide, storied (figure 3B). In charcoal, qualitative characteristics remained, such as solitary vessels (figure 3C), storied rays (figure 3D), aliform axial parenchyma (figure 3E), heterogeneous rays (figure 3G) and simple perforate plate and alternate intervessel pits (figure 3H) and crystals in axial parenchyma cells were also observed (figure 3F).

*Muellera campestris*. In wood samples, growth ring boundaries were distinct, marked by thin lines from marginal parenchyma (figure 4A). Vessels: diffuse porous with irregular distribution, solitary vessels (62 %) or in radial multiples 2-4 (24 %, 9 %, 2 %, respectively for multiples of 2, 3 and 4), simple perforate plate, alternate intervessel pits, gums and other deposits present. Axial parenchyma: lozenge-aliform and confluent, vasicentric, unilateral present (figure 4A). Rays: homogeneous, multiseriate and storied (figure 4B). Carbonization resulted in more distinct vessels (figure 4C), more evident irregular distribution, and some contrast in storied rays (figure 4D). It was possible to observe more contrast of axial parenchyma in more detailed images (figure 4E), presence of crystals in axial parenchyma cells (figure 4F), homogeneous rays (figure 4G), simple perforate plate (figure 4H) and alternate intervessel pits (figure 4F).

*Quantitative characteristics.* In wood samples, increase in vessel diameter and decrease in vessel density from near pith to near bark (table 2) were observed. Ray dimensions showed no linear tendency of variation and ray frequency was not influenced by radial position in trunk (table 3). In charcoal, changes in structural dimensions were different depending on species characteristics (tables 2 and 3)

DISCUSSION

*Tangential diameter of vessels.* In the wood of all species, we observed an increase in vessel diameter from the region of near pith towards near bark, being more accentuated in *Muellera campestris*. In *Inga vera* wood, mean vessel diameter was 129 μm, similar to all species of the genus *Inga*
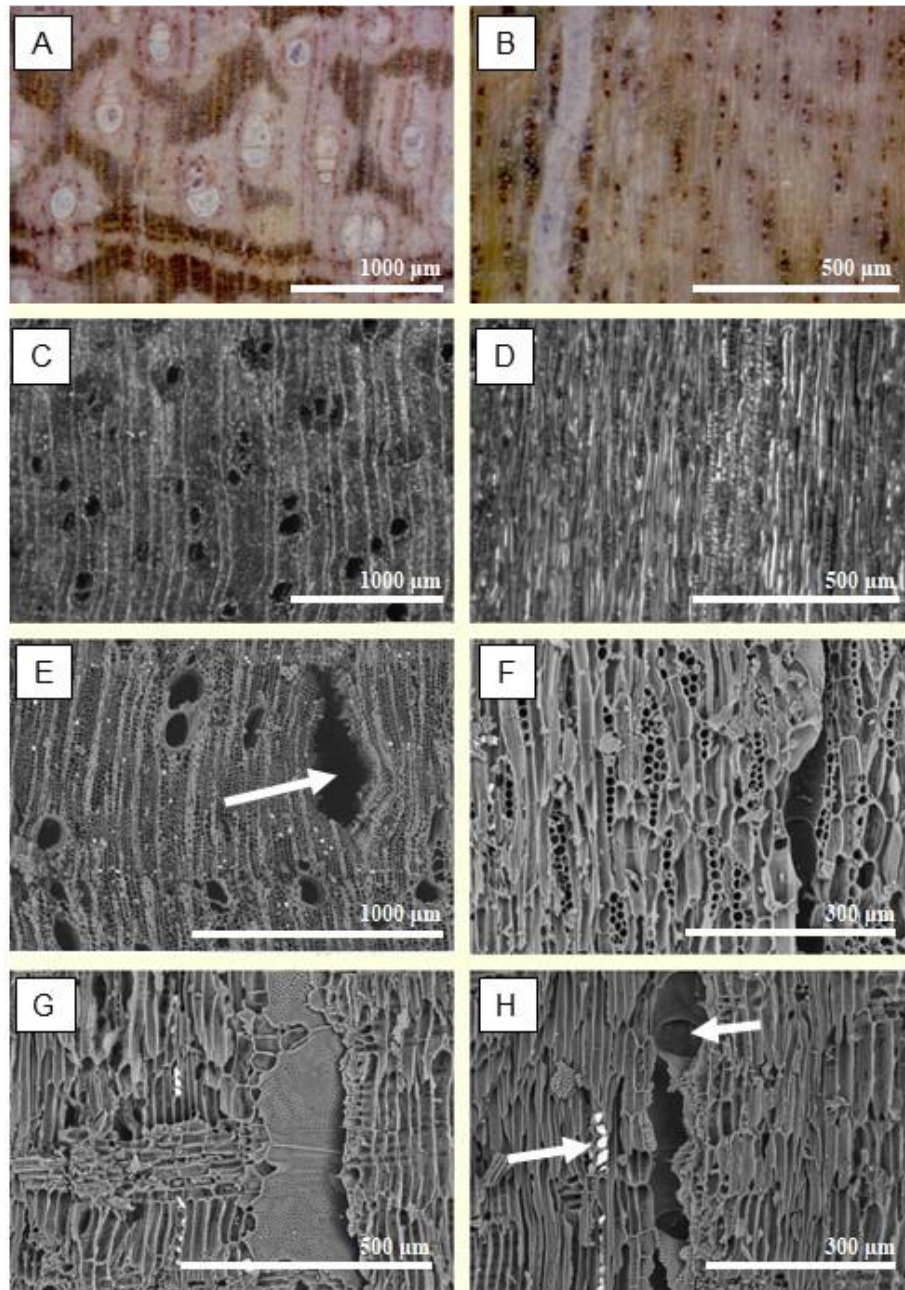


**Figure 2.** Images of *Inga vera* wood (A, B) and charcoal (C, D). SEM images of charcoal (E-H). (A, C) transversal section, (B, D, F) tangential section, (E) transversal section, arrow indicates splits in rays; (G, H) radial section, arrow indicates crystals and simple perforation plate.

Imágenes de la madera (A, B) y carbón (C, D) de *Inga vera*. MEB imágenes del carbón (E-H). (A, C) sección transversal; (B, D, F) sección tangencial; (E) sección transversal, la flecha indica grietas en los radios; (G, H) sección radial, la flecha indica cristales y placa de perforación simples.

published in Inside Wood, along with the study of Ortega *et al*. (1988), who also analyzed *Inga vera*. Furthermore, the results of this study are comparable to those reported by Richter and Dallwitz (2000), with values varying from 60-130-200 µm, for material collected in Mexico, and those reported by Vieira *et al.* (2019), with a mean value of 141 µm. In *Machaerium paraguariense* wood, mean vessel diameter was 107 µm, within the range presented in

Inside Wood for the same genus. The results for both *Machaerium paraguariense* and *Muellera campestris* wood are proportionate to those of Marchiori *et al*. (2009), Richter and Dallwitz (2000) and Vieira (2017), although these authors did not ascertain differences from pith to bark.

In charcoal, differences in vessel diameter from near pith to near bark regions were not linear in accordance with position and varied among the species. After carbo-
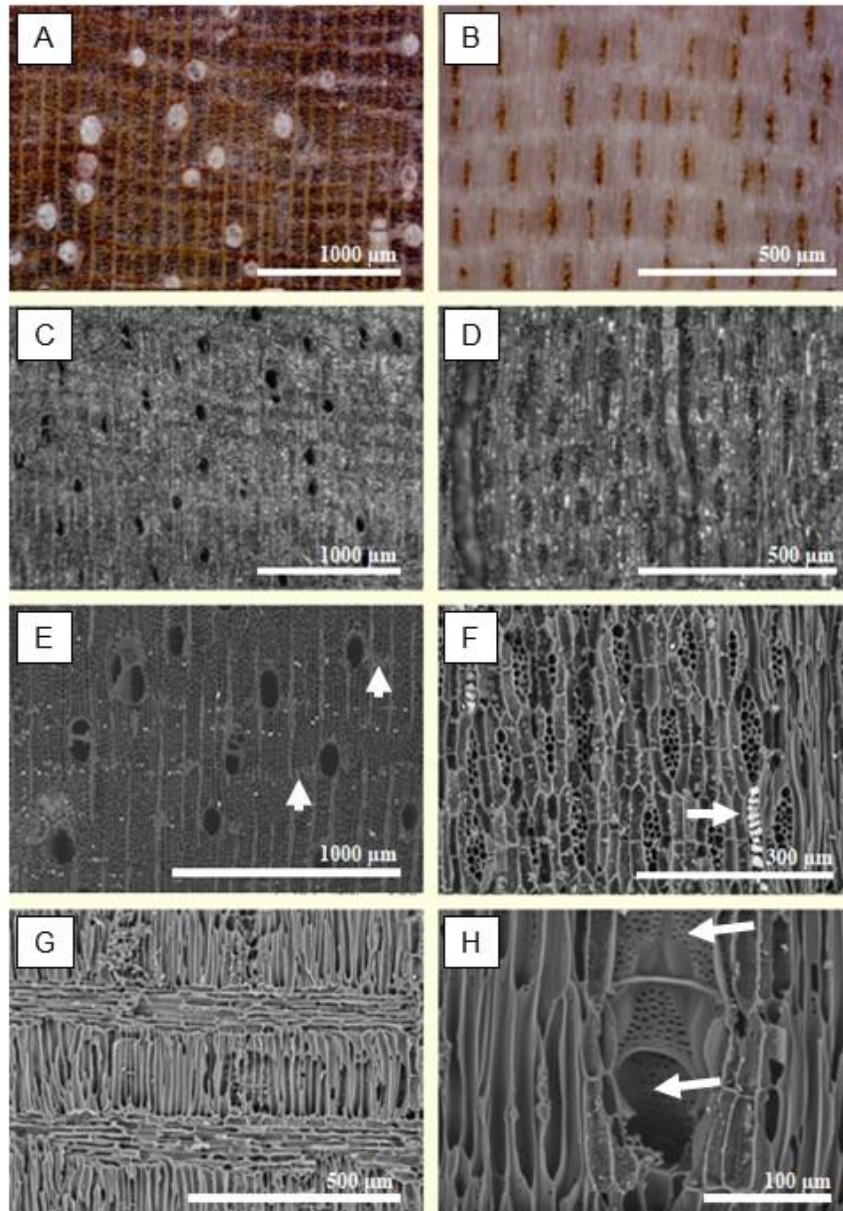


**Figure 3**. Images of *Machaerium paraguariense* wood (A, B) and charcoal (C, D). SEM images of charcoal (E-H). (A, C) Transversal section, (B, D) tangential section, (E) transversal section, arrow indicates axial parenchyma; (F) tangential section, arrow indicates crystals in parenchyma cells; (G, H) radial section, arrow indicates simple perforate plate and intervessel pits.

Imágenes de la madera (A, B) y carbón (C, D) de *Machaerium paraguariense.* MEB imágenes de lo carbón (E-H). (A, C) Sección transversal; (B, D) sección tangencial; (E) sección transversal, la flecha indica parénquima axial aliforme; (F) sección tangencial, la flecha indica cristales en lo parénquima axial; (G, H) sección radial, la flecha indica la placa de perforación simple y las punteaduras intervasculares.

nization, we observed a reduction in vessel diameter for all positions and species. The contraction of cells was more evident in the intermediate position of *Machaerium paraguariense* (32.99 %) and less pronounced in the intermediate position of *Muellera campestris* (14.41 %). Regarding reduction of mean vessel diameter by species after carbonization, *Machaerium paraguariense* had the most important contraction (32.04 %) followed by *Inga vera* (25.41 %) and *Muellera campestris* (20.36 %). Reduction in vessel diameter after carbonization is related to anatomical features, such as the wall thickness of fibers and disposition of axial parenchyma cells, as well as processing conditions such as heating rate. These changes were also reported in other species, such as four Myrtaceae
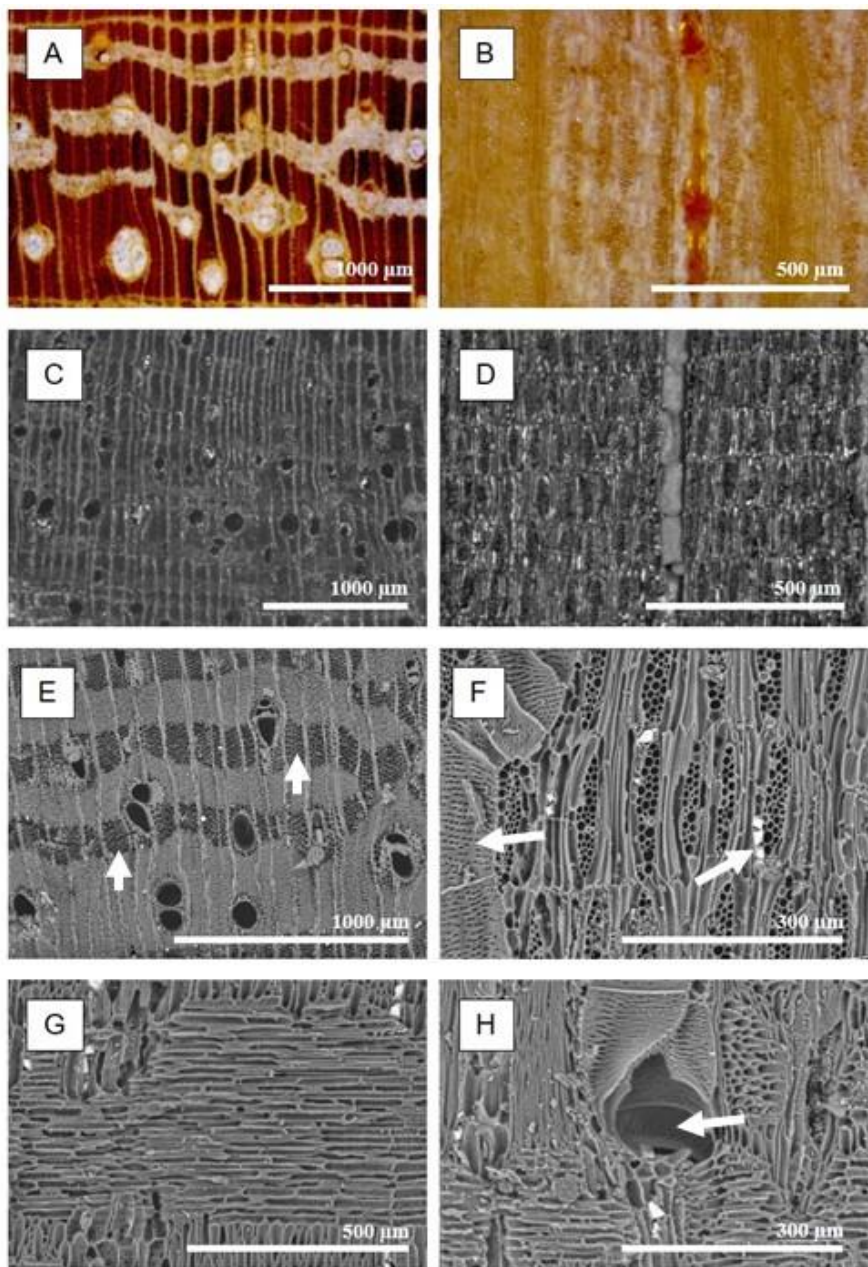


**Figure 4.** Images of *Muellera campestris* wood (A, B) and charcoal (C, D). SEM images of charcoal (E-H). (A, C) Transversal section, (B, D) tangential section, (E) transversal section, arrow indicates the axial parenchyma; (F) tangential section, arrow indicates intervessel pits and crystals in parenchyma cells; (G, H) radial section, arrow indicates simple perforate plate.

Imágenes de la madera (A, B) y carbón (C, D) de *Muellera campestris*. MEB imágenes de lo carbón (E-H). (A, C) Sección transversal; (B, D) sección tangencial; (E) sección transversal, la flecha indica el parénquima axial; (F) sección tangencial, la flecha indica punteaduras intervasculares y cristales en las células del parénquima axial; (G, H) sección radial, la flecha indica placa de perforación simples.

**Table 2.** Mean values and standard deviation of tangential diameter and vessel density of studied species.

Valores medios y desviación estándar del diámetro tangencial y densidad de los vasos de las especies estudiadas.

| Species | Material | Near Bark | Intermediate | Near Pith |
|---|---|---|---|---|
| | | Vessel diameter (μm) | | |
| *Inga vera** | Wood | 139.88 Aa (21.91) | 136.38 Aa (25.26) | 109.17 Ab (31.92) |
| | Charcoal | 106.24 Ba (25.49) | 96.44 Bb (28.30) | 84.18 Bc (28.96) |
| *Machaerium paraguariense* | Wood | 119.82 Aa (23.18) | 103.04 Aa (18.34) | 97.85 Ab (20.69) |
| | Charcoal | 81.52 Ba (22.91) | 69.05 Bb (17.72) | 67.34 Bb (17.55) |
| *Muellera campestris** | Wood | 118.27 Aa (33.21) | 105.33 Ab (23.26) | 94.73 Ac (15.87) |
| | Charcoal | 83.90 Bb (25.53) | 90.15 Ba (23.28) | 78.05 Bb (20.95) |
| | | Vessel density (n/mm$^2$) | | |
| *Inga vera* | Wood | 6.00 Ab (3.42) | 5.77 Ab (3.01) | 7.58 Aa (4.35) |
| | Charcoal | 5.76 Aa (2.62) | 5.46 Aa (2.32) | 6.49 Aa (4.49) |
| *Machaerium paraguariense** | Wood | 4.18 Bb (1.69) | 5.53 Ba (2.29) | 5.76 Ba (1.85) |
| | Charcoal | 7.64 Aa (2.70) | 7.89 Aa (2.13) | 8.18 Aa (2.38) |
| *Muellera campestris** | Wood | 8.42 Ab (3.51) | 7.61 Ab (2.71) | 10.38 Ba (3.55) |
| | Charcoal | 7.49 Ab (2.85) | 7.84 Ab (2.59) | 12.22 Aa (5.08) |

*Species where interaction between material and position was not significant at 95 % probability. For each species, equal letters in means do not present statistical differences by the Scott-Knott test at 95 % probability. Capital letters in column refer to changes after carbonization and small letters are related to radial position in disk (near bark, intermediate, near pith).

species (Stange *et al*. 2018), in angelim species (Muñiz *et al*. 2016) and other species from the Fabaceae family (Nisgoski *et al*. 2012). Another factor that can influence vessel diameter is the possible change in circular shape of cells after carbonization (Gasson *et al.* 2017).

*Vessel density.* Decrease in vessel density was observed in wood from the regions near the pith towards the bark, with statistical significance from the intermediate to near pith region, except in *Machaerium paraguariense*, which had differences between the regions near the bark towards intermediate (33.3 %). In *Inga vera* wood, mean vessel density was 6, similar to the numbers reported by Richter and Dallwitz (2000) and Vieira *et al*. (2019). In wood from *Machaerium paraguariense,* the mean value observed was comparable to that reported by Vieira *et al.* (2019), while for *Muellera campestris* it was similar to that reported by Marchiori *et al*. (2009), Richter and Dallwitz (2000) and Vieira (2017).

In charcoal, changes were only observed in *Muellera campestris,* with decrease in radial direction (33.3 % from near pith towards intermediate and 41.7 % from near pith towards near bark). In other species, there were no differences based on radial position. In a study with Myrtaceae species, Stange *et al.* (2018) also verified that changes in vessel density were not linear regarding position and oc-

curred in accordance with species. Carbonization had little influence on vessel density. Samples from all positions of *Machaerium paraguariense* and the near pith region of *Muellera campestris* had significant increase. The highest change was near the bark for *Machaerium paraguariense* (82.78 %), although considerable values were noted in the other locations (42.68 % in intermediate and 42.01 % near the pith region). This parameter seems to be influenced by species intrinsic characteristics, since Stange *et al.* (2018) observed increases in vessel density in all positions after carbonization of four Myrtaceae species.

Regarding mean vessel density, large divergence was observed among the species. A reduction of 7.92 % occurred in *Inga vera* after carbonization, and increase of 10.60 % in *Muellera campestris* and 32.76 % in *Machaerium paraguariense* were detected. Stange *et al.* (2018) observed values much higher than for the species studied here with samples of *Eugenia pyriformis* Cambess (92.3 %), *Campomanesia xanthocarpa* (Mart.) O. Berg (60.3 %) and *Myrcia retorta* Cambess (50.7 %). Likewise, the influence of species characteristics on changes in vessel density after carbonization has also been reported in literature, such as for Anacardiaceae (Gonçalves and Scheel-Ybert 2016) and Fabaceae species (Muñiz *et al*. 2016). The release of volatile matter and formation of some cracks and voids can also interfere in vessel density (Assis *et al*. 2016).

**Table 3.** Mean values and standard deviation of ray dimensions and frequency of studied species.

Valores medios y desviación estándar de las dimensiones y frecuencia de los radios.

| Species | Material | Near bark | Intermediate | Near pith |
|---|---|---|---|---|
| | | Ray height (µm) | | |
| *Inga vera* | Wood | 189.14 Aa (67.94) | 190.39 Aa (77.81) | 163.39 Ab (68.56) |
| | Charcoal | 165.59 Ba (60.18) | 168.22 Ba (55.47) | 155.26 Aa (78.27) |
| *Machaerium paraguariense* | Wood | 107.41 Aa (21.22) | 109.63 Aa (28.49) | 108.86 Aa (21.42) |
| | Charcoal | 112.05 Aa (18.31) | 111.65 Aa (16.99) | 110.71 Aa (28.75) |
| *Muellera campestris* | Wood | 145.84 Aa (33.82) | 137.60 Aa (37.88) | 139.51 Aa (29.42) |
| | Charcoal | 127.58 Ba (27.96) | 116.28 Bb (22.66) | 118.15 Ba (18.19) |
| | | Ray width (µm) | | |
| *Inga vera\** | Wood | 20.08 Aa (6.81) | 20.32 Aa (8.46) | 15.54 Bb (5.14) |
| | Charcoal | 22.81 Aa (9.05) | 18.95 Ab (6.32) | 23.02 Aa (16.93) |
| *Machaerium paraguariense* | Wood | 16.33 Ba (4.73) | 14.13 Bb (5.18) | 15.77 Ba (5.73) |
| | Charcoal | 25.45 Aa (9.16) | 24.73 Aa (6.04) | 25.28 Aa (7.98) |
| *Muellera campestris* | Wood | 30.17 Ba (11.31) | 26.69 Ab (8.07) | 24.21 Ab (9.69) |
| | Charcoal | 33.23 Aa (6.27) | 28.74 Ab (6.32) | 25.90 Ac (7.07) |
| | | Ray frequency (n/mm) | | |
| *Inga vera* | Wood | 8.40 Ba (2.07) | 8.46 Ba (1.93) | 8.35 Ba (2.13) |
| | Charcoal | 10.42 Aa (1.91) | 10.62 Aa (2.07) | 10.31 Aa (1.76) |
| *Machaerium paraguariense\** | Wood | 7.54 Ba (1.24) | 7.33 Ba (1.18) | 6.90 Bb (1.16) |
| | Charcoal | 9.20 Aa (1.27) | 9.36 Aa (1.45) | 9.46 Aa (1.37) |
| *Muellera campestris\** | Wood | 8.88 Ba (1.87) | 8.64 Ba (2.01) | 8.84 Ba (1.61) |
| | Charcoal | 10.68 Ab (1.88) | 10.82 Ab (1.70) | 12.54 Aa (1.93) |

*Species where interaction between material and position was not significant at 95 % probability. For each species, equal letters in means do not present statistical differences by the Scott-Knott test at 95 % probability. Capital letters in columns refer to changes after carbonization and small letters are related to radial position in disk (near bark, intermediate, near pith).

*Ray height.* In wood, no linear pattern was observed in all three species and the variation among positions was from 0.65 % to 5.99 %. The highest discrepancy (14.18 %) was from intermediate towards the near pith of *Inga vera*. The same species had mean ray height of 181 µm, lower than the 500 µm observed by Richter and Dallwitz (2000). Moreover, in *Machaerium paraguariense,* mean ray height was 109 µm, lower than the values observed by Vieira *et al*. (2019). For *Muellera campestris* wood, the mean value was 141 µm, similar to those obtained by Marchiori *et al*. (2009) in wood from Rio Grande do Sul, and smaller than those observed by Richter and Dallwitz (2000).

In charcoal, reduction in ray height occurred from the near pith towards the intermediate region in *Muellera campestris*. In other species, there was no influence of position on ray height. Carbonization did not statistically influence ray height in *Machaerium paraguariense*. For *Muellera campestris*, all positions presented reduction in ray height

from wood to charcoal (12.52 % near bark, 15.49 % intermediate and 15.31 % near pith), probably as a result of the higher quantity of parenchyma cells in comparison to the other two species. In *Inga vera,* only in the near pith region were there no substantial changes in dimension, while for other positions, reductions of 12.45 % in the near bark position and 11.64 % for intermediate region were observed. According to Muñiz *et al.* (2012), rays are laterally connected to fibers, which limit rays movement, since the contraction of the fibers in the axial direction is small during the carbonization process. On the other hand, Stange *et al.* (2018) described reduction of ray height in *Campomanesia xanthocarpa* and *Eugenia pyriformis* and increase in *Myrcia retorta* species in all radial positions.

With regard to mean ray height values by species, a contrast was observed after carbonization, with reduction of 9.69 % in *Inga vera* and 14.44 % in *Muellera campestris*, and with increase of 2.62 % in *Machaerium pa-*

*raguariense.* Different behavior has also been reported in literature, associated with ruptures of cells due to cell wall expansion, which can vary in accordance with fiber or parenchyma expansion (Gonçalves *et al*. 2012, Muñiz *et al*. 2012, Nisgoski *et al*. 2019). Ruptured rays were verified in some eucalyptus species (Gonçalves *et al*. 2014) and reductions in ray height after carbonization have been described, for example, in *Dipteryx odorata* (Nisgoski *et al*. 2012), *Diplotropis purpurea* (Rich.) Amshoff (Muñiz *et al*. 2016), *Eugenia pyriformis, Campomanesia xanthocarpa and Plinia peruviana* (Poir.) Govaerts (Stange *et al*. 2018). Increase in ray height has been found in *Cedrelinga catenaeformis* (Muñiz *et al*. 2012a), *Ocotea porosa* (Nees *et* Mart.) Barroso (Nisgoski *et al*. 2014) and *Myrcia retorta* (Stange *et al*. 2018).

*Ray width.* For ray width, a difference was observed in wood from near pith towards near bark, nevertheless there was no pattern in all species. Significant increase was observed from near pith towards the bark region in *Inga vera* (23.52 %). The same pattern was also noted from near pith to intermediate (9.29 %) and to near bark (11.54 %) region in *Muellera campestris*. In *Machaerium paraguariense*, the intermediate region had thinner rays than those of the near pith (10.40 %) and near bark regions (13.47 %). Stange *et al.* (2018) also observed divergence in this characteristic in the radial position of Myrtaceae species, with predominance of thinner rays in the near pith region.

In charcoal, there was no difference in ray width concerning sample position in *Machaerium paraguariense*. Increase was observed from near pith towards near bark in *Muellera campestris* (22.06 %). In *Inga vera* charcoal, ray width was lower in the intermediate position when compared to the other regions (16.92 % near bark and 17.68 % near pith). After carbonization, there was significant increase in ray width in all samples of *Machaerium paraguariense*, with variation of 35.83 % for near bark, 42.86 % in intermediate wood and 37.62 % for near pith. Correspondingly, the same behavior was observed for near pith (32.49 %) and near bark (11.97 %) in *Inga vera* and near bark in *Muellera campestris* (10.14 %). According to Stange *et al*. (2018), these results may be related to ruptures that occur due to the expansion of cell walls.

Regarding mean ray width values, increase was observed in all species, varying from 8.27 % in *Muellera campestris* to 38.77 % in *Machaerium paraguariense,* and intermediate in *Inga vera*, with 17.07 % increase. These differences can be the result of multiseriate and uniseriate ray percentage. Literature reports divergent behavior of species related to chemical changes in substances stored in parenchyma cells: decrease in ray width in the Fabaceae family was reported in *Enterolobium schomburgkii* (Muñiz *et al*. 2012a), *Dipteryx odorata* (Nisgoski *et al*. 2012) and *Parkia pendula* (Muñiz *et al*. 2016); while increase in ray width was observed in *Cedrelinga catenaeformis* (Muñiz *et al*. 2012a), *Hymenolobium petraeum* and *Va-*

*tairea paraensis* (Muñiz *et al*. 2016). Moreover, increase in ray width was observed in Cerrado (savanna) species (Gonçalves *et al*. 2012) and Myrtaceae species (Stange *et al*. 2018).

*Ray frequency.* Ray frequency in wood, in general, was not influenced by radial position in the trunk. Only the near pith region of *Machaerium paraguariense* had a value lower (12.5 %) than that presented by the other regions. In *Inga vera* wood, mean ray frequency was 8 / mm, in the range reported by Richter and Dallwitz (2000) and Vieira *et al.* (2019). In *Machaerium paraguariense,* mean ray frequency was 7 / mm, higher than what was observed by Vieira *et al.* (2019). For *Muellera campestris*, 9 rays / mm were observed, lower than what was reported by Marchiori *et al*. (2009), who found mean ray frequency of 12 (10-15) in wood from Rio Grande do Sul, and similar to the value obtained by Vieira (2017).

In charcoal, ray frequency showed reduction of 15.38 % from near pith towards the intermediate/near bark region in *Muellera campestris*, and 9.09 % from intermediate to near pith and near bark of *Inga vera*. In all species and positions, carbonization affected ray frequency. Regarding mean values, ray frequency increased by similar values: 24.35 % in *Inga vera*, 29.12 % in *Muellera campestris* and 28.94 % in *Machaerium paraguariense.* In other species of the Fabaceae family, Muñiz *et al*. (2016) verified significant increase in ray frequency in *Diplotropis purpurea*, *Hymenolobium petraeum* and *Vatairea guianensis.* Different behavior was observed by Ávila *et al*. (2017) regarding mass loss and cell contraction after carbonization, attributed to the influence of intra-specific and ecological characteristics.

CONCLUSIONS

The changes in cell dimensions caused by the carbonization process were confirmed. In all species, the vessel diameter decreased; vessel density decreased in *Inga vera,* though it increased in the other species; ray height decreased in *Inga vera* and *Muellera campestris*, however increased in *Machaerium paraguariense*; and ray width and frequency increased in all species.

Despite the alterations resulting from carbonization, cell arrangement and type were not influenced, therefore the inclusion of these species in a database would be effective to support efforts to control deforestation in the south of Brazil. Charcoal anatomy can be applied for species characterization, and in comparison, with reference data, can support illegal logging control.

# REFERENCES

Assis MR, L Brancheriau, A Napoli, PF Trugilho. 2016. Factors affecting the mechanics of carbonized wood: literature review. *Wood Science and Technology* 50(3): 519–536. DOI: https://doi.org/10.1007/s00226-016-0812-6

Ávila A, C Giongo, R Scheel-Ybert. 2017. Anatomia do lenho carbonizado de 10 espécies nativas da planície costeira do Rio Grande do Sul – subsídio a pesquisas arqueobotânicas e paleoecológicas. *Cadernos do LEPAARQ (UFPEL)* 14(27): 482-511. *DOI*: http://dx.doi.org/10.15210/lepaarq.v14i27.9661

Carvalho AF de, MA Brand, S Nisgoski, GIB Muñiz, G Friederichs, LC Kuster, TS Santos. 2017. Anatomia do carvão oriundo de cinco espécies comercializadas no estado de Santa Catarina. *Ciência da Madeira* 8(3): 158-167. DOI: http://dx.doi.org/10.15210/cmad.v8i3.7542

Gasper AL, L Sevegnani, AC Vibrans, M Sobral, A Uhlmann, DV Lingner, MJ Rigon Júnior, M Verdi, AS Santos, S Dreveck, A Korte. 2013. Inventário florístico florestal de Santa Catarina: espécies da Floresta Ombrófila Mista. *Rodriguésia* 64(2): 201-210. DOI: http://dx.doi.org/10.1590/S2175-78602013000200001

Gasson P, C Cartwright, CL Dias Leme. 2017. Anatomical changes to the wood of *Croton sonderianus* (Euphorbiaceae) when charred at different temperatures. *IAWA Journal* 38: 117–123. DOI: https://doi.org/10.1163/22941932-20170161

Gonçalves TAP, AW Ballarin, S Nisgoski, GIB de Muñiz. 2014. A contribution to the identification of charcoal origin in Brazil I – Anatomical characterization of *Corymbia* and *Eucalyptus*. *Maderas. Ciencia y Tecnología* 16(3): 323-336. DOI: http://dx.doi.org/10.4067/S0718-221X2014005000025

Gonçalves TAP, CR Marcati, R Scheel-Ybert. 2012. The effect of carbonization on wood structure of *Dalbergia violaceae, Stryphnodendron polyphyllum, Tapirira guianensis, Vochysia tucanorum* and *Pouteria torta* from the Brazilian Cerrado. *IAWA Journal* 33(1): 73-90.

Gonçalves TAP, R Scheel-Ybert. 2012. Contra o carvão ilegal: estudo da anatomia da madeira pode ajudar a salvar florestas nativas. *Ciência Hoje* 292: 74-76.

Gonçalves TAP, R Scheel-Ybert. 2016. Charcoal anatomy of Brazilian species. I. Anacardiaceae. *Anais da Academia Brasileira de Ciências* 88(3 Suppl.): 1711-1725. DOI: http://dx.doi.org/10.1590/0001-3765201620150433

IAWA Committee (International Association of Wood Anatomists). 1989. List of microscopic features for hardwood identification. *IAWA Bulletin* 10(3): 219–332.

Marchiori JNC, GIB Muñiz, SR Santos. 2009. *Madeiras do Rio Grande do Sul: 1- Descrição microscópica de 33 espécies nativas*. Vol. 1. Anaterra: Santa Maria. 80 p.

MMA (Ministério do Meio Ambiente, BR). 2014. Lista Nacional Oficial de Espécies da Flora Ameaçadas de Extinção. Ministério do Meio Ambiente. Portaria MMA nº 443.

Muñiz GIB, S Nisgoski, RF França, FZ Schardosin. 2012a. Anatomia comparativa da madeira e carvão de *Cedrelinga catenaeformis* Ducke e *Enterolobium schomburgkii* Benth. para fins de identificação. *Scientia Forestalis* 40(94): 291-297.

Muñiz GIB, S Nisgoski, FZ Schardosin, RF França. 2012b. Anato-

mia do carvão de espécies florestais. *Cerne* 18(3): 471-477.

Muñiz GIB, RF França, AE Fiorese, S Nisgoski. 2013. Análisis de la estructura anatómica de la madera y del carbón de dos especies de Sapotaceae. *Maderas. Ciencia y Tecnología* 15(3): 311-320. DOI: http://dx.doi.org/10.4067/S0718-221X2013005000024

Muñiz GIB, ME Carneiro, FRR Batista, FZS Schardosin, S Nisgoski. 2016. Wood and charcoal identification of five species from the miscellaneous group known in Brazil as "angelim" by near-ir and wood anatomy. *Maderas. Ciencia y Tecnología* 18(3): 505-522. DOI: http://dx.doi.org/10.4067/S0718-221X2016005000045

Nisgoski S, GIB Muñiz, RF França, FRR Batista. 2012. Anatomia do lenho carbonizado de *Copaifera* cf. *langsdorfii* Desf. e *Dipteryx odorata* (Aubl.) Wild. *Ciência da Madeira* 3(2): 66-79.

Nisgoski S, WLE Magalhães, FRR Batista, RF França, GIB Muñiz. 2014. Anatomical and energy characteristics of charcoal made from five species. *Acta Amazonica* 44(3): 367-372. DOI: http://dx.doi.org/10.1590/1809-4392201304572

Nisgoski S, GIB Muñiz, SR Morrone, FZ Schardosin, RF França. 2015. NIR and anatomy of wood and charcoal from Moraceae and Euphorbiaceae species. *Ciência da Madeira* 6(3): 183-190. DOI: http://dx.doi.org/10.15210/cmad.v6i3.7140

Nisgoski S, HC Vieira, TAP Gonçalves, CM Afonso, GIB Muñiz. 2019. Impact of carbonization parameters on anatomic aspects and near infrared spectra of three species from Mozambique. *Wood Science and Technology* 53(6): 1373-1394. DOI: https://doi.org/10.1007/s00226-019-01134-8

Ortega F, L Gerrero, T Carnona, C Córdoba. 1988. Angiospermas Arboreas de Mexico. Núm 1. Anatomica de la madera de veintiocho especies de Cosautlan de Carvajal. La Madera y su Uso 19. Instituo Nacional de Investigaciones sobre Recursos Bioticos.

Osterkamp IC, DM Lara, TAP Gonçalves, M Kauffmann, E Périco, S Stülp, NTG Machado, D Uhl, A Jasper. 2018. Changes of wood anatomical characters of selected species of *Araucaria* during artificial charring: implications for paleontology. *Acta Botanica Brasilica* 32(2): 198-211. DOI: http://dx.doi.org/10.1590/0102-33062017abb0360

Richter HG, MJ Dallwitz. 2000 onwards. Commercial timbers: descriptions, illustrations, identification, and information retrieval. Version: 7th August 2018. Accessed 10 may 2018. Available at http://delta-intkey.com

Scheel-Ybert R, TAP Gonçalves. 2017. Primeiro atlas antracológico de espécies brasileiras. Rio de Janeiro, Brazil. Museu Nacional. 230 p.

Stange R, HC Vieira, PDA Rios, S Nisgoski. 2018. Wood and charcoal anatomy of four Myrtaceae species. *Cerne* 24(3): 190-200. DOI: http://dx.doi.org/10.1590/01047760201824032552

Vieira HC. 2017. Anatomia da madeira de espécies arbóreas da Floresta Ombrófila Mista. Dissertação Mestrado em Engenharia Florestal, Lages, Santa Catarina, Brasil. Universidade do Estado de Santa Catarina, UDESC. 204p.

Vieira HC, PDA Rios, TMGQM Santos, ABD Cunha, MA Brand, D Danielli, JB Florez, R Stange, R Buss, P Higuchi. 2019. Agrupamento e caracterização anatômica da madeira de espécies nativas da Floresta Ombrófila Mista. *Rodriguésia* 70: e04382017. DOI: http://dx.doi.org/10.1590/2175-7860201970038

# Biosolids as planting fertilization of tree species of the Atlantic forest and concentration of nutrients in soil layers

## Biosólidos como fertilización en plantación de especies de árboles nativos del bosque atlántico y concentración de nutrientes en capas del suelo

**Pedro Lima Filho [a], Rodrigo Ferreira Gomes [a]\*, Juçara Garcia Ribeiro [a],**
**Alan Henrique Marques de Abreu [b], Flávio Augusto Monteiro dos Santos [c], Paulo Sérgio dos Santos Leles[a]**

\*Corresponding author: [a] Federal Rural University of Rio de Janeiro, Forest Institute, Department of Forestry,
Seropédica - RJ, Brazil, tel.: 55-21-965023554, rodrigoferreiragomes1@hotmail.com

[b] Water and Sewerage Company of the State of Rio de Janeiro, Rio de Janeiro - RJ, Brazil,
alanhenriquem@gmail.com

[c] Basin Agency of the Paraíba Valley, Resende - RJ, Brazil, monteiro.flaviosantos@gmail.com

### SUMMARY

Sewage sludge biosolids, product from urban sewage treatment, are rich in organic matter and nutrients with potential use in forestry. This work aimed at evaluating the growth of *Ceiba speciosa*, *Peltophorum dubium* and *Sapindus saponaria* and the concentration of nutrients and heavy metals in different soil layers under the application of biosolids as planting fertilizer. Two sequential experiments were set up. First in a pot, to determine the best dose for the growth of *C. speciosa*, using 0.8, 1.6, 3.2 and 6.4 liters of biosolids per pit and the absolute witness. Six months after the planting of *C. speciosa* seedlings, it was concluded that the best dose provided was around 3.9 liters. The field experiment was carried out using the three tree species with witness treatment or application of 3.0 liters of biosolids per pit, at the time of planting. Growth evaluations occurred at 4 and 12 months after planting and it was observed that *C. speciosa* and *P. dubium* responded to the application of biosolids. At 12 months, nitrogen, phosphorus, potassium and heavy metals contents were evaluated in different layers of the soil. It was found that the pits that received biosolids presented significantly higher values for phosphorus (except 75-100 cm soil layer) and heavy metals. There was no leaching of nitrogen, phosphorus and potassium in the soil layers. Heavy metals contents were below the maximum values for levels in the soil profile stipulated by legislation.

*Key words:* sewage sludge, *Ceiba speciosa*, *Peltophorum dubium* and *Sapindus saponaria*.

### RESUMEN

El biosólido de lodos de depuradora, producto del tratamiento de aguas residuales urbanas, es un material rico en materia orgánica y nutrientes con potencial uso en silvicultura. El objetivo fue evaluar el crecimiento de *Ceiba speciosa*, *Peltophorum dubium* y *Sapindus saponaria* y la concentración de nutrientes y metales pesados en diferentes capas del suelo con aplicación de biosólido como fertilizante al plantar. Se establecieron dos experimentos secuenciales. Primero, en maceta para determinar la mejor dosis para el crecimiento de *C. speciosa* (0,8, 1,6, 3,2 y 6,4 litros de biosólidos por taza) y el testigo absoluto. Seis meses después de plantar *C. speciosa* se concluyó que la mejor dosis fue de alrededor de 3,9 litros. Segundo, el experimento de campo utilizó las tres especies de árboles con tratamiento testigo o aplicación de 3.0 litros de biosólidos por hoyo, al momento de plantar. Después de 4 y 12 meses de plantar, *C. speciosa* y *P. dubium* respondieron a la aplicación de biosólidos. A los 12 meses fueron evaluados los contenidos de nitrógeno, fósforo, potasio y metales pesados en diferentes capas del suelo. Se encontró que las tazas que recibieron biosólidos tenían valores de fósforo significativamente mayores (excepto la capa de suelo de 75-100 cm) y metales pesados. No hubo lixiviación de nitrógeno, fósforo ni potasio en las capas del suelo. Los contenidos de metales pesados en el perfil del suelo estuvieron por debajo de los valores máximos estipulados por la legislación.

*Palabras clave:* lodos de depuradora, *Ceiba speciosa*, *Peltophorum dubium*, *Sapindus saponaria*.

## INTRODUCTION

The Atlantic Forest biome corresponds to 15 % of the Brazilian territory area and concentrates around 72 % of the population (IBGE 2014), with the vast majority resi- ding in urban areas. According to data from INPE (2018), 12.4 % of the forest cover remains, usually in the form of forest fragments, thus requiring reforestation actions with species that occur in this biome. Furthermore, in many rural properties in Brazil, there is a need for reforestation in

areas of permanent preservation and constitution of legal reserve areas to adapt to the Federal Law 12.651/12.

The concentration of population in certain regions generates large amounts of waste, such as the production of sanitary sewage, which must be sent to sewage treatment stations. During this treatment, the solid part is decanted and the sewage sludge is obtained, which after due treatment, stabilization and meeting the microbiological and chemical criteria established by CONAMA Resolution 498/2020 (Brazil 2020) is called biosolids. The destination of a large part of the biosolids produced in the sewage treatment stations is still landfills, burdening sanitation companies and contributing to reduce the useful life of landfills.

In the metropolitan region of Rio de Janeiro, which is nestled in Mata Atlântica biome, one of the most populous in Brazil, according to information from engineers, the State Water and Sewer Company pays around U$ 50.00 per ton (price taken in December 2019) for deposition of biosolids in landfills. Considering the chemical and physical characteristics and that the biosolids from sewage treatment stations in the metropolitan region of Rio de Janeiro meet the parameters of CONAMA Resolution 498/2020 and are rich in nutrients and organic matter (Abreu *et al.* 2017, Cabreira *et al.* 2017, Alonso *et al.* 2018, Sousa *et al.* 2019), its use as fertilizer for planting tree species can give a more sustainable destination to this material. In addition, Art. 20, $ 2º and Art. 21, $ 3º of CONAMA resolution 498/2020 mention that "there is no restriction for the application of biosolids in planted forests, soil recovery and degraded areas".

Normally, rural producers in Brazil use the best areas of the property for food production or animal husbandry, therefore forest restoration occurs in areas that are poor in nutrients and organic matter, and it is necessary, according to Gonçalves (1995), in many situations to fertilize planting. For forest restoration, there are some planting fertilization works with sewage sludge biosolids from tree species occurring in the Atlantic forest (Paiva *et al.* 2009, Silva and Pinto 2010, Lopes and Leles 2020, Silva *et al*. 2020) and the responses have been quite different, depending on the edaphic and climatic conditions where the stands are located and the differences in behavior of native tree species. Another characteristic of the biosolid is when applied to the soil, its substances have a high power of adsorption to the soil and thus, according to Campos e*t al.* (2019), there is no leaching to deeper layers of soil, there is no risk of contamination of the water table. Further field studies on this topic are indicated, due to the large differences in soil and climatic conditions existing in Brazil.

In the formation of stands for the restoration of the Atlantic Forest, diversity of tree species is usually used trying to imitate what occurs in the forest. Among the species commonly used are *Ceiba speciosa* (A. St.-Hil.) Ravenna, *Peltophorum dubium* (Spreng.) Taub. and *Sapindus saponaria* L. The first belongs to the Malvaceae family, is clas-

sified as a pioneer stage and has a relatively rapid growth, in addition to being a species that has a wide geographical distribution in the Brazilian territory (Lorenzi 1992). *Peltophorum dubium* belongs to the Fabaceae family, a pioneering species, which is relatively fast-growing and deciduous. Its wood can be used for various purposes, its flowers, in addition to meliferous, have a great ornamental effect (Lorenzi 1992). *Sapindus saponaria* belongs to the Sapindaceae family, according to Lorenzi (1992), it is a species of the secondary successional stage, a characteristic broadleaved semideciduous forest and comparatively slower in growth than the other two species.

The hypothesis of this work is that the three tree species occurring in the Atlantic Forest will be responsive to biosolids as planting fertilizers and that it will not contaminate the soil, based on the "maximum permitted values of chemical substances" of Art. 10 of CONAMA Resolution 498/2020.

The objective is to evaluate the growth of *Ceiba speciosa*, *Peltophorum dubium* and *Sapindus saponaria* and the concentration of nutrients and heavy metals in the different layers of the soil under the application of the biosolid as planting fertilizer.

METHODS

The work was divided into two sequential stages: the first one was an experiment in pots to verify the response of *Ceiba speciosa* to biosolids doses. Based on this information and on the operational aspect of transport and application of biosolids, a field experiment was carried out with the absence and presence of biosolids as fertilization in a pit, in the operation of planting the seedlings of three tree species.

*Stage 1 - Pots conditions.* This stage was carried out in the municipality of Seropédica, State of Rio de Janeiro, from November to May, in pots with volumetric dimensions of 18 liters, with a smaller diameter of 25 cm, larger diameter of 30 cm and a height of 28 cm, simulating a planting pit. The climate of the region, according to Koppen's classification, is of Cwa type. The soil used came from the 0-40 cm layer of a slope, classified expeditiously (in the field) and based on results of chemical analyses by a professor in the field of genesis, soil physics, as dystrophic endoalic Yellow Latosol with clay texture, whose chemical analysis is shown in table 1.

For the definition of biosolids doses, the application of $P_2O_5$ for planting fertilization in native species recommended by Gonçalves (1995) was considered, both in the chemical analysis of pot soil (table 1) and in the chemical analysis of biosolid (table 2). Based on this information, a standard dose of 3.2 liters of biosolids per pot was adopted. The other doses were 1/4, half and twice the standard dose, that is, 0.8, 1.6, 3.2 and 6.4 liters of biosolids per pot, in addition to absolute witness. The biosolid had an avera-

**Table 1.** Chemical analyses of soils used for the growth of tree species in planting fertilization experiments.

Análisis químico de suelos utilizados para el crecimiento de especies arbóreas en experimentos de fertilización de plantaciones.

| Stage | pH | P | K⁺ | Ca²⁺ | Mg²⁺ | Al³⁺ | H+Al | SB | CTC (t) |
|---|---|---|---|---|---|---|---|---|---|
| | $H_2O$ | ------- mg·dm⁻³ -------- | | ---------------------------------- cmol$_c$·dm⁻³ ---------------------------------- | | | | | |
| Pot | 5.1 | 1.0 | 27 | 0.4 | 0.2 | 0.9 | 4.5 | 1.7 | 1.9 |
| Field | 5.7 | 3.3 | 115 | 1.3 | 0.5 | 0.0 | 3.3 | 2.1 | 2.4 |

pH in water; phosphorus and potassium: Mehlich extractor 1; calcium, magnesium and aluminum: 1.0 nitrogen KCl extractor; hydrogen+aluminum: calcium acetate extractor 0.5 N - pH 7.0; SB = sum of exchangeable bases; CTC (t) = effective cation exchange capacity.

**Table 2.** Total elements, organic carbon (CO) and biosolid pH used in the experiments, from the sewage treatment of Alegria, located in Rio de Janeiro City, Brazil.

Elementos totales, carbono orgánico (CO) y pH de biosólidos utilizados en los experimentos, del tratamiento de aguas residuales de Alegría, ubicada en la ciudad de Río de Janeiro.

| Nutrients | Amount | Heavy metals | Content (mg kg⁻¹) | Maximum limit (mg kg⁻¹ total solids)* |
|---|---|---|---|---|
| Nitrogen (g kg⁻¹) | 17.2 | Arsenic | 1.3 | 41 |
| Phosphorus (g kg⁻¹) | 7.5 | Barium | 462.2 | 1.300 |
| Potassium (g kg⁻¹) | 2.1 | Cadmium | 2.3 | 39 |
| Calcium (g kg⁻¹) | 17.2 | Lead | 191.9 | 300 |
| Magnesium (g kg⁻¹) | 3.0 | Copper | 354.0 | 1.500 |
| Sulfur (g kg⁻¹) | 8.5 | Chrome | 172.1 | 1.000 |
| Organic carbon (%) | 17.4 | Mercury | 0.7 | 17 |
| pH (H₂O) | 5.0 | Molybdenum | 1.1 | 50 |
| | | Nickel | 53.2 | 420 |
| | | Selenium | 1.2 | 36 |
| | | Zinc | 1.103 | 2.800 |

Nitrogen - Kjeldahl method; organic carbon - Walkley Method - Black and others determined in the acid extract (nitric acid with perchloric acid). * Maximum permitted levels of chemical substances in Class 1 biosolids to be used for soil use, according to Art. 20, $2º of resolution CONAMA 498/2020.

ge density of 0.65 g cm⁻³, corresponding approximately to 0.5, 1.0, 2.0 and 4.0 kg pot⁻¹, respectively.

The biosolids used in both experiments come from the Alegria Sewage Treatment Station, located in the Caju neighborhood, city of Rio de Janeiro - RJ. The material was provided by the Rio de Janeiro State Water and Sewage Company (CEDAE). The treated sewage is derived from urban households and commercial areas. In this sewage treatment station, the primary treatment is carried out, which consists of the chemically assisted method (use of aluminum sulphate or ferric chloride as a sludge coagulant) and the secondary treatment is using the activated sludge system. The sludge from the secondary treatment is thickened and mixed with the sludge from the primary treatment to pass through a dewatering centrifuge. After

this process, the material is taken to the thermal dryer, where it remains until it reaches low moisture content. Finally, it is deposited in a dry and ventilated place until complete composting. Chemical analyses of the biosolids are shown in table 2.

The biosolids doses were mixed with the soil and afterwards, the pots were filled with the soil-biosolids mixture. For the absolute witness, the pots were filled only with soil. After filling, *Ceiba speciosa* seedlings were planted in tubes of 280 cm³, with a standard height of 50 cm. The substrate used for the production of seedlings was composed by 90 % commercial substrate and 10 % clayey soil.

The experiment was installed in a completely randomized design, composed by five replications of a single plant. Due to temperature and precipitation condi-

tions at the time of the experiment, when it did not rain, once a day the plants were irrigated with 1.5 liters of water. When necessary, spontaneous plants were removed to avoid competition interference.

Six months after planting the seedlings, height and crown diameter of plants were measured. Data were submitted to a regression analysis, in which the growth curves were constructed according to the control and the biosolids doses.

*Stage 2 – Field.* The study was conducted in a settlement formation area for forest restoration in the Municipality of Bom Jardim, State of Rio de Janeiro. According to data from 2012 to 2014 from the nearest meteorological station to the experiment spot, the average annual precipitation in this period was 1.378 mm, with rainfall concentration from November to March and a dry period from June to September. The minimum annual average temperature was 16.0 ºC in July, and the maximum average was 28.0 ºC in February, with average annual temperature of 22.0 ºC. The average altitude of the region is 530 meters.

The experiment was implemented in January (mid-rainy season) 2013, in poorly managed pasture, dominated by weed species belonging to the genus *Urochloa* sp., located in the middle third of a slope. The soil in the experimental area was classified as Yellow Red Latosol with clay texture (46 % clay, 16 % silt and 38 % sand), whose chemical analyses of the 0-30 cm layer are shown in table 1. The experiment was intended to be carried out in the same area that was removed from the pot experiment (stage 1), though, at the time, the area had not been surrounded and the reforestation was not taking place.

Treatments consisted in the application of 3.0 L of biosolids per pit, whose chemical characteristics are shown in the table 2, corresponding to approximately 2 kg mixed with the soil of the pit and absolute witness. This dose of biosolids was based on the results of the pot stage, the chemical analysis of the soil (table 1) and the execution of the operation to transport the biosolids to the middle third of the slope. For each species, each treatment was formed by twelve repetitions, of a plant, adopting a completely randomized design. The planting spacing was 2 m x 2 m.

The species used were *Ceiba speciosa*, *Peltophorum dubium*. and *Sapindus saponaria*. The seedlings were produced in plastic bags of 9.7 x 20 cm (diameter x height), on a substrate composed by tanned bovine manure, clay subsoil and washed sand, in a volumetric ratio of 5: 4: 1. At the time of planting, the seedlings were approximately 80, 35 and 60 cm high for *Ceiba speciosa*, *Peltophorum dubium* and *Sapindus saponaria*, respectively.

To prepare the soil for planting, initially the pits were marked in a level direction, obeying the pre-defined spacing. Next morning and with wind speed below 10 km / h, a glyphosate-based herbicide was applied over a total area (dose of 4.0 L ha⁻¹), using a costal sprayer with capacity of 16 liters. After 20 days, the surrounding of the pits was

crowned, approximately 60 cm in diameter. The pits were opened with the aid of a hoe, with the dimensions of 25 x 25 x 30 cm (length x width x depth). Subsequently, in half of the pits, 3.0 liters of biosolid were fertilized and the seedlings were planted.

The cultural treatments involved control of leaf-cutting ants (before, during and until the end of the experiment) and weed control, with crown and mowing in May and October 2013, and the application of glyphosate (dose of 2.5 L ha⁻¹) in November 2013, to minimize the effects of competition with other plants.

For growth evaluation, the variables shoot height and diameter at 5 cm from the soil surface (D5) were measured at 4 and 12 months after planting. In this last evaluation, the transverse (L1) and longitudinal (L2) widths of the tree planting line were also measured for the calculation of the crown area (Ci), considering them as an ellipse [1]:

$$C_{i} = \pi \, [(L_1 + L_2)/4)^2] \qquad [1]$$

Where: $C_i$ = crown area (m²); $L_1$ = transverse crown width (m); $L_2$ = longitudinal crown width (m).

Soon after measurements and analyses of height and D5 data, performed 12 months after planting, the four plants closest to the average height of *Ceiba speciosa* and *Sapindus saponaria* were chosen from the two treatments used, to analyze the concentration of nitrogen, phosphorus and potassium and also heavy metals (chromium, nickel, cadmium and lead) in the soil profile. The choice of these two species was aimed at covering the species with relatively fast growth (*Ceiba speciosa*) and the slowest (*Sapindus saponaria*), observed with height and diameter measurements. This analysis consisted of collecting soil samples, up to 10 cm away from the base of the plant stem, in layers of depth 0-25, 25-50, 50-75 and 75-100 cm, with a probe. The soil samples from the different layers were dried in air and subjected to chemical analyses at the Laboratory of Chemical Analyses of Soil, Vegetable Tissue and Fertilizers of the Federal University of Viçosa, to obtain the concentration of nitrogen, phosphorus, potassium and heavy metals. These data, together with the growth data, in both seasons were subjected to the homoscedasticity tests of variance and normality of the residues, verifying that there is no need for data transformation. Accordingly, they were submitted to an analysis of variance. Subsequently, for the levels of nutrients and heavy metals between soil layers, with significant differences being verified by the F test, these were subjected to the Tukey test ($P \geq 0.95$).

RESULTS

In the pot experiment evaluation, *Ceiba speciosa* plants showed responses with quadratic equations of height and crown diameter (figure 1) in relation to the treatments, showing that the maximum growth point, for these condi-

tions, is between 3.9 and 4.2 L per pot of biosolids. With this information and in accordance with the logistics of transportation and distribution of biosolids in the pits, it was decided to use the fertilization of 3.0 liters of biosolids per pit, for the field experiment. Another important observation of figure 1 is that the coefficient of determination ($R^2$) was relatively low, mainly in height, indicating a high dispersion of the data, even in pots conditions and the care taken.

On field conditions, it can be seen from table 3 that the plants of *Peltophorum dubium* fertilized with 3.0 liters of biosolids per pit showed a significantly higher growth than that shown by those unfertilized. For *Ceiba speciosa*

the difference was not significant only for height, at four months after planting and for *Sapindus saponaria*, three of the five evaluations did not show significant differences.

In evaluating the concentrations of nitrogen, phosphorus and potassium and heavy metals in the pit region at 12 months after planting, it was found that, for all four layers, there were no significant differences in the concentration of nutrients and heavy metals among samples removed in the pits of *Ceiba speciosa* and *Sapindus saponaria* ($P \geq 0.95$). Thus, the data presented in tables 4 and 5 refer to the average levels, based on data from the two species.

Regardless of the layer of the soil profile evaluated, it appears that there were no significant differences in the
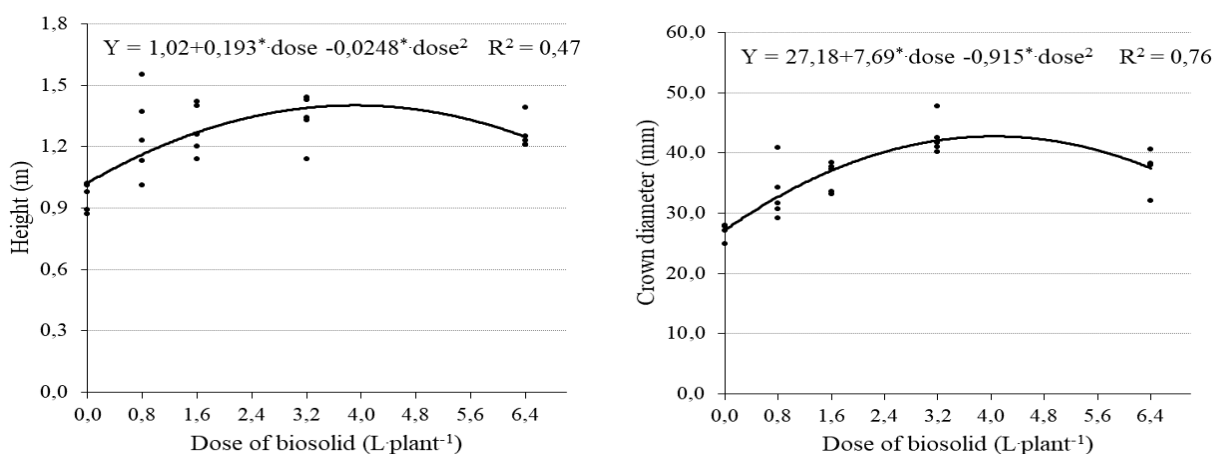


**Figure 1.** Height of the aerial part and crown diameter of the *Ceiba speciosa* on the basis of biosolids per plant grown in pots, six months after planting, in pots. * significant at 1 %, using the t test.

Altura de la parte aérea y diámetro de copa de *Ceiba speciosa* según biosólidos por planta cultivada en maceta, seis meses después de la plantación, en maceta. * significativo al 1 %, utilizando la prueba t.

**Table 3.** Average values (and standard deviation) of three tree species at 4 and 12 months after planting, submitted to fertilization with 3 liters of biosolids or without fertilization, for the formation of stands for forest restoration, in the state of Rio de Janeiro, Brazil.

Valores promedio (y desviación estándar) de tres especies arbóreas a los 4 y 12 meses después de la plantación, sometidas a fertilización con 3 litros de biosólidos o sin fertilización, para la formación de rodales para restauración forestal, en el estado de Río de Janeiro, Brasil.

| Specie | Biosolids | --- 4 months after planting --- | | ------------------12 months after planting ------------- | | |
|---|---|---|---|---|---|---|
| | | Height (m) | D5[1] (cm) | Height (m) | D5[1] (cm) | Crown diameter (m²) |
| *Peltophorumdubium* | 3.0 L pit[-1] | 0.75* (0.15) | 1.83* (0.29) | 1.94* (0.42) | 4.54* (1.10) | 2.31* (1.14) |
| | Absent | 0.41 (0.06) | 0.99 (0.12) | 1.48 (0.37) | 3.42 (0.70) | 0.94 (0.53) |
| *Ceiba speciosa* | 3.0 L pit[-1] | 1.09[n.s] (0.13) | 2.75* (0.58) | 2.43* (0.52) | 8.23* (2.01) | 3.88* (2.66) |
| | Absent | 1.01 (0.08) | 1.56 (0.21) | 1.78 (0.33) | 5.84 (1.50) | 0.97 (0.84) |
| *Sapindus saponaria* | 3.0 L pit[-1] | 0.74[n.s] (0.10) | 1.09* (0.21) | 1.16* (0.24) | 2.59[n.s] (0.70) | 0.18[n.s] (0.10) |
| | Absent | 0.64 (0.10) | 0.76 (0.20) | 0.76 (0.16) | 1.94 (0.61) | 0.13 (0.07) |

[1]Diameter 5 cm from the soil surface. For the same species, age e growth profile, * indicates significantly higher mean by the F test ($P \geq 0.95$) and [n.s] averages do not present significant differences by the F test ($P \geq 0.95$).

levels of nitrogen and potassium of the soil of the pits that received biosolids and levels presented by those that did not receive (table 4). For phosphorus, significantly higher values were found, on average, in the pits that received 3.0 liters of biosolids, except for the 75 to 100 cm layer.

The average values of the concentration of nitrogen, phosphorus and potassium in the four evaluated layers of the soil presented in table 4 indicate that there was no leaching of nutrients in the layer of this soil classified as clayey, when 3 liters per biosolids pit were applied.

It can be seen from table 5 that the application of 3.0 liters of biosolids per pit provided significantly higher nic-

kel, cadmium and lead contents in the pits that received biosolids, except for the last element in the 75 to 100 cm layer. No chromium content was found or it remained below Mehlich -1 method determination limit.

Even with the application of biosolids, the levels of the three heavy metals were much lower, in all layers, than the limits stipulated by Resolution nº. 498/2020 of the National Environment Council - CONAMA for the accumulation of heavy metals in the soil by the application of sewage sludge biosolids (Brasil 2020), corresponding respectively to average values of 9.4, 1.0 and 1.1 % of this maximum value.

**Table 4.** Soil nutrient content after 12 months of 3 liters of biosolids application in the pit during planting of the seedlings and unfertilized treatment in four layers of soil in the area of settlement formation for forest restoration, state of Rio de Janeiro, Brazil.

Contenido de nutrientes del suelo después de 12 meses de aplicación de 3 litros de biosólidos en la taza durante la siembra de las plántulas y el tratamiento sin fertilizar en cuatro capas de suelo en el área de formación de asentamientos para restauración forestal, estado de Río de Janeiro, Brasil.

| Layer of soil | ----- Nitrogen (g kg$^{-1}$) ------ | | --- Phosphorus (mg dm$^{-3}$) ---- | | --- Potassium (mg·dm$^{-3}$) --- | |
|---|---|---|---|---|---|---|
| (m) | 3.0 L pit$^{-1}$ | Absent | 3.0 L pit$^{-1}$ | Absent | 3.0 L pit$^{-1}$ | Absent |
| 0.00 - 0.25 | 1.8$^{n.s}$ a | 1.7 | 29.8* a | 2.8 | 64.0 a | 91.5$^{n.s}$ |
| 0.25 - 0.50 | 1.8$^{n.s}$ a | 1.7 | 7.3* b | 2.1 | 54.1 a | 78.0$^{n.s}$ |
| 0.50 - 0.75 | 1.6$^{n.s}$ a | 1.6 | 4.2* b | 2.1 | 58.5 a | 63.5$^{n.s}$ |
| 0.75 - 1.00 | 1.5$^{n.s}$ a | 2.1 | 3.4$^{n.s}$ b | 4.4 | 57.6 a | 54.9$^{n.s}$ |

Nitrogen = total nitrogen: sulfuric digestion-Kjeldhal distillation; phosphorus and potassium: Mehlich -1 extractor. For each nutrient and layer of soil, * indicates significantly higher mean by the F test ($P \geq 0.95$) between the two treatments and $^{n.s}$ averages do not show significant differences by the F test ($P \geq 0.95$) between the two treatments. For the treatment with biosolids, average of the column followed by the same letter does not statistically differ by Tukey's test ($P \geq 0.95$).

**Table 5.** Heavy metals in the soil (mg dm$^{-3}$), after 12 months of application 3 liters of biosolids in the pit before planting and unfertilized treatment, in an area of settlement formation for forest restoration, state of Rio de Janeiro, Brazil.

Metales pesados en el suelo (mg dm$^{-3}$), después de 12 meses de aplicación 3 litros de biosólidos en la taza antes de la siembra y tratamiento no fertilizado, en un área de formación de asentamientos para restauración forestal, estado de Río de Janeiro, Brasil.

| Layer of soil | Nickel[1] | | Cadmium[1] | | Lead[1] | |
|---|---|---|---|---|---|---|
| (m) | Absent | 3.0 L pit$^{-1}$ | Absent | 3.0 L pit$^{-1}$ | Absent | 3.0 L pit$^{-1}$ |
| 0.00 - 0.25 | 0.09 | 0.30* a | 0.05 | 0.15* a | 0.04 | 0.27* a |
| 0.25 - 0.50 | 0.09 | 0.26* a | 0.08 | 0.14* a | 0.02 | 0.10* b |
| 0.50 - 0.75 | 0.10 | 0.21* a | 0.07 | 0.14* a | 0.01 | 0.06* b |
| 0.75 - 1.00 | 0.08 | 0.13* b | 0.08 | 0.10$^{n.s}$ a | 0.01 | 0.01$^{n.s}$ bc |
| [2]CONAMA 498/2020 | 29.6 | | 1.6 | | 16.4 | |

[1]Extractor Mehlich -1. For each element, * indicates significantly higher mean by the F test ($P \geq 0.95$) between the two treatments and $^{n.s}$ averages do not show significant differences by the F test ($P \geq 0.95$) between the two treatments. For the treatment with biosolids average of the column followed by the same letter does not statistically differ by Tukey's test ($P \geq 0.95$). [2]Maximum limit stipulated pela Resolução CONAMA nº 498/2020 for nickel, cadmium and lead contents in the soil by the application of sewage sludge biosolids.

DISCUSSION

Positive responses for the application of biosolids in pots and field conditions probably occurred because the material had a relatively high content of nutrients and organic matter (table 2), as also reported by Abreu *et al.* (2017, 2019) and Sousa *et al.* (2019). Another factor is the improvement of physical conditions in the pit, as reported by Guerrini *et al.* (2017) and Balduino *et al.* (2020), the organic material of the biosolid acts as a soil conditioner, having a direct influence on the results presented by the plants, as it improves the chemical quality (Caldeira Junior *et al.* 2009) and the physical attributes, acting on the structure and state of aggregation particles, decreasing density and increasing aeration and moisture retention in the soil (Nobrega *et al.* 2007). In addition, tree species in the Atlantic forest live in environments relatively rich in organic matter and normally respond to fertilization with organic materials.

In pots conditions, the decline in growth curves in relation to the higher doses can be attributed to the fact that the biosolids excessively increase the amount of salts in the substrate, which can cause tissue necrosis, especially in roots, interfering in the growth of the plant (Arthur *et al.* 2007). Similar results were found by Maia (1999), in a study with *Pinus taeda* L., in which the biomass of the aerial part and roots showed quadratic effects regarding the increased use of sewage sludge biosolids. The feature of non-proportional gains is probably due to the biosolids, increasing the amount of nutrients in the soil in such a way that *Ceiba speciosa*, being a specie with no degree of improvement, is unable to assimilate nutrients with the same speed, which may cause loss of nutrients by leaching processes (Fernandes and Souza 2006, Novais *et al.* 2007). Silva *et al.* (2008) mention that when the doses of biosolids rise too high, the loss of productivity can be attributed, among other factors, to the possible limitation caused by the scarcest nutrients in the material, such as potassium.

Considering that the largest sewage treatment plants are in large urban centers, where a larger volume where most biosolids are produced (Abreu *et al.* 2017), it is important to analyze transport costs when choosing doses, as *Ceiba speciosa* plants did not respond linearly with increasing doses. Another factor is labor for the distribution of biosolids in the planting pits, which depends on the distance from where the biosolids lot is located in the field and the pits, in addition to the topography of the land.

In the field, responses significantly higher than those presented to the dose of 3.0 liters of biosolids per pit, in relation to the witnesses of the plants of *Peltophorum dubium* and *Ceiba speciosa*, probably occurred because these species are of pioneer successional stage (Lorenzi 1992) and because they present higher growth speed than that presented by *Sapindus saponaria* and, thus, responding more to fertilization. Responses differentiated by tree species in relation to the application of sewage sludge bioso-

lids in the planting pit are also reported by other studies. Paiva *et al.* (2009) observed that *Schinus terebinthifolia* Raddi, *Cytarexyllum myrianthum* Cham. and *Bauhinia forficata* Link, which are considered pioneer species (Carvalho 2003) obtained a response to the application of 80 g biosolids in 4-liter pots better than that obtained by *Myroxylon peruiferum* L. f ., a species considered to be the final stage of succession (Lorenzi 1992).

Silva *et al.* (2020) concluded that *Schinus terebinthifolia* Raddi, *Peltophorum dubium*, *Lafoensia glyptocarpa* Koehne, *Inga laurina* (Sw.) Willd. and *Senna multijuga* (Rich.) benefited from the dose of 4 L biosolid per hole in a sandy texture planosol, while *Genipa americana* (Vell.) Brenan and *Enterolobium contortisiliquum* (Vell.) Morong did not respond to the application of biosolids. Lopes and Leles (2020) observed that in soil of the same classification as the field stage of this work, and relatively poorer in nutrients, the species *Guarea guidonia* L. Sleumer and *Cordia superba* Cham. responded to the application of 4.5 biosolids per pit, nonetheless, *Inga laurina* plants showed no significant differences in the pits that did not receive biosolids 18 months after the application and planting of the seedlings. The result of this work and those of the three other cited works indicate that the responses to the application of sewage sludge biosolids as planting fertilizers vary depending on the tree species and soil conditions. In addition, they show that the application of biosolids as planting fertilizer does not harm the growth of tree species.

Significantly higher means of nitrogen values were expected in the pits that received biosolids 12 months ago, as table 2 shows that this material is relatively rich in nitrogen. One possible explanation for the absence of differences is that, according to Souza and Fernandes (2006), the nitrogen is part of the leaf structures, having a direct influence on the crown area of the plants, being the element that most limits the growth of the plants. Thus, as the application of biosolids promoted more important growth of tree species and, as a consequence, there may have been higher absorption of nitrogen from the soil, no significant differences in the nitrogen content between the soils influenced by the pits of these two treatments may have occurred. Values of phosphorus content in the significantly higher pit, 12 months after application of biosolids in the pit, probably occurred due to the low content of this element in the soil (table 1). Based on data from table 2, the application of about 15 g of phosphorus, which corresponds to 34.4 g of $P_2O_5$ per pit, within the standards of 80 kg of $P_2O_5$ ha$^{-1}$, recommended by Gonçalves (1995), considering the 2 x 2 m planting spacing used, corresponds to 32 g of $P_2O_5$ per pit.

Another factor is that the phosphorus present in organic materials, according to Novais *et al.* (2007) is usually in a complex form and is poorly soluble. In this way, they are gradually made available to the plants (Abreu *et al.* 2019), thus presenting significantly higher values in the pits where 3.0 liters of biosolids were applied 12 months

ago. Absence of potassium ($K^+$) response in the soil to the application of biosolids is due to the low content of this element in the biosolids (table 2). As the material dewatering phase occurs during its treatment, a step that takes some nutrients with water (Abreu *et al.* 2019), especially potassium, since it is an exchangeable base with oxidation number +1, which makes a simple connection with oxyhydroxides and clays, while the exchangeable bases +2 ($Ca^{2+}$ and $Mg^{2+}$) create double bond.

Absence of significant differences in nitrogen, phosphorus (except for a 0-25 cm layer) and potassium indicates that there was no leaching of these nutrients until the depth of 1.0 meter of the soil surface in the pit 12 months after the application of 3.0 liters of biosolid. A significantly higher phosphorus value in the 0-25 cm layer is probably due to the low mobility of this element in the soil (Novais *et al.* 2007), mainly clayey, as in this work, and thus the phosphorus present in the biosolid was accumulated in the region of the pit, which provided values significantly higher than those of the contents in the most superficial layer.

Significantly higher differences in nickel, cadmium and lead in the soils that received 3.0 liters of biosolids in relation to the witness, occurred due to the presence of these elements in the biosolids (table 2), which are below the maximum limits stipulated by Art. 10 of CONAMA Resolution 498/2020. Data also indicate that there was no leaching of these elements in the 75 to 100 cm layer and that the values found in all layers are very low, corresponding to less than 10 % of the maximum limits of CONAMA Resolution 498/2020 (Brasil 2020). Campos *et al.* (2019) studied the leaching from the application of 8 liters of sewage sludge biosolids in the layer of 0-25 cm of soil in columns of 20 cm in diameter, filled with clayey Latosols or sandy Planossols. They found in the samples of all collections, that in the leaching from both soils, the levels of nitrates, phosphates and heavy metals were below the limit stipulated by the CONAMA Resolution 498/2020 (Brasil 2020), showing that there is practically no possibility of soil layer contamination by the application of this dose of biosolids, even in sandy soils. Listing the dose used by Campos *et al.* (2019), with the 2 x 2 spacing used in this work, it corresponds to the application of 20 $m^3$ $ha^{-1}$ and considering the density of 0.65 g $cm^{-3}$ of the biosolids of this study, at 13 Mg $ha^{-1}$.

Among the three heavy metals presented, the significant difference between lead content in the 0-25 cm layer and lower 75-100 cm layer should be highlighted. According to Maciel *et al.* (2012), heavy metals added by biosolids applications tend to remain in the area where the residue is incorporated into the soil (where the planting pit is covered) as a result of the interaction with oxides, clay minerals and organic matter, which will favor its use in forest restoration, since the number of interventions are smaller and less frequent than in agricultural crops. Normally, according to Silva *et al.* (2006) the inorganic constituents of the biosolids adsorb heavy metals, with no increase in

availability expected over time and the tendency is to decrease the levels of metals in the soil, as the process of metal occlusion on the surfaces of the precipitates, which favors the application of biosolids in forest restoration.

## CONCLUSIONS

For the conditions under which the field experiment was carried out, *Ceiba speciosa* and *Peltophorum dubium* plants showed higher growth with the application of 3 liters of biosolids per pit. *Sapindus saponaria* practically did not respond to the application of biosolids.

The pits fertilized with biosolids showed only significantly higher levels of phosphorus than those presented by unfertilized ones 12 months after application and planting of seedlings. Data indicate that there was no leaching of nitrogen, phosphorus and potassium in the soil layers.

Twelve months after the application of biosolids and planting of tree species seedlings, nickel, cadmium and lead contents in the soil were significantly higher in the fertilized pits, nonetheless, corresponding respectively to mean values of 9.4, 1.0 and 1.1 % of the maximum soil limit stipulated by CONAMA Resolution 498/2020. Chromium contents were below those determined by the analytical method.

## ACKNOWLEDGEMENTS

## REFERENCES

Abreu AHM, JM Alonso, LA Melo, PSS Leles, GR Santos. 2019. Caracterização de biossólido e potencial de uso na produção de mudas de Schinus terebinthifolia Raddi. *Engenharia Sanitária e Ambiental* 24(3): 591-599.

Abreu AHM, PSS Leles, JM Alonso, ELS Abel, RR Oliveira. 2017. Characterization of sewage sludge generated in Rio de Janeiro, Brazil, and perspectives for agricultural recycling, *Semina: Ciências Agrárias* 38(4): 2433-2448. DOI: http://dx.doi.org/10.5433/1679-0359.2017v38n4Supl1p2433

Alonso JM, AHM Abreu, LA Melo, PSS Leles, GV Cabreira. 2018. Biosolids as substrate for the production of Ceiba speciosa seedlings. *Cerne* 24(4): 420-429. DOI: https://doi.org/10.1590/01047760201824042568

Arthur AG, MCP Cruz, ME Ferreira, VCM Barretto, R Yagi. 2007. Esterco bovino e calagem para formação de mudas de guanandi. *Pesquisa Agropecuária Brasileira* 42(6): 843-850.

Balduino APC, RS Corrêa, CBR Munhoz, JEQ Faria Júnior, JBA Bringel Junior, LS Barros. 2020. Manipulação de filtros ecológicos para aumentar a cobertura vegetal nativa em jazida tratada com lodo de esgoto no Bioma Cerrado. *Ciência Florestal* 30(2): 436-450. DOI:10.5902/1980509836476

Brasil. Resolução CONAMA nº 498/2020. 2020. Define critérios e procedimentos para produção e aplicação de biossólido em solos. Diário Oficial da República Federativa do Brasil, Brasília, n. 161, p. 265-273. Available in https://www.

in.gov.br/en/web/dou/-/resolucao-n-498-de-19-de-agosto-de-2020-273467970.

Cabreira GV, PSS Leles, JM Alonso, AHM Abreu, NF Lopes, GR Santos. 2017. Biossólido como componente de substrato para produção de mudas florestais. *Floresta* 47(2): 165–176. DOI: http://dx.doi.org/10.5380/rf.v47i2.44291

Caldeira Junior CF, Souza RA, Santos AM, Sampaio RA, Martins ER. 2009. Características químicas do solo e crescimento de *Astronium fraxinifolium* Schott em área degradada adubada com lodo de esgoto e silicato de cálcio. *Revista Ceres* 56(1): 213-218.

Campos T, G Chaer, PS Leles, M Silva, F Santos. 2019. Leaching of heavy metals in soils conditioned with biosolids from sewage sludge. *Floresta e Ambiente* 26: 1-10. DOI: 10.1590/2179-8087.039918

Fernandes MS, SR Souza. 2006. Absorção de nutrientes. *In* Fernandes MS ed. Nutrição mineral de plantas. Viçosa, Brasil. Sociedade Brasileira de Ciência do Solo. p. 115 – 152.

Gonçalves JLM. 1995. Recomendações de adubação para Eucalyptus, Pinus e espécies típicas da Mata Atlântica. *Documentos Florestais* 15: 1-23.

Guerrini IA, CGG Croce, OC Bueno, CPRP Jacon, TAR Nogueira, DM Fernandes. 2017. Composted sewage sludge and steel mill slag as potential amendments for urban soils involved in afforestation programs. *Forestry and Urban Greening* 22: 93–104. DOI: https://doi.org/10.1016/j.ufug.2017.01.015

IBGE (Instituto Brasileiro de Geografia e Estatistica, BR). 2014. Estimativas da população residente nos municípios brasileiros com data de referência em 1º de julho de 2014. Consulted at 14 sep. 2020. Available in http://www.ibge.gov.br/home/estatistica/populacao/estimativa2014/estimativa_dou.shtm

INPE (Instituto Nacional de Pesquisas Espaciais, BR). 2018. Atlas dos Remanescentes Florestais da Mata Atlântica – Período 2016-2017. São Paulo, Brasil. Fundação SOS Mata Atlântica. 63 p.

Lopes LN, PSS Leles. 2020. Biossólido de lodo de esgoto e fertilizantes químicos como adubação de plantio para espécies arbóreas: crescimento inicial e seus efeitos no solo. *Revista Ineana* (8): 28-43.

Lorenzi H. 1992. Árvores brasileiras: manual de identificação e cultivo de plantas arbóreas nativas do Brasil. Nova Odessa, Brasil. Plantarum. 352 p.

Maciel CAC, OA Camargo, SR Vieira, MK Chiba. 2012. Distribuição espacial de cobre, zinco e níquel em um Latossolo após quinze anos da aplicação de lodo de esgoto. *Bragantia* 71(4): 528-537. DOI: 10.1590/S0006-87052013005000008.

Nobrega RSA, RCV Boas, JCA Nobrega, AM Paula, FMS Moreira. 2007. Utilização de biossólido no crescimento inicial de mudas de aroeira (*Schinus terebynthifolius* Raddi). *Revista Árvore* 31(2): 239-246. DOI: 10.1590/S0100-67622007000200006.

Novais RF, TJ Smyth, FN Nunes. 2007. Fósforo. *In* Novais RF, VVH Alvarez, NF Barros, RLF Fontes, RB Canturutti, JCL Neves eds. Fertilidade do solo. 2nd ed. Viçosa, Brasil. Sociedade Brasileira de Ciência do Solo. p. 471-550.

Paiva AV, F Poggiani, JLM Gonçalves, AV Ferraz. 2009. Crescimento de mudas de espécies arbóreas nativas, adubadas com diferentes doses de lodo de esgoto seco e com fertilização mineral. *Scientia Forestalis* 37(84): 499-511.

Silva BVN, LVA Pinto. 2010. Potencial do uso do lodo de esgoto como adubo orgânico em cobertura de espécies florestais nativas plantadas em área degradada por pastagem. *Agrogeoambiental Review* 2(1): 50-56. DOI: 10.18406/2316-1817v2n12010251.

Silva VB, AP Silva, BO Dias, JL Araújo, D Santos, RP Franco. 2014. Decomposition and release of N, P, and K of bovine manure and poultry litter isolated or mixed. *Revista Brasileira de Ciência do Solo* 38(5): 1537-1546.00. DOI: 10.1590/S0100-06832014000500019.

Silva MV, GM Chaer, PSS Leles, AS Resende AS, EV Silva, TO Campos. 2020. Use of biossolid in plantation of atlantic forest species. *Scientia Forestalis* 48(126): e2728. DOI: https://doi.org/10.18671/scifor.v48n126.16

Sousa TJS, JM Alonso, PSS Leles, ELS Abel, JG Ribeiro, JES Santana. 2019. Mudas de Luehea divaricata produzidas com biossólido de duas estações de tratamento de esgoto. Advances in Forestry Science 6: 595-601. DOI: 10.34062/afs.v6i2.6992

Souza SR, MS Fernandes. 2006. Nitrogênio. In Fernandes MS ed. Nutrição mineral de plantas. Viçosa, Brasil. Sociedade Brasileira de Ciência do Solo. p. 215 – 252.

# Stand biomass estimation methods for *Eucalyptus grandis* and *Eucalyptus dunnii* in Uruguay

## Métodos de estimación de biomasa en rodales para *Eucalyptus grandis* y *Eucalyptus dunnii* en Uruguay

**Andrés Hirigoyen [a]\*, Fernando Resquin [a], Rafael Navarro-Cerrillo [b], Jorge Franco [c], Cecilia Rachid-Casnati [a]**

\*Corresponding author: [a] National Institute of Agricultural Research (INIA), Tacuarembó, Ruta 5 km 386, Tacuarembó, Uruguay, +59899268636, andreshirigoyen@gmail.com

[b] University of Cordoba, Department of Forestry Engineering, Laboratory of Silviculture, Dendrochronology and Climate Change, DendrodatLab- ERSAF, Campus de Rabanales, Crta. IV, km 396, E-14071 Córdoba, Spain.

[c] University of the Republic, Faculty of Agronomy, Paysandú, Ruta 3 km 363, Uruguay.

### SUMMARY

Biomass additivity is a desirable characteristic of a system of equations for predicting components and total biomass, since equations independently adjusted generate biologically inconsistent results. The aim of this study was to fit and compare three methods for modelling biomass: (i) total biomass individual regression, (ii) total biomass regression function calculated as the sum of separate biomass components, and (iii) simultaneous equations of biomass components based on Nonlinear Seemingly Unrelated Regression. A total of 208 trees of *Eucalyptus dunnii* and *Eucalyptus grandis* were harvested and destructively sampled to record above-ground biomass. Results indicate that a system of equations adjusted by simultaneous equations provides accurate biomass estimations, guaranteeing additivity. This model system showed good fit and good prediction performance, given that the correlation coefficient was higher than 97 % for total above-ground biomass, for both species; whereas root mean square error was 23.9 kg and 30.2 kg for *E. grandis* and *E. dunnii,* respectively. A system of biomass equations was developed for each eucalyptus species, such that the sum of the estimations of the biomass components equaled the estimate of above-ground biomass. Results showed that the systems of equations have high potential for improving the accuracy of individual tree above-ground biomass estimates for both species.

*Key words:* Additive biomass equations, biomass partitioning, NSUR, system of equations.

### RESUMEN

La aditividad de las ecuaciones empeladas para predecir los componentes y la biomasa total es una característica deseable de un sistema de ecuaciones. Las ecuaciones ajustadas independientemente generan resultados biológicamente inconsistentes. El objetivo de este estudio fue ajustar y comparar tres métodos para estimar la biomasa de rodales de Eucalyptus: (i) regresión clásica individual, (ii) estimación de biomasa total calculada como la suma de las ecuaciones individuales de las fracciones, y (iii) ecuaciones simultáneas aparentemente no relacionadas. Un total de 208 árboles de *Eucalyptus dunnii* y *Eucalyptus grandis* fueron cosechados y muestreados destructivamente para registrar la biomasa aérea. Los resultados indican que el sistema de ecuaciones simultáneas proporciona estimaciones precisas de biomasa, garantizando la aditividad. Este sistema mostró un alto ajuste y desempeño de predicción, dado que registró un coeficiente de determinación mayor al 97 % para la biomasa total, en ambas especies, mientras que la raíz del error cuadrático medio fue 23,9 kg  y 30,2 kg  para *E. grandis* y *E. dunnii,* respectivamente. Se desarrolló un sistema de ecuaciones de biomasa para cada especie de eucalipto, de modo que la suma de las estimaciones de las fracciones equivalía a la estimación de biomasa total. Los resultados muestran que los sistemas de ecuaciones tienen un gran potencial para mejorar la precisión de las estimaciones individuales de biomasa aérea de árboles para ambas especies.

*Palabras claves:* ecuaciones aditivas de biomasa, partición de biomasa, NSUR, sistema de ecuaciones.

## INTRODUCTION

Estimates of the components of the total biomass of individual trees are of interest for researchers and forest managers, either for scientific or commercial purposes. This information is critical for estimating global carbon storage and assessing ecosystem responses to climate change and anthropogenic disturbance (Ni-Meister *et al.* 2010). It is also important for commercial uses and national development planning, as well as for scientific studies of ecosys-

tem productivity and energy and nutrient flows. Therefore, information on the above-ground biomass (AGB) is needed for estimation of site productivity, and stand and tree growth and yield (Poudel and Temesgen 2015).

The traditional numerical approaches for estimating tree biomass from inventory data are biomass expansion factors and biomass equations (allometric models). Allometric models are common tools for biomass prediction (Lei and Shirong 2016), in particular for individual trees, because biomass measurement in the field is difficult and time consuming. Instead, empirical relationships between biomass and easily measured stand variables, such as tree diameter at breast height (*d*) and total height (*h*), are developed through a regression analysis (Parresol 1999).

In Uruguay, several growth models have been developed for *Eucalyptus globulus* Labill*, Eucalyptus grandis* W. Hill ex Maiden, *Eucalyptus dunnii* Maiden and *Pinus taeda* L., for both solid wood and cellulose production (Rachid-Casnati *et al.* 2014, Hirigoyen *et al.* 2018, Resquin *et al.* 2018). It is necessary to adjust systems for Uruguayan plantations, to avoid the use of allometric models from elsewhere or based on unsuitable ranges of predictive variables, which can lead to over- or underestimation of AGB. Traditionally, component models and individual AGB are independently fitted using the ordinary least squares method (OLS) or the weighted least method (WLS), without considering the inherent relationship between measured components and total tree biomass. Thus, estimates are less accurate and do not reflect the additive relationship among component equations (Bi *et al.* 2004). Usually, the sum of the biomass of the components (in this study: branch, foliage, stem) predicted through individual models does not correspond to the value obtained by applying AGB equations. However, additivity is a desired and logical feature of equations for estimating biomass components. According to Bi *et al.* (2004), the lack of additivity means that the sum of the predicted values from biomass models of tree components does not match the value obtained from models predicting the total AGB of the trees. A simultaneous adjustment allows verifying if the sum of the equations of each fraction is equal to the AGB equation, guaranteeing the additivity of the biomass fraction and improving the statistical adjustment (Sanquetta *et al.* 2019).

Since Parresol (2001) introduced the use of seemingly unrelated regression (SUR) for simultaneously fitting equations for component and total biomass, SUR and its nonlinear version (NSUR) have been applied by many forest researchers (Poudel and Temesgen 2015). SUR ensures the additivity among components and total biomass predictions, taking into account possible correlated errors. This study attempts to identify the best total tree biomass estimation method, for *Eucalyptus* spp. forests of Uruguay. The aim was to compare three methods for modelling the AGB of *Eucalyptus dunnii* and *Eucalyptus grandis* plantations in Uruguay. The compatible biomass

models assessed were: i) above-ground biomass individual regression: WLS individual approach; ii) above-ground biomass regression calculated as the sum of separate biomass components: WLS sum approach; iii) simultaneous biomass equations based on nonlinear seemingly unrelated regressions: NSUR approach. Since it is not practical to fell trees to develop equations for each biomass component, and because destructive sampling is tedious and expensive, biomass systems equations that depend on individual tree variables such as *d* and *h* could be useful. The NSUR procedure comprises better biological properties and statistics to adjust allometric equations for fraction and total biomass.

## METHODS

*Study area.* The sampling was located in three different regions prioritized for forest plantations (Lanfranco and Sapriza 2011): northwest (32° 18′ 18″S, 57° 44′ 0.6″ W, next to Guichon city, Paysandu); central east (33° 01′ 43″ S, 55° 31′ 08″ W, next to Sarandi del Yi, Durazno) and central west (33° 21′ 06″ S, 56° 41′ 17″ W, near Trinidad city, Flores). These zones have a temperate subtropical climate, with mean annual temperature of 18 °C (12 °C in the coldest month, 24 °C in the warmest month) and mean annual rainfall between 1,300 and 1,400 mm (Castaño *et al*. 2011).

*Field data collection.* The AGB data used in this study correspond to the PROBIO project carried out by National Research Institute of Agriculture Research (INIA) in 2015 (PROBIO 2015). Data were collected from 90 trees of *Eucalyptus dunnii* and 118 trees of *Eucalyptus grandis*. All 208 trees were harvested and destructively sampled as follows: stems were cut into 1-m sections and each section was weighed; total height (H) and diameter at breast height (D, 1.3 m above the ground) were measured. For each tree, two discs (3 cm thick) were cut, at 50 % and 75 % of commercial height, and weighed. One of the discs was weighed in the field, with and without bark, and oven-dried to constant weight (70±2 ºC) to estimate dry matter percentage (PROBIO 2015). All the green and dry branches and foliage in each crown were classified and weighed in the field. Samples of 0.5 kg of branches and foliage were taken to the laboratory for moisture content determination. The dry weights of branches and foliage per tree were calculated by multiplying fresh weight by dry weight-fresh weight ratios determined in the laboratory through sampling. The dry weight of each stem section with bark was calculated considering green weight and the average ratio of dry weight to green weight of discs sampled at the large and small end of each section. The dry weights of stem wood and bark were calculated using the average bark to stem wood dry weight ratio obtained from discs sampled at both ends. The total stem biomass of each tree was calculated by summing the dry

weight of all stem sections. Descriptive statistics of total above-ground biomass, biomass components and other variables are shown in table 1.

*Model assessment and validation.* To evaluate the fit of models, their accuracy and precision were compared through the graphical and numerical analysis of residuals. Statistical criteria applied were: the adjusted coefficient of determination ($R^2$-adj), during model development stages; the correlation coefficient ($R^2$), which is a simple linear regression between observed and predicted values, employed as a classical method of evaluation of a nonlinear model; and the Akaike information criterion (AIC), to measure the relative quality of each model (Myers 1990). The model performance for the different approaches was assessed based on estimation errors, using the root-mean-square error (RMSE) to indicate the absolute value of the error (Myers 1990).These expressions are summarized as follows:

$$R^2 adj = 1 - \frac{\sum_{i=1}^{n}(y_i - \hat{y}_i)^2}{\sum_{i=1}^{n}(y_i - \bar{y})^2}\left(\frac{n-1}{n-p}\right) \qquad [1]$$

$$R^2 = r^2_{y_i \widehat{y}_y} \qquad [2]$$

$$RMSE = \sqrt{\frac{\sum_{i=1}^{n}(y_i - \hat{y}_i)^2}{n}} \qquad [3]$$

Where $y_i$ and $\hat{y}_i$ are the measured and estimated values of the dependent variable, respectively, *n* is the total number of observations and *p* is the number of equation parameters. $r^2_{y_i \widehat{y}_y}$ is the correlation coefficient for linear regression between observed and predicted values.

In addition, it is necessary to assess whether the goodness of fit reflects the quality of predictions, through validation (Huang 2002). This analysis assists the selection of the best model. To evaluate the prediction quality of the system of simultaneous equations, cross-validation was performed with the fitting dataset (Myers 1990). Cross-validation in forestry is a common practice (Hirigoyen *et al.* 2018) for model selection through consideration of the predictive ability of the assessed model. It consists of the calculation of the residuals of the *i-th* observation using parameters estimated using all the data except the *i-th* observation. This process is named leave-one-out cross-validation (Kohavi 1995). The residue removed from the *i-th* observation is the difference between the observed value of the modelled variable and the value estimated by a function that has been adjusted to all the data except the *i-th* observation. The sum of squares of eliminated residues is called PRESS (predicted residual sum of squares) (Picard and Cook 1984) and it is used to calculate the selection criteria or root-mean-square-error for cross-validation (RMSEcv). A close agreement between RMSEcv and RMSE indicates that the model is not over-fitting the data and has a good predictive value. The efficiency of the model represents the proportion of the variability observed in the original data that is explained by the model, and it varies between 0 (without adjustment) and 1 (perfect fit). The statistics of validation were calculated as follows:

$$PRESS = \sum_{i=1}^{n}(y_i - \hat{y}_{i-1})^2 \qquad [4]$$

$$RMSE_{cv} = \sqrt{\frac{\sum_{i=1}^{n}(y_i - \hat{y}_{i-i})^2}{n-p}} \qquad [5]$$

**Table 1.** Allometric and biomass characteristics of *Eucalyptus grandis* and *Eucalyptus dunnii*. Diameter at breast height (d, cm), total tree height (h, m), stem biomass (SB), foliage biomass (LB), branches biomass (BB) and above-ground biomass (AGB).

Características alométricas y biomasa de *Eucalyptus grandis* y *Eucalyptus dunnii*. Diámetro a la altura del pecho (d, cm), altura total del árbol (h, m); biomasa del fuste (SB); biomasa de follaje (LB); ramas de biomasa (BB); y biomasa aérea total (AGB).

| Species | Summary | d (cm) | h (m) | Age (years) | SB (kg) | LB (kg) | BB (kg) | AGB (kg) |
|---|---|---|---|---|---|---|---|---|
| *E. dunnii* (n=90) | Min | 9.9 | 12.6 | 6.3 | 6.4 | 2.8 | 2.1 | 11.8 |
| | Mean | 18.8 | 23.9 | 8.6 | 344.6 | 21.3 | 20.9 | 389.1 |
| | Max | 31.6 | 33.2 | 12.0 | 1133.7 | 60.8 | 58.4 | 1223.3 |
| | Sd | 5.2 | 4.8 | 2.89 | 246.7 | 13.5 | 14.5 | 272.0 |
| *E. grandis* (n=118) | Min | 11.1 | 16.6 | 6.5 | 69.8 | 1.2 | 2.0 | 73.3 |
| | Mean | 22.3 | 26.7 | 10.0 | 485.7 | 31.4 | 47.3 | 564.5 |
| | Max | 36.9 | 30.8 | 17.0 | 1725.7 | 114.0 | 177.8 | 1.914 |
| | Sd | 5.6 | 5.3 | 3.5 | 332.4 | 25.0 | 33.9 | 377.3 |

$$ME = 1 - \frac{\sum_{i=1}^{n}(y_i - \hat{y}_{i-i})^2}{\sum_{i=1}^{n}(y - \bar{y}_{i-1})^2}\left(\frac{n-1}{n-p}\right) \qquad [6]$$

Where $y_i$ and $\hat{y}_i$ are the measured and estimated values of the dependent variable, respectively, n is the total number of observations and p is the number of equation parameters.

The Proc sql program of SAS (SAS Institute 2004) was used to perform the routine. The characteristic heteroscedasticity of the biomass data was evaluated with the White test (SAS Institute 2004), and was corrected with a residual variance power function as the weighting factor.

*Individual model selection: OLS individual and WLS sum approaches.* Twenty-seven linear and nonlinear regression models available in literature were tested for each tree biomass component and total tree biomass (Appendix). *WLS* was applied to homogenize residuals and to improve the statistics of fit (Parresol 2001, Dong *et al.* 2018). For each biomass component, only the models in which all parameters were significant at $P < 0.05$ were considered. The best model was selected considering the following statistics: the lowest values for the AIC and RMSE, and the largest proportion of the variance explained by the model (R²-adj). The relative error (RE%) of the predicted biomass (AGB$_{predict}$) versus the total measured biomass (AGB$_{measured}$) was calculated to evaluate the general predictive power of the selected models (Chave *et al.* 2005). Mean relative error represents the general bias of the model, whereas precision was assessed through the standard deviation of the relative error.

$$RE\% = 100 * \left(AGB_{predict} - AGB_{measured}\right)/AGB_{measured} \quad [7]$$

*Additive biomass equations: NSUR approach.* Individual models selected for each biomass component were fitted simultaneously using NSUR in an additive system of equations (Parresol 2001). NSUR accounts for the contemporaneous correlations among regression residuals, resulting in a lower variance of regression coefficients. It also incorporates the additivity property into equation systems obtained by constraining the parameters (Parresol 2001). The model residuals of biomass data always exhibit heteroscedasticity, and the variance of the error is often functionally related to one or more explanatory variables of the model (Parresol 2001, Riofrío *et al.* 2015). To deal with the heteroscedasticity and achieve minimum variance estimates, a weight function was defined and used for the biomass models for each component. Caillez and Alder (1980), working with compatible taper and volume functions, proposed a power function of the variable $d_i^2 H h_i$ (the square of $d$ multiplied by $h$) as weight function:

$$\sigma_2^i = (d_i^2 h_i)^k \qquad [8]$$

Where, $d$ is tree diameter at breast height, $h$ is total height total height and $k$ as power.

It was programmed in the model procedure of SAS/ETS (SAS Institute 2004). Statistical analyses and plots were performed using R statistical software (R Core Team 2015), while SAS statistical software (SAS Institute 2004) was used for fitting the weighted nonlinear systems of equations using NSUR.

RESULTS

*Allometric relationships.* The stem, branches, foliage and total biomass of the sampled trees and their relationships with $d$ and $h$ are shown in figure 1. In all cases an exponential relationship was observed. Exponential models with $d$ and $h$ as independent variables were adjusted and were evaluated using R²-adj.

For both species, $d$ was strongly and significantly correlated with stem biomass and AGB, accounting for 95 % and 94 % of the variation for *E. grandis* and *E. dunnii*, respectively. For *E. dunnii*, the R²-adj values for the branch and foliage fractions were 70 % and 66 %, respectively, indicating moderate correlation; however, these values were lower for *E. grandis* (68 and 54 %, respectively). For *h*, all the values were lower in *E. grandis*, 34 %, 25 %, 74 % and 66 % for branches, foliage, stem and AGB, respectively, while *E. dunnii* had values of 85 %, 88 %, 74 % and 71 % for AGB, stem, branches and foliage, respectively.

*Individual biomass equations.* For individual biomass components, the same models were selected for the WLS individual and WLS sum approaches. For the WLS sum approach, total $k$ was estimated as the sum of the independent tree components models. The models selected for biomass components and AGB with their corresponding statistics of fit are given in table 2. For *E. grandis*, the values of the White test were similar. For *E. grandis*, models considering only $d$ showed the best fit, whereas for *E. dunnii*, the selected models included $d$ and $h$ (table 2).

The accuracy of adjusted models was verified by plotting the correlation between model predictions and observed biomass fractions (figure 2). All parameters were significant at the 95 % confidence level. All models fitted total AGB data well, with the model R²-adj ranging from 0.96 to 0.97. The minor adjust was obtained for foliage and branches components.

Incompatibility was observed between AGB and the sum of the fractions estimated independently. Therefore, there was inconsistency between AGB estimation and the sum of the estimated values for biomass fractions, indicating the need to apply simultaneous adjustments to ensure the additivity of biomass fractions.

*Additive biomass equations.* For the NSUR approach, the models for biomass components (table 3) were fitted si-
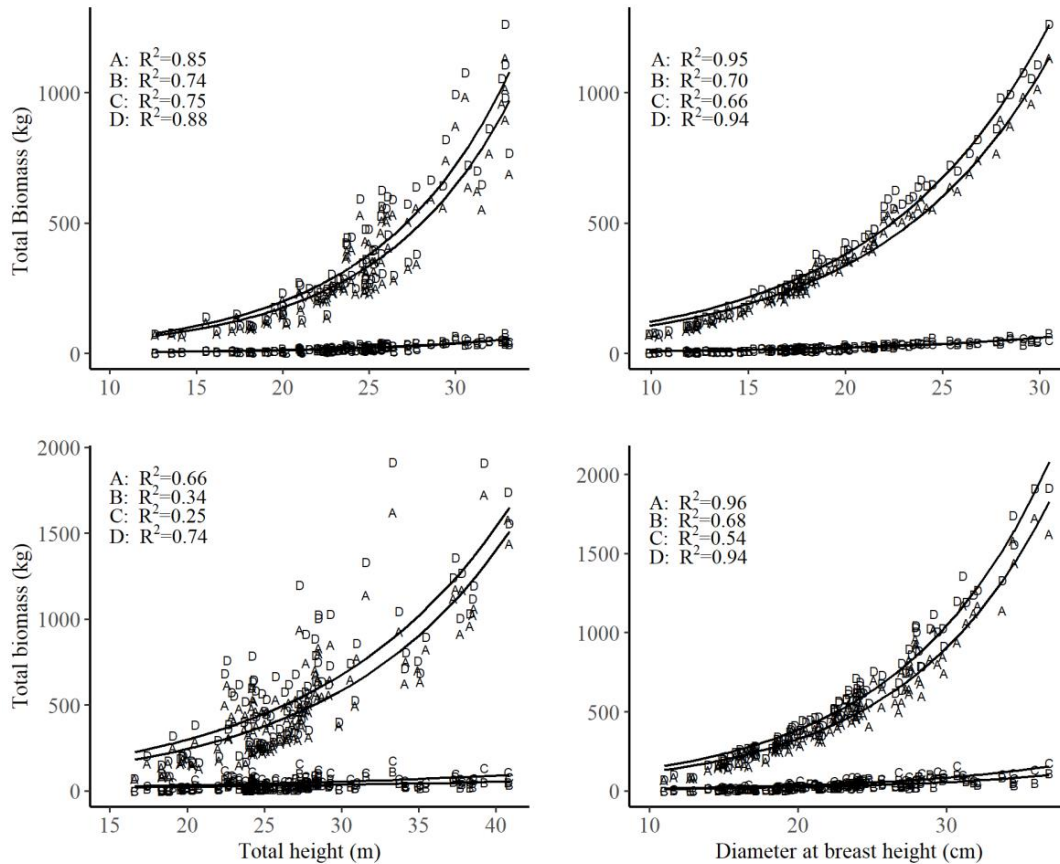
**Figure 1.** Relationships between total (A), branch (B), foliage (C), stem (D) biomass and diameter at breast height and total height for *Eucalyptus dunnii* (upper panel) and *Eucalypts grandis* (bottom panel).

Relaciones entre biomasa total (A), ramas (B), follaje (C) y fuste (D) y diámetro a la altura del pecho y altura total para *Eucalyptus dunnii* (panel superior) y *Eucalyptus grandis* (panel inferior).

**Table 2.** Allometric equations for tree biomass estimation by fractions (kg) and overall aboveground dry weight biomass (AGB, kg) for *Eucalyptus grandis* and *Eucalyptus dunnii* using WLS regression. Independent variables are total height (h, m) and diameter at breast height (d, cm). Adjusted coefficient of determination ($R^2$-adj), root mean squared error (RMSE, kg) and White test.

Ecuaciones alométricas para la estimación de biomasa arbórea por fracciones (kg) y biomasa total sobre el suelo (AGB, kg) para *Eucalyptus grandis* y *Eucalyptus dunnii* empleando regresión WLS. Las variables independientes son la altura total (h, m) y el diámetro a la altura del pecho (d, cm). Coeficiente de determinación ajustado ($R^2$-adj), raíz del error cuadrático medio (RMSE, kg) y prueba de White.

| Species | Biomass fractions | Biomass equation | Model number | RMSE (kg) | $R^2$-adj | Weighting factor | White test |
|---------|------------------|------------------|--------------|-----------|-----------|------------------|------------|
| *E. grandis* | Foliage | $\exp(-2.561 + 3.995\ln(d) - 1.997\ln(h))$ | 15 | 11.8 | 0.77 | $1/d^{2.3}$ | 0.08 |
| | Branches | $\exp(-1.577 + 3.589\ln(d) - 1.776\ln(h))$ | 15 | 13.1 | 0.85 | $1/d^{2.46}$ | 0.09 |
| | Stem | $0.0447d^{2.069}h^{0.835}$ | 3 | 24.2 | 0.98 | $1/d^{2.86}$ | 0.11 |
| | AGB | $d^2(0.656 + 0.0005H)$ | 22 | 34.5 | 0.97 | $1/d^{1.87}$ | 0.60 |
| *E. dunnii* | Foliage | $\exp(-3.248 + 2.890\ln(d) - 0.712\ln(h))$ | 15 | 4.76 | 0.89 | $1/d$ | 0.80 |
| | Branches | $\exp(-3.046 + 2.939\ln(d) - 0.835\ln(h))$ | 15 | 4.38 | 0.90 | $1/d^{2.02}$ | 0.30 |
| | Stem | $0.069d^{2.23}h^{0.566}$ | 3 | 23.6 | 0.97 | $1/d^2h^2$ | 0.08 |
| | AGB | $0.091d^{2.285}h^{0.473}$ | 3 | 24.7 | 0.96 | $1/d^2h^2$ | 0.75 |
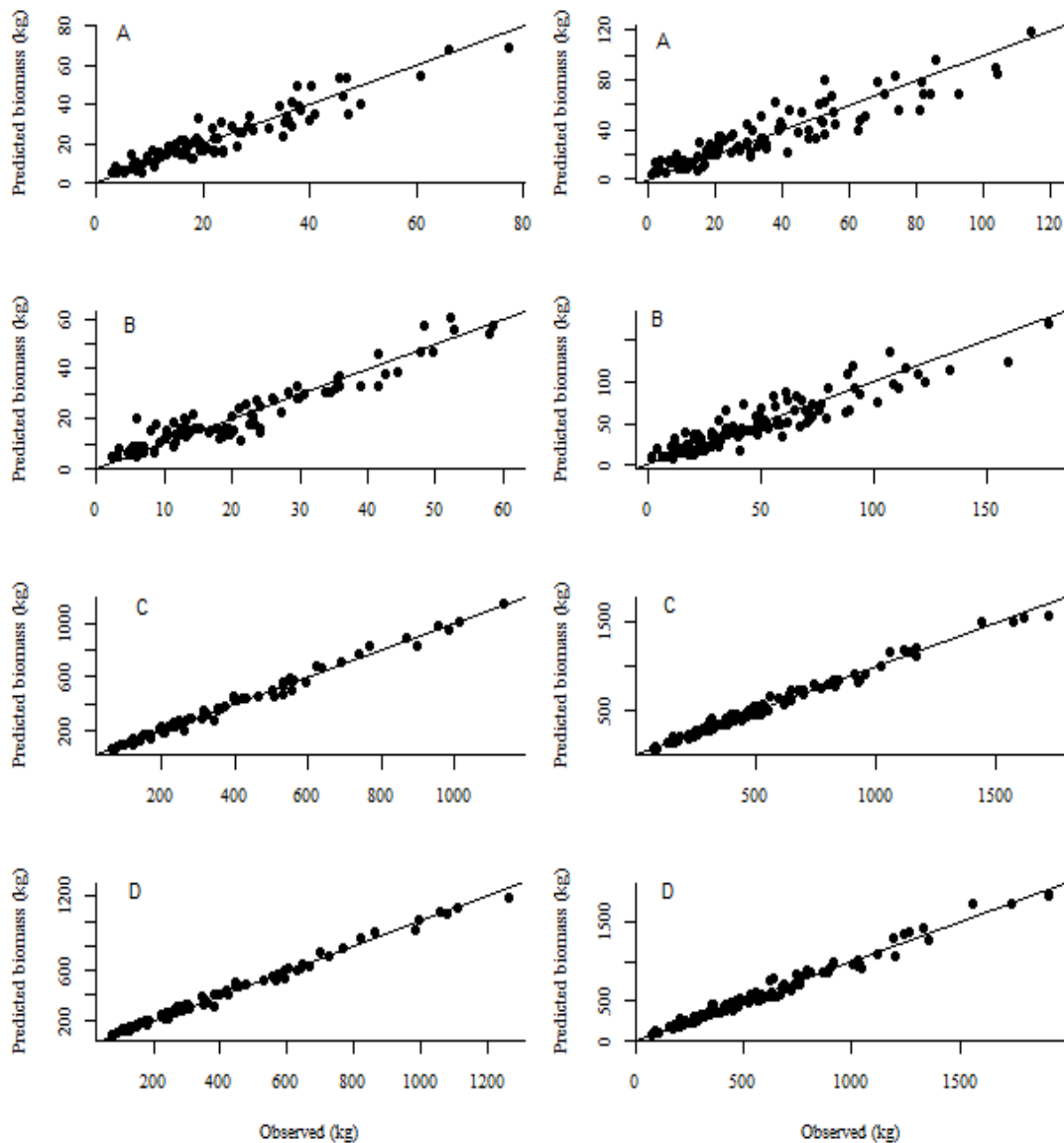
**Figure 2**. Model predictions against observed data; (A) foliage, (B) branches, (C) stem and (D) total tree biomass for *Eucalyptus dunnii* (right) and *Eucalypts grandis* (left).

Predicciones del modelo versus datos observados; (a) follaje, (b) ramas, (c) tallo y (d) biomasa arbórea total para *Eucalyptus dunnii* (derecha) y *Eucalyptus grandis* (izquierda).

multaneously using joint-generalized least squares and restricting the coefficients of regression, ensuring additivity.

The NSUR method consisted first of fitting and selecting the best models for each tree component, since the AGB model was a function of the independent variables used in each tree component model (table 3). The plots of NSUR residuals against predicted values and of predicted values against observed values, for both species, are presented in figures 3 and 4, respectively.

The graphs of the residuals with weighting do not show any trend or heteroscedasticity. All parameters were signi-

ficant ($P < 0.001$) at the 95 % confidence level. All models fitted total AGB data properly ($R^2$ around 0.98). The model fit obtained for biomass of foliage for *E. grandis* ($R^2$ 0.78) was lower than that obtained for *E. dunnii* ($R^2$ 0.90). The relative errors (RE%) of AGB, based on relative stem diameters for individual WLS and adjusted NSUR, were plotted (figure 5) and compared (table 4). For both species, AGB was estimated with a RE% below 1 % for NSUR. The *WLS* individual approach had a RE% value higher than 1 %.

The accuracy of the models was assessed by performing a leave-one-out cross-validation of AGB (table 5).

NSUR yielded the best cross-validation results, with the lowest RMSEcv and best ME; similar values were registered for the WLS individual approach.

DISCUSSION

In this study, we have developed consistent additive biomass functions for *Eucalyptus dunnii* and *E. grandis*

in Uruguay. Models for all components and systems were fitted using the same procedure, which accounted for biological correlation between components. Several growth and yield model systems have been proposed for these species, although few allometric biomass equations are available for eucalypt plantations (Resquin *et al.* 2018). Most equations used for commercial forests of eucalypts and pine species in Uruguay derive from independent fit-

**Table 3.** Biomass equation systems simultaneously fitted for tree biomass estimation by fractions (kg) and overall aboveground dry weight biomass (AGB, kg) for *Eucalyptus grandis* and *Eucalyptus dunnii* using NSUR regression. Independent variables are total height (h, m), diameter at breast height (d, cm), coefficient of correlation ($R^2$) and root mean squared error (RMSE, kg).

Sistemas de ecuaciones ajustadas simultáneamente para la estimación de biomasa por fracciones (kg) y biomasa total sobre el suelo (AGB, kg) para *Eucalyptus grandis* y *Eucalyptus dunnii* utilizando regresión NSUR. Coeficiente de determinación ajustado ($R^2$-adj), raíz del error cuadrático medio (RMSE, kg) y prueba de White.

| Species | Biomass fractions | Biomass equation | $R^2$ | RMSE |
|---|---|---|---|---|
| *E. grandis* | Foliage | $\exp(-2.365 + 4.019\ln(d) - 2.084\ln(h))$ | 0.78 | 11.6 |
| | Branches | $\exp(-1.775 + 3.651\ln(d) - 1.783\ln(h))$ | 0.85 | 12.9 |
| | Stem | $0.044d^{2.077}h^{0.831}$ | 0.98 | 23.1 |
| | AGB | Stem + Foliage + Branches | 0.97 | 30.2 |
| *E. dunnii* | Foliage | $\exp(-3.301 + 2.928\ln(d) - 0.731\ln(h))$ | 0.90 | 4.7 |
| | Branches | $\exp(-3.683 + 2.773\ln(d) - 0.488\ln(h))$ | 0.89 | 4.5 |
| | Stem | $0.082d^{2.269}h^{0.478}$ | 0.97 | 22.5 |
| | AGB | Stem + Foliage + Branches | 0.97 | 23.9 |

**Table 4.** Mean and standard deviation (Sd) of relative error (%) to overall aboveground dry weight biomass (AGB. kg) for *Eucalyptus grandis* and *Eucalyptus dunnii* by method adjusted, induvial equation by weighted least squares (WLS indi), total sum of components fitted by weighted least squares (WLS sum) and fitted by fitted simultaneously (SUR).

Valor medio y desvío estándar (Sd) del error relativo (%) con respecto a la biomasa total sobre el suelo (AGB, kg) para *Eucalyptus grandis* y *Eucalyptus dunnii* por método de ajuste: mínimos cuadrados ponderados individual (WLS indi), suma total de componentes ajustados por mínimos cuadrados ponderados (suma WLS) y ajuste simultáneamente (SUR).

| Species | Approach | Mean | Sd |
|---|---|---|---|
| *E. dunnii* | WLS indi | 1.73 | 6.14 |
| | WLS sum | 1.65 | 7.23 |
| | SUR | 0.25 | 4.07 |
| *E. grandis* | WLS indi | 1.49 | 11.83 |
| | WLS sum | 1.11 | 10.67 |
| | SUR | 0.42 | 8.26 |

**Table 5**. Result for Cross validation to overall aboveground dry weight biomass (AGB, kg) for *Eucalyptus grandis* and *Eucalyptus dunnii* models by method adjusted, induval equation by weighted least squares (WLS indi), total sum of components adjusts by weighted least squares (WLS sum) and adjust by fitted simultaneously (SUR).

Resultado para la validación cruzada de biomasa total en peso seco sobre el suelo (AGB, kg) para *Eucalyptus grandis* y *Eucalyptus dunnii* por método ajustado: mínimos cuadrados ponderados individual (WLS indi), suma total de componentes ajustados por mínimos cuadrados ponderados (WLS sum,) y simultáneo (SUR).

| Species | Approach | Model efficienty | Root-mean-square-error for cross-validation (RSMEcv) |
|---|---|---|---|
| *E. dunnii* | WLS indi | 0.98 | 26.83 |
| | WLS sum | 0.95 | 27.65 |
| | NSUR | 0.98 | 26.48 |
| *E. grandis* | WLS indi | 0.97 | 34.07 |
| | WLS sum | 0.94 | 39.29 |
| | NSUR | 0.97 | 34.14 |
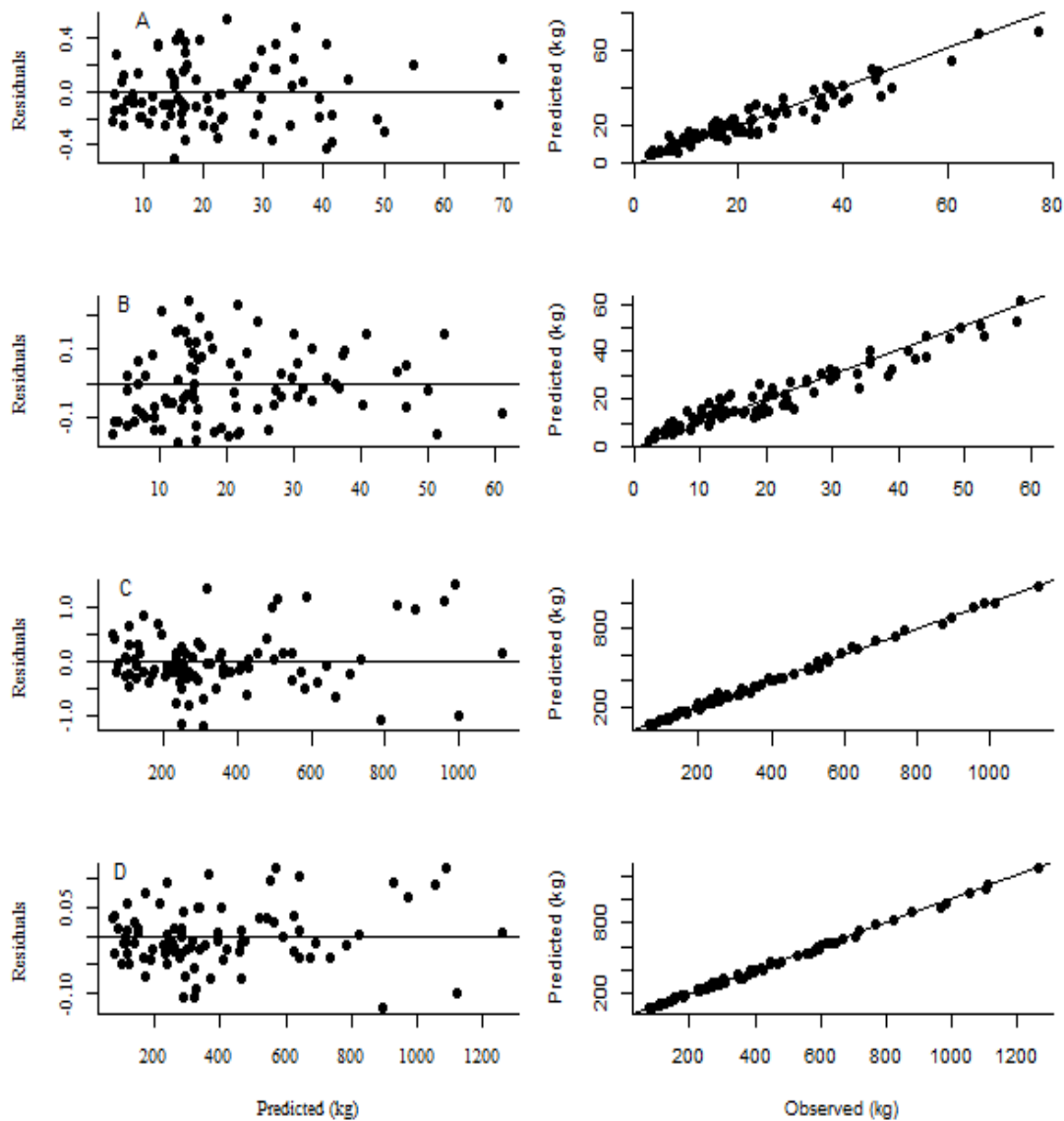
**Figure 3**. Residuals against predicted biomass (right) and predicted against observed data (left) by NSUR: (A) foliage, (B) branches, (C) stem and (D) total tree biomass, to *E. dunnii.*

Residuos versus valores de biomasa predichos (derecha) y predichos versus datos observados (izquierda) por NSUR: (A) hojas, (B) ramas, (C) tallo y (D) biomasa total de árboles, para *E. dunnii*.

tings. Individual approaches do not satisfy the condition of biological consistency, ensured by the restriction that the biomass estimates for components must be additive to equal the estimate of total biomass. Several approaches (Parresol 2001, Li *et al*. 2014, Bi *et al*. 2015) have emphasized the importance of establishing additive equations of biomass. Systems of biomass equations with tree diameter and height as predictors are tools to provide biomass estimates for field inventories. Estimates for the stem and whole tree are more accurate, whereas branch and foliage biomass estimates are less accurate (Li *et al*. 2014, Bi *et al*. 2015).

*Biomass allocation*. Variation in biomass allocation among tree components is usually observed when comparing species or trees of different ages. In this study, stem biomass was the major component of AGB, constituting more than half of the total tree biomass (88.5 % and 86.1 % for *E. grandis* and *E. dunnii* , respectively), while branch biomass represented 8.4 % and 5.4 % and foliage biomass 5.5 % and 6.1 % for *E. grandis*  and *E. dunnii* , respectively.

*Individual tree component and AGB models*. Once the different linear and nonlinear models for each component and total tree biomass had been adjusted, the best model
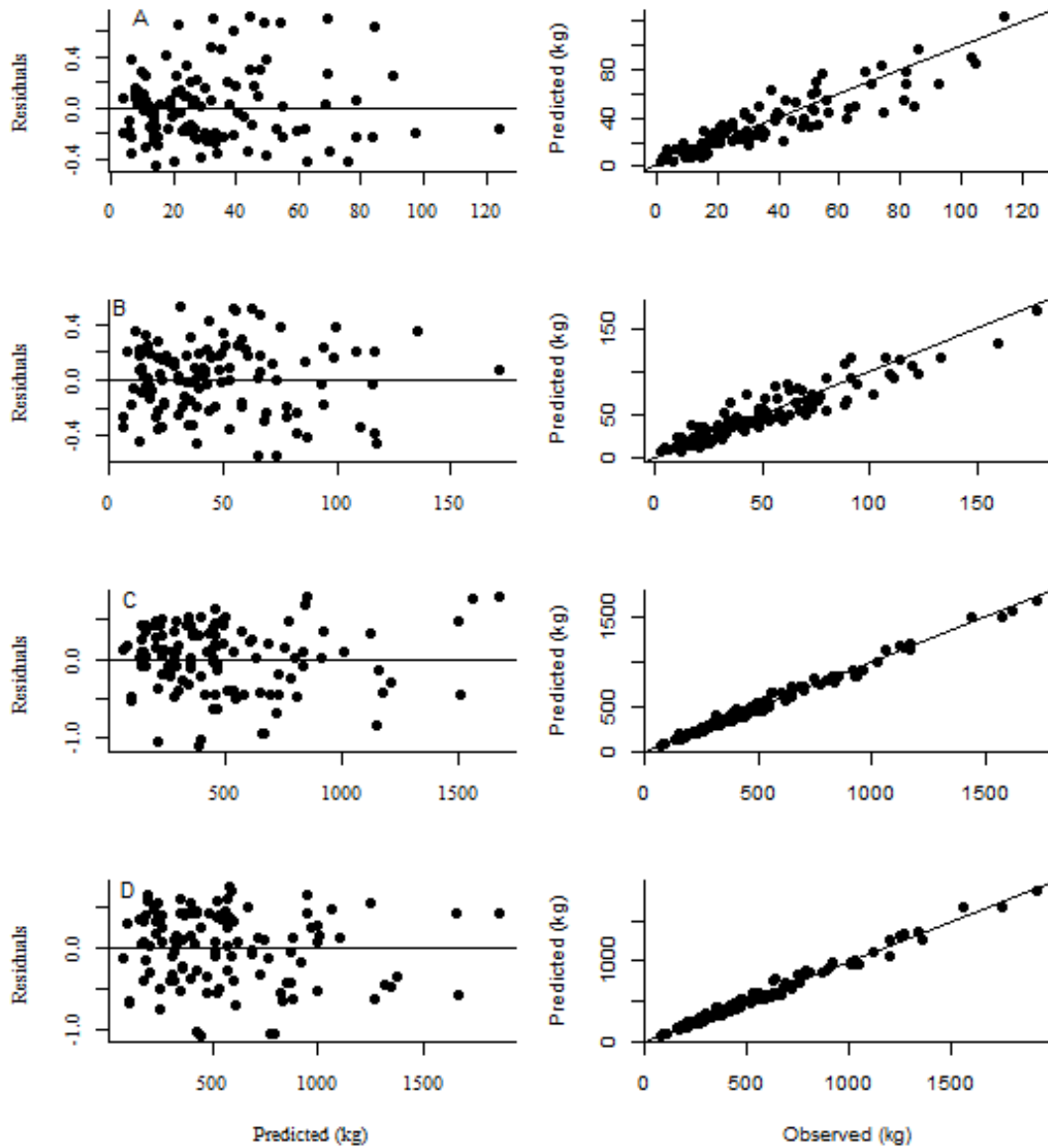
**Figure 4.** Residuals against predicted biomass (right) and predict model against observed data (left) by NSUR: (A) foliage, (B) branches, (C) stem and (D) total tree biomass, to *E. grandis*.

Residuos versus biomasa pronosticada (derecha) y predichos del modelo contra datos observados (izquierda) por NSUR: (A) hojas, (B) ramas, (C) tallo y (D) biomasa total de árboles para *E. grandis*.

was selected in each case based on goodness-of-fit statistics and graphical analyses. The predictive variables tested were D, *h* or both, *d* being a key predictor in growth and yield models as well as in biomass models. Models that include only *d* are simple in structure and require only basic forest inventory data (Wang 2006). Our results show that *d* and *h* had a strong positive relationship with all the biomass components evaluated; they were included as predictor variables in all allometric models and improved the predictive ability of biomass equations (Bi *et al.* 2015, Dong *et al.* 2015). Heteroscedasticity problems are inherent in biomass models since trees with higher *d* and *h* have

more biomass than that presented by small trees. As shown in figure 1, the relationship between biomass and *d* and *h* is exponential. To deal with this issue, logarithmic transformations are commonly applied in the modelling of tree biomass (Wang 2006). To back-transform biomass to its original scale, the use of a correction factor is common to correct for systematic bias introduced by anti-logarithmic transformation. This anti-logarithmic transformation leads to systematic overestimate of biomass (Dong *et al.* 2015). Furthermore, in a system of additive biomass equations, the additivity property of the system may not be achieved (Dong *et al.* 2015).We used weighted least-squares regres-
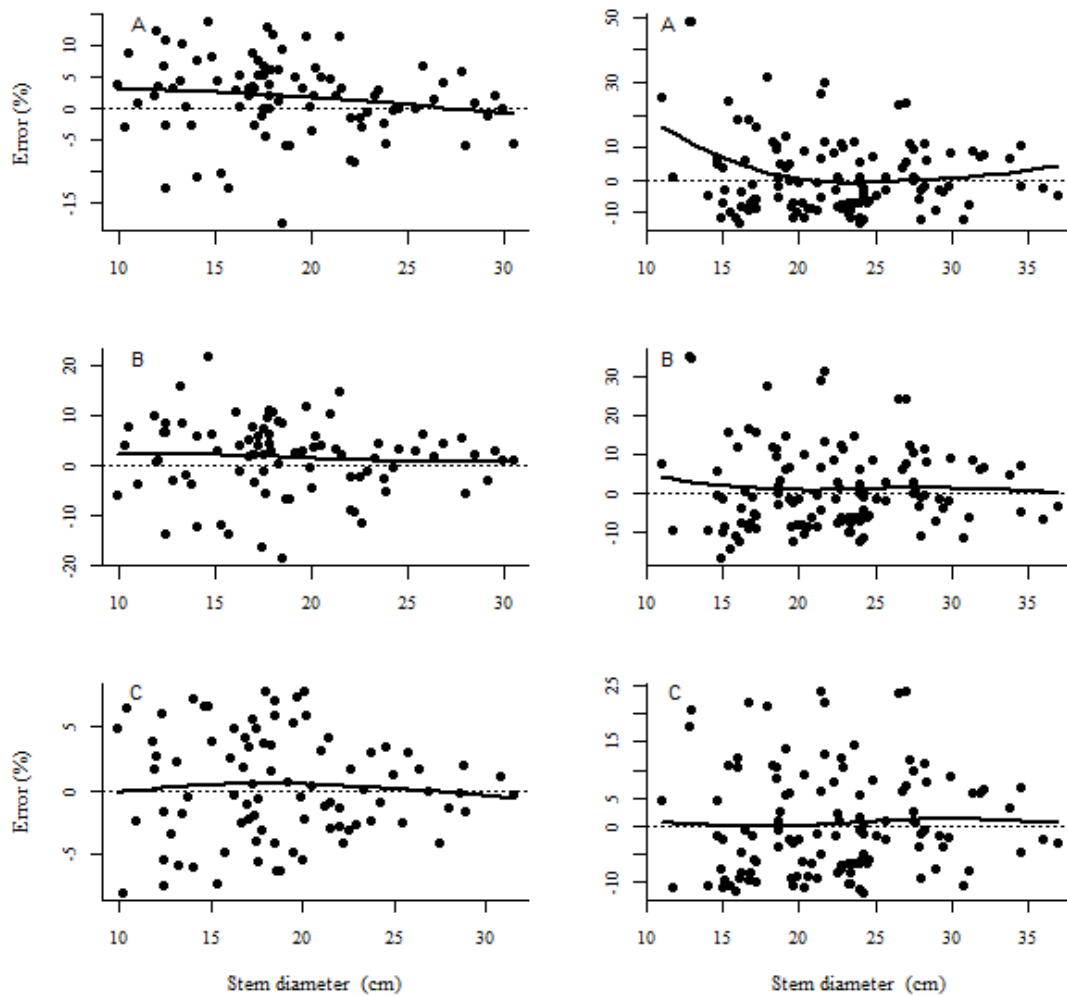
**Figure 5**. Relative error in AGB predictions: (A) individual equation, (B) components sum, (C) additive equation. For *E. dunnii* (right) and *E. grandis* (left) by stem diameter (cm), solid lines are smoothed errors using a lowess method.

Error relativo de las predicciones de AGB: (A) ecuación individual, (B) suma de componentes, (C) ecuación aditiva. *E. dunnii* (derecha) y *E. grandis* (izquierda) por diámetro de troncos (cm), las líneas continuas son errores suavizados utilizando un método *lowess*.

sion to fit individual models, thus accounting for inherent heteroscedasticity (Parresol 1999). Foliage and branches biomass models were less accurate and less precise than biomass models for the stem and AGB, probably due to the variability of the crown structure.

For both species, model [15] was selected to estimate foliage and branches biomass, and model [3] to estimate stem biomass (see Appendix). However, different models were selected for AGB. For stem biomass, both parameters of model [3] were positive, meaning that stem biomass was directly and positively related to *d* and H. For *E. grandis,* in the AGB model [22] the parameter estimated for *h* was positive, implying that, for the same *d*, taller trees have more above-stump stem biomass than that presented by shorter trees. For *E. dunnii,* model [3] shows that the parameters estimated for *h* and *d* were both positive,

indicating that the estimate of AGB is superior in thick-stemmed and tall trees.

*Additive biomass equations.* Biomass additivity is a desirable characteristic of a system of equations for predicting tree component and total tree biomass. Most biomass equations reported in literature are not additive and were developed separately for each biomass component (Lin *et al.* 2017, Resquin *et al.* 2018). The biomass additivity approach has been used by some researchers in the fitting of biomass equations (*e.g.* Riofrío *et al.* 2015, Kralicek *et al.* 2017). However, there is no record of the use of NSUR in Uruguay to estimate tree AGB. Equations adjusted independently generate biologically inconsistent results, which implies that models for the components biomass and total AGB should be comprised of systems of equations. Bio-

mass components were expressed as an individual model, where each model was selected from a group of candidate models. The AGB model was a function of biomass components, resulting in additivity; all the equations of the system had their own weighting function to ensure estimates with minimum variance.

Our additive systems of biomass used only one constraint on total tree biomass. The cross-equation error correlations between total tree biomass and components biomass were accounted (Carvalho and Parresol 2003, Bi *et al.* 2015). Once each biomass component had been individually adjusted, the models selected were simultaneously fitted using NSUR methodology. The results presented in table 3 show high goodness of fit in all the components equation systems (by species) fitted with NSUR methodology. Comparing the two fitting methods (individual fitting and the NSUR approach), the statistics of fitting were similar (with small gains in RSME and $R^2$ for the NSUR approach); however, residuals plots presented different trends (figures 2-4). According to Sanquetta *et al.* (2019), when comparing individual fitting and NSUR, it can be seen that both approaches have similar precision statistics. NSUR models should be used to predict total biomass and its fractions because biological consistency must be considered. For AGB, NSUR achieved an $R^2$ value of approximately 98 % and improvement in the distribution of the residuals. Equations adjusted by means of OLS-WLS do not take into account contemporaneous correlations, which impairs the efficiency of estimation. The inclusion of contemporaneous correlations between the biomass of the components and total biomass in the fitting of equation systems through NSUR resulted in efficiency gain, by reduction of confidence and prediction intervals of biomass estimates (Parresol 1999).

The classical individual approach to the fitting of biomass equations ignores the inherent correlation among the biomass components measured in the same sample trees. Taking this correlation into account in the development of a system of additive biomass equations yields superior statistical efficiency (Parresol 2001). Some authors (Parresol 2001, Carvalho and Parresol 2003) have compared different methods of enforcing additivity, concluding that NSUR achieves more efficient estimates and should be the choice for additivity. In the present work, the simultaneous systems tended to slightly bias AGB estimates, by 0.25 %, 0.42 % for *E. dunnii* and *E. grandis* respectively. According to Chave *et al.* (2005), despite estimation errors that can derive from the use of specific allometric models fitted using a small number of samples, such models are useful because of their ease of implementation. In our study, for both species, estimation by NSUR had a lower bias than that presented by the other methods, ranging from -7.9 to 7.7 and from -11.8 to 24.7 for *E. dunnii* and *E. grandis,* respectively. This represents improvement over the traditional individual approach, which gave values ranging from -18.3 to 13.7 for *E. dunnii* and from -13.2 to 48.5 for *E. grandis,* and the WLS sum approach, with ranges of

-18.3 to 21.9 and -16.7 to 35.2 for *E. dunnii* and *E. grandis,* respectively. The WLS method tended to overestimate AGB. In general, the higher overestimation yielded by WLS approaches compared to NSUR reflects the gain in prediction quality obtained when applying the latter.

To improve the overall biomass stocks estimation and its components, an additive system was proposed which ensures that the estimation functions of components were compatible with the total biomass estimated. The model fit and validation statistics indicate that the systems of equations developed in this study will contribute to the accurate estimation of total biomass. The NSUR method is not intended to improve the precision of AGB estimates, but rather to reconcile estimates of total biomass and the sum of biomass fractions (Coutinho *et al.* 2018). With the application of NSUR, we have developed full allometric models, which can be used to compute the biomass of components for trees of interest.

## CONCLUSIONS

This study represents a first attempt at quantifying total tree biomass in Uruguay through the use of a simultaneously fitted system of weighted nonlinear equations. Our approach, fitting additive biomass functions, led to a consistent set of additive biomass functions for two of the most relevant *Eucalyptus* species in Uruguay. In this work the aboveground biomass of *E. grandis* and *E. dunnii was* estimated using an NSUR approach; to our knowledge, this represents the first attempt at quantifying total tree biomass with a simultaneously fitted system of weighted nonlinear equations for forests in Uruguay. The correlation matrix among biomass equations shows that strong inherent correlations existed among the biomass components measured in the same sample trees. By taking into account this cross-equation error correlation, methods like NSUR result in more efficient estimation of the system of equations than do classical methods. The allometric models adjusted using NSUR methodology provided accurate biomass estimates that guarantee additivity among biomass components for *E. grandis* and *E. dunnii* in Uruguay. Simultaneous fit provided a slight improvement in most goodness-of-fit statistics. This ensures the correct performance of the additive system in new samples. The structural characteristics of models improve the predictive capacity and extend their range of application, since they include total height and diameter as explanatory variables. These models can be implemented in procedures that require a simple and efficient method for estimation of biomass.

## ACKNOWLEDGEMENTS

## REFERENCES

Bi H, S Murphy, L Volkova, C Weston, T Fairman, Y Li, R Law, J Norris, X Lei, G. 2015. Additive biomass equations based on complete weighing of sample trees for open eucalypt forest species in south-eastern Australia. *Forest Ecology and Management* 100(349): 106–121. DOI: https://doi.org/10.1016/j.foreco.2015.03.007

Bi H, J Turner, M Lambert. 2004. Additive biomass equations for native eucalypt forest trees of temperate Australia. *Trees* 18(4): 467–479. DOI: https://doi.org/10.1007/s00468-004-0333-z

Caillez F, D Alder. 1980. Estimación del volumen forestal y predicción del rendimiento con referencia especial a los trópicos. Roma, Italy. FAO 92 p.

Carvalho JP, BR Parresol. 2003. Additivity in tree biomass components of Pyrenean oak (*Quercus pyrenaica* Willd.). *Forest Ecology and Management* 179(1-3): 269–276. DOI: https://doi.org/10.1016/S0378-1127(02)00549-2

Castaño J, A Ceroni, M Furest, J Aunchayna, R Bidegain. 2011. Caracterización agroclimática del Uruguay 1980-2009. Montevideo, Uruguay. INIA. 33 p. (Serie Técnica 193).

Chave J, C Andalo, S Brown, MA Cairns, JQ Chambers, D Eamus, H Fölster, F Fromard, N Higuchi, T Kira, JP Lescure, BW Nelson, H Ogawa, H Puig, B Riera, T Yamakura. 2005. Tree allometry and improved estimation of carbon stocks and balance in tropical forests. *Oecologia* 145(1): 87–99. DOI: https://doi.org/10.1007/s00442-005-0100-x

Coutinho V, C Sanquetta, P Bittencourt, S Alves, K Henkel, W Macedo, J Moreau. 2018. Simultaneous Equations to Estimate Aboveground Biomass of *Pinus caribaea* var. *hondurensis*. *Floresta e Ambiente* 25(3): e20160452. DOI: https://doi.org/10.1590/2179-8087.045216

Dong L, L Zhang, F Li. 2018. Additive Biomass Equations Based on Different Dendrometric Variables for Two Dominant Species (*Larix gmelini* Rupr. and *Betula platyphylla* Suk.) in Natural Forests in the Eastern Daxing'an Mountains, Northeast China. *Forests* 9(5): 261. DOI: https://doi.org/10.3390/f9050261

Dong L, L Zhang, F Li. 2015. Developing additive systems of biomass equations for nine hardwood species in Northeast China. *Trees - Structure and Function* 29(4): 1149–1163. DOI: https://doi.org/10.1007/s00468-015-1196-1

Hirigoyen A, J Franco, U Diéguez. 2018. Modelo dinámico de rodal para *Eucalyptus globulus* (L.) en Uruguay. *Agrociencia Uruguay* 22(1): 63-80. DOI: https://dx.doi.org/10.31285/agro.22.1.7

Huang S. 2002. Validating and localizing growth and yield models: procedures, problems and prospects. *In* Proceedings of IUFRO Workshop on Reality, models and parameter estimation: the forestry scenario. Sesimbra, Portugal (2-5 de junio de 2002).

Kohavi R. 1995. A Study of Cross-Validation and Bootstrap for Accuracy Estimation and Model Selection. *In* International Joint Conference of Artificial Intelligence. Montreal, Quebec, Canada. Morgan Kaufmann, Los Altos, CA. USA. p. 1137–1143.

Kralicek K, H Bao, KP Poudel, H Temesgen, C Salas. 2017. Simultaneous estimation of above- and below-ground biomass in tropical forests of Viet Nam. *Forest Ecology and Management* 100(390): 147–156. DOI: https://doi.org/10.1016/j.foreco.2017.01.030

Lanfranco B, G Sapriza. 2011.El índice CONEAT como medida de productividad y valor de la tierra. Serie Técnica 187 INIA. Montevideo, Uruguay. INIA. 57 p.

Lei S, L Shirong L.2016. Methods of Estimating Forest Biomass: A Review, Biomass Volume Estimation and Valorization for Energy, Jaya Shankar Tumuluru, *IntechOpen* 10: 65733. DOI: http://dx.doi.org/10.5772/65733

Li M, J Im, LJ Quackenbush, T Liu. 2014. Forest biomass and carbon stock quantification using airborne LiDAR data: A case study over huntington wildlife forest in the Adirondack park. IEEE Journal of Selected Topics in *Applied Earth Observations and Remote Sensing* 7(7): 3143–3156. DOI: https://doi.org/10.1109/JSTARS.2014.2304642

Lin K, M Lyu, M Jiang, Y Chen, Y Li, G Chen, J Xie, Y Yang. 2017. Improved allometric equations for estimating biomass of the three *Castanopsis carlesii* H. forest types in subtropical China. *New Forests* 48(1): 115–135. DOI: https://doi.org/10.1007/s11056-016-9559-z

Myers R. 1990. Classical and modern regression with applications. Second ed. Belmont, CA. USA. Duxbury Press. 488 p.

Ni-Meister W, S Lee, AH Strahler, CE Woodcock, C Schaaf, T Yao, KJ Ranson, G Sun, JB Blair. 2010. Assessing general relationships between aboveground biomass and vegetation structure parameters for improved carbon estimate from lidar remote sensing. Journal of *Geophysical Research: Biogeosciences* 115(G2): 1-12. DOI: https://doi.org/10.1029/2009JG000936

Parresol BR. 1999. Assessing tree and stand biomass: a review with examples and critical comparisons. *Forest Science* 45(4): 573–593.

Parresol BR. 2001. Additivity of nonlinear biomass equations. *Canadian Journal of Forest Research* 31(5): 865–878. DOI: https://doi.org/10.1139/x00-202

Picard RR, Cook RD. 1984. Cross-validation of regression models. *Journal of the American Statistical Association* 79(387): 575–583.

Poudel KP, H Temesgen H. 2015. Methods for estimating aboveground biomass and its components for Douglas-fir and lodgepole pine trees. *Canadian Journal of Forest Research* 46(1): 77–87. DOI: https://doi.org/10.1139/cjfr-2015-0256

PROBIO (Producción de Electricidad a partir de Biomasa, UY). 2015. Mejoramiento en la calidad de la información vinculada con la utilización de la biomasa forestal. Montevideo, Uruguay. PROBIO. 157 p.

R Core Team 2015.R: A Language and Environment for Statistical Computing, 3.2.1 ed. R Foundation for Statistical Computing, Vienna, Austria.

Rachid-Casnati C, M Euan, W Richard, F Resquin. 2014. Volume and Taper Equations for *P. taeda* (L.) and *E. grandis* (Hill ex. Maiden). *Agrociencia* 18(2): 47–60. DOI: https://doi.org/10.2477/vol18iss2pp47-60

Resquin F, RM Navarro-Cerrillo, C Rachid-Casnati, A Hirigoyen, L Carrasco-Letelier, J Duque-Lazo. 2018. Allometry, growth and survival of three eucalyptus species (*Eucalyptus benthamii* Maiden and Cambage, *E. dunnii* Maiden and *E. grandis* Hill ex Maiden) in high-density plantations in Uruguay. *Forests* 9(12): 745. DOI: https://doi.org/10.3390/f9120745

Riofrío J, C Herrero, J Grijalva, F Bravo. 2015. Aboveground tree additive biomass models in Ecuadorian highland agroforestry systems. *Biomass and Bioenergy* 100(80): 252–

259. DOI: https://doi.org/10.1016/j.biombioe.2015.05.026

Sanquetta CR, M Minatti, SC Junior, JW Trautenmuller, AP Dalla Corte. 2019. Independent and simultaneous modeling of biomass and carbon of Guinean Elaeis. *Floresta* 49(3): 421–430. DOI: https://doi.org/10.5380/rf.v49i3.58897

SAS Institute Inc. 2004. SAS/ETS 9.1 User's Guide. SAS Institute Inc., Cary, NC, USA.

Wang C. 2006. Biomass allometric equations for 10 co-occurring tree species in Chinese temperate forests. *Forest Ecology and Management* 222(1-3): 9–16. DOI: https://doi.org/10.1016/j.foreco.2005.10.074

West PW. 2017. Simulation studies to examine bias and precision of some estimators that use auxiliary information in design-based sampling in forest inventory. *New Zealand Journal of Forestry Science* 47(1): 22. DOI: https://doi.org/10.1186/s40490-017-0101-7

## Appendix

**Cuadro S1.** Biomass models tested for different tree biomass components ($W_i$, kg); with diameter at breast height (d, cm) and total height (h, m) as dependent variables; $\beta_i$ model parameters.

Modelos de biomasa evaluados para diferentes componentes de biomasa arbórea (Wi, kg); con diámetro a la altura del pecho (d, cm) y altura total (h, m) como variables dependientes; $\beta_i$ Parámetros del modelo.

| Equation number | Model |
|---|---|
| 1 | $W_i = \beta_0 d^{\beta_1}$ |
| 2 | $W_i = \beta_0 (d^2 h)^{\beta_1}$ |
| 3 | $W_i = \beta_0 d^{\beta_1} h^{\beta_2}$ |
| 4 | $W_i = exp(\beta_0 + \beta_1 ln(d))$ |
| 5 | $W_i = \beta_0 W_i = \beta_0 + \beta_1 d^2 \beta_1 d^2$ |
| 6 | $W_i = \beta_0 W_i = \beta_0 + \beta_1 d\beta_1 d + \beta_2 d^2 \beta_2 d^2$ |
| 7 | $W_i = \beta_0 W_i = \beta_0 + \beta_1 d\beta_1 d + \beta_2 h\beta_2 h$ |
| 8 | $W_i = \beta_0 W_i = \beta_0 + \beta_1 \beta_1 (d^2 h d^2 h)$ |
| 9 | $W_i = \beta_0 W_i = \beta_0 + \beta_1 (d^2 h)^{\beta_2} \beta_1 (d^2 h)^{\beta_2}$ |
| 10 | $W_i = \beta_1 d^2 W_i = \beta_1 d^2 + \beta_2 h\beta_2 h + \beta_3 d^2 h\beta_3 d^2 h$ |
| 11 | $W_i = \beta_0 W_i = \beta_0 + \beta_1 d^2 h\beta_1 d^2 h + \beta_2 (dh)^2 \beta_2 (dh)^2$ |
| 12 | $W_i = expW_i = exp(\beta_0 \beta_0 + \beta_1 d\beta_1 d + \beta_2 d^2 \beta_2 d^2)$ |
| 13 | $W_i = expW_i = exp(\beta_0 \beta_0 + \beta_1 d\beta_1 d)$ |
| 14 | $W_i = expW_i = exp(\beta_0 d^{\beta_1} h^{\beta_2} \beta_0 d^{\beta_1} h^{\beta_2})$ |
| 15 | $W_i = exp(\beta_0 W_i = exp(\beta_0 + \beta_1 ln(d)\beta_1 ln(d) + \beta_2 ln(h))\beta_2 ln(h))$ |
| 16 | $W_i = (\beta_0 W_i = (\beta_0 + \beta_1 ln(d))\beta_1 ln(d))$ |
| 17 | $W_i = \beta_0 W_i = \beta_0 + \beta_1 ln(d)\beta_1 ln(d) + \beta_2 ln(h)\beta_2 ln(h)$ |
| 18 | $W_i = \beta_0 (dh)$ |
| 19 | $W_i = \beta_0 W_i = \beta_0 + d^{\beta_1} d^{\beta_1} + h^{\beta_2} h^{\beta_2}$ |
| 20 | $W_i = \beta_0 W_i = \beta_0 + \beta_1 ln\beta_1 ln(d^2 h d^2 h)$ |
| 21 | $W_i = expW_i = exp(\beta_0 d^2 \beta_0 d^2)$ |
| 22 | $W_i = d^2 W_i = d^2 (\beta_0 \beta_0 + \beta_1 h\beta_1 h)$ |
| 23 | $W_i = \beta_0 W_i = \beta_0 + \beta_1 ln\beta_1 ln(d\ h^2\ h^2)$ |
| 24 | $W_i = expW_i = exp(d^2 d^2 / (\beta_0 \beta_0 + \beta_1 \beta_1 / h))$ |
| 25 | $W_i = \beta_0 W_i = \beta_0 + \beta_1 d\beta_1 d + \beta_2 d^2 \beta_2 d^2 + \beta_3 d^2 h\beta_3 d^2 h + \beta_4 dh^2 \beta_4 dh^2 + \beta_5 h\beta_5 h$ |
| 26 | $W_i = \beta_0\ d\ W_i = \beta_0\ d + \beta_1 d^2 \beta_1 d^2 + \beta_2 \beta_2 * dhdh$ |
| 27 | $W_i = exp(\beta_0 W_i = exp(\beta_0 + \beta_1 ln\beta_1 ln(d^2 h d^2 h))$ |

# Soil organic carbon and dead biomass pools
# in woodlands from Monte region (Argentina)

Reservorios de carbono orgánico del suelo y biomasa muerta
en áreas forestales de la región Monte (Argentina)

**Marcos S Karlin [a]\*, Ricardo M Zapata [a], Rubén O Coirini [a,b]**

\*Corresponding author: [a] Universidad Nacional de Córdoba, Facultad de Ciencias Agropecuarias, Departamento Recursos Naturales,
Félix Marrone 746, Ciudad Universitaria, CC 509, CP 5000, Córdoba, Argentina, mkarlin@agro.unc.edu.ar
[b] Red Agroforestal Chaco Argentina, San Lorenzo 1235 Reconquista, CP: 3560, Santa Fe, Argentina.

SUMMARY

Soil and above-ground dead biomass are important carbon pools in drylands. They depend on local controls and patterns that should be studied. The objective of this work is to understand and quantify the influence of the vegetation canopy in the regulation of soil and dead biomass carbon stocks in woodlands of Monte region in Argentina. The hypothesis is that soil and dead biomass carbon stocks are lower in the intercanopy and higher under the canopy, independently of the type of canopy. Thirty sampling plots were selected, identifying three treatments: tree canopy, intercanopy and shrub canopy. In each sampling plot, soil and dead biomass were sampled. Four physiognomic-functional groups were identified. *Prosopis* woodlands accumulated about 38 Mg ha$^{-1}$ of dead organic carbon (from soil, litter, and dead wood), followed by *Suaeda* woodlands with almost 35 Mg ha$^{-1}$. Mixed woodlands showed average values around 27 Mg ha$^{-1}$, while *Bulnesia* woodlands around 25 Mg ha$^{-1}$. The vegetation canopy, and consequently, litter and dead wood input affected soil organic carbon in topsoil. Shrubs such as *Larrea* spp. had a restricted ability to enrich soil compared to *Prosopis* spp. Soil, litter and dead wood are significant pools of carbon and should be included in programs on reducing emissions in arid regions. The hypothesis is accepted partially; there is a remarked contrast in carbon content between soils under the tree canopy and off the canopy. However, the effect of shrub canopy is intermediate between both treatments.

*Key words:* litter, shrub, tree canopy, dead wood.


RESUMEN

El suelo y la biomasa muerta son importantes reservorios de carbono en zonas áridas. Ellos dependen de patrones y factores locales que deben ser estudiados. El objetivo de este trabajo fue cuantificar la influencia del dosel de la vegetación en los contenidos de carbono del suelo y de la biomasa muerta en áreas forestales de la región Monte en Argentina. La hipótesis es que los contenidos de carbono en el suelo y en la biomasa muerta son menores fuera del dosel y mayores bajo dosel, independientemente del tipo de dosel. Treinta parcelas de muestreo fueron seleccionadas, identificando tres tratamientos: bajo dosel arbóreo, espacio sin dosel y bajo dosel arbustivo. Se muestrearon suelo y biomasa muerta. Se identificaron cuatro grupos fisonómico-funcionales. Los bosques de *Prosopis* spp. acumularon ~ 38 Mg ha$^{-1}$ de carbono orgánico muerto (suelo, mantillo y madera muerta), las áreas forestales de *Suaeda* spp. ~ 35 Mg ha$^{-1}$, los bosques mixtos ~ 27 Mg ha$^{-1}$ y los bosques de *Bulnesia* spp. ~ 25 Mg ha$^{-1}$. El dosel de la vegetación y, consecuentemente, los aportes de mantillo y madera muerta influyeron en los contenidos de carbono del suelo superficial. Arbustos como *Larrea* spp. tienen menor capacidad para enriquecer el suelo que *Prosopis* spp. El suelo, mantillo y madera muerta son reservorios significativos de carbono y deberían ser considerados en programas de reducción de emisiones en zonas áridas. La hipótesis fue parcialmente aceptada; hay un marcado contraste en los contenidos de carbono entre suelos bajo y fuera del dosel. Sin embargo, el efecto del dosela arbustivo es intermedio entre ambos tratamientos.

*Palabras clave:* mantillo, arbusto, canopia arbórea, madera muerta.


INTRODUCTION

Soils are an important carbon sink in ecosystems worldwide. Trees, shrubs and herbs can assimilate $CO_2$ from the atmosphere and transform it into biomass. Some of above-ground or subterranean tissues may be assimila-
ted into the soil profile, enriching it with organic carbon. Carbon stocks in ecosystems are the result of the balance between the rates of accumulation and decomposition.

Accumulation rates depend on the net primary production of vegetation, which in turn depends on solar radiation, air temperature, nutrients and water, needed for

plants to grow (Jobbágy and Jackson 2000). Plants physiology and architecture, *e.g.*, deciduousness or canopy volume, also affect carbon accumulation. Decomposition rates depend on soil characteristics and the microclimate under the canopy.

Plants in arid lands have a restricted growth due to harsh environmental conditions such as scarcity of water and nutrients. Only adapted species can develop under arid and hyperarid conditions, and they usually grow in communities within fertile small-scaled patches. Woody plants in arid zones are the primary microclimate regulators, not only by attenuating drastic changes in air temperature and humidity, but also altering soil conditions under the canopy (Rossi and Villagra 2003).

Soil is the most abundant organic carbon pool in the terrestrial biosphere, compared to vegetation and animals. Although many authors studied soil organic matter and litter carbon contents in natural ecosystems (Yang *et al*. 2007), and specifically in arid zones (Charley and West 1975, Rossi and Villagra 2003), local controls should be studied more thoroughly (Yang *et al*. 2007). Such local controls are defined by local climate, soil type and dominant vegetation.

Covering about 47 % of the total terrestrial surface, drylands hold 27 % of the global soil organic carbon reserves (Trumper *et al*. 2008). Desertification may reduce such carbon reserves. With 50,678,905 ha (Karlin *et al*. 2017), Monte region represents 18 % of the total continental area of Argentina, being an important carbon sink due to its extension. It also holds some biogeographic similarities with other regions of South America, North of Mexico and South of the USA (Roig *et al*. 2009). The study of soil carbon stocks in this region might produce relevant information for ecosystem management and conservation practices in arid zones, *e.g.*, for plants arrangement within agroforestry experiences.

The objective of this work is to understand and quantify the influence of the vegetation canopy in the regulation of soil and dead biomass carbon contents in woodlands of Monte region in Argentina. Since the influence of shrubs on carbon inputs is poorly understood, they were compared with the tree canopy effect. The amounts of carbon accumulated in the soil, litter and dead wood in Monte woodlands have been quantified, considering three different treatments: under tree canopy, under shrub canopy and intercanopy.

The hypothesis is that independently of the type of canopy (trees or shrubs; deciduous or semideciduous), the soil, litter and dead biomass carbon stocks in woodlands of Monte region are lower in the intercanopy and higher under the canopy.

METHODS

*Study area.* Monte region is an extended area of about 50 million ha, stretched along 21° of latitude (23°12' to 44°20' S)

at the east of the Andes, and it is the most arid rangeland in Argentina. The elevation ranges between 0 and 3,000 m above sea level (Karlin *et al*. 2017). Water table depth is variable, nonetheless it is usually shallow in forest areas within valleys. The primary soil use is for forestry of native species and extensive livestock of variable intensity. Monte region can be divided into two districts, according to its dominant topography: Southern Monte (of plains and plateaus) and Northern Monte (of mountains and valleys), limiting at 32°50' S latitude (Morello 2012). Despite its extension, the climate, physiognomy and floristic composition, it is relatively homogeneous. Nevertheless, soil features are highly diversified due not only to soil genesis but to anthropic effects such as logging and overgrazing, inducing erosion. Southern Monte is a sandy plain of quaternary fluvial, lacustrine and aeolian origin. Northern Monte is a mountainous area furrowed by intermittent rivers shaping the relief, in which margins the vegetation makes use of the resulting moisture, sometimes resulting in dense forests (Abraham *et al*. 2009).

The climate is arid, with high evapotranspiration rates. Mean annual rainfall varies between < 100 and 450 mm, concentrated in summer, and it is strongly conditioned by topography. Mean annual temperature varies between 10 and 18 °C; the lowest means occur in Northern Monte, with topography-dependent isotherms (Abraham *et al*. 2009). Monte region is a steppe dominated by shrublands of *Larrea* spp. intertwined with open or closed patches of *Prosopis* spp., *Geoffroea decorticans* (Gillies ex Hook. *et* Arn.) Burkart*,* and *Bulnesia retama* (Gillies ex Hook. *et* Arn.) Griseb, (among other species) tree communities. The main species living in Monte region are condensed in table 1, based on Flores *et al*. (2015) and Oyarzábal *et al*. (2018).

The sampling plots were located according to the sampling grid design for the Second National Inventory of Native Forests (Strada *et al*. 2011), consisting of 10 km equidistant points. Sampling plots presenting more than 20 % of tree cover and average height up to 3 m (Argentinian Federal Council for the Environment 2012) and ease of access using 4x4 vehicle and within 2 km by foot from the vehicle were also selected. According to these criteria, 30 sampling plots were selected within Monte region (figure 1), ten from Southern Monte and 20 from Northern Monte. Samplings were made between July and November of 2018, during the dry and windy season.

*Physiognomic-functional traits classification.* In each sampling plot, a plant characterization was made by the phytosociological method (Braun-Blanquet 1979). The sampled area was defined by a radius of 20 m from the central point of the sample plot. Values of cover-abundance of all present plant species were transformed into percent cover values based on the midpoint of each value on the scale (Braun-Blanquet 1979).

With this data, a physiognomic-functional classification of the surveyed woodlands was obtained through con-

glomerate and discriminant analyses. This classification defined environments with different carbon dynamics.

*Sampling design.* In each sampling plot, 20 m long transects were located towards the four cardinal directions (north, south, east, west). Over each transect, two sites were selected as different treatments: under tree canopy (UT) and intercanopy (IC) (figure 2). When any of the described treatments were not present along a transect, samples were taken under shrub canopy (US). A tree is defined as a woody, perennial plant species when over 3 m tall, with one or multiple trunks differentiated from the

**Table 1.** List of the main species living in Monte region.

Lista de las principales especies que viven en la región del Monte.

| Family | Species | Habit |
|---|---|---|
| Asteraceae | *Baccharis salicifolia* (Ruiz *et* Pav.) Pers. | Shrub |
| Asteraceae | *Chuquiraga erinacea* D. Don | Shrub |
| Capparaceae | *Atamisquea emarginata* Miers ex Hook. *et* Arn. | Shrub or tree |
| Celastraceae | *Maytenus viscifolia* Griseb. | Tree |
| Chenopodiaceae | *Allenrolfea vaginata* (Griseb.) Kuntze | Shrub |
| Chenopodiaceae | *Atriplex lampa* (Moq.) D. Dietr. | Shrub |
| Chenopodiaceae | *Suaeda divaricata* Moq. | Shrub |
| Euphorbiaceae | *Jatropha excisa* Griseb. | Shrub |
| Fabaceae | *Vachellia aroma* (Gillies ex Hook. *et* Arn.) Seigler *et* Ebinger | Shrub or tree |
| Fabaceae | *Senegalia gilliesii* (Steud.) Seigler *et* Ebinger | Tree |
| Fabaceae | *Parkinsonia praecox* (Ruiz *et* Pav. ex Hook.) Hawkins | Shrub |
| Fabaceae | *Geoffroea decorticans* (Gillies ex Hook. y Arn.) Burkart | Tree |
| Fabaceae | *Prosopis alpataco* Phil. | Shrub |
| Fabaceae | *Prosopis chilensis* (Molina) Stuntz emend. Burkart | Tree |
| Fabaceae | *Prosopis flexuosa* DC. | Tree |
| Fabaceae | *Prosopis strombulifera* (Lam.) Benth. var. strombulifera | Shrub |
| Fabaceae | *Zuccagnia punctata* Cav. | Shrub |
| Fabaceae | *Parasenegalia visco* (Lorentz ex Griseb.) Seigler *et* Ebinger | Tree |
| Nyctaginaceae | *Bougainvillea spinosa* (Cav.) Heimerl | Shrub |
| Plantaginaceae | *Monttea aphylla* (Miers) Benth. y Hook. | Shrub |
| Poaceae | *Aristida mendocina* Phil. | Grass |
| Poaceae | *Jarava ichu* Ruiz *et* Pav. | Grass |
| Poaceae | *Leptochloa crinita* (Lag.) P.M. Peterson *et* N.W. Snow | Grass |
| Salicaceae | *Salix humboldtiana* Willd. | Tree |
| Solanaceae | *Lycium boerhaviaefolium* L. f. | Shrub |
| Solanaceae | *Lycium chilense* Miers ex Bertero | Shrub |
| Ximeniaceae | *Ximenia americana* L. | Shrub or tree |
| Zygophyllaceae | *Bulnesia retama* (Gillies ex Hook. *et* Arn.) Griseb. | Shrub or tree |
| Zygophyllaceae | *Larrea cuneifolia* Cav. | Shrub |
| Zygophyllaceae | *Larrea divaricata* Cav. | Shrub |
| Zygophyllaceae | *Larrea nitida* Cav. | Shrub |
| Zygophyllaceae | *Plectrocarpa tetracantha* Gillies ex Hook. *et* Arn. | Shrub |

crown. A shrub is defined as a woody, perennial plant species when under 3 m tall, according to Guideline #1.2 Res. 230/12 of the Argentinian Federal Council for the Environment (COFEMA 2012), with the crown undifferentiated from the trunk. In each treatment, the tree and shrub species were identified.

The woody species were classified into two groups, according to deciduousness. Deciduous species are those losing their vegetative or reproductive tissues along a period larger than six months without significant seasonality effects. Semideciduous species are those losing their vegetative or reproductive tissues sporadically or concentrated in only one season. The last group includes those species considered as aphyllous. The deciduous species are represented by *Prosopis* spp., *Geoffroea decorticans*, *Mimozyganthus carinatus*, *Atamisquea emarginata*, *Plectrocarpa tetracantha*, *Vachellia aroma,* and *Allenrolfea* spp. (the last by the release of their strobiles). The semideciduous
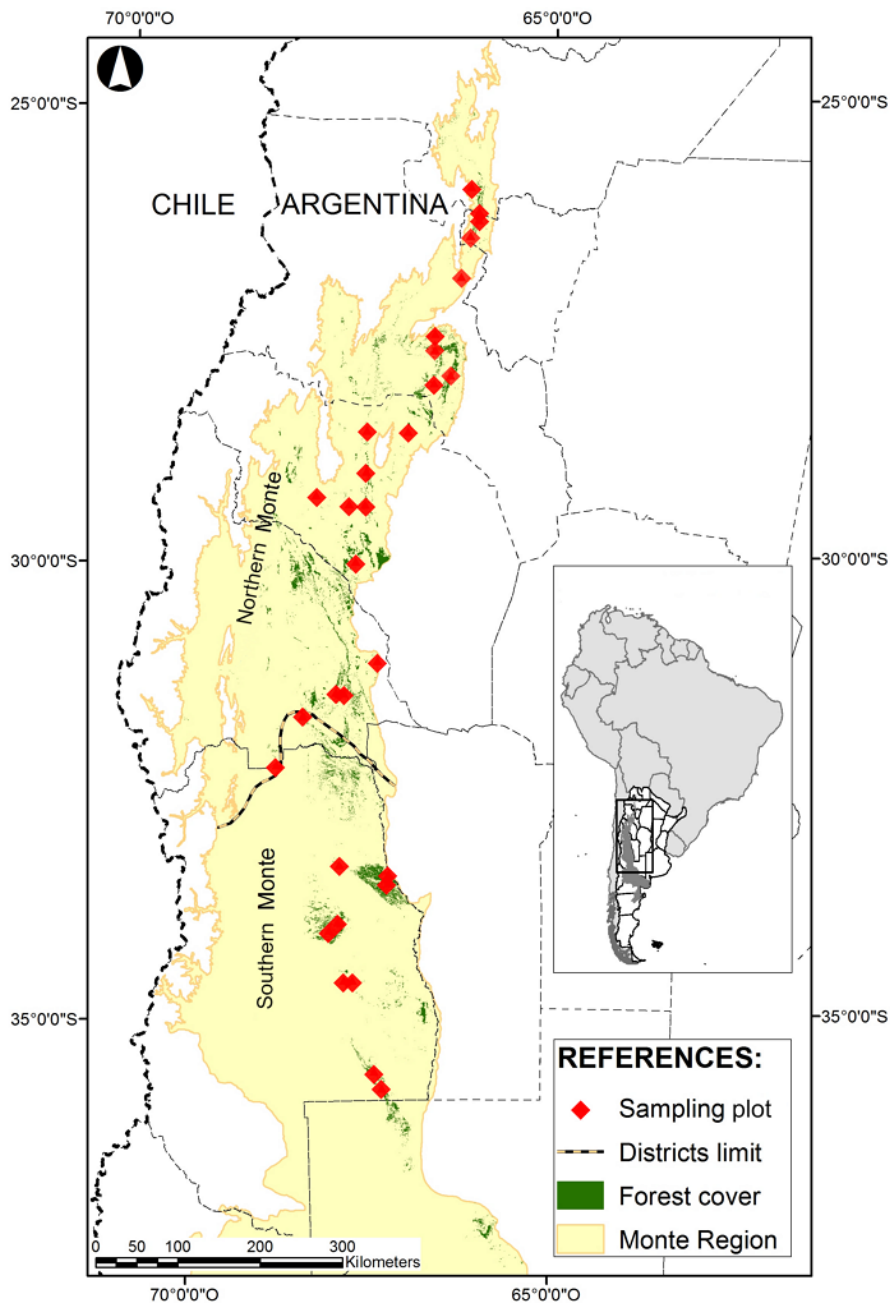


**Figure 1.** Sampling area in Monte region. ♦: Sampling plots. Dark (green) areas: Forest cover.

Área de muestreo en la región Monte. ♦: Parcelas de muestreo. Áreas oscuras (verde): Cobertura forestal.

species are represented by *Bulnesia retama*, *Larrea* spp., *Condalia microphylla,* and *Suaeda divaricata*.

Along each transect, plant cover was measured as the projection of the crown, defining tree and shrub cover in percent. The sectors without crown projection along the transects were identified as intercanopy. In each site, a quadrat of 0.25 m$^2$ was placed to delimit the area for soil and litter sampling. Over each transect, a strip of 10 x 2 m was defined to measure the dead wood presenting more than 5 cm diameter (figure 2).

*Soil bulk density.* A 7 cm diameter and 7 cm height Kopecky cylinder was used to extract undisturbed soil samples for bulk density measurement. The most representative transect in each sample plot was selected, resulting in four soil samples per sample plot: under tree canopy and intercanopy (or under shrub canopy) at 0-7 cm depth and 10-17 cm depth.

Soil samples were carefully pulverized without losing any material and air-dried at 60 °C in a forced-air chamber for three days and weighed. The soil bulk density was the result of the ratio between the dry weight of the sample and the cylinder volume. When soil samples could not be extracted due to the presence of rocks and gravel, soil bulk density was estimated according to its texture, determined by feel analysis (Thien 1979).

With the soil bulk density, soil mass (*SM*) in Mg ha$^{-1}$ was determined for each sample plot, depth and treatment.

*Soil organic carbon stocks.* In each site (under tree canopy and intercanopy –or under shrub canopy–) of each transect, soil samples were taken at 0-5 cm and 5-20 cm depth, following the results of Charley and West (1975). Significant differences in arid soil organic carbon content between these layers were noted. In 20 sites, topsoil samples could not be taken due to the presence of rocks and gravel. In three sample plots from Northern Monte, no 5-20 cm depth samples were taken in any transect for the same reason.

Soil samples were pulverized, sieved and air-dried at 60 °C in a forced-air chamber for three days. Soil organic carbon content (*%C$_s$*) was determined by the method of Walkley and Black (Nelson and Sommers 1974).

Once *%C$_s$* was determined, soil organic carbon stock (*C$_s$*) was calculated in Mg ha$^{-1}$ at the *i$^{th}$* depth, for the *j$^{th}$* treatment:

$$C_{s(i,j)} = SM_{(i,j)} * \%Cs_{(l,j)}/100 \qquad [1]$$

For the determination of soil organic carbon stock per hectare, weighted by the cover (*C$_{s\,W}$*), for each sample plot
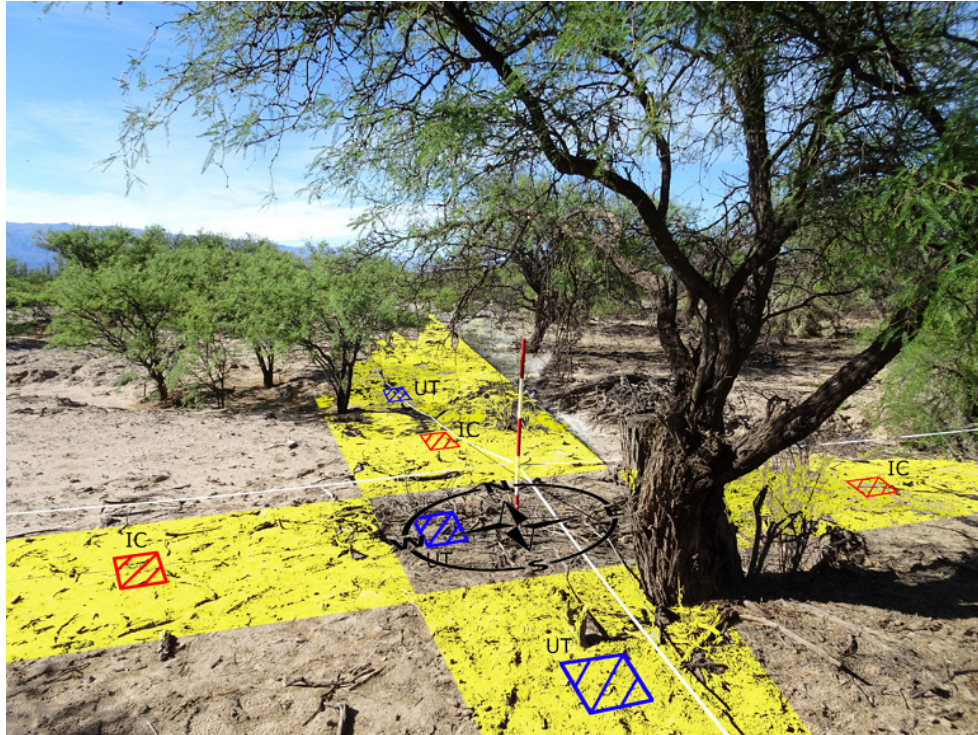


**Figure 2.** Sampling design for each sampling plot. Lighted strips: 10 x 2 m strips for measuring the volume of dead wood with diameter > 5 cm; UT quadrats: under tree canopy treatment; IC quadrats: intercanopy treatment. Photo: R. Zapata.

Diseño del muestreo en cada parcela. Fajas claras: bandas de 10 x 2 m para la medición de volúmenes de madera muerta de diámetro > 5 cm; cuadrantes UT: tratamiento bajo canopia arbórea; cuadrantes IC: tratamiento de intercanopia. Foto: R. Zapata.

at the $i^{th}$ depth and the $j^{th}$ treatment, the following calculation was made:

$$C_{s\,W\,(i,j)} = \sum_j \left( \frac{\sum_n(C_{s\,n} * Cob)}{n} \right)_i \qquad [2]$$

where $\frac{\sum_n(C_{s\,n} * Cob)}{n}$ is the average value (Mg ha$^{-1}$) of the $n$ repetitions for the $C_s$ values, weighted by the canopy percentage.

*Litter carbon stocks.* In each quadrat, litter and dead wood between 1 and 5 cm of diameter were collected separately. No alive grass or herbs were collected, only dead biomass. Samples were air-dried at 60 °C in a forced-air chamber for three days and weighed. From each litter sample, a subsample was extracted, weighed, minced and burned in a muffle furnace (Navarro *et al*. 1993). The muffle was preheated at 100 ºC for 4 h, and afterwards the temperature was increased to 550 ºC for 5 h more. The burned subsample was extracted and weighed, calculating the percentage of organic matter of the sample ($\%OM_L$) from the difference. These values were converted into carbon percentages ($\%C_L$) by using the conversion formula of Navarro *et al*. (1993):

$$\%C_L = \%OM_L * 0.51 + 0.48 \qquad [3]$$

Litter carbon stock ($C_L$) was obtained and extrapolated to an area of 1 ha by multiplying the product of litter mass ($LM$) and $\%C_L$ by 40,000 (0.25 m$^2$ quadrats in 10,000 m$^2$).

For the determination of the litter carbon stock in Mg ha$^{-1}$, weighted by the cover ($C_{L\,W}$) in each sample plot, the following calculation was made:

$$C_{L\,W\,(j)} = \sum_j \left( \frac{\sum_n(C_{L\,n} * Cob)}{n} \right)_j \qquad [4]$$

Where, $\frac{\sum_n(C_{L\,n} * Cob)}{n}$ is the average value (Mg ha$^{-1}$) of the $n$ repetitions of the $C_L$ values, weighted by the canopy cover percentage, and $j$ represents each treatment.

The ratio between the weighted litter carbon stocks under tree and shrub canopy was calculated for each site. This ratio was obtained as an index to quantify the influence of each cover category regarding litterfall.

*Dead wood (1 to 5 cm in diameter) carbon stocks.* The dead wood between 1 and 5 cm in diameter was collected from the quadrats and weighed. Dead wood samples originated predominantly from the species *Prosopis flexuosa* and *Bulnesia retama*. The carbon percentage ($\%C_{DW}$) of one sample of *P. flexuosa* and two samples of *B. retama* were analyzed by the same method and conversion formula as that of litter [3]. Navarro *et al*. (1993) demonstrated that the percentage of carbon in wood is homogeneous.

The carbon stock of the dead wood samples was obtained by multiplying the dead wood mass and $\%C_{DW}$.

The weighted stock ($C_{DW<5\,W}$) in Mg ha$^{-1}$ of the dead wood (1-5 cm in diameter) was calculated with the same formula as that of litter [4].

*Dead wood (diameter > 5 cm) carbon stocks.* Diameter and height of the portions of dead wood branches found inside the 10 x 2 m strips were measured for volume in each quadrant. Seven to nine wood samples per species were immersed in a beaker of water that was placed on a high-precision balance, and the weight of water displacement was converted into volume (Martínez-Cabrera *et al*. 2009). Afterwards, samples were dried in a chamber of forced air at 40 °C for 48 h and weighed. The average value of wood density per species was obtained. Carbon stock ($C_{DW>5}$) was obtained by multiplying dead wood mass to $\%C_{DW}$.

The dead wood larger than 5 cm diameter was extrapolated to one hectare. The total dead wood stock larger than 5 cm diameter ($C_{DW>5}$) per each sample plot was obtained by averaging the values in Mg ha$^{-1}$.

*Statistical analyses.* With the cover-abundance values, characteristic species were selected by discriminating those who had more than 3 % of the cover, on average. With these species, a conglomerate analysis (average linkage; Phi coefficient) was performed for a first tentative classification. Subsequently, with the tentative classification, a discriminant analysis was performed. A physiognomic-functional classification was finally obtained, identifying four plant clusters with different floristic characteristics.

The carbon stocks in each pool were compared between physiognomic-functional traits, treatments and plant deciduousness through ANOVA (LSD Fisher test). Simple regression analyses were made between different carbon pools. All the statistical analyses were performed with InfoStat statistical software (Di Rienzo *et al*. 2018).

RESULTS

*Physiognomic-functional classification.* From the phytosociological analysis, 12 species were selected as characteristic species: *Prosopis flexuosa*, *Bulnesia retama*, *Lycium tenuispinosum*, *Geoffroea decorticans*, *Atamisquea emarginata*, *Larrea cuneifolia*, *Aristida adscensionis*, *Suaeda divaricata*, *Larrea divaricata*, *Jarava ichu*, *Condalia microphylla*, and *Prosopis alpataco*.

The conglomerate and the discriminant analyses defined four physiognomic-functional groups (figure 3):

1) Communities of *Suaeda divaricata*, co-dominated by *Prosopis flexuosa* (n = 2). They were present in mudlands, with silt loam Entisols and shallow water tables.
2) Mixed woodlands (n = 8). Populations of *P. flexuosa*, *G. decorticans*, *L. divaricata*, and *P. alpataco* co-dominated in these woodlands. They were the dominant woody formations in the Southern Monte

district, over Entisols with loamy sand (one plot), sandy loam (five plots), loam (one plot) or silt loam (one plot) textures.

3) Communities of *P. flexuosa* (n = 8). *P. flexuosa* dominated, although some species such as *A. emarginata* or *G. decorticans* stood out. They were associated with Salids with loamy sand (two plots), sandy loam (three plots) or silt loam (one plot) topsoil textures, or Cambids with abundant gravel (2 plots).

4) Communities of *B. retama* (n = 12). Populations of *B. retama* were dominant, but *P. flexuosa* co-dominated sometimes. Their soils were diverse, from Argids or Cambids with abundant gravel and clay (two plots) to Salids (mudflats) with sandy loam (four plots) or silt loam (six plots) topsoil textures.

*Soil organic carbon stocks*. The soil organic carbon stock at 0-5 cm depth ($C_{s\,0-5}$) showed significant differences (table 2) between the intercanopy and tree canopy. The shrub canopy treatment showed no differences with the intercanopy or the tree canopy (F = 14.01; $P < 0.0001$; DF = 2). The intercanopy had approximately half the amount of soil organic carbon than that found under tree canopy treatment. The values shown in table 2 were derived from

the following soil organic carbon percentages: IC = 0.75 ± 0.11 %; UT = 1.68 ± 0.11 %; US = 1.16 ± 0.21 %.

The soil organic carbon stock at 5-20 cm depth ($C_{s\,5-20}$) was significantly lower in the intercanopy than under the tree canopy (F = 6.05; $P = 0.0030$; DF = 2). Under shrub canopy showed no difference with either the intercanopy or the under-tree canopy treatment (table 2). The values shown in table 2 were derived from the following soil organic carbon percentages ($\%C_s$): IC = 0.61 ± 0.07 %; UT=0.99 ± 0.07 %; US = 0.78 ± 0.12 %. Differences among treatments at 5-20 cm depth were less contrasting than those in the surface.

Soil organic carbon percentage ($\%C_s$) showed significant differences between 0-5 and 5-20 cm depth under tree canopy (n = 139; F = 15.83; $P < 0.0001$), and a marginal difference ($0.1 > P > 0.05$) under shrub canopy (n = 42; F = 3.60; $P = 0.0652$) and in the intercanopy (n = 143; F = 2.90; $P = 0.0908$).

When weighted by the cover percentages (table 2), soil organic carbon showed similar differences between treatments at the surface (F = 3.93; $P = 0.0019$; DF = 2), nevertheless did not differ statistically among treatments in the deeper layer (F = 0.61; $P = 0.5466$; DF = 2). The surveyed covered area (under tree canopy plus shrub canopy) was on average 40 % of the total surface.
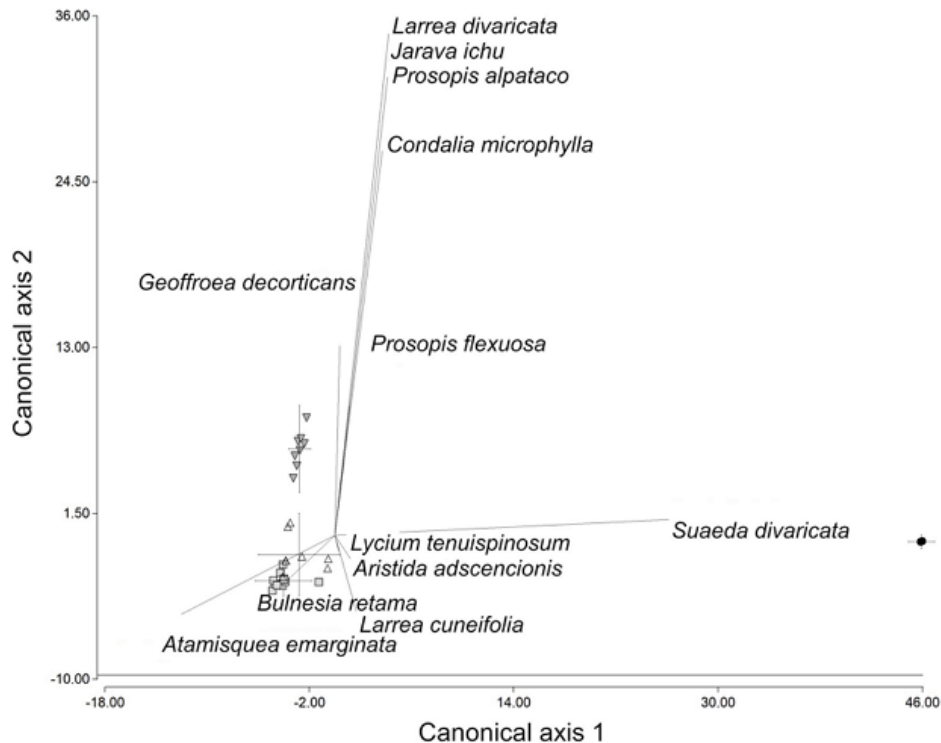


**Figure 3.** Discriminant analysis, with prediction intervals associated with the four groups: ●, communities of *S. divaricata*, co-dominated by *P. flexuosa*; ▼, mixed woodlands; Δ, communities of *P. flexuosa*; □, communities of *B. retama*.

Análisis discriminante, con intervalos de predicción asociados a los cuatro grupos: ●, comunidades de *S. divaricata*, co-dominados por *P. flexuosa*; ▼, bosques mixtos; Δ, comunidades de *P. flexuosa*; □, comunidades de *B. retama*.

**Table 2.** Stocks (Mg ha$^{-1}$) of soil organic carbon, litter carbon, and dead wood carbon, by treatment. IC: Intercanopy, UT: under tree canopy, US: under shrub canopy. Different letters show statistically significant differences among treatments at $P = 0.05$.

Contenidos (Mg ha$^{-1}$) de carbono orgánico del suelo, carbono de mantillo y carbono de madera muerta, por tratamiento. IC: espacio fuera del dosel, UT: bajo dosel arbóreo, US: bajo dosel arbustivo. Letras diferentes indican diferencias estadísticamente significativas entre tratamientos al $P = 0,05$.

| Treatment | | IC | By soil cover | | By deciduousness | |
|---|---|---|---|---|---|---|
| | | | UT | US | Semideciduous | Deciduous |
| Soil organic carbon stock (0-5 cm depth) | n | 74 | 72 | 21 | 27 | 66 |
| | Mean | 5.74 ± 0.77 (aA) | 11.52 ± 0.78 (b) | 8.33 ± 1.44 (ab) | 8.26 ± 1.26 (A) | 11.84 ± 0.81 (B) |
| Soil organic carbon stock (5-20 cm depth) | n | 69 | 67 | 21 | 25 | 63 |
| | Mean | 14.60 ± 1.43 (aA) | 21.76 ± 1.47 (b) | 18.26 ± 2.62 (ab) | 16.19 ± 2.37 (A) | 22.80 ± 1.49 (B) |
| Weighted soil organic carbon stock (0-5 cm depth) | n | 74 | 72 | 21 | 27 | 66 |
| | Mean | 3.44 ± 0.53 (aA) | 5.53 ± 0.54 (b) | 3.93 ± 1.00 (ab) | 4.05 ± 0.88 (AB) | 5.62 ± 0.56 (B) |
| Weighted soil organic carbon stock (5-20 cm depth) | n | 69 | 67 | 21 | 25 | 63 |
| | Mean | 8.79 ± 1.70 | 10.03 ± 0.95 | 8.33 ± 1.70 | 7.66 ± 1.55 | 10.40 ± 0.98 |
| Litter carbon stock | n | 98 | 94 | 26 | 29 | 91 |
| | Mean | 0.38 ± 0.39 (aA) | 5.64 ± 0.40 (b) | 3.02 ± 0.75 (c) | 2.68 ± 0.70 (B) | 5.83 ± 0.39 (C) |
| Weighted litter carbon stock | n | 98 | 94 | 26 | 29 | 91 |
| | Mean | 0.20 ± 0.22 (aA) | 2.67 ± 0.22 (b) | 1.76 ± 0.42 (b) | 1.44 ± 0.39 (B) | 2.81 ± 0.22 (C) |
| Dead wood carbon stock (diameter < 5 cm) | n | 98 | 94 | 26 | 29 | 91 |
| | Mean | 0.15 ± 0.13 (aA) | 1.05 ± 0.13 (b) | 0.67 ± 0.24 (ab) | 0.46 ± 0.23 (A) | 1.14 ± 0.13 (B) |
| Weighted dead wood carbon stock (diameter < 5 cm) | n | 98 | 94 | 26 | 29 | 91 |
| | Mean | 0.09 ± 0.08 (aA) | 0.52 ± 0.08 (b) | 0.35 ± (0.15) (ab) | 0.24 ± 0.14 (A) | 0.56 ± 0.08 (B) |

**Table 3.** Stocks (Mg ha$^{-1}$) of the weighted soil organic carbon, litter carbon and dead wood carbon, by physiognomic-functional group.

Contenidos (Mg ha$^{-1}$) del carbono orgánico del suelo ponderado, del carbono de la hojarasca y del carbono de la madera muerta, por grupo fisonómico-funcional.

| Group | | Comm. *S. divaricata* | Mixed woodland | Comm. *P. flexuosa* | Comm. *B. retama* |
|---|---|---|---|---|---|
| Weighted soil organic carbon stock (0-5 cm depth) | n | 2 | 8 | 8 | 12 |
| | Mean | 7.98 ± 4.59 | 7.56 ± 2.30 | 13.83 ± 2.30 | 7.09 ± 1.88 |
| Weighted soil organic carbon stock (5-20 cm depth) | n | 2 | 8 | 7 | 10 |
| | Mean | 20.04 ± 5.60 | 15.95 ± 2.80 | 21.28 ± 2.99 | 15.72 ± 2.51 |
| Weighted litter carbon stock | n | 2 | 8 | 8 | 12 |
| | Mean | 2.60 ± 1.57 | 2.99 ± 0.79 | 3.85 ± 0.79 | 2.16 ± 0.64 |
| Weighted dead wood carbon stock (diameter < 5 cm) | n | 2 | 8 | 8 | 12 |
| | Mean | 1.15 ± 0.45 | 0.38 ± 0.23 | 0.98 ± 0.23 | 0.34 ± 0.18 |
| Dead wood carbon stock (diameter > 5 cm) | n | 2 | 8 | 8 | 12 |
| | Mean | 2.41 ± 1.25 | 0.59 ± 0.62 | 2.20 ± 0.62 | 1.07 ± 0.51 |
| Total carbon stock | n | 2 | 8 | 7 | 10 |
| | Mean | 34.18 ± 8.53 | 27.48 ± 4.27 | 38.62 ± 4.56 | 25.55 ± 3.82 |

Deciduous plant cover showed significantly larger amounts of soil organic carbon mass (table 2) than those shown by semideciduous plant cover and the intercanopy (0-5 cm: F = 15.10, $P < 0.0001$, DF = 2; 5-20 cm F = 8.30, $P = 0.0004$, DF = 2). Deciduous plant cover differed at the surface from the intercanopy though not from the semideciduous cover (F = 4.08, $P = 0.0186$; DF = 2) in the weighted soil organic carbon stock (table 2). In the deeper layer, no significant differences were found (F = 1.34; $P = 0.2637$; DF = 2).

When soil organic carbon stock was compared among physiognomic-functional groups at both depths (table 2), no significant differences were found in the average values per sample plot (0-5 cm: F = 1.96, $P = 0.1446$, DF = 3; 5-20 cm: F = 0.87; $P = 0.4714$, DF = 3). The sample plot with the largest contents of soil organic carbon stock for the 0-20 cm layer represented 47.44 Mg ha$^{-1}$ in carbon. This plot was from a closed *P. flexuosa* woodland located in the Pipanaco saline basin (Catamarca).

The total soil organic carbon stock (0-20 cm) did not differ significantly between districts. Northern Monte District showed average values of 25.00 ± 2.69 Mg ha$^{-1}$ (n = 17), while Southern Monte District had 26.44 ± 3.50 Mg ha$^{-1}$ (n = 10) (F = 0.11, $P = 0.7464$). The former derived from the weighted average (0-20 cm depth) in soil organic percentages of 1.32 % under canopy and 0.66 % in the intercanopy.

The soil organic carbon stock at both depths were significantly correlated ($C_{s\ 5-20}$ = 5.98 + 1.47 * $C_{s\ 0-5}$; $R^2$ = 0.52; $P < 0.0001$; n = 157), indicating that subsoil carbon stock can be estimated by topsoil carbon stock with regression equation.

*Litter carbon stocks.* Despite the variety of materials accumulated as litter in the topsoil, litter carbon contents ($\%C_L$) were relatively constant with 40.76 % average, 41.89 % median and 13.77 % coefficient of variation (n = 212). No statistically significant differences were obtained between the litter carbon contents related to the covering species (n = 126; F = 0.94; $P = 0.5078$). No difference was found comparing plant cover (n = 212; F = 0.68; $P = 0.5073$) or deciduousness (n = 212; F = 0.94; $P = 0.3928$).

Litter carbon stock ($C_L$) showed significant differences (table 2) among the intercanopy, under shrub canopy and tree canopy (F = 45.73; $P < 0.0001$; DF = 2). The weighted litter carbon stock showed similar tendencies although did not differ between shrub and tree canopy treatments (F = 32.35; $P < 0.0001$; DF = 2).

When compared between districts, no significant differences were obtained for the weighted litter stocks ($C_{L\ W}$), discriminating by each soil cover type (IC: n = 98; F = 1.74; $P = 0.1897$. UT: n = 94; F = 2.09; $P = 0.1521$. US: n = 26; F = 0.82; $P = 0.3733$). However, the average UT:US weighted litter stock ratio differed between Northern (1.03:1) and Southern (2.45:1) Monte Districts. The average litter stock ratio for all sites was 1.52:1.

Deciduousness had a clear and significant effect over the stocks of litter accumulated above the soil (table 2), with deciduous cover almost doubling the effect of semideciduous cover, for both unweighted and weighted values ($C_L$: F = 49.69, $P < 0.0001$, DF = 2; $C_{L\ W}$: F = 35.87, $P < 0.0001$, DF = 2). Litter carbon stock did not significantly differ between physiognomic-functional groups (F = 0.94; $P = 0.4344$; DF = 3). Nevertheless, a tendency for higher litter carbon stock was noted for the communities of *P. flexuosa* (table 3). *Prosopis* had twice as large litterfall input as that of *Bulnesia* cover (3.03 vs. 1.50 Mg ha$^{-1}$ when values were weighted by plant cover). Litter carbon input seems to explain soil organic carbon at both depths by significant regressions. The following regression was found for topsoil organic carbon stock: $C_{s\ 0-5}$ = 6.08 + 0.95 * $C_L$ ($R^2$ = 0.30; $P < 0.0001$; n = 166). For subsoil organic carbon stock, the following regression was found: $C_{s\ 5-20}$ = 14.87 + 1.33 * $C_L$ ($R^2$ = 0.15; $P = 0.0001$; n = 156) (figure 4).



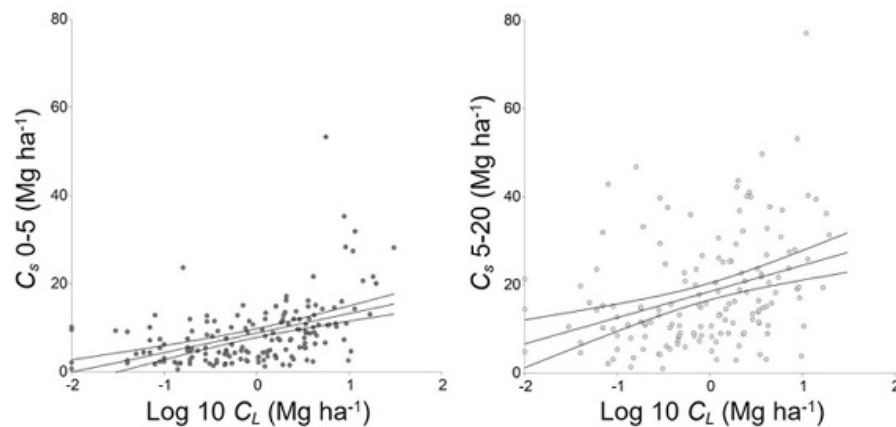**Figure 4.** Soil organic carbon stocks ($C_s$) at 0-5 and 5-20 cm depth and Log 10 litter carbon stock ($C_L$) regression. Midline: mean regression line; lateral lines: confidence bands.

Regresión entre los contenidos de carbono orgánico del suelo ($C_s$), a profundidades de 0-5 y 5-20 cm, y Log 10 de los contenidos de carbono de mantillo ($C_L$). Línea media: función de regresión; líneas laterales: bandas de confianza.

*Dead wood (1 to 5 cm in diameter) carbon stocks.* Trees produced substantial amounts of small branches and twigs that were deposited on the soil, significantly different from the dead wood stocks accumulated in the intercanopy (table 2). Shrubs made a modest input of dead wood, although did not differ significantly from the intercanopy ($C_{DW<5}$: F = 12.97, $P < 0.0001$, DF = 2; $C_{DW<5\ W}$: F = 7.34, $P = 0.0008$, DF = 2).

The litter accumulated under deciduous vegetation was twice as that of semideciduous vegetation, and it was six times larger than that in the intercanopy ($C_{DW<5}$: F = 15.61, $P < 0.0001$, DF = 2; $C_{DW<5\ W}$: F = 8.97, $P = 0.0002$, DF = 2) (table 2).

Physiognomic-functional groups did not differ significantly in the diameter < 5 cm dead wood inputs (table 3). However, there was a marginal difference between mixed woodlands and communities of *B. retama*, when compared to the communities of *S. divaricata* and *P. flexuosa*, with p-values at 0.1 (F = 2.64; $P = 0.0912$; DF = 3). The latter accumulated large amounts of dead wood under 5 cm in diameter.

*Dead wood (diameter > 5 cm) carbon stocks.* Dead wood volumes were multiplied by the following densities; *P. flexuosa*: $0.75 \pm 0.03$ Mg m$^{-3}$ (n = 7); *S. divaricata*: $0.66 \pm 0.02$ Mg m$^{-3}$ (n = 9); *B. retama*: $0.80 \pm 0.02$ Mg m$^{-3}$ (n = 9); *G. decorticans*: $0.53 \pm 0.02$ Mg m$^{-3}$ (n = 8).

Since the dead wood compartment was quantified independently from the identified treatments within each sample plot, it was only possible to compare among physiognomic-functional groups (table 3). This variable showed no statistical difference among groups (F = 1.45; $P = 0.2524$; DF = 3). The two dead wood categories had a positive and significant relationship between each other ($C_{DW>5} = 0.29 + 1.81 * C_{DW<5}$; $R^2 = 0.47$; $P < 0.0001$; n = 30).

*Total dead organic carbon stocks.* The sum of the three pools (soil organic carbon, litter, and dead wood) represented significant stocks for all the four physiognomic-functional groups (table 3). *Prosopis* spp. woodlands accumulated more than 38 Mg ha$^{-1}$ of dead organic carbon, followed by *Suaeda* spp. woodlands with almost 35 Mg ha$^{-1}$. Mixed woodlands, representative from Southern Monte District, showed average values around 27 Mg ha$^{-1}$, while *Bulnesia* spp. woodlands were the poorest with around 25 Mg ha$^{-1}$. No statistical differences were found among groups (F = 1.84; $P = 0.1683$; DF = 3); nevertheless, *P. flexuosa* communities were marginally different ($P < 0.1$) from *B. retama* communities, when separately compared from the rest (F = 4.09; $P = 0.0614$; DF = 1).

DISCUSSION

Deciduousness, *i.e.*, deciduous vs. semideciduous, has a more significant effect over soil organic carbon stocks than does soil cover, *i.e.*, tress vs. shrubs. The deciduousness has an important influence in the topsoil (0-5 cm), although its effect is diluted in the subsoil (5-20 cm).

Few studies have surveyed soil organic carbon stocks in arid land regions by discriminating strata within the first five centimeters of soil depth. For example, Charley and West (1975) found for Utah rangelands important differences in the soil organic carbon stocks by comparing three depths within the top 20 cm depth. They suggest that the lack of soil mixing, litter input, and the low precipitations in arid lands, are the leading causes of carbon layering, even within the first centimeters of soil depth.

Soil organic carbon stocks per site are strongly dependent on the proportion of soil under the canopy and off the canopy. Alvarez *et al*. (2009) made the same conclusions for Ñacuñán woodlands in Southern Monte. Therefore, the elimination of plant cover should have a substantial effect on the total amounts of organic carbon accumulated in arid environments.

Tree and herbaceous plant suppression may promote encroaching of semideciduous species such as *Larrea* spp. (Villagra *et al*. 2009). Shrub encroachment reduces the amount of total litter deposited in the soil by almost 50 % (see $C_L$ under tree canopy vs. under shrub canopy in table 2). Since litter is the primary source of soil organic carbon, a reduction in its deposition may affect the stocks of soil organic carbon. *Larrea* spp., a common shrubby species in Monte woodlands, may contribute to soil carbon stocks (as Eldridge *et al*. 2011, state for *Larrea* shrublands in the USA), though it may never reach the litter input levels of *Prosopis* spp. due to its semideciduousness and lower canopy volume.

The average ratio between the UT:US weighted litter carbon stocks found in this work (1.52:1) is similar to the annual litterfall ratio measured by Alvarez *et al*. (2009), who compared *Prosopis* spp. and *Larrea* spp. litterfall (1.4 to 1.8 in 1). By district, the average ratio for the Southern Monte (2.45:1) recorded here (and where these authors made their study) surpasses those obtained by Alvarez *et al*. (2009), while the ratio for Northern Monte (1.03:1) is quite lower. The differences between districts are mainly due to the species found in each; no communities of *B. retama*, with lower inputs of litter, were measured in Southern Monte. Differences with Alvarez *et al*. (2009) might depend on the sampling moment and the input of other species rather than *Prosopis* spp. and *Larrea* spp.

The difference between the unweighted and the weighted litter input between under tree canopy and shrub canopy suggests that trees and shrubs release different amounts of litter per surface unit (m$^2$). However, ultimately this effect will be dependent on the relative cover of each type within each sample plot. Litter contents in the intercanopy are quite low due probably to slope effect, high rainfall intensity and, consequently, to runoff effect. Intercanopy areas are away from canopy influence, where cattle can move freely producing significant erosive impact. Such effect alters microtopography, forming pedes-

tals under trees and shrubs, and gullies in inter-patches. During the rainy season, water moves through gullies dragging litter away.

Dead wood is an important carbon pool. Nevertheless, the fraction of dead wood between 1 and 5 cm in diameter represents approximately one-fifth of the litter fraction, while dead wood with more than 5 cm in diameter represents almost half. Both dead wood fractions are quite variable, and their inputs depend on the climatic conditions such as rainfall or wind (Alvarez *et al*. 2009). The values obtained for dead wood in this study are slightly superior to those reported by Woodall and Liknes (2008) for drylands in the United States. Unfortunately, these authors do not detail to which species corresponds the measured dead wood, nor the sampling season.

Deciduousness is the cause that explains the large carbon stocks found in the communities of *P. flexuosa*, despite the lack of significant differences ($P = 0.05$) from other plant communities. Soil organic carbon and litter are the main carbon pools in these communities. These communities are usually associated with shallow water tables, increasing the total productivity, and therefore, the amount of litter input.

In the mixed woodlands, predominantly from Southern Monte, organic carbon contents in soil and dead wood are below the average. In this group, soil organic carbon percentages are similar to those reported by Rossi and Villagra (2003) for the same district. When converted into organic matter ($f = 0.58$), weighted by soil depth (0-20 cm) and discriminated by quadrant and soil cover, organic matter percentages are 2.28 % in under canopy and 1.14 % in the intercanopy. These can be compared with 2.06 % of under canopy and 0.74 % of the intercanopy, obtained by these authors.

The communities of *B. retama* have the lowest total carbon stocks, also due to deciduousness. *Bulnesia retama* is an aphyllous species that produces small amounts of litter, and this is reflected in low soil organic carbon stocks (Tapia and Martinelli 2019).

The communities of *S. divaricata* show relevant carbon stocks as soil organic carbon at 5-20 cm depth and dead wood. During the dry season in the mudflats, dust is removed from adjacent denuded areas and accumulated by deposition at the feet of the shrubs, burying the topsoil organic matter and incorporating it into the soil. Such a phenomenon is quite usual in arid lands and is the cause of the soil mixing and the inclusion of organic matter into the soil, increasing subsoil fertility (Moorhead and Reynolds 1991).

The total dead organic carbon stocks in these four communities can be related to the above-ground biomass contents measured by Iglesias *et al*. (2012) in Telteca Reserve (figure 5). The alive/dead carbon biomass ratio for the communities of *P. flexuosa,* compared with the 48 Mg ha⁻¹ of carbon in "mature forests of *P. flexuosa*," is 1.24. In the mixed woodlands compared with the 33 Mg ha⁻¹ carbon in "mixed forests," it is 1.20. In the *S. divaricata* communi-

ties compared with the 21 Mg ha⁻¹ carbon in "open forests with shrubs," it is 0.61. Finally, in *B. retama* communities compared with the 8 Mg ha⁻¹ carbon in "open shrublands," it is 0.31. The latter relates with a reduced total plant cover, characteristic in the *B. retama* communities (Tapia and Martinelli 2019), a reduced litter production and a reduced decay of dead wood due to its high density and hardness.

In this analysis (and for all the four groups), we missed the soil organic carbon from below 20 cm of depth, which according to Jobbágy and Jackson (2000), constitute considerable stocks.

Soil organic carbon and litter stocks can be compared with other ecosystems. In semiarid Chaco, with 550 mm y⁻¹ of precipitation, Abril and Bucher (2001) report 70.5, 31.0, and 15.0 Mg ha⁻¹ of soil organic carbon (0-20 cm depth) for highly restored, moderately restored and highly degraded woodlands, respectively. Regarding litter stocks, these authors report 2.60, 2.29 and 0 Mg ha⁻¹ for the same types of woodland, respectively. The four physiognomic-functional groups can be compared with the moderately restored woodland in terms of soil organic carbon (ranging between ca. 23 and 37 Mg ha⁻¹ for 0-20 cm depth) and litter stocks (ranging between *ca.* 2.5 and 5 Mg ha⁻¹, by adding litter and dead wood < 5 cm). Compared with a subtropical rainforest in Misiones (Argentina), with 1,800 mm y⁻¹
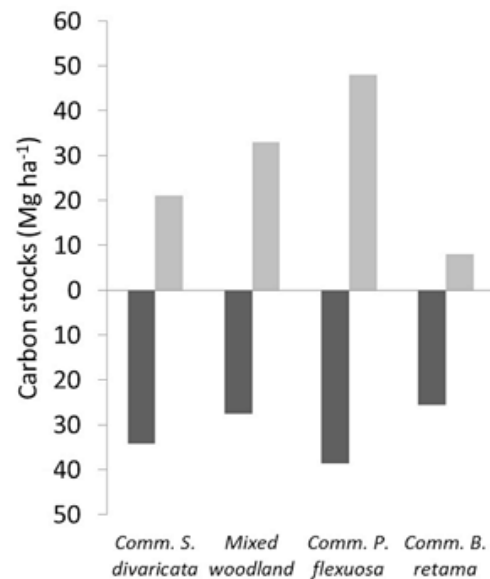


**Figure 5.** Carbon stocks in each physiognomic-functional group. In light gray, above-ground biomass carbon contents obtained by Iglesias *et al*. (2012) for Telteca Reserve; in dark gray, dead carbon biomass (soil organic carbon, litter carbon, and dead wood carbon) obtained in this study.

Contenidos de carbono en cada grupo fisonómico-funcional. En gris claro, contenidos de carbono de la biomasa aérea obtenidos por Iglesias *et al*. (2012) para la Reserva Telteca; en gris oscuro, el carbono de la biomasa muerta (carbono orgánico del suelo, carbono del mantillo y carbono de la madera muerta) obtenido para este estudio.

of precipitation, the average soil organic carbon stock in Monte region is less than half. Piccolo *et al*. (2008) report soil organic carbon contents (at 0-15 cm depth) in a Kandihumult soil of 58.9 Mg ha$^{-1}$. It can be contrasted with the 47.44 Mg ha$^{-1}$ obtained in a closed *P. flexuosa* woodland (at 0-20 cm depth). The reported litter stocks in a mature rainforest, also in Misiones, are of *ca*. 5 Mg ha$^{-1}$ (Vaccaro *et al*. 2003). Despite the evident ecological differences from rainforests, especially in soil organic carbon content, *P. flexuosa* woodlands have the potential for reaching slightly lesser levels of soil carbon content than that reached by rainforests.

These results partially confirm the hypothesis. The carbon contents in the intercanopy are significantly reduced compared to areas under canopy. However, trees, and especially deciduous ones, produce larger amounts of litter that affect the soil organic carbon stocks. Despite that shrubs drive the soil into reduced carbon contents compared to trees, they might be important as transitional functional types to regulate carbon stocks along successional pathways.

## CONCLUSIONS

The vegetation canopy, and consequently, the litter input within fertile patches affect soil organic carbon in the topsoil. Nevertheless, carbon inputs are intimately dependent on plant functionality, such as deciduousness or canopy volume. Therefore, shrubs (especially semideciduous such as *Larrea* spp.) have a restricted ability to enrich the soil compared to deciduous trees such as *Prosopis* spp.

Soil, litter and dead wood are important pools of carbon compared to above-ground biomass in Monte region. The communities of *P. flexuosa* are the largest carbon sinks in this region. Closed *Prosopis* spp. formations can even be compared in terms of accumulated carbon, with ecosystems from more humid regions.

Soils and dead biomass can become significant pools of carbon storage in drylands compared to above-ground biomass. This aspect should be considered in programs on reducing emissions in arid regions.

## ACKNOWLEDGMENTS

## REFERENCES

Abraham E, HF Del Valle, F Roig, L Torres, JO Ares, F Coronato, R Godagnone. 2009. Overview of the geography of the Monte Desert biome (Argentina). *Journal of Arid Environments* 73(2): 144-153. DOI: https://doi.org/10.1016/j.jaridenv.2008.09.028

Abril A, EH Bucher. 2001. Overgrazing and soil carbon dynamics in the western Chaco of Argentina. *Applied Soil Ecology* 16(3): 243-249. DOI: https://doi.org/10.1016/S0929-1393(00)00122-0

Alvarez JA, PE Villagra, BE Rossi, EM Cesca. 2009. Spatial and temporal litterfall heterogeneity generated by woody species in the Central Monte desert. *Plant Ecology* 205(2): 295-303. DOI: https://doi.org/10.1007/s11258-009-9618-z

Braun-Blanquet J. 1979. Fitosociologia. Bases para el estudio de las comunidades vegetales. Madrid, España. Blume Ediciones. 820 p.

COFEMA (Consejo Federal de Medio Ambiente, AR). 2012. Res. 230/12. http://argentinambiental.com/legislacion/nacional/resolucion-23012-bosques-nativos/

Charley JL, NE West. 1975. Plant-induced soil chemical patterns in some shrub-dominated semi-desert ecosystems of Utah. *Journal of Ecology* 63(3): 945-963. DOI: https://www.jstor.org/stable/2258613

Di Rienzo JA, F Casanoves, MG Balzarini, L Gonzalez, M Tablada, CW Robledo. 2018 InfoStat versión 2018. Grupo InfoStat, FCA, Universidad Nacional de Córdoba, Argentina. URL http://www.infostat.com.ar

Eldridge DJ, MA Bowker, FT Maestre, E Roger, JF Reynolds, WG Whitford. 2011. Impacts of shrub encroachment on ecosystem structure and functioning: towards a global synthesis. *Ecological Letters* 14(7): 709-722. DOI: https://doi.org/10.1111/j.1461-0248.2011.01630.x

Flores DG, G Suvires, A Dalmasso. 2015. Distribución de la vegetación nativa en ambientes geomorfológicos cuaternarios del Monte Árido Central de Argentina. *Revista Mexicana de Biodiversidad* 86(1): 72-79. DOI: http://dx.doi.org/10.7550/rmb.40248

Iglesias MR, A Barchuk, MP Grilli. 2012. Carbon storage, community structure and canopy cover: A comparison along a precipitation gradient. *Forest Ecology and Management* 265: 218-229. DOI: https://doi.org/10.1016/j.foreco.2011.10.036

Jobbágy EG, RB Jackson. 2000. The vertical distribution of soil organic carbon and its relation to climate and vegetation. *Ecological Applications* 10(2): 423-436. DOI: https://doi.org/10.1890/1051-0761(2000)010[0423:TVDOSO]2.0.CO;2

Karlin UO, MS Karlin, RM Zapata, RO Coirini, AM Contreras, M Carnero. 2017. La Provincia Fitogeográfica del Monte: límites territoriales y su representación. *Multequina* 26: 63-75.

Martínez-Cabrera HI, CS Jones, S Espino, HJ Schenk. 2009. Wood anatomy and wood density in shrubs: responses to varying aridity along transcontinental transects. *American Journal of Botany* 96(8): 1388-1398. DOI: https://doi.org/10.3732/ajb.0800237

Moorhead DL, JF Reynolds. 1991. A general model of litter decomposition in the northern Chihuahuan Desert. *Ecological Modelling* 56: 197-219. DOI: https://doi.org/10.1016/0304-3800(91)90200-K

Morello J. 2012. Ecorregión del Monte de Sierras y Bolsones. *In* Morello J, SD Matteucci, AF Rodriguez, ME Silva eds. Ecorregiones y complejos ecosistémicos argentinos. Buenos Aires, Argentina. FADU-GEPAMA. p. 265-291.

Navarro AF, J Cegarra, A Roig, D Garcia. 1993. Relationships between organic matter and carbon contents of organic wastes. *Bioresource Technology* 44(3): 203-207. DOI: https://doi.org/10.1016/0960-8524(93)90153-3

Nelson DW, LE Sommers. 1974. A rapid and accurate procedure for estimation of organic carbon in soils. *Proceedings of the Indiana Academy of Science* 84: 456-462.

Oyarzábal M, JR Clavijo, LJ Oakley, F Biganzoli, PM Tognetti, IM Barberis, HM Maturo, R Aragón, PI Campanello, D Prado, M Oesterheld, R León. 2018. Unidades de vegetación de la Argentina. *Ecología Austral* 28(1): 40-63. DOI: https://doi.org/10.25260/EA.18.28.1.0.399

Piccolo GA, AE Andriulo, B Mary. 2008. Changes in soil organic matter under different land management in Misiones province (Argentina). *Scientia Agricola* 65(3): 290-297. DOI: http://dx.doi.org/10.1590/S0103-90162008000300009

Roig FA, S Roig-Juñent, V Corbalán. 2009. Biogeography of the Monte Desert. *Journal of Arid Environments* 73: 164-172. DOI: https://doi.org/10.1016/j.jaridenv.2008.07.016

Rossi BE, PE Villagra. 2003. Effects of *Prosopis flexuosa* on soil properties and the spatial pattern of understorey species in arid Argentina. *Journal of Vegetation Science* 14(4): 543-550. DOI: https://doi.org/10.1111/j.1654-1103.2003.tb02181.x

Strada M, MG Parmuchi, E Wabo. 2011. Propuesta de Programa Nacional de Inventario de Bosques Nativos para la República Argentina. Grilla Nacional. Buenos Aires, Argentina.

Dirección de Bosques, Secretaría de Ambiente y Desarrollo Sustentable de la Nación.

Tapia R, M Martinelli. 2019. Impacto de *Bulnesia retama* (Zigofilácea) sobre la tasa de infiltración en un sitio piloto ubicado en la zona sur de la cuenca del Bermejo, San Juan (Argentina). *Multequina* 28: 47-57.

Thien SJ. 1979. A flow diagram for teaching texture by feel analysis. *Journal of Agronomic Education* 8(1): 54-55. DOI: https://doi.org/10.2134/jae.1979.0054

Trumper K, C Ravilious, B Dickson. 2008. Carbon in drylands: desertification, climate change and carbon finance. Istanbul, Turkey. UNEP-UNDP-UNCCD. 12 p.

Vaccaro S, MF Arturi, JF Goya, JL Frangi, G Piccolo. 2003. Almacenaje de carbono en estadios de la sucesión secundaria en la provincia de Misiones, Argentina. *Interciencia* 28(9): 521-527.

Villagra PE, GE Defossé, HF Del Valle, S Tabeni, M Rostagno, E Cesca, E Abraham. 2009. Land use and disturbance effects on the dynamics of natural ecosystems of the Monte Desert: implications for their management. *Journal of Arid Environments* 73(2): 202-211. DOI: https://doi.org/10.1016/j.jaridenv.2008.08.002

Woodall CW, GC Liknes. 2008. Climatic regions as an indicator of forest coarse and fine woody debris carbon stocks in the United States. *Carbon Balance and Management* 3(1): 5. DOI: https://doi.org/10.1186/1750-0680-3-5

Yang Y, A Mohammat, J Feng, R Zhou, J Fang. 2007. Storage, patterns and environmental controls of soil organic carbon in China. *Biogeochemistry* 84(2): 131-141. DOI: https://doi.org/10.1007/s10533-007-9109-z

# Oribatid mite (Acari, Oribatida) richness and diversity in Oak forests of West Azerbaijan Province (Northwestern Iran)

## Riqueza y diversidad del ácaro oribátido (Acari, Oribatida) en los bosques de robles de la provincia de Azerbaiyán occidental (noroeste de Irán)

**Mahtab Jabbari [a], Javad Eshaghi Rad [a*], Zahra Hashemi Khabir [b], Seyed Rostam Mousavi Mirkala [a]**

*Corresponding author: [a] Urmia University, Faculty of Natural Resources, Department of Forestry, Urmia, Iran, tel.: +98 4432770489, j.eshagh@urmia.ac.ir

[b] Agricultural and Natural Resources Research center, Department of Plant protection, Urmia, Iran.

### SUMMARY

Up to now, oribatid mite richness and diversity have not been studied in oak forests of Iran. This study aimed at determining the relationships among Oribatid mite composition, richness and diversity as well as ecological factors such as elevation, soil pH and soil moisture, tree species and stand density in oak forests in northwestern Iran. Thirty samples were randomly arranged at three elevation levels (1,000-1,300 m, 1,300-1,500 m and 1,500-1,650 m). Results indicated that 42 oribatid mite species were recorded in the study area. Nine and six species were exclusively observed in the elevations 1,100-1,300 and 1,300-1,500 m, respectively; while five mite species were commonly recorded in these two elevation categories. The study revealed that oribatid mite composition was affected by elevation gradient; however, the mean differences of species richness and diversity indices were not significant among elevation categories. Moreover, there were no significant correlations either between the densities of most frequent species of oribatid mite species and soil pH (except for *Tectoribates* sp.), soil moisture (except for *Tectocepheus velatus*), elevation, density of *Quercus infectoria* and density of *Quercus libani* in study area. Generally, variations in oribatid mite composition were more affected by physiographic factors *e.g.*, altitude than by soil properties and oak species densities, nevertheless no environmental factors influenced oribatid mite richness and diversity in this region.

*Key words:* leaf litter, soil, stand density, Zagros forests.

### RESUMEN

Hasta ahora, la riqueza y diversidad de ácaros oribátidos no se han estudiado en bosques de robles de Irán. Este estudio tuvo como objetivo determinar las relaciones entre la composición, riqueza y diversidad de los ácaros oribátidos, así como factores ecológicos como: elevación, pH y humedad del suelo, especies de árboles y densidad del rodal en los bosques de robles en el noroeste de Irán. Se dispusieron 30 muestras de forma aleatoria en tres niveles de elevación (1.100-1.300 m, 1.300-1.500 m, 1.500-1.650 m). Se registraron 42 especies de ácaros oribátidos en el área de estudio. Se observaron nueve y seis especies exclusivamente en las elevaciones 1.100-1.300 y 1.300-1.500 m, respectivamente; mientras que cinco especies de ácaros se registraron en ambas categorías de elevación. La composición de ácaros oribátidos se vio afectada por el gradiente de elevación; sin embargo, las diferencias medias de los índices de riqueza y diversidad de especies no fueron significativas entre categorías de elevación. Tampoco hubo correlaciones significativas entre las densidades de las especies más frecuentes de ácaros oribátidos y el pH del suelo (excepto *Tectoribates* sp.), humedad del suelo (excepto *Tectocepheus velatus*), elevación, densidad de *Quercus infectoria* y densidad de *Quercus libani*. En general, las variaciones en la composición de los ácaros oribátidos se vieron más afectadas por factores fisiográficos, por ejemplo, la altitud que por las propiedades del suelo y la densidad de las especies de robles, pero ningún factor ambiental influyó en la riqueza y diversidad de los ácaros oribátidos en esta región.

*Palabras clave:* hojarasca, suelo, densidad del rodal, bosques de Zagros.

## INTRODUCTION

The main objective of natural resource management is the biodiversity conservation in natural ecosystems. Species richness, which is the most fundamental level of diversity, is defined as the species count in a given geogra-phic area. Ecosystems with higher diversity include large number of species with equivalent population size. The study of density and structure of soil macro- or microor-ganisms is important as the segments of the structure of the food web. Oribatid mites are the most abundant and diverse species of soil mesofauna (Schatz and Behan-

Pelletier 2008). Oribatid mites, in particular, inhabit the soil-litter system and tend to be the dominant arthropod group in highly organic soils of temperate forests (Norton and Behan-Pelletier 2009). They play a significant role in decomposition processes in the soil because they fragment organic matter and influence biomass and species composition of fungi and bacteria (Wallwork 1983, Seastedt 1984, Yoshida and Hijii 2005). Up to now, more than 10,000 species of mites have been described in more than 1,200 genera and 177 families (Schatz *et al*. 2011, Walter and Proctor 2013). Soil is the most favorable condition for the development of oribatid mites in the forest ecosystem (Manu 2013). The composition of oribatid mite assemblage in soil reflects the stress situation in the soil ecosystem and is useful as a bio-indicator for evaluating soil quality (Ivan 2009). Researchers have already stated that the density of oribatid mites is usually related to climatic factors (Gergócs *et al*. 2011), the type of forest stands (Murvanidze and Mumladze 2014), vegetation structure (Manu 2013), soil moisture (Corral-Hernández *et al*. 2016), type of microhabitats (Gergócs *et al*. 2011) and anthropogenic factors (Ivan 2009). Moreover, Reiff *et al*. (2016) stated that vegetation could influence the distribution and density of edaphic oribatid mites. In this context it was illustrated that oribatid mite communities were indirectly influenced by litter qualities (Murvanidze and Mumladze 2014, Gergócs *et al*. 2015) or were not affected by type of leaf litter (Bokhorst *et al*. 2018, Bluhm *et al*. 2019). Thus, the relationships between oribatid mite diversity and environmental variables, canopy species composition and stand quantitative characteristics are still complicated and unclear.

According to the latest reports, 380 species belonging to 191 genera from 86 families of oribatid mites have been reported for the Iranian fauna (Akrami 2015). There are few studies concerning the oribatid mites in different habitats in Iran *e.g.* in pastures (Hashemi-Khabir *et al*. 2015) and agro-ecosystems (Rahgozar *et al*. 2019). Similarly, some poronotic oribatid mites (Acari: Oribatida: Poronotic Brachypylina) from Arasbaran forests, North of East Azarbayjan Province, were introduced by Azimi *et al*. (2018). Zagros forests (*ca*. 5 million hectares) are the largest forest area in Iran, which is covered with oak trees. The northern parts of these forests are the specific habitat of *Quercus infectoria* Olivier and *Quercus libani* Olivier, while the southern parts are solely covered by *Quercus brantii* Lindley (Eshaghi Rad *et al*. 2018). It is very valuable to conduct an investigation on oribatid mite species even on regional scale regarding the lack of related data in Zagros forests. Oribatid mite richness and diversity have not been studied in Zagros forests so far and this research was the first case examining oribatid mites in oak forests of Iran. Zagros forests are mainly located on mountainous area and elevation could be a fundamental driver of species composition and species richness and diversity. Indeed, it was illustrated that the patterns of species oc-

currence at high altitudes were expected to resemble the species distribution patterns observed at lower altitudes (Hugo-Coetzee and Le Roux 2018). On the other hand, soil pH, soil moisture and stand characteristics could be considered as important factors affecting oribatid mite species composition and diversity. Thus, in this study we hypothesized that a) elevation, soil pH and soil moisture influenced oribatid mite composition, richness and diversity, b) oribatid mite species responded to stand characteristics such as tree species types and density. The aim of this study is to determine the relationships among oribatid mite composition, richness and diversity as well as some ecological factors such as elevation, soil pH and soil moisture, tree species and stand density in oak forests in northwestern Iran.

METHODS

*Study area.* The research area was located in west Azarbaijan province (Iran), latitude 36°25' N and longitude 45°53'E. The study area is mainly covered by *Quercus infectoria* Olivier and *Quercus libani* Olivier situated on north-facing sites with mean slope of 30 % and elevation ranges from 1,100 to 1,650 m above sea level. Mean annual temperature is 13.5 °C and mean annual rainfall is 724 mm.

*Data collection.* For this study three elevation categories (1,100-1,300 m, 1,300-1,500 m and 1,500-1,650) were determined for allocating the samples. Ten square 400 m² (20×20 m) sampling plots were randomly taken in each elevation category (Mumladze *et al*. 2015). Totally, 30 samples were randomly arranged in the forests of the region. The selection criteria for the samples were as follows:

- - Habitat conditions within stands were homogeneous.
- - No illegal pole and fuel wood cutting within stands.

In each sample, the density and type of tree species in the canopy were recorded. The geographical coordination of the center of each sample was recorded using GPS. Soil samples were taken from the surface (20×20 cm) up to 20 cm deep of soil using trowel around the center of each sample plot and afterwards transported to the laboratory at the Urmia Agricultural and Natural Resources Research Center. Soil pH (soil reaction) and soil moisture were determined for the mixed samples in the soil laboratory.

*Field sampling and mite extraction.* As no significant variation had been observed in the structure of the community and abundance of oribatid mites during the year in oak forests (Gergócs *et al*. 2011), the oribatid mites were studied by taking 30 mixed litter and soil samples (from surface to a maximum depth of 20 cm) in May 2018. Mites

were extracted by using the Berlese funnel and stored in 75 % ethanol, cleared by Nesbitt's fluid and mounted on microscopic slides using Hoyer's medium. The slides were kept in an oven at 45–50 ºC for 2–3 weeks and only adult oribatid mites were identified using valid keys (Balogh 1992, Akrami 2015).

*Data analysis*. Species richness index, Shannon evenness, Shannon diversity index and Simpson diversity index were calculated based on mite species density via software PC-ORD version 4. Kolmogorov-Smirnov test was applied to check data normality. Tukey test was used to test for significant differences among different elevation categories regarding the species richness, species diversity and evenness indices, and soil properties. The Pearson correlation analysis was applied to analyze relationships between environmental factors (elevation, soil pH, soil moisture, stand density) and the abundance of the most frequent oribatid mites. Further, mite interspecies correlations, mite species density, and tree species types were calculated through this method. SPSS ver. 21.0 for Windows was used for data analyses.

The dominance index (%) was calculated using the formula $D = 100\% * n/N$, where: $n$ = number of individuals of one species in all samples; $N$ = total number of individuals of all species in all samples.

The identified orbatid mites were distributed by dominance as follows: eudominants with $D > 10.0$ % (D5), dominants with $D$ of 5.1– 10.0 % (D4), subdominants with $D$ of 2.1–5.0 % (D3), recedents with $D$ of 1.1–2.0 % (D2), and subrecedents with $D < 1.1$ % (D1). The constancy index (%) was obtained using the formula: $C = 100$ % * $pA/P$, where: $pA$ = number of samples with species A; $P$ = total number of samples. Identified mites were classified in four constancy classes: constant species with $C$ of 75.1–100 % (C4), constant species with $C$ of 50.1–75 % (C3), accessory species with $C$ of 25.1–50 % (C2), and accidental species with $C$ of 1–25 % (C1) (Selvin and Vacca 2004).

RESULTS

*Environmental parameters and tree densities.* Table 1 reports the mean of studied environmental variables and tree species densities in different elevations categories. It is important to mention that the compositions of all sampling plots were a mixture of *Q. infectoria* and *Q. libani;* nevertheless, the density of each species was different. Soil pH and soil moisture were similar in the different elevation categories.

*Oribatid mite distribution along the elevation gradient.* A total of 42 oribatid mite species belonging to 29 genera and 24 families were recorded in this study (oak forests in Iran) (table 2). Oribatids mites *e.g. Ramusella* (*Ramusella*) *sengbuschi tokyoensis* (Aoki 1974), *Ramusella* (*Ramusella*) *sengbuschi* s. str. (Hammer 1968), *Ramusella* (*Ramusella*) *puertomonttensis* (Hammer 1962), *Ramusella (Insculptoppia) insculpta* (Paolo 1908), *Ramusella* (*Rectoppia*) *mihelcici* (Pérez-Ínigo 1965), *Lasiobelba* (*Lasiobelba*) *decui* (Vasiliu *et* Ivan 1995), *Rhinoppia* (*Rhinoppia*) *obsoleta* (Paoli 1908), *Punctoribates punctum* (Koch 1839), *Punctoribates angulatus* (Bayartogtokh, Grobler and Cobanoglu 2000), *Tectocepheus velatus* (Michael 1880), *Sphaerochthonius splendidus* (Berlese 1904), *Papillacarus aciculatus* (Berlese 1905), *Plesiodamaeus ornatus* (Pérez-Ínígo 1972) were observed in all elevation levels.

Oribatid mites such as *Ramusella* (*Insculptoppiella*) *varians* (Wallwork 1961), *Galumna iranensis* (Mahunka *et* Akrami 2001), *Berlesezetes aegypticus* (Balogh *et* Mahunka 1981), *Atropacarus* (*Atropacarus*) *striculus* (Koch 1836), *Ceratoppia quadridentata* (Haller 1882), *Epilohmannia cylindrica cylindrica* (Berlese 1904) and *Suctobelbella* (*Flagrosuctobelba*) *elegantula* (Hammer 1958) were only found in the elevation 1,100-1,300 m. In addition, *Licnodamaeus fissuratus* (Balogh *et* Mahunka 1965), *Aleurodamaeus setosus* (Berlese 1883), *Oribatula* (*Oribatula*) *pallida* (Banks 1906) and *Passalozetes africanus* (Grand-

**Table 1.** The mean ± standard error of studied environmental variables and tree species densities in the study area.

Media ± error estándar de las variables ambientales estudiadas y las densidades de especies arbóreas en el área de estudio.

| Characteristics | Elevation categories (m) | | | Total |
|---|---|---|---|---|
| | 1,100–1,300 | 1,300–1,500 | 1,500–1,650 | |
| pH | 7.5 ± 0.25 | 7.4 ± 0.21 | 7.6 ± 0.30 | 7.5 ± 0.26 |
| Moisture (%) | 12.4 ± 3.3 | 11.3 ± 1.5 | 13.9 ± 3.1 | 12.6 ± 3.2 |
| Elevation (m) | 1,200.2 ± 70.3 | 1,410.3 ± 59.2 | 1,584.4 ± 24.1 | 1,398.3 ± 51.9 |
| *Q. infectoria* density | 42.1 ± 11.3 | 28.1 ± 5.4 | 17.3 ± 6.5 | 29.2 ± 7.7 |
| *Q. libani* density | 10.7 ± 4.4 | 24.4 ± 7.5 | 21.3 ± 4.1 | 18.8 ± 5.3 |
| Total density | 52.8 ± 16.2 | 52.5 ± 15.1 | 38.6 ± 12.1 | 47.9 ± 14.4 |

jean 1932) were collected in the elevation 1300–1500 m. Similarly, *Lasiobelba* (*Lasiobelba*) *kuehnelti* (Csiszár 1961), *Oribatula* (*Zygoribatula*) *connexa ucrainica* (Iordansky 1990), *Scheloribates fimbriatus* (Thor 1930) and *Indoribates* )*Haplozetes*) *fusifer* (Berlese, 1908) were observed in both 1100-1300 m and 1300-1500 m categories.

Half of the collected species (21 species) had dominance lower than 1 % (table 2). *Punctoribates punctum* had the highest dominance (D= 11.9 %). In the study area, 41 mite species had constancy index lower than 50 %. *Tectocepheus velatus* had the highest constancy (C=53 %) (table 2).

*Species richness and diversity indices*. Table 3 indicates the species richness, evenness, Shannon diversity and Simpson diversity indices of mites recorded in oak stands located in various elevation categories in the study area. There were no significant differences in the mean of species diversity indices among the elevation categories (*P*-value < 0.05 based on Tukey test results).

*Mite species abundance-environment relationship*. The correlations between the abundance of most frequent species of oribatid species and the studied environmental factors (elevation, soil pH, soil moisture, oak species density, and total stand density) in the study area are indicated in table 4. The abundance of *Tectocepheus velatus* is significantly correlated with soil moisture. There is also a significant correlation between *Tectoribates* sp. and soil pH; however, other mite species do not respond to soil pH or soil moisture. In addition, there is no significant correlation between the abundance of most frequent species of oribatid species and elevation, density of *Q. infectoria* and density of *Q. libani* in the study area.

*Mite interspecies correlation*. Table 5 indicates the correlation among different species of oribatid mites recorded in the sampling plots in the study area. There appears to be a significant positive correlation between the *Pilogalumna* sp. and *R.*(*R.*) *sengbuschi tokyoensis*, *Sphaerochthonius splendidus* and *Tectoribates* sp. species as well as between *Tectocepheus velatus* and *Punctoribates angulatus*. Likewise, there is a significant negative correlation between the *Tectoribates* sp. and *R.*(*R.*) *sengbuschi tokyoensis* and *R.*(*R.*) *puertomonttensis*. Other pair correlations among mite species were not significant in the study area.

DISCUSSION

A total of 42 oribatid mite species were recorded in this study (oak forests in Iran). Species including *Ramusella* (*Insculptoppiella*) *varians*, *Ramusella* (*Rectoppia*) *mihelcici, Lasiobelba (Lasiobelba) decui, Lasiobelba* (*Lasiobelba*) *kuehnelti, Scheloribates laevigatus* (C.L. Koch, 1835), *Epilohmannia cylindrica cylindrica, Ceratoppia quadridentata, Suctobelbella* (*Flagrosuctobelba*) *elegantula* and *Papillacarus aciculatus* (Berlese, 1905) were new records

for oak forests of this region, which were previously reported in different habitats in Iran *e.g.* in pastures (Hashemi-Khabir *et al.* 2015) and Arasbaran temperate forests (Azimi *et al.* 2018). Likewise, *Ramusella* (*Insculptoppia*) *insculpta, Oppiella* (*Oppiella*) *nova nova* (Oudemans, 1902) and *Rhinoppia* (*Rhinoppia*) *obsoleta* were reported in oak forests in Turkey (Toluk and Akin 2017) as well as *Scheloribates laevigatus* and *Oppiella* (*Oppiella*) *nova nova* in Romania (Ivan 2009).

Approximately 67 % of the collected species (28 from 42 species) had dominance under 2 % and most mite species (41 species) in the study area belonged to accessory and accidental species classes (table 2). According to literature, the high numbers of recedent, subrecedent, accessory and accidental species indicate an unfavorable impact of environmental conditions on stability of the studied populations (Manu 2013).

Nine and six species were exclusively observed in the elevations 1,100–1,300 m and 1,300–1,500 m respectively. In addition, five mite species were recorded in the elevations 1,100–1,300 m, 1,300–1,500 m, although absent above 1,500 m. Thus, oribatid mite composition was affected by elevation gradient. In agreement with this result, Mumladze *et al.* (2015) illustrated that the oribatid mite composition was influenced by elevation gradient. This could be related to lower temperatures and generally harsher environment in high elevations (Hugo-Coetzee and Le Roux 2018) or a combination of increasing biotic harshness with decreasing availability of food resources as the driving factors for changing species composition along gradients (Fischer *et al.* 2014).

The absence of a significant difference in mite species richness and diversity indices among elevation categories of the study area may be due to the higher resistance of mites to changes in environmental variables (Reiff *et al.* 2016) as well as minor variations of soil pH and soil moisture in the study area. Nevertheless, many studies indicated that mite species richness and diversity declined with increasing elevation (Hugo-Coetzee and Le Roux 2018, Bokhorst *et al.* 2018). These contrasting responses may be related to variation in vegetation or soil type, precipitation, elevation range and temperature range (Hodkinson 2005).

Our results also indicated no significant correlation between the abundance of most frequent oribatid species and the density of oak species in study area. Reportedly, a dense stand makes a great amount of leaf litter on the forest floor that can serve as protection for soil biota (Reiff *et al.* 2016). However, the stands in the Zagros forests in the region were dominated by oak species which did not make dense stands. Meanwhile, oak litter is favorable for all types of oribatid communities (Gergócs *et al.* 2015). In line with this result, Hugo-Coetzee and Le Roux (2018) illustrated that plant characteristics did not affect mite and springtail species patterns. Further, Bokhorst *et al.* (2018) proved that mite abundance was unaffected by vegetation type. In addition, Bluhm *et al.* (2019) stated that tree spe-

**Table 2.** Family, scientific name, frequency, abundance, dominance and constancy indices of Oribatid mite in study area.

Familia, nombre científico, frecuencia, abundancia, dominancia e índices de constancia del ácaro oribátide en el área de estudio.

| Family | Species | Frequency in elevation categories (m) | | | D% | C% | n | % abundance |
|---|---|---|---|---|---|---|---|---|
| | | <1,300 | 1,300–1,500 | >1,500 | | | | |
| Sphaerochthoniidae | *Sphaerochthonius splendidus* | 2 | 3 | 3 | 4.4 | 27 | 38 | 4.42 |
| Steganacaridae | *Atropacarus (Atropacarus) striculus* | 1 | 0 | 0 | 0.1 | 3 | 1 | 0.11 |
| Phthiracaridae | *Phthiracarus lentulus* | 1 | 0 | 1 | 0.4 | 7 | 4 | 0.46 |
| Lohmanniidae | *Papillacarus aciculatus* | 2 | 3 | 2 | 2.2 | 23 | 19 | 2.2 |
| Epilohmanniidae | *Epilohmannia cylindrica cylindrica* | 1 | 0 | 0 | 0.6 | 3 | 6 | 0.69 |
| Hermanniellidae | *Hermanniella* sp. | 1 | 0 | 0 | 0.1 | 3 | 1 | 0.11 |
| Gymnodamaeidae | *Plesiodamaeus ornatus* | 1 | 3 | 1 | 1.6 | 17 | 14 | 1.62 |
| Aleurodamaeidae | *Aleurodamaeus setosus* | 0 | 2 | 0 | 0.2 | 7 | 2 | 0.23 |
| Licnodamaeidae | *Licnodamaeus fissuratus* | 0 | 1 | 0 | 0.1 | 3 | 1 | 0.11 |
| Damaeolidae | *Belba* sp. | 1 | 1 | 2 | 1.8 | 13 | 16 | 1.86 |
| Xenillidae | *Xenillus (Xenillus) setosus* | 0 | 1 | 0 | 0.1 | 3 | 1 | 0.11 |
| | *Xenillus (Xenillus)* sp.nr. *singularis* | 0 | 1 | 1 | 0.5 | 7 | 5 | 0.58 |
| Metrioppidae | *Ceratoppia quadridentata* | 3 | 0 | 0 | 0.3 | 10 | 3 | 0.34 |
| Tectocephidae | *Tectocepheus minor* | 0 | 1 | 0 | 0.1 | 3 | 1 | 0.11 |
| | *Tectocepheus velatus* | 6 | 6 | 4 | 7.4 | 53 | 64 | 7 |
| Oppiidae | *Ramusella (Ramusella) sengbuschi tokyoensis* | 3 | 3 | 4 | 2.9 | 33 | 25 | 2.91 |
| | *Ramusella (Ramusella) sengbuschi* s.str. | 7 | 2 | 4 | 0.1 | 43 | 86 | 10.01 |
| | *Ramusella (Ramusella) puertomonttensis* | 3 | 2 | 2 | 1.8 | 23 | 16 | 1 |
| | *Ramusella (Insculptoppia) insculpta* | 2 | 1 | 1 | 0.8 | 13 | 7 | 0.81 |
| | *Ramusella (Insculptoppiella) varians* | 1 | 0 | 0 | 0.1 | 3 | 1 | 0.11 |
| | *Ramusella (Rectoppia) mihelcici* | 1 | 1 | 1 | 0.9 | 10 | 8 | 0.93 |
| | *Lasiobelba (Lasiobelba) decui* | 3 | 1 | 1 | 3.6 | 17 | 34 | 3.95 |
| | *Lasiobelba (Lasiobelba) kuehnelti* | 2 | 2 | 0 | 5.3 | 13 | 46 | 5.35 |
| | *Oppiella (Oppiella) nova nova* | 2 | 0 | 2 | 1.2 | 13 | 11 | 1.28 |
| | *Rhinoppia (Rhinoppia) obsoleta* | 1 | 1 | 1 | 0.5 | 10 | 5 | 0.58 |
| Epimerellidae | *Epimerella* sp. | 4 | 0 | 0 | 5.8 | 13 | 50 | 5.82 |
| Suctobelbidae | *Suctobelbella (Flagrosuctobelba) elegantula* | 1 | 0 | 0 | 0.1 | 3 | 1 | 0.11 |
| Microzetidae | *Berlesezetes aegypticus* | 1 | 0 | 0 | 0.1 | 3 | 1 | 0.11 |
| Passalozetidae | *Passalozetes africanus* | 0 | 3 | 0 | 0.6 | 10 | 6 | 0.6 |
| Oribatulidae | *Oribatula (Oribatula) pallida* | 0 | 1 | 0 | 0.1 | 3 | 1 | 0.11 |
| | *Oribatula (Oribatula) tibialis allifera* | 1 | 0 | 1 | 1.3 | 7 | 12 | 1.39 |
| | *Oribatula (Zygoribatula) connexa ucrainica* | 1 | 1 | 0 | 2.2 | 7 | 19 | 2 |
| | *Oribatula (Zygoribatula)debilitranslamellata* | 1 | 0 | 1 | 2.5 | 7 | 22 | 2.56 |
| Scheloribatidae | *Scheloribates fimbriatus* | 1 | 2 | 0 | 1 | 10 | 9 | 1.04 |
| | *Scheloribates laevigatus* | 1 | 0 | 1 | 0.2 | 7 | 2 | 0.23 |
| Haplozetes | *Indoribates) Haplozetes (fusifer* | 2 | 2 | 0 | 3.7 | 13 | 32 | 3.72 |
| Punctoribatidae | *Punctoribates punctum* | 5 | 4 | 1 | 11.9 | 33 | 103 | 11 |
| | *Punctoribates angulatus* | 3 | 3 | 6 | 5.1 | 40 | 44 | 5 |
| Achipteriidae | *Tectoribates* sp. | 4 | 2 | 0 | 6.6 | 20 | 57 | 6.63 |
| | *Achipteria* sp. | 1 | 1 | 2 | 1.5 | 13 | 13 | 1.51 |
| Galumnidae | *Pilogalumna* sp. | 5 | 1 | 4 | 5.3 | 33 | 71 | 8 |
| | *Galumna iranensis* | 1 | 0 | 0 | 0.1 | 3 | 1 | 0.11 |

D: dominance index, C: constancy index, n: number of individuals.

**Table 3.** Species richness and diversity indices of Oribatid mites in the elevation categories.

Índices de riqueza y diversidad de especies de ácaros oribátidos en las categorías de elevación.

| Parameter | Elevation categories (m) | | | |
|---|---|---|---|---|
| | 1,100–1,300 | 1,300–1,500 | 1,500–1,650 | Total |
| Species richness | 8.44 ± 1.95 | 6.22 ± 1.37 | 5.11 ± 0.96 | 6.60 ± 3.50 |
| Evenness | 0.69 ± 0.10 | 0.62 ± 0.10 | 0.90 ± 0.30 | 0.74 ± 0.27 |
| Shannon index | 1.43 ± 0.27 | 1.08 ± 0.24 | 1.29 ± 0.13 | 1.27 ± 0.67 |
| Simpson Index | 0.62 ± 0.10 | 0.48 ± 0.09 | 0.67 ± 0.03 | 0.59 ± 0.26 |

**Table 4.** Pearson correlation between most frequent Oribatid mite species and environmental factors (elevation, soil pH, soil moisture, stand density) in the study area.

Correlación de Pearson entre las especies de ácaros oribátidos más frecuentes y factores ambientales (elevación, pH del suelo, humedad del suelo, densidad del rodal) en el área de estudio.

| | pH | Soil moisture | Elevation | *Q. infecoria* density | *Q. libani* density | Total density |
|---|---|---|---|---|---|---|
| *Punctoribates punctum* | 0.26 | 0.36 | 0.36 | -0.22 | 0.37 | -0.64 |
| *Tectocepheus velatus* | 0.03 | 0.55* | 0.12 | 0.19 | -0.11 | 0.38 |
| *Punctoribates angulatus* | 0.16 | -0.03 | -0.01 | -0.01 | 0.01 | 0.24 |
| *Ramusella (R.) puertomonttensis* | -0.21 | -0.09 | -0.59 | 0.73 | -0.18 | 0.72 |
| *Sphaerochthonius splendidus* | -0.25 | -0.40 | 0.04 | -0.14 | -0.05 | -0.32 |
| *Papillacarus aciculatus* | -0.56 | -0.17 | -0.30 | 0.19 | 0.66 | -0.30 |
| *Ramusella (R.) sengbuschi tokyoensis* | -0.33 | -0.59 | -0.63 | 0.38 | -0.55 | 0.55 |
| *Ramusella (R.) sengbuschi* s.str. | 0.41 | -0.06 | -0.31 | -0.01 | 0.07 | 0.28 |
| *Pilogalumna* sp. | 0.29 | 0.58 | 0.22 | -0.23 | 0.16 | 0.18 |
| *Tectoribates* sp. | 0.85** | 0.16 | 0.19 | -0.36 | 0.01 | 0.15 |

*Significant differences *P* < 0.05.  **Significant differences *P* < 0.01

cies (*Fagus sylvatica* L., *Acer pseudoplatanus* L., *Fraxinus excelsior* L. and *Tilia cordata* Mill.) with different leaf litter quality did not affect species richness or community structure of oribatid mites. However, contrasting results were obtained in other studies regarding mite–vegetation relationships based on the type of vegetation. Rieff *et al*. (2016) found a superior number of mites in soil samples from the area under eucalyptus compared to the native grassland area. Besides, Murvanidze and Mumladze (2014) observed that different types of litter (beech versus hornbeam) had a significant impact on the overall number of species and abundance of oribatid mites.

Furthermore, we observed a weak correlation between the abundance of different oribatid mites in the study area (table 5). It was stated that oribatid mites coexisted in the same habitat since mite species where found to have di-

fferent diets (Schneider *et al*. 2004) and oribatid species were known to be general feeders (Maraun *et al*. 2003). Alternatively, it might be due to partitioning of the feeding resource in a competitive way (Murvanidze and Mumladze 2014).

CONCLUSIONS

Overall, oribatid mite species composition in Zagros oak forests was different at different elevations. However, no significant correlation was observed among most of frequent mite densities and the species diversity indices and elevation, soil pH and soil moisture. Generally, variations in oribatid mite composition were more affected by physiographic factors *e.g.* altitude than by soil properties and oak species densities. In addition, no environmental

**Table 5.** Pearson correlation among most frequent Oribatid mite species in the study area.

Correlación de Pearson entre las especies de ácaros oribátidos más frecuentes en el área de estudio.

| | *Pilogalumna* sp. | *Punctoribates punctum* | *Tectocepheus velatus* | *Punctoribates angulatus* | *R. (R.) puertomonttensis* | *Sphaerochthonius splendidus* | *Papillacarus aciculatus* | *R. (R.) sengbuschi tokyoensis* | *R. (R.) sengbuschi* s. str. | *Tectoribates* sp. |
|---|---|---|---|---|---|---|---|---|---|---|
| *Pilogalumna* sp. | 1.00 | | | | | | | | | |
| *Punctoribates punctum* | -0.29 | 1.00 | | | | | | | | |
| *Tectocepheus velatus* | 0.13 | -0.40 | 1.00 | | | | | | | |
| *Punctoribates angulatus* | 0.22 | -0.02 | 0.76* | 1.00 | | | | | | |
| *R.(R.)puertomonttensis* | -0.32 | -0.46 | 0.41 | a | 1.00 | | | | | |
| *Sphaerochthonius splendidus* | 0.99** | -0.06 | -0.11 | 0.35 | -0.50 | 1.00 | | | | |
| *Papillacarus aciculatus* | -0.40 | a | -0.41 | 0.82 | a | 0.50 | 1.00 | | | |
| *R. (R.) sengbuschi tokyoensis* | 0.99** | -0.47 | -0.10 | -0.11 | a | 0.08 | -0.94 | 1.00 | | |
| *R.(R.) sengbuschi* s. str. | 0.07 | -0.39 | -0.16 | 0.31 | 0.33 | 0.02 | -0.19 | 0.26 | 1.00 | |
| *Tectoribates* sp. | 0.99** | -0.40 | -0.16 | -0.88 | -0.99** | -0.53 | -0.84 | -0.99** | -0.24 | 1.00 |

*Significant differences $P < 0.05$.  **Significant differences $P < 0.01$.  a: one of species is absent.

factors impacted oribatid mite richness or diversity in this region and Oribatid mite species did not respond to stand characteristics such as tree species types and density.

ACKNOWLEDGMENTS

REFERENCES

Akrami MA, A. Saboori. 2012. Acari of Iran, Vol. 2, Oribatid mites. Tehran, Iran. Tehran University Press. 261p.

Akrami MA. 2015. An annotated checklist of oribatid mites (Acari: Oribatida) of Iran. *Zootaxa* 3963(4): 451–501. DOI: http://dx.doi.org/10.11646/zootaxa.3963.4.1

Azimi N, D Shirdel, P Lotfollahi, A Khalil Ariya. 2018. Introduction of Some Poronotic Oribatid Mites (Acari: Oribatida: *Poronotic Brachypylina*) from Arasbaran Forests, North of East Azerbaijan Province. *Applied Research in Plant Pathology* 7(3): 117–123.

Balogh J, P Balogh. 1992a. The oribatid mites genera of the world. Vol. 1. Budapest, Hungary. The Hungarian National Museum Press. 263 p.

Balogh J, P Balogh. 1992a. The oribatid mites genera of the world. Vol. 2. Budapest, Hungary. The Hungarian National Museum Press. 375 p.

Bluhm C, O Butenschoen, M Maraun, S Scheu.2019. Effects of root and leaf litter identity and diversity on oribatid mite abundance, species richness and community composition. *PLos One* 14(7): 1–16. DOI: https://doi.org/10.1371/journal.pone.0219166

Bokhorst S, GF Veen, M Sundqvist, JR De Long, P Kardol, DA Wardle. 2018. Contrasting responses of springtails and mites to elevation and vegetation type in the sub-Arctic. *Pedobiologia* 67: 57–64. DOI: https://doi.org/10.1016/j.pedobi.2018.02.004

Corral-Hernández E, I Balanzategui, JC Iturrondobeitia. 2016. Effect of progressive drying of pedunculate oak (*Quercus robur* L.) and holm oak (*Quercus rotundifolia* Lam.) forest soils on the composition of the oribatid mite community (Acari: Oribatida) in laboratory conditions. *International Journal of Acarology* 42(7): 358–365. DOI: https://doi.org/10.1080/01647954.2016.1194470

Eshaghi Rad J, G Valadi, O Salehzadeh, H Maroofi. 2018. Effects of anthropogenic disturbance on plant composition, plant diversity and soil properties in oak forests, Iran. *Journal of Forest Science* 64(8): 358–370. DOI: https://doi.org/10.17221/13/2018-JFS

Fischer BM, E Meyer, M Maraun, 2014. Positive correlation of trophic level and proportion of sexual taxa of oribatid

mites (Acari: Oribatida) in alpine soil systems. *Experimental and Applied Acarology* 76: 112–123. DOI: https://doi.org/10.1007/s10493-014-9801-3

Gergócs V, Á Garamvölgyi, R Homoródi, L Hufnagel. 2011. Seasonal change of oribatid mite communities (Acari, Oribatida) in three different types of microhabitats. *Applied Ecology and Environmental Research* 9(2): 181–195. DOI: http://dx.doi.org/10.15666/aeer/0902_181195

Gergócs V, G Rétháti, L Hufnagel. 2015. Litter quality indirectly influences community composition, reproductive mode and trophic structure of oribatid mite communities: a microcosm experiment. *Experimental and Applied Acarology* 67(3): 35–56. DOI: https://doi.org/10.1007/s10493-015-9959-3

Hashemi-Khabir Z, K Haddad Irani-Nejad, M Moghaddam, M Khanjani. 2015. Community structure of oribatid mites (Acari: Oribatida) in rangelands of West Azerbaijan Province, Iran. *International Journal of Acarology* 41(4): 344–355. DOI: https://doi.org/10.1080/01647954.2015.1033458

Hodkinson ID. 2005. Terrestrial insects along elevation gradients: species and community responses to altitude. *Biological Review* 80: 489–513. DOI: https://doi.org/10.1017/S1464793105006767

Hugo-Coetzee EA, PC Le Roux. 2018. Distribution of microarthropods across altitude and aspect in the sub-Antarctic: climate change implications for an isolated oceanic island. *Acarologia* 58: 43–60. DOI: http://dx.doi.org/10.24349/acarologia/20184278

Ivan O. 2009. Structure and dynamics of the oribatid mite communities (Acari,Oribatida) in some *Quercus* forests, in relation with the treatments used in the control of defoliating insects. *Annals of Forest Research* 52: 5–10.

Manu M. 2013. Diversity of soil mites (Acari: Mesostigmata: Gamasina) in various deciduous forest ecosystems of Muntenia region (southern Romania). *Biological Letters* 50(1): 3–16. DOI: http://dx.doi.org/10.1016/S1164-5563(03)00006-2

Maraun M, H Martens, S Migge, A Theenhaus, S Scheu. 2003. Adding to the enigma of soil animal diversity: fungal feeders and saprophagous soil invertebrates prefer similar food substrates. *European Journal of Soil Biology* 39: 85–95. https://doi.org/10.2478/biolet-2013-0001

Mumladze L, M Murvanidze, M Maraun, M Salakaia. 2015. Oribatid mite communities along an elevational gradient in Sairme gorge (Caucasus). *Experimental and Applied Acarology* 66(1): 41-51. https://doi.org/10.1007/s10493-015-9893-4

Murvanidze M, L Mumladze. 2014. Article Oribatid mite (Acari: Oribatida) diversity in different forest stands of Borjom-Kharagauli National Park (Georgia). *Persian Journal of Acarology* 3(4): 257–276. DOI: http://dx.doi.org/10.22073/pja.v3i4.10169

Ndri JK, SD Zon, JE Tondoh, J Lagerlöf. 2017. Changes in mite richness and diversity along a gradient of land-use intensity from mid-west Ivory Coast. *Tropical Ecology* 58(3): 497–506.

Rahgozar M, K Iraninejad, MN Zargaran, A Saboori. 2019. Biodiversity and species richness of oribatid mites (Acari: Oribatida) in orchards of East Azerbaijan province, Iran. *Persian Journal of Acarology* 8(2): 147–159. DOI: http://dx.doi.org/10.22073/pja.v8i2.43052

Rieff GG, T Natal-da-Luz, J Paulo Sousa, MO Wallau, M Hahn, EL de Sá1.2016.Collembolans and mites communities as a tool for assessing soil quality: effect of eucalyptus plantations on soil mesofauna biodiversity. *Current Science* 110(4): 713–719. DOI: https://doi.org/ 10.18520/cs/v110/i4/713-719

Schatz H, V Behan-Pelletier. 2008. Global diversity of oribatids (Oribatida: Acari: Arachnida). *Hydrobiologia* 595: 323–328. DOI: https://doi.org/10.1007/s10750-007-9027-z

Schatz H, NM Behan-Pelletier, BM Oconnor, RA Norton. 2011. Suborder Oribatida van der Hammen, 1968. *In* Zhang ZQ ed. Animal biodiversity: An outline of higher-level classification and survey of taxonomic richness. *Zootaxa* 3148: 141–148. DOI: http://dx.doi.org/10.11646/zootaxa.3148.1.26

Schneider K, C Renker, S Scheu, M Maraun. 2004. Feeding biology of oribatid mites: a mini review. *Phytophaga* 14: 247–256.

Seastedt TR. 1984. The role of microarthropods in decomposition and mineralization processes. *Annual Review of Entomology* 29: 25–46.

Selvin S, A Vacca. 2004. Biostatistics. How it works.London, England. 408 p.

Subías LS. 2004. Listado sistematico, sinonimico y biogeografico de los acaros oribatidos (Acariformes, Oribatida) del Mundo (1758–2002). *Graellsia* 60: 3–305. DOI: https://doi.org/10.3989/graellsia.2004.v60.iExtra.218

Toluk A, AT Akin. 2017.Oribatid mite fauna (Acari) of Çat Forest, Sivas Province, Turkey. *Turkish Journal of Entomology* 41(3): 293–307. DOI: http://dx.doi.org/10.16970/entoted.322866

Wallwork JA. 1983. Oribatids in forest ecosystems. *Annual Review of Entomology* 28:109–130.

Walter DE, HC Proctor. 2013. Mites: Ecology, Evolution, and Behavior. 2nd edition. Dordrecht, Netherlands. Springer. 470 p.

Yoshida T, N Hijii. 2005. The composition and abundance of microarthropod communities on arboreal litter in the canopy of *Cryptomeria japonica* trees. *Journal of Forest Research* 10:35–42. DOI: https://doi.org/10.1007/s10310-004-0098-7

# Functional structure of the landscape and seed dispersal of *Araucaria angustifolia* in Canoas River Basin (Southern Brazil)

## Estructura funcional del paisaje y dispersión de semillas de *Araucaria angustifolia* en la cuenca del río Canoas (Sur de Brasil)

**Amanda Köche Marcon ᵃ\*, Gisley Paula Vidolin ᵃ, Daniela Biondi ᵇ**

\*Corresponding author: ᵃ Federal University of Paraná, Graduate Program in Forestry,
Av. Prefeito Lothário Meissner, 632, Curitiba, Paraná, Brazil, amandakoche@gmail.com
ᵇ Federal University of Paraná, Department of Forest Sciences, Curitiba, Paraná, Brazil.

SUMMARY

*Araucaria angustifolia* is one of the main species of the Mixed Ombrophilous Forest and has been threatened by extinction. Additionally, a low number of regenerating individuals can be seen in forest remnants. For these reasons, this study aimed at evaluating the functional structure of Canoas River Basin (state of Santa Catarina, Brazil) using landscape ecology metrics, and at verifying whether or not the proximity between remnants is compatible with this species displacement of the main dispersers. Thus, a landscape structure analysis was performed using metrics of area, shape, edge and connectivity of habitat fragments based on satellite images. Landscape metrics were related to maximum distances of displacement of dispersers and to effective dispersion distance based on a genetic estimate derived from secondary data. Results indicate that Canoas River Basin has natural vegetation cover in 19.6 % of its territory and is highly fragmented. A total of 80.8 % of the fragments have an area smaller than 50 ha. The proximity between patches concerning the mean displacement of dispersers (87 m) is zero for 100 % of fragments. The proximity is zero in 43.5 % landscape, considering the effective seed dispersion based on the genetic estimate of dispersion distance. Therefore, the connectivity between fragments is very low, which may justify the fact that this species is often not found in the regenerating components of forest inventories.

*Key words:* landscape ecology, connectivity, forest fragmentation, Brazilian pine, landscape metrics.


RESUMEN

Una de las principales especies de los bosques mixtos, *Araucaria angustifolia*, está en peligro de extinción y también tiene un bajo número de individuos en regeneración. Por estas razones, el objetivo de este estudio fue evaluar, a través de métricas de ecología del paisaje, la estructura funcional de la cuenca del río Canoas, SC, Brasil, y verificar si la proximidad entre los remanentes es compatible con el desplazamiento de los principales dispersores de la especie. Para esto, se utilizaron métricas de área, forma, borde y conectividad de fragmentos de hábitat, utilizando imágenes satelitales. Las métricas del paisaje se relacionaron con las distancias máximas de desplazamiento de los dispersores y con la distancia de dispersión efectiva de la estimación genética, derivada de datos secundarios. Los resultados obtenidos indican que la cuenca del río Canoas tiene una cubierta de vegetación natural en el 19,6 % de su territorio y está altamente fragmentada, con un 80,8 % de los fragmentos con un área menor a 50 ha. La proximidad entre los remanentes en vista del desplazamiento de los dispersores (87 m) es nula para el 100 % de los fragmentos. Considerando la medida efectiva de dispersión de semillas a partir de la estimación genética de la distancia de dispersión, en el 43,5 % del paisaje la proximidad es nula. Se puede concluir que la conectividad entre fragmentos es muy baja, lo que puede justificar el hecho de que la especie a menudo no se encuentre en los componentes regenerativos de los estudios forestales.

*Palabras clave:* ecología del paisaje, conectividad, fragmentación forestal, pino paraná, métricas del paisaje.


INTRODUCTION

*Araucaria angustifolia* (Bertol.) Kuntze (Araucariaceae) is a symbolic tree of the Mixed Ombrophilous Forest and was overexploited in a recent past. Currently, it is a threatened species, and its suppression is prohibited (IBAMA 1992). Nonetheless, there are indications that *A. angustifolia* has often low natural regeneration since regenerating individuals are found in lower proportion contrasted with adult individuals (Chami *et al*. 2011). In addition, the long-term species perpetuation in the landscape is worrisome due to increasing temperature related to climate change and conversion of natural areas caused by land-use changes (Marchioro *et al*. 2020).

The seed dispersal of *A. angustifolia* occurs mainly by small mammals, because it depends on animals to carry

seeds after the pine nut falls (Iob and Vieira 2008). Thus, the effect of landscape functional connectivity plays a crucial role in maintaining the interaction networks between plants and animals, as it can impose barriers and limit pollination and seed dispersal (Hadley and Betts 2011).

Most fragments of the Mixed Ombrophilous Forest are small, having an area of up to 50 hectares (Sevegnani *et al.* 2013). Therefore, they suffer high anthropogenic pressure. In fragmented landscapes, habitat filters influence propagules availability: isolation decreases the abundance of dispersers and impact vegetation composition (Dea´k *et al.* 2018). In view of this situation, there is an evident need to develop and apply non-invasive methods to examine the effects of fragmentation on the seed dispersal of *A. angustifolia* at a local scale (Finch *et al.* 2020), such as those used in satellite image-based landscape ecology and geographic information systems (GIS).

Therefore, this study aimed at evaluating the functional structure of Canoas River Basin (state of Santa Catarina, Brazil) using landscape ecology metrics, and at relating the structure to the seed dispersal of *A. angustifolia*, a species of the Mixed Ombrophilous Forest. It sought to answer the following questions regarding Canoas River Basin: i) How is the landscape structure, especially considering the vegetation cover, degree of fragmentation and connectivity between fragments? and ii) is the proximity between natural remnants compatible with the displacement of the main seed dispersers of *A. angustifolia*?

## METHODS

The study area is Canoas River Basin, one of the main rivers located in the Hydrographic Region (HR) 4 – Plateau of Lages, in Serrano Plateau of the state of Santa Catarina, comprising 28 municipalities (figure 1).

For the landscape metrics analysis, an inventory of the Atlantic Forest remnants (shapefile) was used. It was provided by the non-governmental organization SOS Mata Atlântica in partnership with National Institute for Space Research (INPE) based on images from the Landsat 8 satellite for 2016, with spatial resolution of 30 m (SOS Mata Atlântica and INPE 2017), and the Ottocodified Hydrographic Base, provided by National Water Agency of Brazil (ANA 2012) (figure 2). The Atlantic Forest remnants shapefile from SOS Mata Atlântica has two classes of natural areas: forest fragments (Mixed Ombrophilous Forest) and other non-forest natural fragments (Grasslands or "Campos" – figure 1). However, for this study, both were considered as habitat fragments, without distinction.

The landscape ecology analysis was conducted for the fragments and for the whole landscape, considering only habitat fragments (forest remnants and other non-forest natural remnants). Non-forest natural remnants were included because these natural vegetation patches allow the transit of seed dispersers. To assess landscape structure, the area, shape, edge and connectivity metrics were calculated (table 1). They enabled the assessment of fragments size and shape, relating them to the edge effect
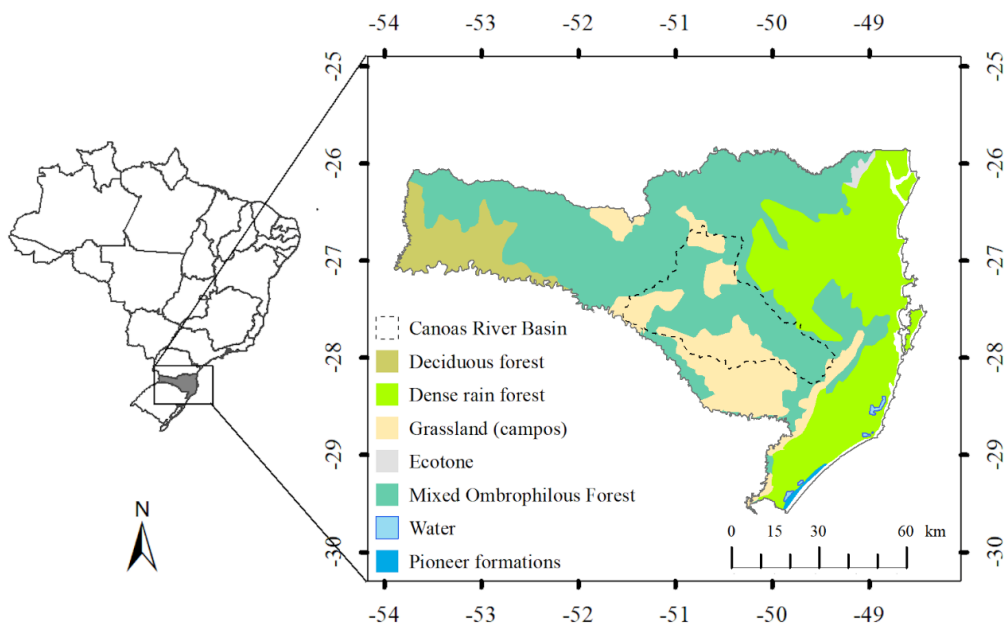


**Figure 1.** Location map of Canoas River Basin and phytogeographic formations in the state of Santa Catarina, Brazil.

Mapa de ubicación de la cuenca del río Canoas y formaciones fitogeográficas en el estado de Santa Catarina, Brasil.
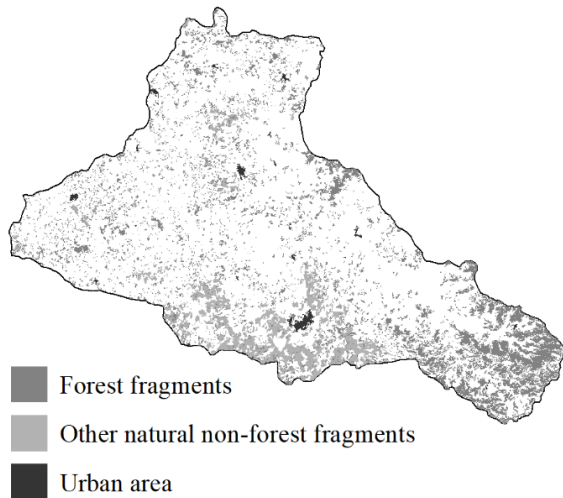
**Figure 2.** Atlantic Forest remnants in Canoas River Basin (Santa Catarina, Southern Brazil) provided by SOS Mata Atlântica and National Institute for Space Research (INPE). Based on images from the Landsat 8 satellite (2016, spatial resolution of 30 m) (SOS Mata Atlântica and INPE 2017).

Remanentes del bosque atlántico en la cuenca del río Canoas (Santa Catarina, sur de Brasil) proporcionados por SOS Mata Atlântica y el Instituto Nacional de Investigaciones Espaciales (INPE). Basado en imágenes del satélite Landsat 8 (2016, resolución espacial de 30 m).

and proximity and allowing inferences about the landscape connectivity.

To assess the core areas, an edge effect of 50 m was considered, based on other studies performed in the region that evaluated the environmental, floristic and structural conditions at different edge distances (Guidini *et al*. 2014, Dalla Rosa *et al*. 2015). SHAPE, CORE, and CAI metrics were evaluated by fragment size classes (<5 ha, 5-50 ha, 50-100 ha, and >100 ha) using boxplots.

For connectivity metrics, a standard search radius of 1,000 m was used, which is a commonly measure for landscape ecology studies. In addition, to check if there were neighboring fragments compatible with the displacement distances of the main seed dispersers of *A. angustifolia*, other two search radii were considered (table 2). The maximum values found in each study were used, seeking to not underestimate animals' displacement capacity since the methodologies of the studies were different. Seed dispersal distance data from the genetic structure were also employed, based on studies that assessed seed dispersal distances regarding the location of mother trees and regenerating individuals. Based on the maximum values found in each study, two average distances were calculated: 1) for the displacement distances of dispersers; and 2) for seed dispersal distances based on genetic proximity.

**Table 1.** Metrics for fragments and landscape of Canoas River Basin, state of Santa Catarina, Brazil.

Métricas para fragmentos y paisaje de la cuenca del río Canoas, estado de Santa Catarina, Brasil.

| | Category | Metric | Range | Description |
|---|---|---|---|---|
| Fragments | Area | AREA | > 0 | Fragment area (ha). |
| | Shape | SHAPE | ≥ 1 | Fragment shape. The closer to 1, the more regular the shape. |
| | Core area | CORE | ≥ 0 | Core area considering edge size (ha). |
| | | NCORE | ≥ 0 | Number of core areas. |
| | | CAI | $0 \leq CAI < 100$ | Fragment percentage corresponding to the core area. |
| | Connectivity | ENN | > 0 | Euclidean nearest neighbor distance (m). |
| | | PROX | ≥ 0 | Proximity index. When it is equal to zero, there are no neighbors in the search radius; it rises as the neighborhood is increasingly occupied by patches of the same type. |
| Landscape | Area | CA/TA | > 0 | Landscape area (ha). |
| | | LPI | $0 < LPI \leq 100$ | Landscape percentage composed of the largest fragment. |
| | Core area | TCA | ≥ 0 | Total core area (ha). |
| | Connectivity | NP | ≥ 1 | Number of fragments. |
| | | ENN | > 0 | Euclidean nearest neighbor distance (m). |
| | | PROX | ≥ 0 | Mean proximity index. |

**Table 2.** Displacement distances for the dispersers of *A. angustifolia* used in this study, according to studies developed in the phytogeographic region of the Mixed Ombrophilous Forest.

Distancias de desplazamiento para los dispersores de *A. angustifolia* utilizados en este estudio.

| Sources | | | Maximum distance (m) | Average distance (m) |
|---|---|---|---|---|
| Dispersers displacement distances | Small rodents | Lamberts (2003) | 26.7 | |
| | | Marques *et al.* (2011) | 70 | |
| | | Nicola (2009) | 225 | |
| | Jays | Anjos (1991) | 80 | 87[a] |
| | | Kindel (1996) | 100 | |
| | | Solórzano-filho (2001) | 120 | |
| | Agouti | Lamberts (2003) | 50 | |
| | Squirrels | Bordignon and Monteiro-Filho (2000) | 25 | |
| Seed dispersal distances (genetic proximity of mother tree and regenerants) | | Cristofolini (2013) | 237 | |
| | | Bittencourt and Sebbenn (2007) | 291 | 287[b] |
| | | Sant'anna (2011) | 334 | |

[a] Based on the average of all dispersers displacement distances.

[b] Based on the average of all seed dispersal distances considering genetic proximity of mother trees and regenerating individuals.

Euclidean nearest neighbor distance (ENN) was assessed using a frequency histogram, and PROX metric was assessed using absolute and relative frequencies in different classes.

Geoprocessing activities were performed using ArcGis 10.3 software (ESRI 2013), and landscape metrics were calculated using Fragstats 4.2 software (McGarigal *et al.* 2012). Charts were constructed using the R programming language (R Core Team 2020).

RESULTS

*Landscape structure.* A total of 3,436 patches of habitat were recorded in Canoas River Basin, which corresponds to an area of 291,391 ha. Considering the total calculated area of the basin in this study (1,488,846 ha), 19.6 % are habitat areas, *i.e.* forest remnants and other non-forest natural remnants. Of the total number of patches in Canoas River Basin, 80.8 % have an area smaller than 50 ha (table 3, figure 3). It could be found that fragments larger than 50 ha occupy 16.4 % of the landscape when assessing the proportion of habitat areas in relation to the total area of the Canoas River basin. The landscape percentage composed of the largest fragment (LPI) is only 1.9 %.

The mean value obtained for the landscape shape index (SHAPE) was 1.87, indicating that, in general, fragments are little shredded and presented shapes similar to a rectangle. Fragments with shape metrics of up to 1.5 correspond to 36.9 % of the total value; shape between 1.5 and 2 to 34.3 %, and shape from 2 to 28.8 %. Regarding the

**Table 3.** Number of patches of habitat (forest natural remnants) by area size class in Canoas River Basin, state of Santa Catarina, Brazil.

Número de fragmentos de hábitat (bosques naturales remanentes) por clase de tamaño del área de la cuenca del río Canoas, estado de Santa Catarina, Brasil.

| Class (ha) | Number | % in class | Total area (ha) | Occupation in the landscape (%) |
|---|---|---|---|---|
| < 5 | 266 | 7.7 | 783.5 | 0.1 |
| 5 - 50 | 2,513 | 73.1 | 47,040.3 | 3.2 |
| 50 - 100 | 349 | 10.2 | 23,860.8 | 1.6 |
| > 100 | 308 | 9.0 | 219,706.3 | 14.8 |
| Total | 3,436 | 100.0 | 291,390.8 | 19.6 |
| Total basin area (ha) | | | 1,488,846.0 | |

size classes of the fragments, the most important variation in shape is in fragments with the largest size (> 100 ha), whereas the smaller ones (<5 ha) have a shape close to 1 and are more regular (figure 4A). Fragments with shape metrics above 4 are the largest in relation to the total area. Even though they have a highly irregular shape, they also correspond to the largest core areas of Canoas River Basin (figures 4B and 4C). The largest fragments (areas of 28,000 and 21,000 hectares) had very high values for shape metrics (10 and 17), although they were also the patches
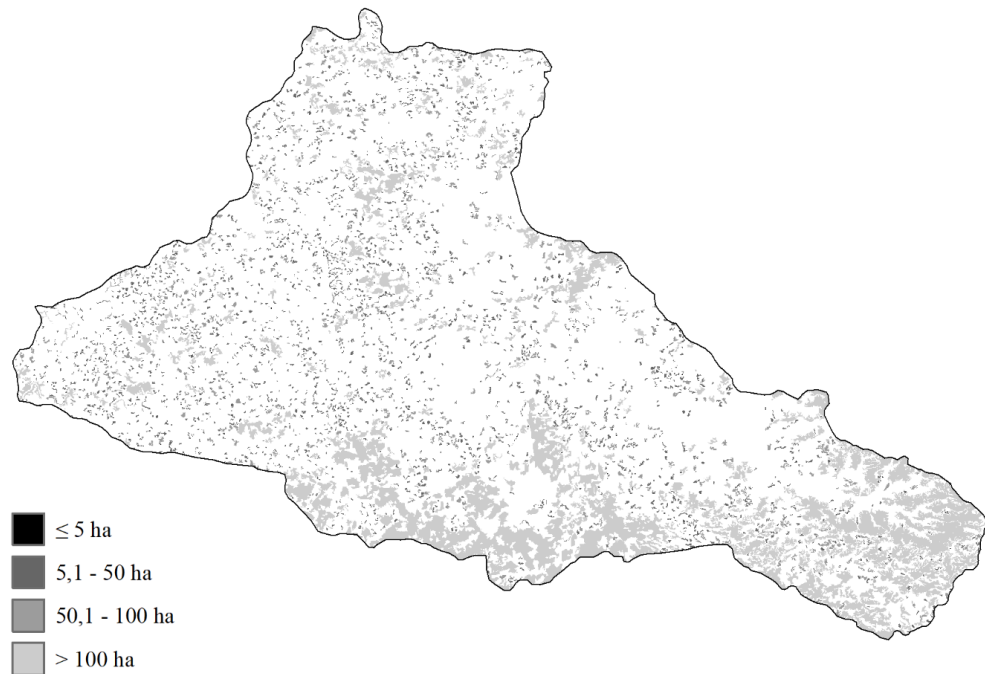
**Figure 3.** Size classes of habitat fragments in Canoas River Basin, state of Santa Catarina, Brazil.

Clases de tamaño de fragmentos de hábitat en la cuenca del río Canoas, estado de Santa Catarina, Brasil.

with the highest proportions of core areas, corresponding to 91 and 83 % of the total area, respectively.

For the total area (fragments with forest remnants and other non-forest natural remnants) of Canoas River Basin, the core area (CORE) was of 2,173.2 km². This result implies a reduction of 25.4% when compared to the total area. Among the fragments, 46 had no core area, *i.e.,* when the edge size was applied, the whole fragment consisted of an edge habitat. Based on the metric that calculates the percentage of a fragment that corresponds to the core area (CAI), it could be noticed that 61% of fragments have less than 50 % core area in relation to the total area (2,091 fragments).

*Connectivity between fragments and relation to seed dispersal of* A. angustifolia. Canoas River Basin has a density of 0.23 fragments per 100 hectares. The mean proximity index (PROX) found for a generalist search radius (1,000 m) was 344, and the nearest neighbor distance (ENN) was 362 m. The distance to the nearest and most frequent fragment was 100 to 200 m (figure 5).

Using a search radius of 87 m, which corresponds to the mean displacement distance of the dispersers of *A. angustifolia* considered in this study, the proximity index was equal to 0 (zero) for all fragments. This result suggests that there are no neighboring fragments within this radius of distance throughout Canoas River Basin. For seed dispersal distance considering genetic proximity and

applying a search radius of 287 m, 1,495 fragments with a proximity index equal to 0 (zero) were found (table 4). This number indicates that 43.5 % of the remaining fragments do not have a neighbor within the seed dispersal limit of *A. angustifolia*, considering the genetic distance. Equivalently, results of the metric that measures the nearest neighbor distance (ENN) indicate that 1,941 fragments have at least one neighbor within the seed dispersal limit, considering the distance between mother and regenerating trees.

DISCUSSION

*Landscape structure.* Considering the total number of fragments, Canoas River Basin presents the same reality as those of Mixed Ombrophilous Forest as a whole and the Atlantic Forest biome, having approximately 80 % of the forest remnants with an area of less than 50 ha (Ribeiro *et al.* 2009, Sevegnani *et al.* 2013). The large number of small fragments indicates high degree of landscape destruction and, consequently, a more important edge effect. Likewise, the landscape percentage composed of the largest fragment (LPI) was exceptionally low, demonstrating the intense fragmentation since the largest fragment comprises only a small area in relation to the total landscape. These results already indicate that seed dispersal may be impaired as many small fragments may not be sufficient for long-term survival of large vertebrates, and the lack of

connectivity between the remnants may hinder seed dispersal of the local flora, particularly those with large seeds (Bueno *et al.* 2013).

Fragments with an area larger than 50 ha are located mainly in the South and Southeast regions of the basin. In the South, it comprises the municipalities of Campo Belo do Sul, Capão Alto, Lages and Painel. In the Southeast, the fragments are mainly in the following municipalities close to Serra Geral: Urubici, Bom Retiro and Rio Rufino. The proximity to the mountain range may have led to better conservation in this region since the larger slopes



**Figure 5.** Frequency histogram of the Euclidean nearest neighbor distance (ENN) for Canoas River Basin, state of Santa Catarina, Brazil.

Histograma de frecuencia de la distancia euclidiana al vecino más cercano (ENN) para la cuenca del río Canoas, estado de Santa Catarina, Brasil.



**Figure 4.** Boxplots for the metrics of SHAPE (A), CORE (B) and CAI (C) by fragment size class from Canoas River Basin, state of Santa Catarina, Brazil. Closed triangles correspond to the mean and open circles represent the outliers.

Gráficos de caja para las métricas de SHAPE (A), CORE (B) y CAI (C) por clase de tamaño de fragmento de la cuenca del río Canoas, estado de Santa Catarina, Brasil. Los triángulos cerrados corresponden a la media y los círculos abiertos representan los valores atípicos.

**Table 4.** Frequencies of the PROX connectivity metric for Canoas River Basin fragments, state of Santa Catarina, Brazil (AF = absolute frequency; RF = relative frequency).

Frecuencias de la métrica de conectividad PROX para los fragmentos de la cuenca del río Canoas, estado de Santa Catarina, Brasil (AF = frecuencia absoluta; RF = frecuencia relativa).

| PROX | Seed dispersal (mother and regenerating tree) (287 m) | |
|---|---|---|
| | AF | RF (%) |
| 0 | 1495 | 43.5 |
| 0.1 - 200 | 1660 | 48.3 |
| 200.1 - 400 | 48 | 1.4 |
| 400.1 - 600 | 35 | 1.0 |
| 600.1 - 800 | 22 | 0.6 |
| 800.1 - 1000 | 21 | 0.6 |
| >1000 | 155 | 4.5 |
| Total amount of fragments | 3436 | 100 |

found there may hinder the processes of occupation by man. Land use for economic purposes is preferably done in less sloping areas and at lower altitudes, leading to a more drastic reduction in forest cover in these situations, while more remote and hard-to-reach areas usually have higher vegetation cover (Cunha *et al.* 2012).

Regarding shape, fragments with a shape index above 2 were observed, reaching values such as 10 and 17. These fragments with more irregular shape are also those of larger total area and core area, contrary to what was expected. Shape index is influenced by the fragment size and is expected to commonly decrease as the size increases (Turner *et al.* 2001). Nevertheless, according to the results obtained in this study, even large fragments can have quite complex shapes and may suffer important effects of surrounding matrix. Perhaps, due to the type of land use of neighboring fragments, such as urban area or agriculture, these large fragments are shredded. However, the composition of fragments with large areas can be highly influenced by their shape and edge effect, factors that are often considered more important than the area itself (Didham and Ewers 2012). Ewers and Didham (2007) found that large fragments with highly complex shape can have 80 % of their diversity reduced when compared to smaller circular fragments, a result of the dominance of groups of species that are tolerant to the edge, which impairs the presence of demanding species in shade.

On the other hand, it could be observed that some very small fragments have no core area, according to the edge size adopted. Ferreira *et al.* (2016) assessed a fragment in the region of Mixed Ombrophilous Forest and concluded that it did not present variations in its organization, structure and relative participation of regeneration guilds in the arboreal community of the edge-interior gradient. Similar result are described by Ferreira *et al.* (2016), which added to those results on the core area metrics found in this study, suggests that, in fact, some of Mixed Ombrophilous Forest fragments are composed entirely of a habitat with edge characteristics mainly due to the size, shape and large anthropization of the matrix.

*Connectivity between fragments and relation to seed dispersal of A. angustifolia.* Connectivity between remnants in Canoas River Basin is low, and considering the displacement of the main dispersers of *A. angustifolia,* it could be inferred that these animals' walking between fragments is quite difficult due to the distance between them and the non-forest matrix. Considering that the seed dispersal of *A. angustifolia* by small rodents is limited to a mean displacement distance of 107 m, and by jays, to 100 m – according to studies conducted in the phytogeographic region –, and that the mean nearest neighbor distance was less than or equal to the movement of these dispersers in only 314 fragments, *i.e.*, 91 % of cases, there is no connectivity between remnants for these classes of dispersers. As for the seed dispersal by agouti and squirrels, considering the dis-

placement distances of 50 and 25 m respectively, the connectivity between fragments is inexistent since there are no nearby fragments within this limit. If the displacement of dispersers between fragments is difficult, and therefore possibly occurs less frequently, the seeds of this species will likely have greater difficulties of establishment due to factors such as competition and predation. For plants, external factors, such as abundance and disperser behavior, habitat quality and quantity, and interactions between these elements, influence the movement of propagules in ecological and evolutionary time (Damschen *et al.* 2008).

The large distances between the remnants may justify the low occurrence of *A. angustifolia* regenerants detected in the Mixed Ombrophilous Forest (Chami *et al.* 2011). Cain *et al.* (2000) claim that landscape fragmentation can cause populations of many plant species to be spatially isolated from each other, often by hundreds of meters or more. The authors also suggest that most plant seeds do not go far, often only one or a few meters, hindering the reach of new areas by propagules even more. A previous study has found that human interferences as fragmentation and selective logging have had negative effects on the seed disperser communities and the natural availability of seeds of *A. angustifolia*, which reduces seed survival and recruitment (Brocardo *et al.* 2018). Their results indicated that recruitment has decreased in mean fourfold in forest fragments in relation to continuous forests, suggesting a scenario with low seed dispersal effectiveness on fragmented landscapes.

It is worth mentioning that the edge effect distance considered was 50 m, which makes it impossible for very small fragments to be considered in this metric. However, depending on the landscape matrix, the existence of these small remnants can assist in the displacement of dispersers between larger patches, serving as stepping stones or trampolines.

In view of the genetic estimates of seed dispersal – *i.e.*, a measure of "effective seed dispersal" since it allows to accurately identify the distance between the mother tree and its regenerants (Cain *et al.* 2000) –, the proximity to other remnants is zero for almost half of the fragments. Even in an optimistic scenario, in which seed dispersal is effective in half the landscape, the situation of the species is worrisome. Assuming that the seed is dispersed, there is still a high probability that it will be degraded or consumed by other animals before germinating; or even, the seedling may suffer from the trampling of cattle, common practice in the forest remnants of the region. For such reasons, both awareness and preservation of the species, as well as commitment to the creation of conservation units that act as connectors of larger fragments are necessary as they can assist in the movement of dispersers of this species.

CONCLUSIONS

From the results of this study, it can be inferred that Canoas River Basin has a high degree of fragmentation, having a large proportion of small fragments (less than 5

ha of area). In comparison with the Atlantic Forest biome, the vegetation cover is higher than average, although the number of fragments smaller than 50 ha is compatible with the studies for this biome.

Considering the displacement distance of the main dispersers of *A. angustifolia*, connectivity and proximity between fragments are very low, which may explain the fact that this species is often not found in the regenerating components of forest inventories. On the other hand, considering the results based on genetic proximity and using distance data between the mother tree and regenerating individuals, it can be concluded that a connection would be possible in more than 50 % of fragments. Therefore, other factors may be interfering with the low regeneration of the species, *e.g*., seed predation. Actions such as the creation of small conservation units and the preservation of ciliary areas that connect habitat fragments can help in increasing the regeneration of the species.

## ACKNOWLEDGEMENTS

## REFERENCES

ANA (Agência Nacional de Águas, BR). 2012. Bacias Hidrográficas Ottocodificadas (Níveis Otto). Accessed 21 feb. 2018. Available at http://metadados.ana.gov.br/geonetwork.

Anjos L. 1991. O ciclo anual de *Cyanocorax caeruleus* em floresta de araucária (Passeriformes: Corvidae). *Ararajuba* 2(1): 19–23.

Bittencourt JVM, AM Sebbenn. 2007. Patterns of pollen and seed dispersal in a small, fragmented population of the wind-pollinated tree *Araucaria angustifolia* in southern Brazil. *Heredity* 99(6): 580–591. DOI: 10.1038/sj.hdy.6801019

Bordignon M, ELDA Monteiro-Filho. 2000. O serelepe *Sciurus ingrami* (Sciuridae: Rodentia) como dispersor do pinheiro do Paraná *Araucaria angustifolia* (Araucariaceae: Pinophyta). *Arquivos de Ciências Veterinária e Zoologia da UNIPAR* 3(2): 139–144.

Brocardo CR, F Pedrosa, M Galetti. 2018. Forest fragmentation and selective logging affect the seed survival and recruitment of a relictual conifer. *Forest Ecology and Management* 408: 87-93. DOI: 10.1016/j.foreco.2017.09.046

Bueno RS, R Guevara, MC Ribeiro, L Culot, FS Bufalo, M Galetti. 2013. Functional redundancy and complementarities of seed dispersal by the last neotropical megafrugivores. *PloS one* 8(2): e56252. DOI: 10.1371/journal.pone.0056252

Cain ML, BG Milligan, AE Strand. 2000. Long-Distance Seed Dispersal in Plant Populations. *American Journal of Botany* 87(9): 1217-27. DOI: 10.2307/2656714

Chami LB, MM Araújo, SJ Longhi, P Kielse, AD Lúcio. 2011.

Mecanismos de regeneração natural em diferentes ambientes de remanescente de Floresta Ombrófila Mista, São Francisco de Paula, RS. *Ciência Rural* 41(2): 251–259. DOI: 10.1590/S0103-84782011000200012

Cristofolini C. 2013. Dinâmica da diversidade genética de *Araucaria angustifolia* (Bertol.) Kuntze em paisagem de campo no estado de Santa Catarina. Science Master Thesis. Florianópolis, Brazil. Universidade Federal de Santa Catarina. 93 p.

Cunha JEBL, IAA Rufino, BB Silva, IB Chaves. 2012. Dinâmica da cobertura vegetal para a Bacia de São João do Rio do Peixe, PB, utilizando-se sensoriamento remoto. *Revista Brasileira de Engenharia Agrícola e Ambiental* 16(5): 539–548. DOI: 10.1590/S1415-43662012000500010

Dalla Rosa A, AC Silva, P Higuchi, AL Guidini, FR Spiazzi, M Negrini, RD Ansolin, MA Bento, DA Gonçalves, TS Ferreira. 2015. Diversidade e guildas de regeneração de espécies arbóreas na borda de uma floresta nativa em contato com plantio de pínus. *Floresta* 45(2): 273–280. DOI: 10.5380/rf.v45i2.34676

Damschen EI, LA Brudvig, NM Haddad, DJ Levey, JL Orrock, JJ Tewksbury. 2008. The movement ecology and dynamics of plant communities in fragmented landscapes. *Proceedings of the National Academy of Sciences* 105(49): 19078–19083. DOI: 10.1073/pnas.0802037105

Deák, B., O Valkó, P Török, A Kelemen, Á Bede, AI Csathó, B Tóthmérész. 2018. Landscape and habitat filters jointly drive richness and abundance of specialist plants in terrestrial habitat islands. *Landscape Ecology* 33(7): 1117-1132. DOI: 10.1007/s10980-018-0660-x

Didham RK, RM Ewers. 2012. Predicting the impacts of edge effects in fragmented habitats: Laurance and Yensen's core area model revisited. *Biological Conservation* 155: 104–110. DOI: 10.1016/j.biocon.2012.06.019

Environmental Systems Research Institute (ESRI). 2013. ArcGIS for Desktop: release 10.3. Redlands, CA.

Ewers RM, RK Didham. 2007. The effect of fragment shape and species' sensitivity to habitat edges on animal population size: Contributed papers. *Conservation Biology* 21(4): 926–936. DOI: 10.1111/j.1523-1739.2007.00720.x

Ferreira TS, AK Marcon, B Salami, CCC Rech, AR Mendes, AF Carvalho, FF Missio, F Pscheidt, AL Guidini, RS Dornelles, AC Silva, P Higuchi. 2016. Composição florístico-estrutural ao longo de um gradiente de borda em fragmento de Floresta Ombrófila Mista Alto-Montana em Santa Catarina. *Ciência Florestal* 26(1): 123-134.

Finch D, DP Corbacho, H Schofield, S Davison, PGR Wright, RK Broughton, F Mathews. 2020. Modelling the functional connectivity of landscapes for greater horseshoe bats *Rhinolophus ferrumequinum* at a local scale. *Landscape Ecology* 35(3): 577-589. DOI: 10.1007/s10980-019-00953-1

Guidini AL, AC Silva, P Higuchi, A Dalla Rosa, FR Spiazzi, M Negrini, TS Ferreira, B Salami, AK Marcon, F Buzzi Junior. 2014. Invasão por espécies arbóreas exóticas em remanescentes florestais no Planalto Sul Catarinense. *Revista Árvore* 38(3): 469-478. DOI: 10.1590/S0100-67622014000300009

Hadley AS, MG Betts. 2011. The effects of landscape fragmentation on pollination dynamics: absence of evidence not evidence of absence. *Biological Reviews* 87(3): 526-544. DOI: 10.1111/j.1469-185X.2011.00205.x

Instituto Brasileiro do Meio Ambiente e dos Recursos Naturais

Renováveis (IBAMA). 1992. Portaria IBAMA Nº 06-N, de 15 de janeiro de 1992, Ministério do Meio Ambiente. Consulted 13 mar. 2018. Available in http://www.mma.gov.br/estruturas/179/_arquivos/179_05122008033646.pdf.

Iob G, EM Vieira. 2008. Seed predation of *Araucaria angustifolia* (Araucariacae) in the Brazilian Araucaria Forest: influence of deposition site and comparative role of small and 'large' mammals. *Plant Ecology* 198: 185-198. DOI: 10.1007/s11258-007-9394-6

Kindel EAI. 1996. Padrões de dispersão e disposição espacial de *Araucaria angustifolia* (Bert.) O. Ktze. e suas relações com aves e mamíferos na Estação Ecológica de Aracuri, Esmeralda, RS. Master in Ecology. Porto Alegre, Brazil. Universidade Federal do Rio Grande do Sul.

Lamberts AH. 2003. Predação e sobrevivência de sementes de *Araucaria angustifolia* (Bert.) Kuntze em áreas de mata nativa e plantação de *Pinus eliotii* na Floresta Nacional de São Francisco de Paula, RS. Master in Ecology. Campinas, Brazil. Universidade Estadual de Campinas. 165 p.

Marques RV, CV Cademartori, SM Pacheco. 2011. Mastofauna no Planalto das Araucárias, Rio Grande do Sul, Brasil. *Revista Brasileira de Biociências* 9(3): 278–288. DOI: 10.11606/T.17.2006.tde-01082007-105409

Marchioro CA, KL Santos, A Siminski. 2020. Present and future of the critically endangered *Araucaria angustifolia* due to climate change and habitat loss. *Forestry: An International Journal of Forest Research* 93(3): 401–410. DOI: 10.1093/forestry/cpz066

McGarigal K, Cushman SA, Ene E. 2012. FRAGSTATS v4: Spatial Pattern Analysis Program for Categorical and Continuous Maps. Amherst: University of Massachusetts. Accessed 13 jan. 2020. Available at http://www.umass.edu/landeco/research/fragstats/fragstats.html.

Nicola PA. 2009. Comunidades de pequenos mamíferos como indicadores de qualidade ambiental no planalto norte catarinense. Forestry Engineer Thesis. Curitiba, Brazil. Universidade Federal do Paraná. 118 p.

R Core Team. 2020. R: A language and environment for statistical computing. R Foundation for Statistical Computing, Vienna, Austria. Accessed 21 dez. 2020. Available at https://www.R-project.org/.

Ribeiro MC, JP Metzger, AC Martensen, FJ Ponzoni, MM Hirota. 2009. The Brazilian Atlantic Forest: How much is left, and how is the remaining forest distributed? Implications for conservation. *Biological Conservation* 142(6): 1141–1153. DOI: 10.1016/j.biocon.2009.02.021

Sant'Anna CS. 2011. Diversidade genética, estrutura genética espacial e dispersão realizada de pólen e sementes em uma população contínua de *Araucaria angustifolia* (Bertol.) Kuntze no planalto norte de Santa Catarina. Science Master Thesis. Florianópolis, Brazil. Universidade Federal de Santa Catarina. 89 p.

Sevegnani L, AC Vibrans, AL Gasper. 2013. Considerações finais sobre a Floresta Ombrófila Mista em Santa Catarina. *In* Vibrans AC, L Sevegnani, AL Gasper. DV Lingner eds. Inventário Florístico Florestal de Santa Catarina. Volume III - Floresta Ombrófila Mista. Blumenau, Brazil. Edifurb. p. 275–278.

Solórzano-Filho JA. 2001. Demografia, fenologia e ecologia da dispersão de sementes de *Araucaria angustifolia* (Bert.) Kuntze (Araucariaceae), numa população relictual em Campos do Jordão, SP. Ecology Thesis. São Paulo, Brazil. Universidade de São Paulo. 115 p.

SOS Mata Atlântica and INPE (Instituto Nacional de Pesquisas Espaciais, BR). 2017. Atlas dos Remanescentes Florestais da Mata Atlântica: Relatório Técnico Período 2015-2016. Accessed 21 feb. 2018. Available at http://mapas.sosma.org.br/site_media/download/atlas_2015-2016_relatorio_tecnico_2017.pdf.

Turner MG, RH Gardner, RV O'Neill. 2001. Landscape ecology in theory and practice: pattern and process. New York, USA. Springer. 401 p.

# Anatomy and cell wall chemistry of tension wood in *Hibiscus cannabinus*

Anatomía y química de la pared celular de la madera de tensión en *Hibiscus cannabinus*

**Pramod Sivan [a, c], Karumanchi S Rao [b], Kishore S Rajput [c]\***

[a] Swedish University of Agricultural Sciences, Umea Plant Science Centre,
Department of Forest Genetics and Plant Physiology, Umea, Sweden.

[b] Sardar Patel University, Department of Biosciences, Vallabh Vidyanagar, Gujarat, India.

*Corresponding author: [c] The Maharaja Sayajirao University of Baroda, Faculty of Science,
Department of Botany, Tilak Road, Vadodara 390002, India, phone: +91 265 2791891, ks.rajput15@yahoo.com

## SUMMARY

*Hibiscus cannabinus* (kenaf) is well known as a source for textile fibers and as an alternate source for cellulosic fibers for paper and pulp industry. Formation of reaction xylem alters the chemical properties of fibers, which may affect its uses. To the best of our knowledge, there are no reports on the occurrence of reaction xylem in kenaf. The present study examines reaction xylem (*i.e.* tension wood and its opposite side) formed in response to bending of stems in Kenaf by anatomical, histochemical and biochemical methods. The reaction xylem found on the upper side of leaning stems showed an eccentric growth pattern, thin walls, shorter and wider fibers without gelatinous layer, decrease of vessel or ray density as compared to wood formed on opposite sides. Histochemical localization of lignin using Weisner reaction and Maule's test indicated presence of more syringyl units in the fiber wall of tension wood. Gravimetric quantification of cell wall polymers showed relatively more amount of holocellulose and hemicellulose in tension wood (69 and 46 %, respectively) compared to those of opposite wood (63 and 42 %, respectively). There was no significant difference noticed in the klason lignin content between opposite (17.4 %) and tension wood (16.7 %). Lignin characterization by the thioacidolysis method revealed that the tension wood lignin in kenaf was composed of more amount of syringyl and p-hydroxyphenyl monomers compared to that of opposite side wood. This analysis also suggests that the tension wood lignin is rich in β-aryl ether linkages in syringyl units resulting in high S/G ratio.

*Key words:* kenaf, reaction xylem, lignin characterization, wood chemistry.

## RESUMEN

*Hibiscus cannabinus* (kenaf) es utilizada para producción de fibras textiles, papel y pulpa. La formación del xilema de reacción altera las propiedades químicas de las fibras, la cual puede afectar sus usos finales. No existen reportes sobre la aparición del xilema de reacción en kenaf. Por ello, el presente estudio describe el xilema de reacción de kenaf, el cual abarca cambios anatómicos, histoquímicos y bioquímicos como respuesta a la inclinación del tallo. El xilema de reacción en el lado superior del tallo inclinado mostró un patrón de crecimiento excéntrico, paredes delgadas, fibras más cortas y menor diámetro, y sin la presencia de una capa gelatinosa característica de la madera de reacción, menor frecuencia de vasos y rayos en comparación con el xilema formado en el lado opuesto. La localización de la lignina por histoquímía (método de Weisner y prueba de Maule) indicó una mayor cantidad de grupos siringilo en la pared celular del xilema de tensión. La cuantificación gravimétrica de los polímeros en la pared celular mostró mayor porporción de holocelulosa y hemicelulosa en el xilema de tensión, pero no hubo diferencia significativa en el contenido de lignina klason entre el xilema de tensión y el xilema opuesto. El método de tioacidólisis mostró que la lignina en el xilema de tensión estaba compuesta por mayor cantidad de grupos de siringilo y p-hidroxifenilo en relación con la madera opuesta. Estos resultados sugieren que la lignina en el xilema de tensión del kenaf presenta mayor proporción de enlaces de éter β-arílico en unidades de siringilo, resultando una alta relación S/G.

*Palabras clave:* kenaf, madera de reacción, caracterización de lignina, química de la madera.

## INTRODUCTION

Formation of reaction xylem is a dynamic characteristic in the developmental biology of higher plants. In woody angiosperms, reaction xylem is called as tension wood, which is formed as eccentric growth on the upper side of the leaning stems or branches. When the orientation of the main stem is shifted from vertical, formation of tension wood provides the required mechanical reinforcement for optimal architecture of the dicotyledons species in the space (Almeras and Clair 2016, Groover 2016). The physiology of maintaining stems and branches with secondary

growth in appropriate positions by allowing them to bend through generating tensional longitudinal stress is also attributed to tension wood formation (Clair *et al.* 2013). In general, tension wood is characterized by the occurrence of gelatinous (G) fiber in which the inner lignified secondary wall layer is replaced by a crystalline cellulosic G layer. Due to the high proportion of G-fibers, tension wood has less lignin content while, high cellulose quantity in the cell wall chemical composition (Baba *et al.* 1996). On the other hand, there are also reports on the occurrence of reaction xylem, without G-fibers on the side of eccentric growth (Yoshida *et al.* 2000).

Because of the variation in tissue composition, cell wall structure and chemical composition, tension wood is considered to be important in understanding the relation between physical and physiological stress on plant growth pattern, especially structure and function of cell wall of plants. Plant fibers are the most important raw materials for versatile usage, especially in pulp and paper industry. Therefore, structure and chemical composition of cell wall polymers play a significant role in their commercial use (Ramage *et al.* 2017). It is therefore necessary to understand the distribution pattern of cell wall polysaccharides and monomeric composition of lignin in plant fibres having commercial importance.

The current understanding on the chemistry of reaction xylem is mainly based on the xylem with gelatinous fibers on the upper side of the bending stem associated with eccentric growth. However, the information available on the cell wall chemistry of reaction xylem showing eccentric growth without gelatinous fibers is meagre. *Hibiscus cannabinus* L. (kenaf) belongs to Malvaceae, and is well known as a source for textile fibers and as an alternate source for cellulosic fibers for paper and pulp industry (Neto *et al.* 1996). *Hibiscus cannabinus* fibers are also suggested to be applied for cellulose derivatives (Saikia *et al.* 1993), particle boards (Seller *et al.* 1993) and feedstock for energy and chemicals (Cunninghan *et al.* 1986). Due to the immense importance of *H. cannabinus* fibers, the structure and chemistry of cell walls have been studied extensively (Jin *et al.* 2012). The functional properties of reaction xylem have been mainly attributed to the cell wall chemistry variation associated with gelatinous layers (Groover 2016, Pramod *et al.* 2019). Plausibly, the lignified part of the cell wall may also play a role in functional mechanics of reaction xylem. The major limitation for quantification of chemical variation in lignified walls of typical reaction or tension wood fibers is due to the presence of a thick G-layer. In the present study, we noticed an eccentric growth pattern in the stem of *H. cannabinus*. Anatomical studies revealed the absence of gelatinous fibers in the eccentric growth side suggesting this reaction xylem is an ideal system for evaluating the structure and chemistry of reaction xylem without G-layers. Therefore, the main aim of the study is to describe the anatomy, distribution pattern of lignin, chemical composition and characterization of lignin

monomers in the tension and opposite wood of *H. cannabinus*. To the best of our knowledge, there are no reports on the occurrence of reaction xylem in *H. cannabinus* and our results suggest the dynamic change in lignin chemistry could play a key role in reaction xylem mechanics during upright growth of stems without gelatinous fibers.

## METHODS

*Plant material.* Samples from bending stems (main) were collected from two-year-old *H. cannabinus* plants growing in the premises of Department of Biosciences, Sardar Patel University, Gujarat, India. Tension wood and opposite wood samples were selected from the area of eccentric growth on the upper side and less growth on lower side respectively. For microscopy, samples were fixed in 2 % glutaraldehyde in phosphate buffer (pH 7.2). For biochemical studies, wood pieces were frozen in liquid nitrogen for 1 hour and subsequently dried for 72 hours at -80 ˚C. Cell-wall residue (CWR) was obtained by pulverizing the samples in a Wiley mill to pass through an 80 μm sieve. The powdered wood (CWR) was afterwards sequentially extracted with distilled water, ethyl alcohol, alcohol: toluene (1:1) and acetone (Merck, Germany) in Soxhlet extractor and dried to get Extractive free xylem residue (EXR). The analysis was conducted in triplicate.

*Light microscopy.* Transverse, tangential and radial longitudinal sections (15-20 μm thick) were taken from the upper side of the bending stem and its opposite side wood sample using sliding microtome (Leica SM2010R, Germany). Sections were stained with safranin-astra blue (Srebotnik and Messener 1994), dehydrated in ethanol-xylene series and embedded in DPX. Lignin was localized in the xylem elements using Wiesner reaction by pouring few drops of 1 % phloroglucinol in ethanol solution on the section mounted on a glass slide followed by adding a drop of 10 % HCl and covering the sections with cover slip (Vallet *et al.* 1996). Maule's reaction (Meshitsuka and Nakano 1979) was used to localize the abundance of syringyl lignin moieties in the cell wall. Sections were immersed in 1 % $KMnO_4$ for 5 minutes, washed in distilled water, immersed in 3 % HCl for 1 minute, washed in distilled water, added few drops of ammonium hydroxide solution and covered with a glass slide. Observations and photography of stained sections were carried out using Leica SM2000 microscope attached with digital camera (Leica DMC2900, Germany).

For measuring the dimension details of xylem elements, small pieces of xylem were macerated by incubating them in Jeffrey's fluid (Berlyn and Miksche 1976) 36-48 hrs. After thorough washing in water, the macerated xylem elements were stained with 0.5 % safranin O (Sigma, USA) before being mounted in 50 % glycerol. The length and width of fibers and vessel elements were measured with an ocular micrometer scale mounted in a research microsco-

pe. Ray dimension and density/mm$^2$ area were measured from tangential longitudinal sections using ocular micrometer. Wall thickness of fibers and vessels, and vessel density were measured from transverse sections. For each parameter, 30 measurements were taken randomly for each cell types and statistically analyzed to determine the mean values. Student t-test was carried out to determine statistically significant differences of anatomical parameters at a 0.05 confidence level using Sigmastat software (Version 3.5, San Jose, CA, USA).

*FTIR Spectroscopy.* Cell wall residues (CWR) and Klason lignin (KL) were used for an FTIR analysis. KBr pellets for IR spectroscopy were prepared using macro-technique (13 mm ø pellet; Ca. 1.5 mg sample with 350 mg KBr). Spectra were recorded with the FTIR spectrometer with TGS detector (Perkin Elmer, Spectrum GS, USA) at resolution of 4 cm$^{-1}$ for 32 scans in the range from 600 to 4000 cm$^{-1}$. Background spectra of clear window was recorded prior to acquisition of the sample spectra. The spectrum of the background was subtracted from the spectra of the sample before conversion into absorbance units. For each sample, three different sub samples were analyzed and averaged to give mean spectrum per individual sample.

*Determination of holocellulose and α-cellulose.* The holocellulose and α-cellulose was determined using a microanalytical method developed by Yokoyama *et al.* (2002), 200 mg of EXR were weighed into a 15 ml round bottom flask and placed in water bath at 90 ˚C. The reaction was initiated by the addition of 1ml of reaction mixture (400 mg of 80 % Sodium chlorite + 4ml distilled water + 0.4 ml acetic acid). An additional 1ml reaction mixture was added every 30 min. The samples were removed to cold water bath after 2 h. The sample was then filtered through a course sintered glass filter (Whatmann, GD 1UM), washed with deionized water (3×50 ml), dried in oven at 105 ˚C and holocellulose content was determined gravimetrically. For determination of α-cellulose, 50 mg of dried holocellulose samples were weighed into reaction flask and allowed to equilibrate for 30 min, subsequently 4 ml of 17.5 % sodium hydroxide were added and allowed to react for 30 min and next 4 ml of distilled water were added. The sample was macerated for 1 min, allowed to react for 29 min and after filtered through a sintered glass filter. Following a 5min soaking in 1.0 M acetic acid, the sample was washed with 90 ml of distilled water (3×30 ml) and dried overnight. The α-cellulose was determined gravimetrically.

*Determination of lignin content.* A lignin analysis was carried out on dry extract free cell wall residue and ground to pass through a 180 micron sieve before exhaustive solvent extraction (2:L$^1$ (v/v) toluene: ethanol, ethanol and water). The lignin content in juvenile and mature wood was determined by Klason lignin method (Dence 1992).

*Thioacidolysis.* Thioacidolysis was carried out according to Lapierre *et al.* (1995). The reagent was prepared by introducing 2.5 ml of BF3 etherate (Aldrich) and 10 ml of ethanethiol EtSh (Aldrich) into a 100 ml flask and adjusting the final volume to 100 ml with dioxane. A mixture of the sample (12 mg) and 12 ml of reagent were put in tube fitted with Teflon lined screw cap. Thioacidolysis was performed at 100 ˚C (Oil bath) for 4 hours with occasional shaking. The cooled reaction mixture, followed by washings with water, was combined with and the mixture was poured over 1 ml Dichloromethane (Fluka, Germany) including internal standard (0.50 mg tetracosane from Sigma, Germany). After adjusting the pH of the aqueous phase to pH 3-4 with 0.4 M sodium carbonate aqueous solution, the aqueous phase was extracted with dichloromethane (20 ml×3). The combined organic extracts were dried over Na$_2$SO$_4$ and the solvent was evaporated under reduced pressure at 40 ˚C in a rotary evaporator. The residue was re-dissolved in dichloromethane (1ml). The thioacidolysis products (7 μl) were sylated with 50 μl of N, O-bis (trimethylsilyl) trifluoroacetamide (BSTFA, Sigma, Germany) and 5 μl of pyridine (Sigma, Germany) in a 200 μl GC vial with Teflon lined screw cap and kept at room temperature for overnight. The sylated products were separated by Gas chromatography using silicon based capillary column (30 m×0.25 μm×250 μm) and each peak was identified by GC/MS. The temperature program of the GC increased at a rate of 5 ˚C/min from 100 ˚C/280 ˚C and final temperature was maintained for 60 minutes.

RESULTS

*Anatomical characteristics tension and opposite wood.* The secondary xylem of *H. cannabinus* was composed of fibers, vessels (as solitary and radial multiples), paratracheal parenchyma and ray parenchyma cells (figure 1A). Vessels and fibers were characterized by the presence of thick, lignified secondary walls (figure 1A, B). Although axial and ray parenchyma showed lignified cell walls, the thickness of their secondary wall was relatively thin as compared to that of vessel and fibers (figure 1B). Rays were tri-to multiseriate and heterocellular (figure 1C). In terms of tissue composition, tension wood was similar to opposite wood except the ratio of fibers to vessels was found to be higher in tension wood. The thickness of the secondary wall decreased significantly in fibers. On the other hand, the gelatinous layer, a typical characteristics of tension wood was found absent in the fibers in the reaction xylem of *H. cannabinus* (figure 1D). Fibers were identical to axial parenchyma due to similar wall thickness, while distinct by the absence of intercellular spaces and narrow tip compared to parenchyma cells (figure 1D). Ray parenchyma in tension wood appeared to be wider than those of opposite wood (figure 1E).

Measurements from the macerated xylem tissue revealed the dimensional difference of various elements in
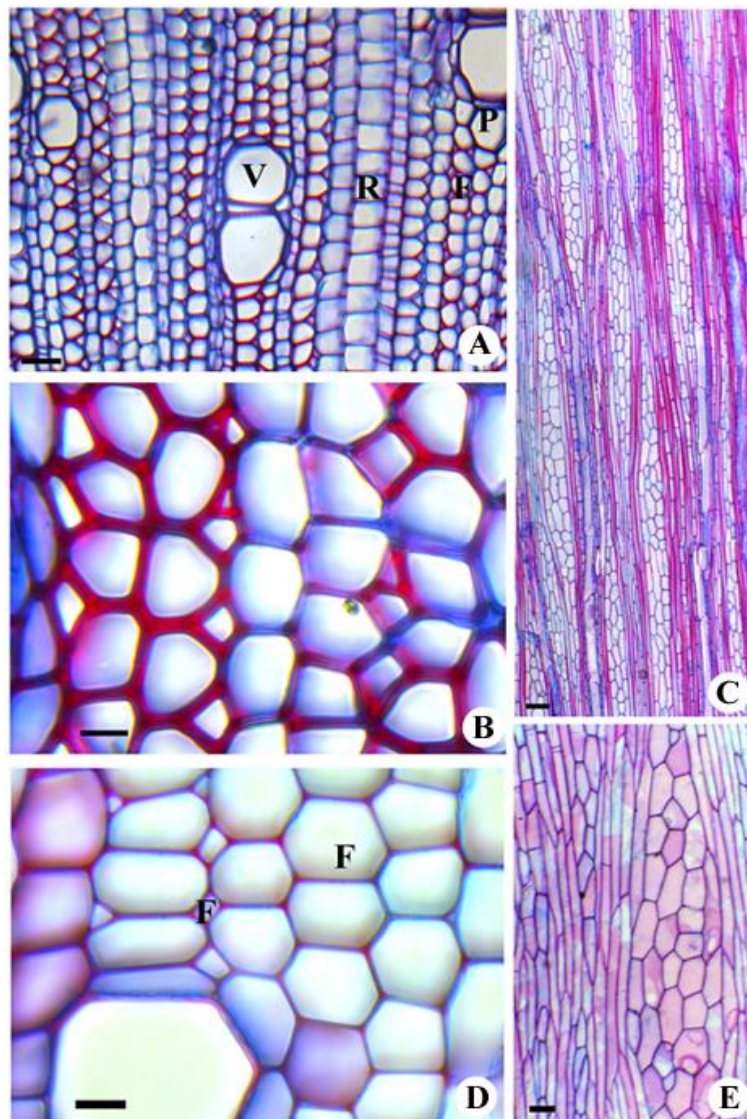
**Figure 1 (A-E).** Transverse (A, B, D) and tangential longitudinal (C, E) sections of normal wood (A-C) and tension wood (D-E) of *H. cannabinus*.

Cortes microtómicos de secciones transversales (A, B, D) y tangenciales de madera normal (A-C) y madera en tensión (D-E) de *H. cannabinus*.

the tension and opposite wood of *H. cannabinus*. Tension wood showed a significant decrease in fiber length, wall thickness of fibers and vessel elements, height of rays and density of vessels and rays per unit area as compared to those of opposite wood (table 1). On the other hand, a significant increase in width of fibers and rays was evident in tension wood (table 1). Dimensions of vessel elements did not show any significant variation between tension and opposite wood.

*Histochemical localization of lignin in tension wood and opposite wood.* Weisner reaction revealed variation of lignification patterns in different xylem elements of opposite

and tension wood elements. Opposite wood showed presence of lignin in all xylem elements (figure 2A). Staining intensity was more in the vessel wall suggesting higher lignin concentration compared to other elements (figure 2B). Maules reaction revealed a negative staining reaction from vessel walls, which indicates the presence of more condensed guaiacyl lignin units (figure 2C). Fiber walls showed positive staining reaction due to the presence of more syringyl lignin units (figure 2D). Weisner reaction of tension wood samples showed similar lignin distribution as compared to opposite wood elements (figure 2E). Cell walls of fibers, on the other hand, showed a relatively stronger positive staining reaction to Maule's test indicating the

**Table 1.** Anatomical characteristics of normal wood and tension wood of *H. cannabinus*.

Características anatómicas de la madera de tensión y la madera normal de *H. cannabinus*.

| Variable | | Normal wood | Tension wood | P-value |
|---|---|---|---|---|
| Fiber | Length | 1093 ± 234 | 897 ± 165 | *0.001 |
| | Width | 35 ± 4 | 44 ± 3 | *<0.001 |
| | Wall thickness | 3.6 ± 0.5 | 1.46 ± 0.3 | *<0.001 |
| Vessel element | | | | |
| | Length | 559 ± 52 | 527 ± 60 | [n.s.]0.398 |
| | Width | 97 ± 32 | 100 ± 17 | [n.s.]0.838 |
| | Wall thickness | 4.6 ± 0.7 | 3.25 ± 0.4 | *<0.001 |
| | Vessel density | 15 ± 2 | 10 ± 2 | *<0.001 |
| Ray | | | | |
| | Height | 4016 ± 102 | 2747 ± 95 | *<0.001 |
| | Width | 169 ± 42 | 244 ± 56 | *<0.001 |
| | Density | 19 ± 2 | 13 ± 1 | *<0.001 |

*Significant difference following student t-test ($\alpha=0.05$), n.s.; non-significant difference, measurements are in µm
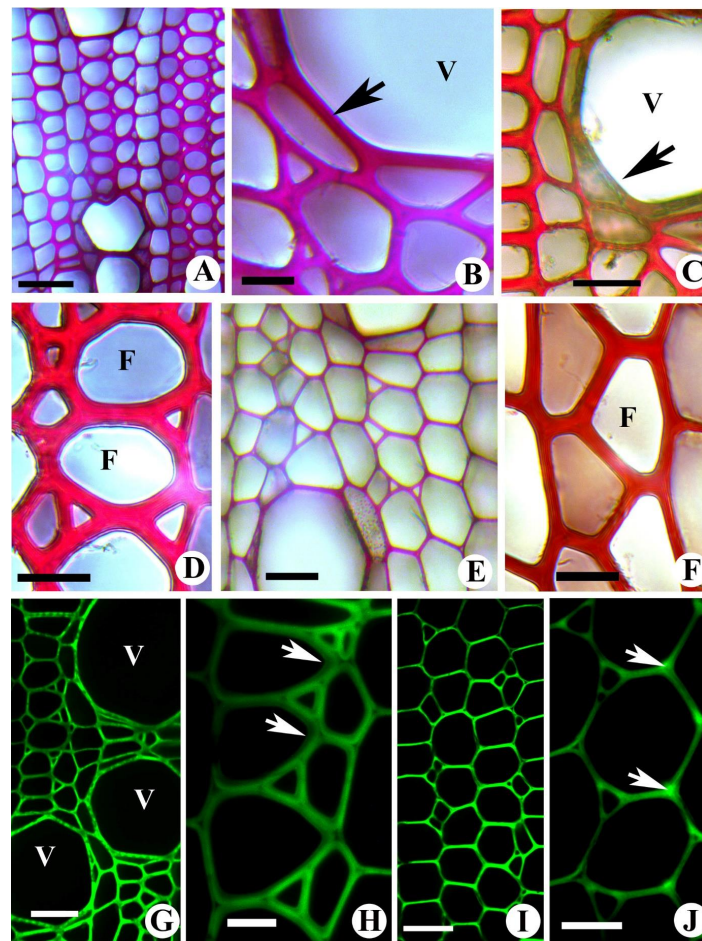


**Figure 2 (A-J).** Light (A-F) and epi-fluorescence (G-J) images from the transverse section of normal wood (A-D) and tension wood (E-J) of *H. cannabinus*.

Imágenes al microscopio de luz (A-F) y epi-fluorescencia (G-J) de cortes transversales de la madera normal (A-D) y madera en tensión (E-J) de *H. cannabinus*.

presence of more syringyl lignin units (figure 2F). Epi-fluorescence microscopy of opposite wood xylem showed high intensity of fluorescence from the vessel walls while a weak signal from the secondary wall fibers suggesting the presence of highly condensed lignin units in the former (figure 2G, H). Tension wood also showed a similar pattern of fluorescence compared to opposite wood elements (figure 2I). The cell corners of tension wood fibers showed relatively high fluorescence intensity indicating presence of condensed lignin units in this region (figure 2J).

*Analysis of chemical composition of opposite and tension wood by FTIR and gravimetric methods.* The analysis of

FTIR spectra of tension and opposite wood showed prominent peaks in the fingerprint region of 1800-600 cm$^{-1}$ (figure 3). Peaks were numbered and assigned to functional groups and structures according to published literature (table 2).

Most peaks observed in the cell wall residue (CWR) such as 1, 6, 9, 10 and 11 (1738, 1376, 1160, 1112 and 1053 cm$^{-1}$ respectively) corresponded to polysaccharides (Cellulose and hemicelluloses). Peaks 2, 3, 4, 7 and 8 (1602, 1506, 1461, 1328, 1246 cm$^{-1}$, respectively) were assigned to aromatic skeletal vibration, C=O stretching and CH3 bending vibration in the lignin. These peaks appeared more prominent in the FTIR spectra of klason lignin
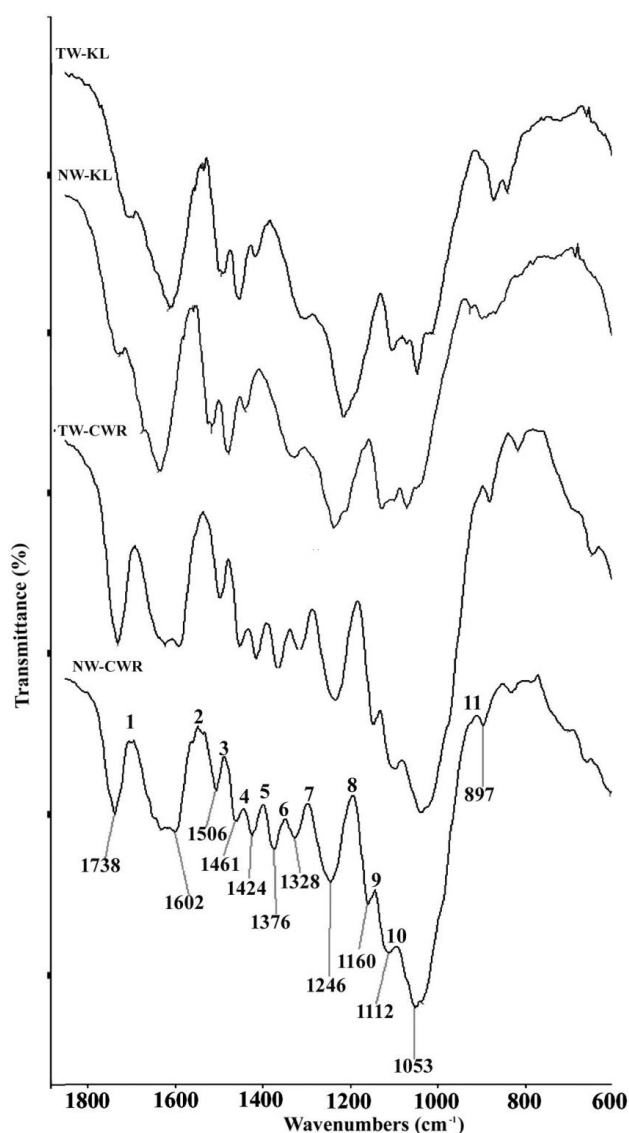


**Figure 3.** FTIR spectra of cell wall residue (CWR) and Klason lignin (KL) from the normal wood (NW) and tension wood (TW) of *H. cannabinus*.

Espectros FTIR de residuos de pared celular (CWR) y lignina Klason (KL) de la madera normal (NW) y madera de tensión (TW) de *H. cannabinus*.

(KL). On the other hand, peaks 1, 6 and 9 of CWR spectra, which correspond to C=O stretching, CH3 bending and COC anti-symmetric bridge vibration in the cellulose and hemicellulose, did not appear in the KL spectra suggesting their removal during acid hydrolysis. Peaks 2 and 8, which correspond to benzene ring stretching vibration and C=O stretching vibration in lignin, showed a shift in peak position from 1602 cm$^{-1}$ (CWR) to 1619 cm$^{-1}$ (KL) and 1246 cm$^{-1}$ (CWR) to 1223 cm$^{-1}$ (KL), respectively. The gravimetric quantification of cell wall polysaccharides showed a relatively higher content holocellulose, α-cellulose and

hemicelluloses in tension wood compared to that of opposite wood (tables 2, 3). There was no significant difference in the lignin content between opposite and tension wood (tables 2, 3).

*Characterization of lignin by thioacidolysis method.* The results of the gas chromatographic separation of thioacidolytic monomers from opposite and tension wood lignins of *H. cannabinus* are displayed in figure 4.

The monomers of *H. cannabinus* lignin were detected according to Rolando *et al.* (1992) as both the erythro

**Table 2.** Chemical composition in normal and tension wood of *H. cannabinus*.

Composición química de la madera de tensión y la madera normal de *H. cannabinus*.

| Chemical constituent | Normal wood | Tension wood |
|---|---|---|
| Holocellulose (%) | 63.23 ± 0.4 | 69.50 ± 0.5 |
| α-cellulose (%) | 42.61 ± 1.5 | 46.45 ± 0.42 |
| Hemicellulose (%) | 20.62 ± 2.4 | 23.05 ± 0.5 |
| Lignin (%) | 17.42 ± 0.3 | 16.7 1± 0.5 |

**Table 3.** Band assignments of cell wall residue (CWR) and Klason lignin (KL) from normal and tension wood of *H. cannabinus*.

Asignaciones de bandas para residuos de lignina en pared celular (CWR= y lignina Klason para la madera de tensión y la madera normal de *H. cannabinus*.

| No. | Wave number (cm$^{-1}$) | | | | Band origin, short comments | References |
|---|---|---|---|---|---|---|
| | Normal wood | | Tension wood | | | |
| | CWR | KL | CWR | KL | | |
| 1 | 1738 | -- | 1739 | -- | C=O stretching vibration in xylan | Harington *et al.* (1964) |
| 2 | 1602 | 1619 | 1602 | 1619 | Aromatic skelton vibration plus C=O stretch; S>G; G condensed > G etherified | Faix (1991) |
| 3 | 1506 | 1499 | 1506 | 1499 | Benzene ring stretching vibration in lignin | Harington *et al.* (1964) |
| 4 | 1461 | 1460 | 1462 | 1460 | CH$_2$ deformation vibration in lignin and Xylan+benzene vibration in lignin | Faix (1991), Harington *et al.* (1964) |
| 5 | 1424 | 1421 | 1425 | 1421 | CH$_2$ scissor vibration in cellulose + CH$_3$ bending Vibration in lignin | Harington *et al.* (1964) |
| 6 | 1376 | -- | 1377 | -- | CH bending vibration in cellulose and hemicellulose | Faix (1991) |
| 7 | 1328 | -- | 1329 | -- | C=O stretching vibration | Faix (1991), Harington *et al.* (1964) |
| 8 | 1246 | 1221 | 1246 | 1223 | C=O stretching vibration in lignin | Harington *et al.* (1964) |
| 9 | 1160 | -- | 1166 | -- | C-O-C antisymmetric bridge stretching vibration in cellulose and hemicellulose | Faix (1991), Harington *et al.* (1964) |
| 10 | 1112 | 1113 | 1112 | 1113 | OH association band in cellulose and hemicellulose | Harington *et al.* (1964) |
| 11 | 1053 | 1053 | 1052 | 1053 | C=O stretching vibration in cellulose and hemicellulose | Harington *et al.* (1964) |

and threo isomers of p-hydroxyphenyl (H), guaiacyl (G) and syringyl (S) lignin units (H-CHSEt-CHSEt-CH$_2$SEt, G-CHSEt-CHSEt-CH$_2$SEt, S-CHSEt-CHSEt-CH$_2$SEt respectively) as well as G- CH$_2$-CHSEt-CH(SEt)$_2$ and S- CH$_2$-CHSEt-CH(SEt)$_2$. It is apparent from the figure 4 and table 4 that monomeric composition of tension wood lignin was characterized by higher content of p-hydroxyphenyl and syringyl units resulted in higher and H/G and S/G ratios compared to those of opposite wood (table 4). The relative proportion of β-O-4 linkages in H, G and S units determined from the major thioacidolytic products, erythro and

threo forms of different monolignol units showed that tension wood of *H. cannabinus* characterized by more β-aryl ether linkages in S and H units (figure 5).

DISCUSSION

The tension wood of *H. cannabinus* is characterized by the absence of a gelatinous layer. Although G-layer is considered as a typical feature of angiosperm reaction xylem, there are several reports on the occurrence of fibers without G-layers in the wood on upper side of lea-
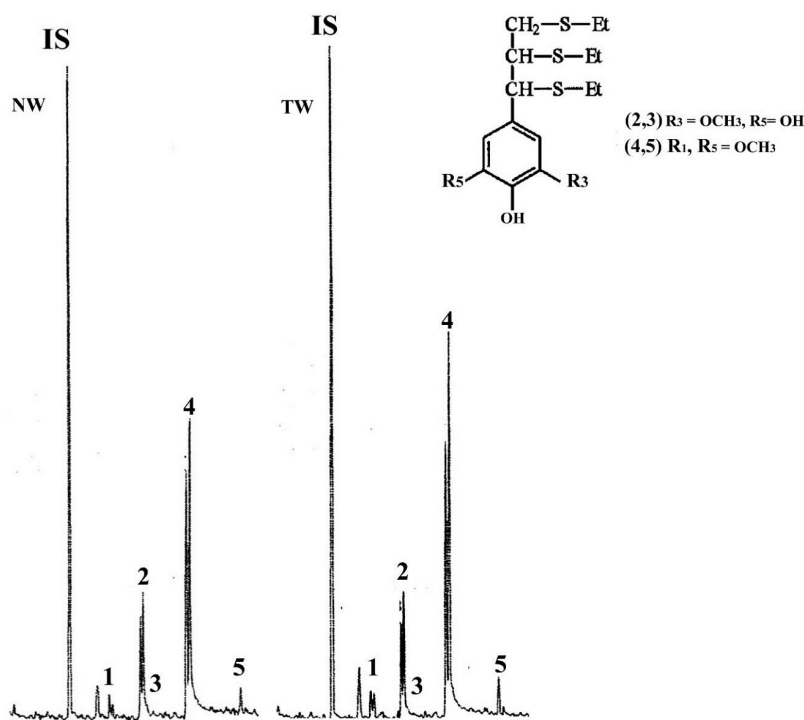


**Figure 4.** Partial gas chromatographs of TMS thioacidolysis products recovered from normal wood (NW) and tension wood (TW) lignin of *H. cannabinus*.

Cromatografía de gases de los productos de tioacidólisis de TMS recuperados de la lignina de madera normal (NW) y madera en tensión (TW) de *H. cannabinus*.

**Table 4.** Monomeric composition of lignin in normal and tension wood of *H. cannabinus*.

Composición monomérica de la lignina en la madera de tensión y la madera normal de *H. cannabinus*.

| | Normal wood | Tension wood |
|---|---|---|
| p-hydroxyphenyl unit (µmol g$^{-1}$) | 70.15 ± 6 | 90.35 ± 3 |
| Guaiacyl unit (µmol g$^{-1}$) | 310.75 ± 15 | 285.35 ± 12 |
| Syringyl unit (µmol g$^{-1}$) | 709.17 ± 16 | 761.68 ± 24 |
| H/G ratio | 0.23 ± 0.03 | 0.32 ± 0.04 |
| S/G ratio | 2.29 ± 0.02 | 2.67 ± 0.15 |
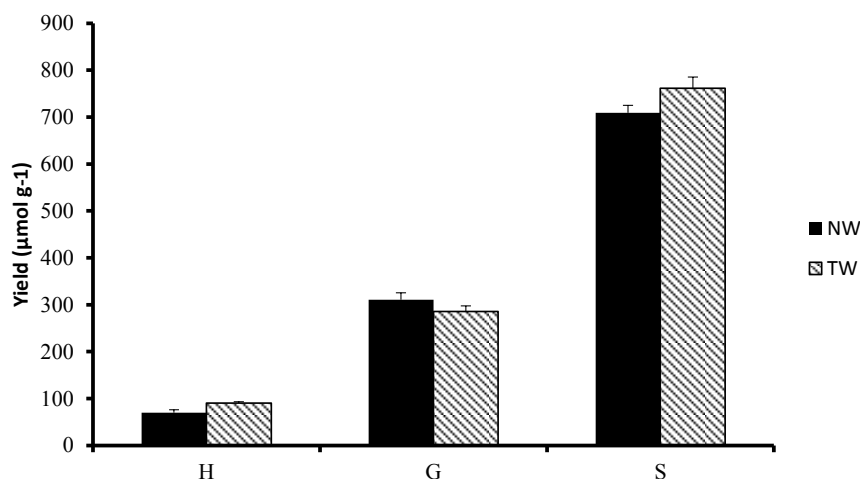
**Figure 5.** Relative richness of β-aryl ether linkages in p-hydroxyphenyl (H), guaiacyl (G) and syringyl (S) lignin units. (Calculated from the prominent peaks of erythro/threo forms of each monomeric unit appeared in the gas chromatograph).

Riqueza relativa de enlaces β-aril éter en unidades de lignina tipo p-hidroxifenil (H), guaiacil (G) y siringil (S). Nota: el cálculo fue hecho a partir de los picos prominentes de las formas eritro/treo en cada unidad monomérica en el cromatógrafo de gases.

ning stem and branches of hard wood species (Bailliers *et al*. 1996). Clair *et al*. (2006), reported the absence of G-layer in the tension wood fibers of 14 tropical rain forest species having highly tensile stressed wood. The present study suggests the similar pattern of tension wood formation in the herbaceous plant, *H. cannabinus,* which shows absence of G-fibers on the upper side of the leaning stem. Anatomical studies revealed that the fibers in the *H. cannabinus* TW are shorter and wider compared to those of opposite wood. In case of G-fibers of tree species, vessel elements and fibers are reported to be significantly longer in tension wood compared to opposite wood in poplar (Jourez *et al*. 2001), while no significant difference in the dimensions of vessels and fibers was noticed in *Leucaena leucocephala* (Lam) de Wit (Pramod *et al*. 2013). The fibers without G-layer found in the eccentric growth side of *Viburnum oderatissimum* (L.) Ker Gawl. were shorter than those found in opposite wood (Wang *et al*. 2010). These authors suggested that the decrease in fiber length could be due to increasing frequency of anticlinal division during eccentric growth. Therefore, decrease in fiber length and ray height with an increase in their width may be associated with the variation in the frequency of anticlinal/periclinal division in tension and opposite xylem development in *H. cannabinus*. The cell-wall thickness of fibers and vessel elements and vessel density have been found to be decreased in the tension wood of *H. cannabinus*. In typical tension wood, increased differentiation of G-fibers generally accompanied by a significant decrease of size and density of vessel elements due to the priority for development of elements responsible for mechanical strength (Timel 1986, Pramod *et al*. 2013). In spite of the lack of G-layers in fibers, the occurrence of typical ten-

sion wood associated anatomical features in *H. cannabinus* secondary xylem suggests that G-layer can be considered as one of the characteristics rather than a specific feature of tension wood formation in angiosperms (Clair *et al*. 2006).

The histochemical analysis of distribution pattern of lignin and syringyl lignin units using Weisner reaction and Maule's test suggests relatively high syringyl lignin units in the tension wood fibers of *H. cannabinus*. In typical tension wood fibers with gelatinous layers, reports on distribution pattern of syringyl units are controversial within different species. More syringyl units are reported in the G-fibers of *Populous deltoids* (Joseleau *et al*. 2004), while more amount of guaiacyl units were noticed in the G-fibers of *Leucaena leucocephala* (Pramod *et al*. 2013). On the other hand, *Magnolia* species showed no difference in the distribution of lignin monomers between tension and opposite wood (Yoshizawa *et al*. 2000). In herbaceous plants, *Liriodendron tulifera* L., less syringyl units have been reported in tension wood fibers (Jin and Kwon 2009). The unusual reaction xylem in the *Viburnum odoratissimum* characterized by eccentric growth on the lower side of branches (region opposite to larger growth stress) showed fibers without G-layer although possessing less syringyl lignin units (Wang *et al*. 2010). The reaction xylem fibers without G-layer in *H. cannabinus* xylem, on the contrary, showed an increase in syringyl lignin distribution on the region of eccentric growth.

The FTIR analysis has revealed the presence of prominent peaks in the fingerprint region (1800-600 cm$^{-1}$) reported to be specific to cellulose, hemicelluloses and lignin (Faix 1991). IR spectra of Klason lignin show that peaks corresponding to lignins have shifted to new posi-

tions from those found in CWR. According to Rana *et al*. (2009), this kind of peak shift in FTIR spectra might be caused by inductive effects of substituents (*e.g.*, $H_3CO_3$) in the aromatic ring system of lignin.

The relative proportion of monolignol units (H, G and S) is believed to be an important feature determining the biological origin of lignin, physical and mechanical characteristics of xylem. In the present study, results of the thioacidolysis analysis showed higher proportion of syringyl lignin units compared to H and G units in the *H. cannabinus* xylem. A previous study on isolated lignin from bast fibers (Ralph 1996) and core xylem (Jin *et al*. 2012) of *H. cannabinus* reported it to contain a high syringyl: guaiacyl ratio, and to have high β-aryl ether units with predominantly erythro form as the predominant form of aryl β-ether intermonomer linkage in the stereo chemistry of lignin. On the contrary, determination of lignin monomeric composition using the permanganate oxidation method showed higher content of H and G units while relatively low S units in the core xylem of *H. cannabinus* grown in Portugal (Neto *et al*. 1996). The selective degradation of aliphatic side chains attached to aromatic moieties in lignin during permanganate oxidation can be useful to analyze only a small fraction of lignin structure (Gellerstedt 1992). Thioacidolysis is specific for degradation of aryl β-ether linkages, which form the most abundant binding form in lignin polymer (Nishimura *et al*. 2002). Therefore, the degradation mechanism of methods and samples employed could probably be responsible for the variation in H:G:S ratio of *H. cannabinus* lignin. The efficient and specific cleavage of β-aryl ether linkages of *H. cannabinus* lignin by thioacidolysis was evident from the observed prominent peaks (3,5) in the chromatograph (figure 4) corresponds to the amount of uncondensed alkyl aryl ether linkages in guaiacyl and syringyl lignin units. Therefore, the S/G ratio calculated from these peaks reflects the proportion of β-aryl ether subunits in S and G lignin units. The high S/G ratio in *H. cannabinus* tension wood suggests more amount of β-aryl ether linkages in syringyl lignin units compared to that of opposite wood.

The major difference found in the lignin monomeric composition of *H. cannabinus* tension wood was an increase in H and S monomers compared to those of opposite wood. Previous studies on characterization of lignin in the tension wood of different dicots have showed a high heterogeneity between different species. In poplar, thioacidolysis data showed an S/G ratio lower than that of opposite wood (Lapierre and Monties 1986). The branches of *Viburnum odoratissimum* also showed an S/G ratio in the eccentric growth side lower than that shown by opposite growth side (Wang *et al*. 2010). These authors suggested that the altered proportion of S/G ratio and β-O-4 linkages in the lower side of branches provides high rigidity and lower viscosity to sustain downward bending due to gravitational force. Rodrigues *et al*. (2001), reported that tension wood of *Eucalyptus globulus* has no significant variation in S/G ratio as compared to opposite wood. On the contrary, Aguayo *et al*. (2010), noticed a high syringyl lignin content in the tension wood of *Eucalyptus* sp. Our results also suggested higher syringyl lignin content in the tension wood of *H. cannabinus*. It is also noteworthy a relatively higher content of p-hydroxyphenyl (H) units in *H. cannabinus* tension wood compared to that of opposite wood. Compression wood in gymnosperms reported to have more H-units than those found in normal wood (Timel 1986, Bailers *et al*. 1996). According to Bailleres *et al*. (1996), the proportion of H units increased significantly during transition from normal to compression wood in *Buxus sempervirens* L. The increase in H units of *H. cannabinus* tension wood suggests a chemical resemblance in the variation pattern of monomeric composition to that of compression wood. The rigidity and strength properties are mainly attributed to a condensed form of G and H units, which form more carbon-carbon linkages compared to S units rich in β-O-4 linkages (Boerjan *et al*. 2003). Hence, increase in H lignin units in *H. cannabinus* tension wood may be an alternative mechanism to balance the rigidity and strength properties. Further, from the industrial perspective, the presence of longer xylem fibers, higher cellulose content and the increase in S/G ratio in tension wood is a desirable feature for textile fibers or processing of lignocellulose biomass for paper and pulp or bioenergy applications.

## CONCLUSIONS

The present study demonstrated that the tension wood (upper side of the bending stem) of *H. cannabinus* is a variant due to the absence of G-layer in fibers. However, it shows several typical tension wood anatomical features such as decrease in vessel density, thickness of fiber wall, density and height of xylem rays etc. The histochemical analysis revealed a higher distribution of syringyl lignin units in the tension wood fiber wall. Although, there is no difference in the amount of lignin between tension wood and opposite wood, TW lignin was also characterized by the presence of more syringyl and p-hydroxyphenyl units in its monomeric composition. The thioacidolysis analysis also suggested TW lignin is rich in β-aryl ether linked syringyl units resulting an S/G ratio higher than that of opposite wood.

## ACKNOWLEDGEMENTS

# REFERENCES

Aguayo MG, L Quintupill, R Castillo, J Baeza, J Freer, RT Mendonça. 2010. Determination of differences in anatomical and chemical characteristics of tension and opposite wood of 8-year-old *Eucalyptus globulus*. *Maderas. Ciencia y Tecnología* 12(3): 241-252.

Almeras T, B Clair. 2016. Critical review on the mechanism of maturation stress generation in trees. *Journal of the Royal Society Interface* 13: 20160550. DOI: https://doi.org/10.1098/rsif.2016.0550

Baba K, T Ona, K Takabe, T Itoh, K Ito 1996. Chemical and anatomical characterization of the tension wood of *Eucalyptus camaldulensis* L. *Mokuzai Gakkaishi* 42: 795–798

Bailleres H, M Castin, B Monties, B Pollet, C Lapierre. 1996. Lignin structure in *Buxus sempervirens* reaction wood. *Phytochemistry* 44: 35-39. DOI: https://doi.org/10.1016/S0031-9422(96)00499-2

Berlyn GP, JP Mikshe. 1976. Botanical microtechnique and cytochemistry. Ames, Iowa, USA. Iowa State University Press. 326 p.

Boerjan W, J Ralph, M Baucher. 2003. Lignin biosynthesis. *Annual Review of Plant Biology* 54: 519-546. DOI: https://doi.org/10.1146/annurev.arplant.54.031902.134938

Clair B, J Ruelle, J Beauchene, M-F Prevost, M Fournier. 2006. Tension wood and opposite wood in 21 tropical rain forest species. 1. Occurrence and efficiency of G-layer. *International Association of Wood Anatomists Journal* 27: 329-338. DOI: http://doi.org/10.1163/22941932-90000158

Clair B, J. Alteyrac, A Gronvold, J Espejo, B Chanson, T. Alméras. 2013. Patterns of longitudinal and tangential maturation stresses in *Eucalyptus nitens* plantation trees. *Annals of Forest Science* 70: 801–811. DOI: http://doi.org/10.1007/s13595-013-0318-4

Cunningham RL, ME Carr, MO Bagby. 1986. Hemicellulose isolation from annual plants. *Biotechnology and Bioengineering Symposium* 17: 159-168.

Dence CW. 1992. The determination of Lignin. *In* Lin SY, CW Dence eds. Methods in lignin chemistry. Springer-Verlag. p 33-61.

Faix O. 1991. Classification of lignin from different botanical origin by FTIR spectroscopy. *Holzforschung* 45: 21–27. DOI: https://doi.org/10.1515/hfsg.1991.45.s1.21

Gellerstedt G. 1992. Permanganate oxidation. *In* Lin SY, CW Dence eds. Methods in lignin chemistry. Springer-Verlag. p. 322-332.

Groover A. 2016. Gravitropism and reaction wood of forest trees-evolution, function and mechanism. *New Phytologists* 211: 790–802. DOI: https://doi.org/10.1111/nph.13968

Jin H, M Kwon. 2009. Mechanical bending-induced tension wood formation with reduced lignin biosynthesis in *Liriodendron tulipifera*. *Journal of Wood Science* 55: 401–408. DOI: https://doi.org/10.1007/s10086-009-1053-1

Jin Z, G Jin, S Shao, KS Katsumata. 2012. Lignin characteristics of bast fibre and ore in kenaf, bark and wood of paper mulberry and mulberry. *Journal of Wood Science* 58: 144-152. DOI: https://doi.org/10.1007/s10086-011-1228-4

Joseleau JP, T Imai, K Kuroda, K Ruel. 2004. Detection *in situ* and characterization of lignin in the G-layer of tension wood fibres of *Populus deltoids*. *Planta* 219: 338–345. DOI: https://doi.org/10.1007/s00425-004-1226-5

Jourez B, A Riboux, A Leclercq. 2001. Anatomical characteristics of tension wood and opposite wood in young inclined stem of Poplar (*Populus euramericana* cv 'Ghjoy'). *International Association of Wood anatomists Journal* 22: 133–157

Lapierre C, B Monties. 1986. Thioacidolysis of poplar lignins: identification of monomeric syringyl products and characterization of Guaiacyl-Syringyl lignin fractions. *Holzforschung* 40: 113–118. DOI: http://doi.org/10.1515/hfsg.1986.40.2.113

Lapierre C, B Pollet, C Ronaldo. 1995. New insights into the molecular architecture of hard wood lignins by chemical degradative methods. *Research on Chemical Intermediates* 21: 397-412. DOI: https://doi.org/10.1007/BF03052266

Mehistsuka G, J Nakano. 1979. Studies on the mechanism of lignin colour reaction (XIII): Maüle colour reaction (9). *Mokuzai Gakkaishi* 25: 588-594. DOI: https://doi.org/10.1016/S0926-6690(01)00101-7

Neto C, A Seca, D Fradinho, MA Coimbra, F Domingues, D Evtuguin, A Silvestre, JAS Cavaleiro. 1996. Chemical composition and structural features of macromolecular components of *Hibiscus cannabinus* grown in Portugal. *Industrial Crops and Products* 5: 189-196. DOI: https://doi.org/10.1016/0926-6690(96)89448-9

Nishimura N, A Izumi, K-I Kuroda. 2002. Structural characterization of kenaf lignin: differences among kenaf verities. *Industrial Crops and Products* 15: 115-122.

Pramod S, KS Rao, A Sundberg. 2013. Structural, histochemical and chemical characterization of normal, tension and opposite wood of Subabul (*Leucaena leucocephala*). *Wood Science and Technology* 47: 777-796. DOI: https://doi.org/10.1007/s00226-013-0528-9

Pramod S, KS Rajput, KS Rao. 2019. Immunolocalization of β (1-4) D-galactan, xyloglucans and xylans in the reaction xylem fibres of *Leucaena leucocephala* (Lam.) de Wit. *Plant Physiology and Biochemistry* 142: 217-223. DOI: 10.1016/j.plaphy.2019.07.013

Ralph J. 1996. An unusual lignin from kenaf. *Journal of Natural Products* 59: 341-342. DOI: https://doi.org/10.1021/np960143s

Ramage MH, H Burridge, M Busse-Wicher, Feredey G, T Reynolds, DU Shah, G Wu, L Yu, P Fleming, DD Tingley, J Allwood, P Dupree, PF Linden, O Scherman. 2017. The wood from the trees: The use of timber in construction. *Renewable and Sustainable Energy Reviews* 68: 333-359. DOI: https://doi.org/10.1016/j.rser.2016.09.107

Rana R, RL Heyser, R Finkeldey, A Polle. 2009. FTIR spectroscopy, chemical and histochemical characterization of wood and lignin of five tropical timber wood species of the family Dipterocarpaceae. *Wood Science and Technology* 44(2): 225–242. DOI: https://doi.org/10.1007/s00226-009-0281-2

Rodrigues J, J Graca, H Pereira. 2001. Influence of tree eccentric growth on syringyl/guaiacyl ratio in *Eucalyptus globulus* wood lignin assessed by analytical pyrolysis. *Journal of Analytical and Applied Pyrolysis* 58: 481–489. DOI: https://doi.org/10.1016/S0165-2370(00)00121-2

Rolando, C, B Monties, C Lapierre. 1992. Thioacidolysis. *In* Lin S, C Dence eds. Methods in Lignin Chemistry. Berlin, Germany. Springer-Verlag. p. 334– 349.

Saikia CN, NN Dutta, M Borah. 1993. Thermal behaviour of some homogeneously esterified products of high a-cellulo-

se pulps of fast-growing plant species. *Thermochimica Acta* 219(1-2): 191-203. DOI: https://doi.org/10.1016/0040-6031(93)80497-X

Sellers T, GD Miller, MJ Fuller. 1993. Kenaf core as a board raw material. *Forest Products Journal* 43: 69-71.

Srebotnik E, K Messener. 1994. A simple method that uses differential staining and light microscopy to assess the selectivity of wood delignification by white rot fungi. *Applied and Environmental Microbiology* 60: 1383-1386.

Timel TE. 1986. Compression wood in Gymnosperms. Vol. I. Springer, Berlin.

Vallet C, B Chabbert, Y Czaninski, B Monties. 1996. Histochemistry of lignin deposition during sclerenchyma differentiation in alfalfa stems. *Annals of Botany* 78: 625-632. DOI: https://doi.org/10.1006/anbo.1996.0170

Wang Y, J Grill, B Clair, K Minato, J Sugiyama. 2010. Wood properties and chemical composition of the eccentric growth branch of *Viburnum odoratissimum* var. *awabuki*. *Trees: Structure and Function* 24(3): 541–549. DOI: http://doi.org/10.1007/s00468-010-0425-x

Yokoyama T, JF Kadla, H-M Chang. 2002. Microanalytical method for the characterization of fibre components and morphology of woody plants. *Journal of Agricultural and Food Chemistry* 50: 1040-1044. DOI: http://doi.org/10.1021/jf011173q

Yoshida M, T Okuda, T. Okuyama. 2000. Tension wood and growth stress induced by artificial inclination in *Liriodendron tulifera* Linn. and *Prunus spachiana* Kitamura f. ascendens Kitamura. *Annals of Forest Science* 57: 739-746. DOI: https://doi.org/10.1051/forest:2000156

Yoshizawa N, A Inami, S Miyake, F Ishiguri, S Yokota. 2000. Anatomy and lignin distribution of reaction wood in two *Magnolia* species. *Wood Science and Technology* 34: 183–196. DOI: http://doi.org/10.1007/s002260000046

# Impact of sand mining:
# A case study of initial growth of forest species for recovery of degraded areas

## Impacto de la extracción de arena:
## Un estudio de caso del crecimiento inicial de especies forestales para la recuperación de áreas degradadas

**Jair Augusto Zanon [a]\*, Francisca Alcivania de Melo Silva [b], Reginaldo Barboza da Silva [b],
Ricardo Cordeiro de Paula [c], Lucas Florencio Mariano [b]**

\*Corresponding author: [a] Universidade Federal do Paraná (UFPR), Curitiba, Paraná, Brasil, zanon.augusto@bol.com.br
[b] Universidade Estadual Paulista "Júlio de Mesquita Filho", Campus Experimental de Registro, Registro, São Paulo, Brasil.
[c] Pirâmide Extração e Comércio de Areia Ltda., Registro, São Paulo, Brasil.

## SUMMARY

The Vale do Ribeira region has a large extension of Brazilian Atlantic Forest, and in most cities, low environmental impact activities predominate, such as sand mining. Sand mining has been trying to adapt their industrial activities to low environmental impact, aiming at the protection of permanent preservation areas (PPAs) of riparian forests. The objective of this work was to conduct a case study focused on monitoring and initial growth of forest species by 18 months. This study was performed in a riparian forest site on the Ribeira de Iguape River, Registro, state of São Paulo, Brazil, in a PPA with extraction of river bed sand. Forest species height, stem diameter and mortality index, and rainfall were evaluated in the period. Non-pioneer species accounted for 42.7 % of the forest, while pioneer species accounted for 53.1 %. These proportions are in accordance with local legislation, which establishes a lower limit of 40 % in planting for both groups. Drought periods and leaf-cutting ants at the beginning of growth stages contributed to a higher mortality index and irregular development of some species, however, even during such adversities, forest species indicated resistance to these conditions. Pioneer species had more important development, with emphasis on *Senna multijuga*, *Alchornea triplinervia*, *Citharexylum myrianthum* and *Trema micranta*, these species must be taken into consideration during the first stages of a project which aims at recovering degraded areas in riparian forests of Atlantic Forest.

*Key words:* permanent preservation areas, land restoration, Ribeira de Iguape River.


## RESUMEN

La región de Vale do Ribeira tiene una gran extensión de selva Atlántica brasileña, y en la mayoría de las ciudades predominan las actividades de bajo impacto ambiental, como la minería de arena de río. La extracción de arena ha estado tratando de adecuar sus actividades con menor impacto ambiental, apuntando a la protección de áreas de preservación permanente (APP). El objetivo fue realizar un estudio de caso con enfoque en el monitoreo y crecimiento inicial de especies forestales hasta 18 meses. Este estudio se realizó en un bosque ribereño del río Ribeira de Iguape, municipalidad de Registro, estado de São Paulo, Brasil, en una APP con extracción de arena de lecho de río. Se evaluó la altura de las especies forestales, el diámetro del tallo, el índice de mortalidad y la precipitación en el período. Las especies no pioneras tuvieron una proporción del 42,7 % del total y las pioneras el 53,1 %; las proporciones están de acuerdo con la ley local. Los períodos de sequía y las hormigas cortadoras de hojas al inicio del crecimiento de las especies contribuyeron para o mayor índice de mortalidad y al desarrollo irregular de algunas especies, sin embargo, incluso las adversidades, las especies forestales indican resistencia en estas condiciones. Las especies pioneras tuvieron mayores desarrollos, con énfasis en *Senna multijuga*, *Alchornea triplinervia*, *Citharexylum myrianthum* y *Trema micranta*. Estas especies deben ser tomadas en consideración al inicio del proyecto de recuperación de área degradada en bosque ribereño de selva atlántica.

*Palabras clave:* áreas de preservación permanente, restauración de tierras, río Ribeira de Iguape.

## INTRODUCTION

The Atlantic Forest is one of the main biomes in Brazil and is highly important for biodiversity, soil and water conservation (Skorupa *et al.* 2012, Thomazini *et al.* 2015). Among the characteristics of this biome, the forest formation is heterogeneous, extending from tropical to subtropical regions of Brazil (Lima *et al.* 2014). Several authors have

studied forest fragments (Ribeiro *et al.* 2009, Esposito *et al.* 2018), and many forest areas are in extremely degraded conditions, thus, forest recovery should be an instrument to mitigate this situation (Costa *et al.* 2019). Sustainable management practices are instruments that may be used to long-term recovery of these forests, which are mainly focused on planting a community of native species of the Atlantic Forest biome (Hatfield *et al.* 2018, Pastório *et al.* 2020).

In Brazil, the forest formations located on the banks of rivers, lakes, water springs and hilltops are called riparian forests (Suganuma and Durigan 2014). These forests are included in the category of permanent preservation areas (Nunes *et al.* 2020), and their importance is due to the maintenance of water quality, soil stability, regularization of hydrological alteration and stabilization of riverbanks, avoiding siltation and soil erosion (Holanda *et al.* 2010, Keram *et al.* 2019). The riparian forests are established as forest formations to be conserved or recovered, therefore, to avoid degradation, planning and strategies are priorities for the preservation of riparian zones (Webb and Erskine 2003, Iori *et al.* 2019).

For a successful recovery of riparian lands, the chosen forest species should be adapted for their local environment, including characteristics as drought tolerance, deep root system, vigorous growth, survival in conditions of low fertility and effectiveness in soil cover (Silva *et al.* 2018, Nunes *et al.* 2020). The lack of knowledge of the environmental impacts caused by riparian forest exploitation puts at risk the sustainability of land and water resources in Ribeira de Iguape river basin (Iori *et al.* 2012), and although the agricultural use of permanent preservation areas is prohibited, a part of these areas has been used for agriculture and sand extraction in river beds (Soares-Filho *et al.* 2014, Marçal *et al.* 2017).

The Ribeira de Iguape River is located between southern São Paulo State and eastern Paraná State, comprising approximately 470 km. It is considered the longest river without dams in the state of São Paulo (SIGRB, 2020). The Vale do Ribeira Region has large biodiversity and there is also the estuary-lagoon complex Cananéia-Iguape, a region of rich biological diversity (SOS Mata Atlântica/INPE 2018). Due to its important biodiversity, studies are needed to provide information on the degradation status of protected areas in this fragment of the Atlantic forest (Prado *et al.* 2019, Dalmaso *et al.* 2020). Currently, sand extraction in riverbeds is an industrial process that has been increasing in the Vale do Ribeira Region (SOS Mata Atlântica/ INPE 2018), and the industrial activity is called sand mining. The activity is an anthropogenic action that causes drastic disturbances in the ecosystem, and rebuilding a soil profile is one of the main tasks for successful recovery (Bradshaw and Hüttl 2001). The effects and impacts of sand mining on the riparian forest are understudied in Brazilian Atlantic Forest (Boëchat *et al.* 2013) and evaluating the influences of sand extraction from the river bed on the growth of forest species can contribute to the

recovery of a riparian forest (Seitz *et al.* 2019, Qin *et al.* 2020). Sand extraction in the riverbed can alter river flow, inhibiting the growth of forest species. Moreover, during the extraction process, large amounts of water and sand are captured and released, this action, combined with the hydrodynamics of the river, can become critical in periods of flood and increase erosion in soils under riparian forests (Souza *et al.* 2001).

The objective of this work is to evaluate the relationship between the initial growth of forest species and the impact of sand mining in a permanent preservation area in the recovery process, taking into consideration aspects of plant classification and mortality index of forest species. We hope to contribute to the recommendation of best management practices in recovery areas of riparian forest by answering the following questions: Can sand mining influence the initial growth of forest species in degraded areas of riparian forest in the process of recovery? What are the best forest species to be implemented in future projects for the recovery of degraded areas in the Atlantic Forest?

METHODS

*Study area.* The study was performed in Registro, state of São Paulo, Brazil (24°30'16.85" S, 47°48'18.47" W, 7 m altitude) in a riparian zone in the process of forest recovery. The regional climate is classified as Cfa - humid subtropical (Köppen) with average annual rainfall of 1,700 mm, which is mostly concentrated between December and March (Iori *et al.* 2019).

The study area was pasture until 2009 and was characterized by permanent preservation areas deforestation caused by anthropic action over the years. The sand mining company Pirâmide Extração e Comércio de Areia Ltda. acquired the area in 2010 and started planting forest species in March 2014. The total area of riparian forest has 1.55 ha, from which 0.10 ha was considered in this study, thus, nine plots were delimited, each plot delimited by 2 planting lines of forest species and in each line nine species were planted, with the spacing of 2.5 m x 2.0 m (figure 1).

The monitoring of forest species started in May 2014, two months after the planting of the last recovery stage in the permanent preservation areas and the monitoring occurred until the 18th month.

*Plant classification and chemical soil analyses.* All forest species were identified (table 1), classified by family, species, successional group and seed dispersal syndrome (Barbosa *et al.* 2017). A total of 143 individuals from 24 different forest species were classified and evaluated over 18 months. Morphological attributes of the forest species were measured, such as species height and stem diameter, assessed by using a measuring tape and a caliper. During measurements, the mortality and pest incidence indexes were evaluated.
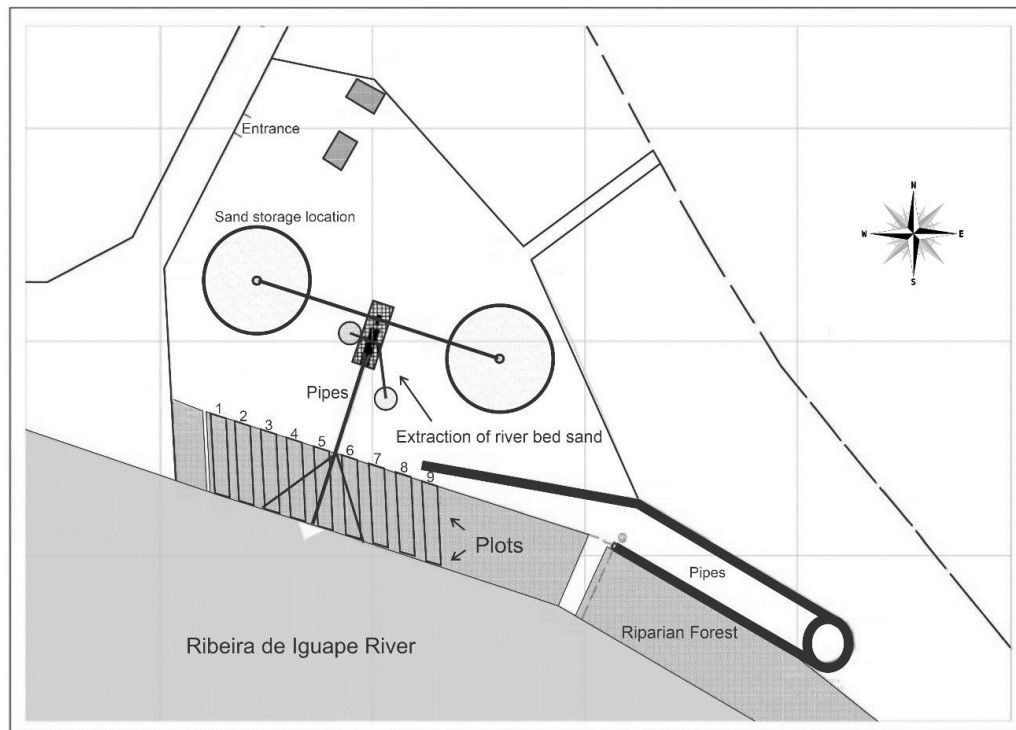
**Figure 1.** Area of the riparian forest (PPA) with extraction of riverbed sand, plots 1, 2, 3, 4, 5, 6, 7, 8 and 9 were monitored and evaluated until the 18th month.

Ubicación del área del bosque ribereño (APP) con extracción de arena de lecho de río, se monitorearon y evaluaron las parcelas 1, 2, 3, 4, 5, 6, 7, 8 y 9 hasta el mes 18.

For soil analyses, samples were collected in the 0-20 cm-deep layer, at the beginning of the experiment. The chemical attributes of the soil were performed according to the methodology recommended by Brazilian Agricultural Research Corporation (EMBRAPA 2017). The sum of bases had the following order of concentration: $Ca^{2+} > Mg^{2+} > K^+$ (table 2). For the pH value ($CaCl_2$) in the layer 0-20 cm deep, the soil was slightly acidified (5.4). Overall organic matter was 3.2 %, the riparian soil had a low concentration of nutrients, which was already expected for an area without chemical fertilizers.

*Statistical analyses.* Sixteen forest species were selected for statistical analyses of height and stem diameter, eight species from the successional group of pioneers: (*Cecropia pachystachya*, *Schinus terebinthifolius*, *Cytharexyllum myrianthum*, *Senna multijuga*, *Alchornea triplinervia*, *Trema micranta*, *Jacaranda caroba*, *Tibouchina mutabilis*) and eight species from the successional group of non-pioneers: (*Ocotea corymbosa*, *Daphnopsis fasciculata*, *Matayba elaeagnoides*, *Clitoria falcata*, *Anadenanthera colubrina*, *Eugenia pyriformes*, *Tabebuia umbellata*, *Ficus guaranitica*). Analyses of variance and Scott-Knott's test ($P < 0.05$) for average comparisons were performed, using the SISVAR 5.6 software (Ferreira 2011).

RESULTS

*Diversity of forest species.* In total, 143 individuals from 24 different forest species were identified and registered in the study area, among pioneer and non-pioneer species. It is observed that 95.8 % of the total forest individuals are native species of the Atlantic forest (table 3).

The percentage of pioneer species identified were 53.1 % and non-pioneer species were 42.7 % and that of the 143 forest individuals, whereas 113 were classified as zoochorous species, that is 79 %.

*Mortality index of forest species.* The mortality of forest species was caused by three reasons: Flooding in the area, drought period and attack by leaf-cutting ants (table 4).

For one month, flooding was observed in three plots (6, 7 and 8) due to a work in the pipes of the extraction of riverbed sand. The pipes showed leakage from river water, which was driven by hydraulic pumps to the sand storage location. In this stretch, less development and a higher mortality index of forest species were observed.

The atypical rainfall in the region during the months of monitoring was another factor that contributed to the mortality index of forest species. The area presented months with very high rainfall and above the monthly average and

**Table 1.** Identification of 24 forest species monitored in the riparian forest area over 18 months.

Identificación de 24 especies forestales monitoreadas en el área de bosque ribereño durante 18 meses.

| Forest species | Family | SG | DS | NI |
|---|---|---|---|---|
| *Alchornea triplinervia* (Spreng.) Müll. Arg. | Euphorbiaceae | P | Zoochorous | 5 |
| *Anadenanthera colubrina* (Vell.) Brenan | Fabaceae | NP | Autochorous | 14 |
| *Cecropia pachystachya* Trécul. | Urticaceae | P | Zoochorous | 5 |
| *Citharexylum myrianthum* Cham. | Verbenaceae | P | Zoochorous | 11 |
| *Clitoria falcata* Lam. | Fabaceae | NP | Autochorous | 7 |
| *Daphnopsis fasciculata* (Meisn.) Nevling | Thymelaeaceae | NP | Zoochorous | 5 |
| *Erythrina falcata* Benth. | Fabaceae | NP | Zoochorous | 3 |
| *Eugenia pyriformes* Cambess. | Myrtaceae | NP | Zoochorous | 5 |
| *Ficus guaranitica* Chodat | Moraceae | NP | Zoochorous | 5 |
| *Gaylussacia brasiliensis* (Spreng.) Meisn. | Ericaceae | P | Zoochorous | 5 |
| *Inga vera* subsp. affinis (DC.) T.D.Penn. | Fabaceae | P | Zoochorous | 16 |
| *Jacaranda caroba* (Vell.) DC. | Bignoniaceae | P | Anemochorous | 9 |
| *Leucaena leucocephala* (Lam.) de Wit | Fabaceae | E | Autochorous | 2 |
| *Matayba elaeagnoides* Radlk. | Sapindaceae | NP | Zoochorous | 9 |
| *Miconia ligustroides* (DC.) Naudin | Melastomataceae | NP | Zoochorous | 4 |
| *Morus nigra* L. | Moraceae | E | Zoochorous | 1 |
| *Ocotea corymbosa* (Meisn.) Mez | Lauraceae | NP | Zoochorous | 3 |
| *Schinus terebinthifolius* Raddi. | Anacardiaceae | P | Zoochorous | 7 |
| *Senna multijuga* (Rich.) H. S. Irwin *et* Barneby | Fabaceae | P | Autochorous | 7 |
| *Syagrus romanzoffiana* Cham. | Arecaceae | NP | Zoochorous | 4 |
| *Syzygium jambos* (L.) Alston | Myrtaceae | E | Zoochorous | 3 |
| *Tabebuia umbellata* (Sond.) Mattos. | Bignoniaceae | NP | Anemochorous | 2 |
| *Tibouchina mutabilis* (Vell.) Cogn. | Melastomataceae | P | Zoochorous | 4 |
| *Trema micranta* (L.) Blume. | Cannabaceae | P | Zoochorous | 7 |

Legend: SG = Successional Group; DS = Dispersal Syndrome; P = Pioneer Species; NP = Non-pioneer Species; E = Exotic; NI = Number of Individuals.

**Table 2.** Chemical property of soil samples from the riparian forest at depth 0-0.20 m.

Propiedad química de muestras de suelo del bosque ribereño a una profundidad de 0-0,20 m.

| pH | OM | P resin | $Al^{3+}$ | H+Al | $K^+$ | $Ca^{2+}$ | $Mg^{2+}$ | SB | CEC | BS |
|---|---|---|---|---|---|---|---|---|---|---|
| $CaCl_2$ | g $dm^{-3}$ | mg $dm^{-3}$ | ------------------------mmol$_c$ $dm^{-3}$------------------------ | | | | | | | --%-- |
| 5.4 | 32 | 22 | - | 31 | 2.2 | 22 | 14 | 38.2 | 69 | 55 |

Legend: OM = Organic Matter; SB = Sum of Bases; CEC = Cation Exchange Capacity; BS = Base Saturation.

other months of low rainfall, with the forest species *Syagrus romanzoffiana*, being the most sensitive to drought. The mortality index of this species was the highest (50 %), along with *Gaylussacia brasiliensis*; the high mortality index in the latter was caused by leaf-cutting ants.

The attack by ants was one of the main reasons for the increase in mortality of forest species. The species most attacked by ants were from the group of non-pioneer species. Some forest species resisted the attacks by the insects, but some did not resist and died, however, in most of them, the forest species attacked by ants resisted and sprouted, developing satisfactorily throughout the evaluated period.

**Table 3.** Percentage of native, exotic, pioneer, non-pioneer, zoochorous forest species, and mortality index about the total number of individuals in the riparian forest area over 18 months of monitoring.

Porcentaje de especies forestales nativas, exóticas, pioneras, no pioneras, zoocorosas e índice de mortalidad sobre el número total de individuos en el área de bosque ribereño durante 18 meses de monitoreo.

|  | Number of individuals | Total percentage (%) |
|---|---|---|
| Total of individuals | 143 | 100.0 |
| Native species | 137 | 95.8 |
| Exotic species | 6 | 4.2 |
| Pioneer species | 76 | 53.1 |
| Non-pioneer species | 61 | 42.7 |
| Zoochorous species | 113 | 79.0 |

*Development of pioneer and non-pioneer forest species.* In general, the species of riparian forest developed satisfactorily, with good performance in the initial growth, even under some adversities. Some forest species showed a high standard deviation due to a high mortality index or a severe attack by leaf-cutting ants or flooding in the area. However, 16 forest species had similar development and were used for the statistical analysis of the initial growth. The average height and average stem diameter of 8 pioneer forest species and 8 non-pioneer forest species were measured from the 2nd to the 18th month, and therefore the Scott-Knott's test was applied to verify the level of significance of the species (tables 5 and 6).

Up to month 2, the eight pioneer species showed no significant difference, probably because of their initial fast-growth. After month 2, the species *Senna multijuga*, *Alchornea triplinervia* and *Trema micranta* had superior growth regarding the other species. Species such as *Cytharexyllum myrianthum* also developed more in the months 14 and 18.

By contrast, non-pioneer species had higher heterogeneity in development up to month 2, both for average height and for average stem diameter. From month 8, the species followed a more homogeneous tendency and had low variation in average height and average stem diameter. There was no significant difference among forest species because these species were adapted in the riparian forest area, therefore, pioneer species with fast growth already offered shade conditions for non-pioneer species to develop under suitable settings.

Pioneer and non-pioneer species had the highest mortality index. For example: *Inga vera*, *Daphnopsis fasciculata*, *Clitoria falcata* and *Gaylussacia brasiliensis* were the fo-

**Table 4.** Mortality index (%) for pioneer and non-pioneer forest species and the cause of mortality in the riparian forest area over 18 months of monitoring.

Lista de especies forestales pioneras y no pioneras que presentaron índice de mortalidad (%) y causa de mortalidad en el área de bosque ribereño durante 18 meses de monitoreo.

| Forest species | Successional group | Number of individuals | Dead individuals | Mortality (%) | Cause of mortality |
|---|---|---|---|---|---|
| *Syagrus romanzoffiana* | NP | 4 | 2 | 50.0 | Drought |
| *Trema micranta* | P | 7 | 1 | 14.3 | Flooding |
| *Jacaranda caroba* | P | 9 | 2 | 22.2 | Flooding |
| *Inga vera* | P | 16 | 3 | 18.8 | Leaf-cutting ants |
| *Daphnopsis fasciculata* | NP | 5 | 1 | 20.0 | Leaf-cutting ants |
| *Matayba elaeagnoides* | NP | 9 | 1 | 11.1 | Flooding |
| *Clitoria falcata* | NP | 7 | 2 | 28.6 | Leaf-cutting ants |
| *Anadenanthera colubrina* | NP | 14 | 4 | 28.6 | Flooding |
| *Gaylussacia brasiliensis* | P | 4 | 2 | 50.0 | Leaf-cutting ants |

Legend: P = Pioneer Species; NP = Non-pioneer Species.

**Table 5.** Average height and average stem diameter of eight pioneer forest species in the riparian forest area over 18 months of monitoring.

Altura promedio y diámetro promedio del tallo de ocho especies forestales pioneras en el área de bosque ribereño durante 18 meses de monitoreo.

| Months | 2 | 8 | 14 | 18 | 2 | 8 | 14 | 18 |
|---|---|---|---|---|---|---|---|---|
| Species | Average height (cm) | | | | Average stem diameter (mm) | | | |
| *Cecropia pachystachya* | 66.4ns | 86.0a | 121.4a | 192.0a | 7.8ns | 18ns | 32.4a | 42.6a |
| *Schinus terebinthifolius* | 75.7ns | 86.7a | 114.6a | 174.0a | 7.0ns | 14ns | 28.2a | 39.2a |
| *Cytharexyllum myrianthum* | 80.4ns | 82.3a | 174.3b | 222.8b | 7.1ns | 18ns | 46.6b | 59.6b |
| *Senna multijuga* | 88.9ns | 138.4b | 230.7b | 315.6b | 10ns | 34ns | 66.9b | 83.3b |
| *Alchornea triplinervia* | 76.6ns | 149.8b | 219.8b | 235.6b | 9.6ns | 33ns | 69.8b | 75.6b |
| *Trema micranta* | 70.3ns | 117.2b | 136.0a | 220.5b | 7.5ns | 24ns | 48.8b | 55.9b |
| *Jacaranda caroba* | 52.0ns | 60.8a | 95.7a | 116.5a | 5.0ns | 12ns | 26.9a | 30.3a |
| *Tibouchina mutabilis* | 54.0ns | 82.0a | 104.0a | 133.5a | 6.3ns | 17a | 21.0a | 28.5a |

Average means followed by the same letter in the column are not significantly different by Scott-Knott's test ($P < 0.05$); ns = Not Significant.

**Table 6.** Average height and average stem diameter of eight non-pioneer forest species in the riparian forest area over 18 months of monitoring.

Altura promedio y diámetro promedio del tallo de ocho especies forestales no pioneras en el área de bosque ribereño durante 18 meses de monitoreo.

| Months | 2 | 8 | 14 | 18 | 2 | 8 | 14 | 18 |
|---|---|---|---|---|---|---|---|---|
| Species | Average height (cm) | | | | Average stem diameter (mm) | | | |
| *Ocotea corymbosa* | 63.3a | 73.3ns | 112ns | 150ns | 6.1a | 8.3a | 19.9a | 33.0a |
| *Daphnopsis fasciculata* | 114b | 133ns | 180ns | 204ns | 13.6b | 26.0c | 50.4b | 56.4b |
| *Matayba elaeagnoides* | 74.6a | 83.1ns | 105ns | 149ns | 7.9a | 13.5a | 24.6a | 29.5a |
| *Clitoria falcata* | 91.2b | 103ns | 141ns | 174ns | 9.9b | 17.4a | 35.1a | 46.2b |
| *Anadenanthera colubrina* | 78.9a | 100ns | 172ns | 190ns | 7.1a | 12.7a | 24.9a | 30.3a |
| *Eugenia pyriformes* | 129b | 132ns | 173ns | 135ns | 10.9b | 15.9a | 23.0a | 29.6a |
| *Tabebuia umbellata* | 57.0a | 100ns | 159ns | 216ns | 5.7a | 11.3a | 27.0a | 29.6a |
| *Ficus guaranitica* | 40.3a | 83.7ns | 173ns | 243ns | 6.5a | 19.3b | 45.3b | 54.0b |

Average means followed by the same letter in the column are not significantly different by Scott-Knott's test ($P < 0.05$); ns = Not Significant.

rest species with the maximum attack by leaf-cutting ants. Even under attack by leaf-cutting ants, *Clitoria falcata* had one of the largest stem diameters at month 18. There was no statistical difference in the months 14 and 18 for average height, although *Daphnopsis fasciculata* and *Ficus guaranitica* had the highest mean for average stem diameter these months for the non-pioneers group. Moreover, *Daphnopsis fasciculata* was one of the species that had an attack by leaf-cutting ants at the beginning of development, which proves the high regenerative capacity of this forest species.

DISCUSSION

The percentage of pioneer and non-pioneer species were 53.1 % and 42.7 %, respectively. These values are in the percentage range found by other authors in reforestation studies in the Atlantic forest (Souza *et al.* 2012, Machado *et al.* 2013). Moura and Montavani (2017) found 42 % of non-pioneer species in areas of regeneration of the Atlantic forest and according to the São Paulo state legislation, SMA 32/2014, the total proportion of species from

the same successional group must not exceed 60 % (São Paulo 2014). In the area of this study, neither group exceeded this percentage. The biodiversity of forest species and the species distribution of both successional groups (pioneer and non-pioneer) are essential for the success of forest restoration projects in areas of the Atlantic Forest (Esposito *et al.* 2018).

The importance of zoochorous species needs to be highlighted, which is mainly linked to the enrichment of the region flora, increasing the presence of seed-dispersing animals (Reznik *et al.* 2012, Colmanetti *et al.* 2016). In degraded or recovering land, the planting of zoochorous species is particularly important due to the seed spread of forest species by wild animals when the forest is in an advanced stage of ecological succession (Sangsupan *et al.* 2018). In month 18 of monitoring, the presence of birds was observed because of the first fruiting of *Schinus terebinthifolius*. Table 5 shows that of the three pioneer forest species showing the fastest growth (height and stem diameter means), two species (*Alchornea triplinervia* and *Trema micranta*) have common morphophysiological characteristics, as they have seed dispersion syndrome classified as zoochorous. Zama *et al.* (2012) also observed that zoochorous forest species were important for advancing in the recovery of degraded areas and influenced the success of the Atlantic Forest.

The non-pioneer forest species had a more heterogeneous behavior, probably because the riparian forest was not in satisfactory conditions for the development of non-pioneer species since the pioneer species were also in an initial growth stage. Shadow is a key component for the growth of non-pioneer species (Piñarodrigues *et. al.* 1997), nonetheless it was not achievable in the studied area as both groups were planted at the same time. Moreover, these species were classified in the same group (non-pioneer), however, initial secondary species, late-stage species and climax species are in this group, hence it was naturally more heterogeneous than the group of pioneer species (Pontes *et al.* 2019).

For the chemical analysis of soil, the values were in the slightly acidic range. Thomazini *et al.* (2015) found pH values (CaCl$_2$) between 4.6 and 4.7 in Atlantic forest areas in Brazil, and other authors also identified pH in the acidic range, showing that Atlantic forest soils are naturally acidic (Pinheiro *et al.* 2004, Marques *et al.* 2015). The importance of soil pH is associated with plants absorption of nutrients from the soil solution and with its significance as indicator of soil chemical conditions, as it can influence the chemical disposition of various nutrients in plant development, changing nutrient availability for the plant (Brandão and Lima 2002).

Higher concentrations of Ca$^{2+}$ and Mg$^{2+}$ compared to K$^+$ are also reported by Souza *et al.* (2001) in the Atlantic Forest in the state of Minas Gerais, Brazil. In the soil-plant system, K$^+$ is one of the most leached nutrients, not being part of any organic compound, therefore, among the main nutrients, it is the one with the biggest leaching loss (Marques *et al.* 2015, Zanon *et al.* 2020). Although Ca$^{2+}$ and Mg$^{2+}$ have structural functions in plant tissues, Ca$^{2+}$ is found in a higher rate in the sum of bases due to the low mobility of this nutrient, furthermore, Ca$^{2+}$ is the main element of the cell wall, including leaf, bole and roots; therefore, the fall of these parts of the species contributes to the supply and cycling of this nutrient.

Three factors were the causes of the mortality of species in the riparian forest, and the flooding of three plots (6, 7, and 8) was the one with the highest index. Keram *et al.* (2019) studied the hydrological dynamics of the river and the implications for reforestation of riparian forest, and they observed that the survival of forest species in wetlands varies according to the species. In our study, mortality occurred mainly in non-pioneer species (table 4). This group has a slower growth compared to pioneer species, being more demanding in water and nutrients (Esposito *et al.* 2018), however, excess water was very harmful. The physiological factor of this group presents morphoclimatic characteristics more susceptible than those presented by pioneer species (Brandão *et al.* 2017); besides, non-pioneer species were implanted in larger proportion, which contributed to the higher proportion in the mortality index of forest species.

The attack by leaf-cutting ants was another serious mortality problem in the riparian forest, however, in general, the forest species had an efficient regeneration. Xavier *et al.* (2019) also had problems with leaf-cutting ants in forest planting, the authors suggested the introduction of forest species diversity to minimize the impacts of ants in highly degraded ecosystems. However, several authors have found positive effects of ants for the transport of nutrients in forest soil (Madureira *et al.* 2013, Almeida *et al.* 2019), thus the extermination of ants is not the best option to eliminate the problem (Alvarez-Loayza and Terborgh 2011), rather a solution may be to carry out effective management with biological control (Roos *et al.* 2011), as some species of ants, even the leaf-cutting, have a fundamental role in improving soil fertility (Farji-Brener and Werenkraut 2017).

CONCLUSIONS

Sand mining in the river bed has altered the initial growth of forest species in riparian forest areas of the Atlantic Forest, however, the effects were mitigated by the implementation of adequate proportions of non-pioneer and pioneer forest species (42.7 % and 53.1 %). Furthermore, forest species had a low mortality index due to drought and flooding tolerance and regeneration by leaf-cutting ants.

The forest species with the highest average height and average stem diameter during initial growth were: *Senna multijuga*, *Alchornea triplinervia*, *Citharexylum myrianthum* and *Trema micranta*. All pioneer species, therefore, are the most suitable to be implemented at initiation of a project to recovery of degraded area in riparian forest of Atlantic Forest.

## ACKNOWLEDGMENTS

## REFERENCES

Almeida FS, L Elizalde, LMS Silva, JM Queiroz. 2019. The effects of two abundant ant species on soil nutrients and seedling recruitment in Brazilian Atlantic Forest. *Revista Brasileira de Entomologia* 63(4): 296-301. DOI: 10.1016/j.rbe.2019.08.001.

Alvarez-Loayza P, J Terborgh. 2011. Fates of seedling carpets in an Amazonian floodplain forest: intra-cohort competition or attack by enemies? *Journal of Ecology* 99(4): 1045-1054. DOI: 10.1111/j.1365-2745.2011.01835.x.

Barbosa LM, RT Shirasuna, FC Lima, PRT Ortiz, KC Barbosa, TC Barbosa. 2017. Lista de espécies indicadas para restauração ecológica para diversas regiões do Estado de São Paulo. São Paulo, Brasil. Instituto de Botânica. 344 p.

Boëchat IG, ABM Paiva, S Hille, B Gücker. 2013. Land-use effects on river habitat quality and sediment granulometry along a 4th-order tropical river. Revista Ambiente & Água 8(3): 54-64. DOI: 10.4136/ambi-agua.1232.

Bradshaw AD, RF Hüttl. 2001. Future mine site restoration involves a broader approach. *Ecological Engineering* 17(2): 87-90. DOI: 10.1016/S0925-8574(00)00149-x.

Brandão SE, P Bulbovas, MEL Lima, M Domingos. 2017. Biochemical leaf traits as indicators of tolerance potencial in tree species from the Brazilian Atlantic Forest against oxidative environmental stressors. *Science Total Environmental* 575(1): 406-417. DOI: 10.1016/j.scitotenv.2016.10.006.

Brandão SL, SC Lima. 2002. pH e condutividade elétrica em solução do solo, em áreas de Pinus e cerrado na chapada, em Uberlândia (MG). *Caminhos da Geografia* 3(6): 46-56. DOI: http://www.seer.ufu.br/index.php/caminhosdegeografia/article/view/15294.

Colmanetti MAA, LM Barbosa, RT Shirasuna, HTZ Couto. 2016. Phytosociology and structural characterization of woody regeneration from a reforestation with native species in southeastern Brazil. *Revista Árvore* 40(2): 209-218. DOI: 10.1590/0100-67622016000200003.

Costa RO, CM José, MTG Guaratini, DMS Matos. 2019. Chemical characterization and phytotoxicity of the essential oil from the invasive Hedychium coronarium on seeds of Brazilian riparian trees. *Flora* 257(1): 151411. DOI: 10.1016/j.flora.2019.05.010.

Dalmaso CA, MCM Marques, P Higuchi, VP Zwiener, R Marques. 2020. Spatial and temporal structure of diversity and demographic dynamics along a successional gradient of tropical forests in southern Brazil. *Ecology and Evolution* 10(7): 3164-3177. DOI: 10.1002/ece3.5816.

EMBRAPA (Empresa Brasileira de Pesquisa Agropecuária, BR). 2017. Centro Nacional de Pesquisa de Solos. Manual de métodos de análises de solo. 3 ed. Brasília, Brasil. 574 p.

Esposito MP, RK Nakazato, ANV Pedroso, MEL Lima, MA Figueiredo, AP Diniz, AR Kozovits, M Domingos. 2018. Oxidant-antioxidant balance and tolerance against oxidative stress in pioneer and non-pioneer tree species from the remaining Atlantic Forest. *Science of Total Environment* 625(1): 382-393. DOI: 10.1016/j.scitotenv.2017.12.255.

Farji-Brener AG, V Werenkraut. 2017. The effects of ant nests on soil fertility and plant performance: a meta-analysis. *Journal of Animal Ecology* 86(4): 866-877. DOI: 10.1111/1365-2656.12672.

Ferreira DF. 2011. Sisvar: a computer statistical analysis system. *Ciência e Agrotecnologia* 35(6): 1039-1042. DOI: 10.1590/S1413-70542011000600001.

Hatfield JH, CDL Orme, CL Leite. 2018. Using functional connectivity to predict potential meta-population sizes in the Brazilian Atlantic Forest. *Perspectives in Ecology and Conservation* 16(4): 215-220. DOI: 10.1016/j.pecon.2018.10.004.

Holanda FSR, LGN Gomes, IP Rocha, TT Santos, RNA Filho, TRS Vieira, JB Mesquita. 2010. Crescimento inicial de espécies florestais na recomposição da mata ciliar em taludes submetidos à técnica de bioengenharia de solos. *Revista Ciência Florestal* 20(1): 157-166. DOI: 10.5902/198050981770.

Iori P, RB Silva, MSD Júnior, JM Lima. 2012. Pressão de preconsolidação como ferramenta de análise da sustentabilidade estrutural de classes de solos com diferentes usos. *Revista Brasileira de Ciência do Solo* 36(5): 1448-1456. DOI: 10.1590/S0100-06832012000500008.

Iori P, RB Silva, MSD Júnior, R Nakamura, LCF Almeida. 2019. Soil quality analysis in riparian areas for soil and water resource management. *Archives of Agronomy and Soil Science* 66(5): 572-585. DOI: 10.1080/03650340.2019.1630822.

Keram A, Ü Halik, M Keyimu, T Aishan, Z Mamat, A Rouzi. 2019. Gap dynamics of natural *Populus euphratica* floodplain forests affected byhydrological alteration along the Tarim River: Implications for restoration of the riparian forests. *Forest Ecology and Management* 438(1): 103-113. DOI: 10.1016/j.foreco.2019.02.009.

Lima GC, MLN Silva, MS Oliveira, N Curi, MA Silva, AH Oliveira. 2014. Variabilidade de atributos do solo sob pastagens e mata atlântica na escala de microbacia hidrográfica. *Revista Brasileira de Engenharia Agrícola e Ambiental* 18(5): 517-526. DOI: 10.1590/S1415-43662014000500008.

Machado SA, NT Zamin, RGM Nascimento, ALD Augustynczik, CS Menegazzo. 2013. Comparação dos parâmetros fitossociológicos entre três estratos de um fragmento de floresta ombrófila mista. *Cerne* 19(3): 365-372. DOI: 10.1590/S0104-77602013000300002.

Madureira MS, JH Schoereder, MC Teixeira, TG Sobrinho. 2013. Why does *Atta robusta* (Formicidae) not change soil features around their nests as other leaf-cutting ants do? *Soil Biology and Biochemistry* 57(1): 916-918. DOI: 10.1016/j.soilbio.2012.11.005.

Marçal M, G Brierley, R Lima. 2017. Using geomorphic understanding of catchment-scale process relationships to support the management of river futures: Macaé Basin, Brazil. *Applied Geography* 84(1): 23-41. DOI: 10.1016/j.apgeog.2017.04.008.

Marques R, GEP Piazza, H Blum, CB Pinto, JE Bianchin, CA Dalmaso, KMC Dickow. 2015. Contribuição da precipitação interna para o aporte de nutrientes em estágios sucessionais da floresta altântica no Paraná. *Revista Scientia Agraria* 16(4): 80-95. DOI: 10.5380/rsa.v16i3.46879.

Moura C, W Mantovani. 2017. Regeneração natural da floresta ombrófila densa após oito anos de abandono de atividades agrícolas em Miracatu, Vale do Ribeira, SP. *Revista Instituto Florestal* 9(1): 91-119. DOI: 10.24278/2178-5031.201729106.

Nunes S, M Gastauer, RBL Cavalcante, SJ Ramos, CF Caldeira JR, D Silva, RR Rodrigues, R Salomão, M Oliveira, PWM Souza-Filho, JO Siqueira. 2020. Challenges and opportunities for large-scale reforestation in the Eastern Amazon using native species. *Forest Ecology and Management* 466(1): 118120. DOI: 10.1016/j.foreco.2020.118120.

Pastório FF, AL Gasper, ACB Vibrans. 2020. Successional stages of Santa Catarina atlantic subtropical evergreen rainforest: a classification method proposal. *Cerne* 26(2): 162-171. DOI: 10.1590/01047760202026022651.

Piñarodrigues FCM, LR Lopes, S Marques. 1997. Sistema de plantio adensado para revegetação de áreas degradadas da Mata Atlântica: bases ecológicas e comparações de estudo-benefício com o sistema tradicional. *Floresta e Ambiente* 4(1): 30-41. DOI: https://www.academia.edu/32618852/Pi%C3%B1a_Rodrigues_plantio_adensado_Floram_4_1997_pdf.

Pinheiro RA, STV Fisch, A. Almeida. 2004. A cobertura vegetal e as características do solo em área de extração de areia. *Revista de Biociências* 10(3): 103-110. DOI: http://periodicos.unitau.br/ojs/index.php/biociencias/article/view/167/134.

Pontes DMF, VL Engel, JA Parrota. 2019. Forest structure, wood standing stock, and tree biomass in different restoration systems in the brazilian Atlantic Forest. *Forests* 10(7): 588. DOI: 10.3390/f10070588.

Prado HM, MN Schlindwein, RSS Murrieta, DRN Junior, EP Souza, MC Lignon, MM Mahiques, PCF Giannini, RF Contente. 2019. The Valo Grande channel in the Cananéia-Iguape estuary-lagoon complex (SP, Brazil): Environmental history, ecology, and future perspectives. *Ambiente e Sociedade* 22(1): e01822. DOI: 10.1590/1809-4422aso-c0182r2vu19l4td.

Qin Y, Z Chen, B Ding, Z Li. 2020. Impact of sand mining on the carbon sequestration and nitrogen removal ability of soil in the riparian area of Lijiang River, China. *Environmental Pollution* 261(1):114220. DOI: 10.1016/j.envpol.2020.114220.

Reznik G, JPA Pires, L Freitas. 2012. Efeito de bordas lineares na fenologia de espécies arbóreas zoocóricas em um remanescente de Mata Atlântica. *Acta Botanica Brasílica* 26(1): 65-73. DOI: 10.1590/S0102-33062012000100008.

Ribeiro MC, JP Metzger, AC Martensen, FJ Ponzoni, MM Hirota. 2009. The Brazilian Atlantic Forest: How much is left, and how is the remaining forest distributed? Implications for conservation. *Biological Conservation* 142(6): 1141-1153. DOI: 10.1016/j.biocon.2009.02.021.

Roos K, HG Rödel, E Beck. 2011. Short and long-term effects of weed control on pastures infested with Pteridium arachnoideum and an attempt to regenerate abandoned pastures in South Ecuador. *Weed Research* 51(2): 165-176. DOI: 10.1111/j.1365-3180.2010.00833.x.

Sangsupan HA, DE Hibbs, BAW Robinson, S Elliott. 2018. Seed and microsite limitations of large-seeded, zoochorous trees in tropical forest restoration plantations in northern Thailand. *Forest Ecology and Management* 419-420(1): 91-100. DOI: 10.1016/j.foreco.2018.03.021.

São Paulo. 2014. Resolução nº 32, de 03 de abril de 2014. Secretaria de Meio Ambiente do Estado de São Paulo. Diário Oficial do Estado de São Paulo, São Paulo, 05/04/2014. Seção Meio Ambiente. Accessed in: July 10th 2020. Available at https://cetesb.sp.gov.br/licenciamentoambiental/licenca-previa-documentacao-nescessaria/autorizacao-para-supressao-de-vegetacao-nativa-intervencao-em-areas-de-preservacao-permanente-legislacao/resolucao-sma-no-32-2014/.

Seitz N, D VanEngelsdorp, SD Leonhardt. 2019. Conserving bees in destroyed landscapes: The potentials of reclaimed sand mines. *Global Ecology and Conservation* 19(1): e00642. DOI: 10.1016/j.gecco.2019.e00642.

SIGRB (Sistemas de Informações Geográficas da Bacia do Ribeira de Iguape e Litoral Sul). 2020. CBH-RB. SIG-RB. Accessed in: June 10th 2020. Available at https://www.sigrb.com.br/index.php.

Silva AO, AM Costa, AFS Teixeira, AA Guimarães, JV Santos, FMS Moreira. 2018. Soil microbiological attributes indicate recovery of an iron mining area and of the biological quality of adjacent phytophysiognomies. *Ecological Indicators* 93(1): 142-151. DOI: 10.1016/j.ecolind.2018.04.073.

Skorupa ALA, LRG Guilherme, N Curi, CPC Silva, JRS Scolforo, JJGSM Marques. 2012. Propriedades de solos sob vegetação nativa em Minas Gerais: Distribuição por fitofisionomia, hidrografia e variabilidade espacial. *Revista Brasileira de Ciência do Solo* 36(1): 11-22. DOI: 10.1590/S0100-06832012000100002.

Soares-Filho B, R Rajão, M Macedo, A Carneiro, W Costa, M Coe, H Rodrigues, A Alencar. 2014. Cracking Brazil's forest code. *Science* 344(6182): 363-364. DOI: 10.1126/science.1246663.

Sos Mata Atlântica, INPE (Fundação SOS Mata Atlântica e Instituto Nacional de Pesquisas Espaciais) 2018. Atlas dos Remanescentes Florestais da Mata Atlântica período 2016-2017, São Paulo, Brasil. Accessed in: June 2nd 2020. Available at https://www.sosma.org.br/wp-content/uploads/2019/05/Atlas-mata-atlantica_17-18.pdf.

Souza PA, N Venturin, RLG Macedo, MIN Alvarenga, VF Silva. 2001. Estabelecimento de espécies arbóreas em recuperação de área degradada pela extração de areia. *Cerne* 7(2): 43-52. DOI: https://www.redalyc.org/pdf/744/74470205.pdf.

Souza LM, RAVB Faria, SA Botelho, MAL Fontes, JMR Faria. 2012. Potencial da regeneração natural como método de restauração do entorno de nascente perturbada. *Cerne* 18(4): 565-576. DOI: 10.1590/S0104-77602012000400006.

Suganuma MS, G Durigan. 2014. Indicators of restoration success in riparian tropical forests using multiple reference ecosystems. *Restoration Ecology* 23(3): 238-251. DOI: 10.1111/rec.12168.

Thomazini A, ES Mendonça, IM Cardoso, ML Garbin. 2015. SOC dynamics and soil quality index of agroforestry systems in the Atlantic rainforest of Brazil. *Geoderma Regional* 5(1): 15-24. DOI: 10.1016/j.geodrs.2015.02.003.

Webb AA, WD Erskine. 2003. A practical scientific approach to riparian vegetation rehabilitation in Australia. *Journal of Environmental Management* 68(4): 329-341. DOI: 10.1016/S0301-4797(03)00071-9.

Xavier RO, P Dodonov, DMS Matos. 2019. Growth and mortality patterns of the Neotropical bracken (*Pteridium arachnoideum*) and their response to shading in a savanna–ripa-

rian forest transition. *Flora* 252(1): 36-43. DOI: 10.1016/j.flora.2019.02.005.

Zama MY, YR Bovolenta, ES Carvalho, DR Rodrigues, CG Araujo, MAF Sorace, DG Luz. 2012. Florística e síndrome de dispersão de espécies arbutisvo-arbóreas no Parque Estadual Mata São Francisco. PR, Brasil. *Hoehnea* 39(3): 369-378. DOI: 10.1590/S2236-89062012000300002.

Zanon JA, N Favaretto, GD Goularte, J Dieckow, G Barth. 2020. Manure application at long-term in no-till: Effects on runoff, sediment and nutrients losses in high rainfall events. *Agricultural Water Management* 228(1): 105908. DOI: 10.1016/j.agwat.2019.105908.

# Factores abióticos sobre aspectos ecofisiológicos
## de *Handroanthus impetiginosus* y *Handroanthus serratifolius*

## Abiotic factors on ecophysiological aspects
### of *Handroanthus impetiginosus* and *Handroanthus serratifolius*

**João Everthon da Silva Ribeiro [a*], Ester dos Santos Coêlho [b]**

[*]Corresponding author: [a] State University of Maranhão (UEMA), Department of Technology in Agribusiness Management, Strees Hernani Pereira n°458, Itapecuru-Mirim, Maranhão, Brazil, tel.: +558398171-6327, j.everthon@hotmail.com
[b] Federal Rural University of Semi-arid (UFERSA), Department of Plant Sciences, Mossoró, Rio Grande do Norte, Brazil.

SUMMARY

The objective of this research was to evaluate the influence of abiotic factors on the ecophysiological aspects of *Handroanthus impetiginosus* and *Handroanthus serratifolius* throughout the day, as well as to indicate the ideal time for ecophysiological evaluations. The design was entirely randomized, with ten treatments and six repetitions for each species. The treatments used were ten evaluation times throughout the day (8h-17h) with an interval of one hour between them. Climatic variables evaluated were internal and external temperature, relative humidity of the internal and external air of the greenhouse and the photosynthetically active radiation of the environment. Ecophysiological aspects evaluated were: net $CO_2$ assimilation, stomatal conductance, transpiration, internal $CO_2$ concentration, vapor pressure deficit, instantaneous water use efficiency, intrinsic water use efficiency and instantaneous carboxylation efficiency. The canonical correlation analysis and principle component analysis were used to verify associations between climatic and ecophysiological variables. In both species, climatic variables were correlated with ecophysiological variables, with higher association between photosynthetically active radiation, internal and external temperature of environment, with the rate of net $CO_2$ assimilation, stomatal conductance, transpiration, instantaneous carboxylation efficiency and vapor pressure deficit. The influence of climatic factors on the ecophysiological aspects of *H. impetiginosus* and *H. serratifolius* was verified. In both species, the ideal time of day for measuring ecophysiological variables is between 11h and 13h.

*Key words:* Bignoniaceae, gas exchange, ipê-amarelo, ipê-roxo, irradiance.

RESUMEN

El objetivo de la investigación fue evaluar la influencia de los factores abióticos en aspectos ecofisiológicos de *Handroanthus impetiginosus* y *Handroanthus serratifolius* a lo largo del día, así como indicar el momento ideal para las evaluaciones ecofisiológicas. Se utilizo un diseño experimental completamente aleatorizado, con diez tratamientos y seis repeticiones para cada especie. Los tratamientos utilizados fueron diez momentos de evaluación a lo largo del día (8 h-17 h) con un intervalo de una hora entre ellos. Las variables meteorológicas evaluadas fueron la temperatura del aire interior y exterior, y la humedad relativa del aire interior y exterior del ambiente. Los aspectos ecofisiológicos evaluados fueron: tasa de asimilación neta de $CO_2$, conductancia estomática, transpiración, concentración interna de $CO_2$, déficit de presión de vapor, eficiencia instantánea en el uso del agua, eficiencia intrínseca en el uso del agua y eficiencia instantánea de carboxilación. El análisis de la correlación canónica y los componentes principales se utilizaron para verificar las asociaciones entre las variables meteorológicas y ecofisiológicas. En ambas especies, las variables meteorológicas se correlacionaron con las variables ecofisiológicas, con una mayor asociación entre la radiación fotosintéticamente activa, temperatura interna y externa del ambiente, con la tasa de asimilación neta de $CO_2$, conductancia estomática, transpiración, eficiencia instantánea de carboxilación y déficit de presión de vapor. Se verificó la influencia de los factores meteorológicos en los aspectos ecofisiológicos de *H. impetiginosus* y *H. serratifolius*. En ambas especies, la hora ideal del día para medir las variables ecofisiológicas es entre las 11 h y las 13 h.

*Palabras clave:* Bignoniaceae, intercambio gaseoso, ipê-amarelo, ipê-roxo, irradiación.

## INTRODUCCIÓN

Conocido popularmente como ipê-roxo, pau d'arco roxo y ipê-roxo-da-mata, *Handroanthus impetiginosus* (Mart. ex DC.) Mattos (Bignoniaceae Juss.) es una especie de árbol caducifolio nativo de Brasil, que puede alcanzar hasta 20 m de altura. Tiene una amplia distribución geográfica, desde México hasta el norte de Argentina, y en Brasil se da en las regiones Norte, Noreste, Centro-Oeste y Sureste. Se encuentra en todos los dominios fitogeográficos, ex-

cepto en la Pampa, en altitudes que varían desde el nivel del mar hasta los 1.400 metros. Esta especie presenta una gran importancia económica, ya que se utiliza principalmente para fines madereros en la construcción de muebles, además, la corteza tiene compuestos químicos bioactivos que se utilizan con fines medicinales con potencial para actividades antiinflamatorias, antibióticas y analgésicas (Beltreschi *et al*. 2019). Se utiliza en el paisajismo en general y en la recuperación de zonas degradadas (Ferreira *et al*. 2020), como también tiene un potencial alimenticio para la fauna, por ejemplo, las abejas (Benevides y Carvalho 2009).

*Handroanthus serratifolius* (Vahl) S. Grose, conocido popularmente como ipê-amarelo y pau d'arco amarelo, es una especie de árbol de tamaño medio a grande, con una altura que varía entre 5 y 25 m. Se distribuye en Colombia, el Ecuador, Guyana, Bolivia, la Guayana Francesa, el Perú, Suriname, Venezuela y el Brasil.  En el Brasil está ampliamente distribuida y se da en varios dominios fitogeográficos, que van desde el Amazonas hasta la región meridional del país. La madera de la especie tiene importancia económica principalmente en la construcción civil y con fines tecnológicos, como los mangos de herramientas y los muebles (Oliveira *et al*. 2019). La corteza del tronco tiene propiedades farmacológicas, utilizándose en la medicina tradicional para el tratamiento de inflamaciones generales, enfermedades respiratorias, así como metabolitos secundarios con actividades antipalúdicas, antitumorales y antiparasitarias (Costa *et al*. 2017). Se cultiva ampliamente en las zonas urbanas para la ornamentación y puede utilizarse en la recuperación de zonas degradadas y en la reforestación, adaptándose a los suelos secos de baja fertilidad (Vieira y Weber 2017).

Debido a la importancia de estas especies para las regiones de ocurrencia, se necesitan estudios para evaluar el comportamiento y el desempeño ecofisiológico debido a los diferentes factores abióticos. Entre los principales factores que influyen en la fisiología de las plantas, destacan la radiación solar (irradiación), la temperatura del aire y la humedad relativa (Lambers y Oliveira 2019). Las especies forestales, debido a sus características intrínsecas, pueden presentar respuestas diferentes a las condiciones ambientales y, por lo tanto, la actividad fotosintética de las plantas se ven significativamente alteradas (Dias *et al*. 2017).

La radiación solar (irradiación) a lo largo del día promueve efectos directos en la fotosíntesis de las plantas para influir en la absorción y transferencia de energía en el aparato fotosintético, así como para causar cambios en la asimilación neta de $CO_2$, la conductancia estomática y la transpiración (Cruces *et al*. 2017). La temperatura del aire puede influir en el proceso fotosintético de las plantas directa o indirectamente. El efecto indirecto está relacionado con la actividad de los  estomas, tales como la apertura y el cierre de los mismos, provocando la regulación de las relaciones hídricas en las hojas a través de la transpiración. El efecto directo de la temperatura del aire sobre la asimilación del $CO_2$ implica la regeneración de Ribulosa 1,5-bifosfato (RuBP), así como modificaciones en la actividad de Rubisco (Bhatla y Lal 2018).

En vista de lo anterior, los estudios relacionados con los aspectos ecofisiológicos en las especies forestales, como *H. impetiginosus* y *H. serratifolius*, son de gran importancia, por lo que se trata de comprender la adaptación y estabilización de estas especies en condiciones ambientales adversas. Sin embargo, la información en la literatura sobre los mecanismos fisiológicos de estas especies en respuesta a condiciones ambientales adversas es escasa. Esta información puede ser útil en la elaboración de modelos que tengan como objetivo predecir escenarios sobre la fijación de carbono, y también puede ayudar a explicar la dinámica de estas especies en fragmentos de vegetación. La hipótesis de investigación fue que *H. impetiginosus* y *H. serratifolius* presentan diferentes respuestas ecofisiológicas a lo largo del día, con menor rendimiento fotosintético en el período de menor radiación fotosintética (irradiancia) y baja temperatura del aire. Así pues, el objetivo de la investigación fue evaluar la influencia de los factores abióticos en los aspectos ecofisiológicos de *H. impetiginosus* y *H. serratifolius* a lo largo del día, así como indicar el momento ideal para las evaluaciones ecofisiológicas.

## MÉTODOS

La investigación se llevó a cabo en un invernadero, perteneciente al Departamento de Ciencias Vegetales y Ambientales de la Universidad Federal de Paraíba (Campus II) (6°57'59" S y 35°42'57" O), ubicado en el municipio de Areia, estado de Paraíba, Noreste de Brasil. La región está situada en la microrregión de Brejo y la mesorregión de Agreste Paraibano y tiene una altitud que varía entre 400 y 600 m, con una temperatura media del aire de 22 °C y una precipitación anual de 1.400 mm (Ribeiro *et al*. 2018). El clima de la región es tropical, caracterizado por ser cálido y húmedo con lluvias de otoño-invierno, clasificado según Alvares *et al*. (2013) como As. Durante el período experimental, el medio ambiente presentó una temperatura media y una humedad relativa del aire de 24,2°C y 53,5 %, respectivamente, cuyas mediciones se realizaron con un termohigrómetro digital portátil (Minipa, modelo MT-241A).

Las semillas de *H. impetiginosus* y *H. serratifolius* se recogieron en enero de 2019 en matrices adultas en los remanentes forestales de Caatinga, situados en el municipio de Solânea, ubicado en la mesoregión de Agreste, microrregión de Curimataú Oriental, en el estado de Paraíba, al Noreste de Brasil [altitud de 626 m (06º46'40" S y 35º41'49" W)].  Para la producción de plántulas, se recogieron las semillas que alcanzaron la fase de maduración, es decir, con dehiscencia en una etapa temprana. Después de la cosecha, las semillas se seleccionaron manualmente y se sumergieron en una solución de hipoclorito de sodio al 2 % durante cinco minutos para su desinfección antes de la siembra.

Para la siembra se utilizaron macetas de plástico con capacidad para 8 dm³ y un sustrato compuesto de tierra vegetal y Bioplant® (3:1), con los atributos químicos presentados en el cuadro 1. Se utilizaron seis semillas por maceta y a los 40 días de su aparición se realizó un raleo, manteniendo la uniformidad de los individuos de la especie. Durante el período de investigación, la irrigación de las plantas se mantuvo al 80 % de la capacidad de la maceta, siendo controlada mediante lisimetría de drenaje.

Se utilizó un diseño experimental completamente aleatorizado, con diez tratamientos y seis repeticiones para cada especie, dos plantas por unidad experimental (parcela), totalizando 24 individuos. Los tratamientos utilizados fueron diez momentos de evaluación a lo largo del día (8:00 a 17:00 h) con un intervalo de una hora entre ellos.

Las variables meteorológicas evaluadas fueron la temperatura del aire interna (Tin) y externa (Tex) (ºC), y la humedad relativa interna (HRin) y externa (HRex) del ambiente, con la ayuda de un termómetro digital portátil (Minipa, modelo MT-241A). Para la cuantificación de la radiación fotosintética activa (RFA) ($\mu$mol m$^{-2}$ s$^{-1}$), se utilizó el sensor de luz acoplado al analizador portátil de gas por infrarrojo (IRGA) (Licor, modelo LI-6400XT).

Los aspectos ecofisiológicos evaluados fueron la asimilación neta de $CO_2$ (A) ($\mu$mol m$^{-2}$ s$^{-1}$), conductancia estomacal (gs) (mol m$^{-2}$ s$^{-1}$), transpiración (E) (mmol de $H_2O$ m$^{-2}$ s$^{-1}$), concentración interna de $CO_2$ (Ci) ($\mu$mol de $CO_2$ mol$^{-1}$) y déficit de presión de vapor (DPV). A partir de estas variables se calcularon la eficiencia instantánea del uso del agua (EUA: A/E) [($\mu$mol m$^{-2}$ s$^{-1}$) / (mmol $H_2O$ m$^{-2}$ s$^{-1}$)], eficiencia intrínseca del uso del agua (EiUA: A/gs) [($\mu$mol m$^{-2}$ s$^{-1}$) / (mol m$^{-2}$ s$^{-1}$)] y eficiencia instantánea de carboxilación (EiC: A/Ci) [($\mu$mol m$^{-2}$ s$^{-1}$) / ($\mu$mol $CO_2$ mol$^{-1}$)]. Las mediciones se realizaron de acuerdo con el siguiente protocolo: humedad relativa entre 50-60 %; flujo de aire de 300 $\mu$mol s$^{-1}$, concentración de $CO_2$ de 400 $\mu$mol mol$^{-1}$ (mezclador, modelo 6400-01) y sensor de luz natural acoplado a una cámara de hojas de 6 cm². Para las evaluaciones se utilizó el IRGA, que se realizó en cuatro hojas sanas y completamente expandidas, en el tercio medio de cada individuo.

Las evaluaciones se llevaron a cabo 360 días después de la emergencia, en condiciones ideales de luminosidad (pleno sol), a fin de inferir los efectos de los parámetros meteorológicos en los aspectos ecofisiológicos de los individuos.

Se utilizó el análisis de correlación canónica (ACC) y el análisis de componentes principales (ACP) para verificar las asociaciones entre las variables meteorológicas (RFA, Tin, Tex, HRin y HRex) y las variables ecofisiológicas (A, gs, E, Ci, DPV, EUA, EiUA y EiC), así como la prueba de significación multivariante de Lambda de Wilks (aproximación de la distribución de F) para observar la significación de las raíces canónicas juntas. Los análisis estadísticos se realizaron con el software SAS® 9.4M6.

RESULTADOS

Según la prueba de significación de Lambda de Wilks, las variables ecofisiológicas presentaron correlaciones con las variables meteorológicas, obteniendo significación en las cuatro primeras parejas canónicas de cada especie estudiada, con valores de R² que oscilan entre 0,64 y 0,99 en *H. impetiginosus* , y entre 0,56 y 0,99 en *H. serratifolius*, respectivamente (cuadro 2).

En ambas especies se observó en el primer par canónico que las variables meteorológicas más importantes fueron la radiación fotosintéticamente activa (cc = 0,87 y 0,76), la temperatura interna (cc = 0,75 y 0,69) y la temperatura externa del ambiente (cc = 0,72 y 0,67), correlacionándose positivamente con la asimilación neta de $CO_2$ (cc = 0,90 y 0,83), conductancia estomática (cc = 0,83 y 0,69), transpiración (cc = 0,79 y 0,77), eficiencia instantánea de carboxilación (cc = 0,71 y 0,79) y déficit de presión de vapor (cc = 0,66 y 0,64) (cuadro 3).

En cuanto al análisis de los componentes principales (ACP), se observó que en *H. impetiginosus* los ejes concentraban el 77,54 % de la variabilidad total de los datos (49,38 % en CP1 y 28,16 % en CP2), observándose que la asimilación neta de $CO_2$, conductancia estomática, transpiración y eficiencia instantánea de carboxilación estuvieron fuertemente correlacionadas con la radiación fotosintéticamente activa, así como el déficit de la presión de vapor correlacionó con la temperatura interna y la temperatura externa del ambiente (figura 1A). En *H. serratifolius* las dimensiones del eje (44,74 % en CP1 y 24,00 % en CP2), concentraron el 68,74 % de la variabilidad total de los datos (figura 1B). Hubo correlaciones positivas entre la radiación fotosintéticamente activa con la asimilación neta de $CO_2$, la transpiración, la eficiencia instantánea de carboxilación y la conductancia estomática, y entre la tem-

**Cuadro 1.** Análisis de fertilidad del sustrato utilizado en el experimento.

Fertility analysis of the substrate used in the experiment.

| pH (H$_2$0) | P | K | Na | H+Al | Al | Ca | Mg | SB | CIC | V | M.O. |
|---|---|---|---|---|---|---|---|---|---|---|---|
| | mg dm$^{-3}$ | | cmolc dm$^{-3}$ | | | | | | | % | g kg$^{-1}$ |
| 5,42 | 118,7 | 217,2 | 0,43 | 4,62 | 0,00 | 3,50 | 3,10 | 7,58 | 12,2 | 62,1 | 29,86 |

SB: suma de bases; CIC: capacidad de intercambio catiónico; V: saturación de bases; M.O.: materia orgánica.

**Cuadro 2.** Prueba multivariante Lambda de Wilks (aproximación de la distribución F). R²: correlación canónica; Fa: valor aproximado de F; GL-Num: grado de libertad del numerador; GL-Den: grado de libertad del denominador.

Wilks's Lambda multivariate test (F distribution approximation).

| | | *Handroanthus impetiginosus* | | | |
|---|---|---|---|---|---|
| Función canónica | R² | Fa | GL-Num | GL-Den | $Pr > F$ |
| 1 | 0,99 | 23,64 | 40 | 207,66 | < 0,0001 |
| 2 | 0,91 | 9,21 | 28 | 174,49 | < 0,0001 |
| 3 | 0,76 | 5,40 | 18 | 139,08 | < 0,0001 |
| 4 | 0,64 | 3,78 | 10 | 100,00 | 0,0002 |
| 5 | 0,32 | 1,54 | 4 | 51,00 | 0,2037 |
| | | *Handroanthus serratifolius* | | | |
| Función canónica | R² | Fa | GL-Num | GL-Den | $Pr > F$ |
| 1 | 0,99 | 17,21 | 40 | 207,66 | < 0,0001 |
| 2 | 0,82 | 5,28 | 28 | 174,49 | < 0,0001 |
| 3 | 0,62 | 3,46 | 18 | 139,08 | < 0,0001 |
| 4 | 0,56 | 3,16 | 10 | 100,00 | 0,0015 |
| 5 | 0,38 | 2,27 | 4 | 51,00 | 0, 0747 |

**Cuadro 3.** Correlaciones canónicas y par canónico entre las variables meteorológicas y ecofisiológicas de *Handroanthus impetiginosus* y *Handroanthus serratifolius*. ** Significativo al 1 % de probabilidad por prueba de ji-cuadrado; S1: *Handroanthus impetiginosus*; S2: *Handroanthus serratifolius*; R² = correlación canónica.

Canonic correlations and canonical pair between the climatic and ecophysiological variables of *Handroanthus impetiginosus* and *Handroanthus serratifolius*.

| Variables | Par canónico | |
|---|---|---|
| Grupo I: Meteorológicas | S1 | S2 |
| Radiación fotosintética activa (RFA) | 0,87 | 0,76 |
| Temperatura interna (Tin) | 0,75 | 0,69 |
| Temperatura externa (Tex) | 0,72 | 0,67 |
| Humedad relativa- interna (HRin) | - 0,50 | - 0,39 |
| Humedad relativa- externa (HRex) | - 0,54 | - 0,42 |
| Grupo II: Ecofisiológicas | | |
| Asimilación neta de $CO_2$ (A) | 0,90 | 0,83 |
| Conductancia estomacal ($g_s$) | 0,83 | 0,69 |
| Transpiración (E) | 0,79 | 0,77 |
| Concentración interna de $CO_2$ (Ci) | - 0,49 | - 0,55 |
| Déficit de presión de vapor (DPV) | 0,66 | 0,64 |
| Eficiencia instantánea del uso del agua (EUA) | - 0,55 | - 0,44 |
| Eficiencia intrínseca del uso del agua (EiUA) | - 0,58 | - 0,47 |
| Eficiencia instantánea de carboxilación (EiC) | 0,71 | 0,79 |
| R² | 0,99 | 0,99 |
| Significación | ** | ** |

peratura del ambiente externo e interno con el déficit de presión de vapor (figura 1B). En ambas especies se observó que los autovectores de las variables ecofisiológicas, excepto la concentración interna de $CO_2$, se localizan en la porción más extrema de la derecha, presentando valores positivos, mientras que la humedad relativa interna y externa se localizaron en la porción externa de la izquierda (con valores negativos), evidenciando la distinción de estos parámetros y los demás analizados (figura 1A y B).

Las variables meteorológicas presentaron variaciones, en las que la radiación fotosintéticamente activa (RFA) aumentó significativamente a lo largo del día, con valores que oscilaron entre 29,01 μmol s⁻¹ m⁻² y 1506,14 μmol s⁻¹ m⁻², registrados a las 17 h y 12 h, respectivamente (figura 2). La temperatura del ambiente interno y externo alcanzó los valores máximos en el período de 12h y 13h, con valores de 40,6 °C y 39,9 °C en el interior de la casa de la vegetación, y 38,5 °C y 36,7 °C en el área externa (figura 2). La humedad relativa del aire interior y exterior presentó reducción durante el período de mayor temperatura y radiación fotosintéticamente activa, con los valores más bajos observados a la 13 h (HRin de 29 % y HRex de 32 %) y los valores más altos durante el período de 8 h y 17 h (figura 2).

La asimilación neta de $CO_2$ (A) mostró un aumento significativo en las primeras horas del día (figura 3A), junto con la radiación fotosintéticamente activa (RFA) y la temperatura interna y externa del ambiente (Tin y Tex). En *H. impetiginosus* se observaron las mayores tasas de asimilación neta de $CO_2$, con valores registrados a las 11 h y 12 h (6,7301 μmol m⁻² s⁻¹ y 8,2402 μmol m⁻² s⁻¹, respectivamente) (figura 3A),

mientras que en *H. serratifolius* los valores aumentaron hasta las 12 h y 13 h (5,8567 µmol m$^{-2}$ s$^{-1}$ y 6,0748 µmol m$^{-2}$ s$^{-1}$, respectivamente) (figura 3A). En ambas especies, los valores más bajos se registraron a las 17 h (figura 3A).

La conductancia estomática (gs) mostró un comportamiento similar a la tasa de asimilación neta de $CO_2$, con incrementos graduales a lo largo del día en ambas espe-

cies, registrándose en *H. impetiginosus* 0,1505 mol m$^{-2}$ s$^{-1}$ y 0,1844 mol m$^{-2}$ s$^{-1}$ a las 11 h y 12 h, y 0,1295 mol m$^{-2}$ s$^{-1}$ y 0,1540 mol m$^{-2}$ s$^{-1}$ a las 12 h y 13 h en plantas de *H. serratifolius*, con considerables descensos hasta las 17 h (figura 3B).

La transpiración (E) mostró la misma tendencia que la asimilación neta de $CO_2$ y la conductancia estomática, con
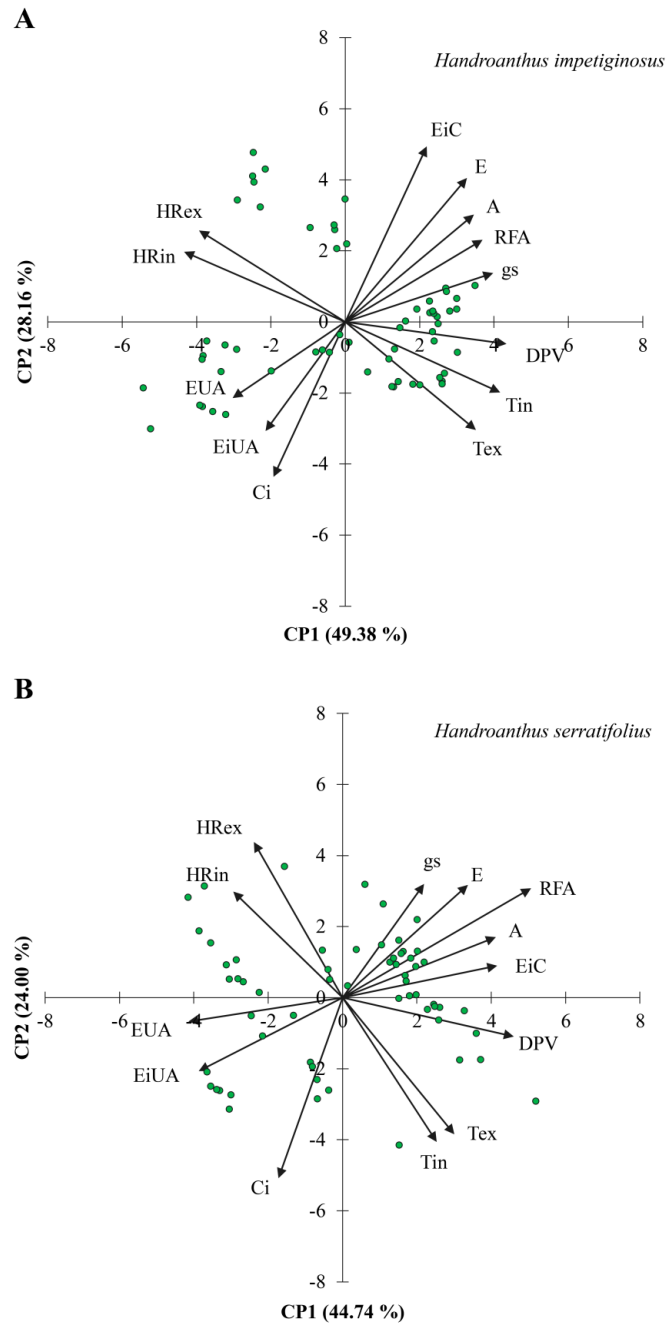


**Figura 1.** Análisis de los componentes principales (CP1 y CP2) entre las variables meteorológicas y ecofisiológicas de *Handroanthus impetiginosus* (A) y *Handroanthus serratifolius* (B).

Principal component analysis among the climatic and ecophysiological variables of *Handroanthus impetiginosus* (A) and *Handroanthus serratifolius* (B).
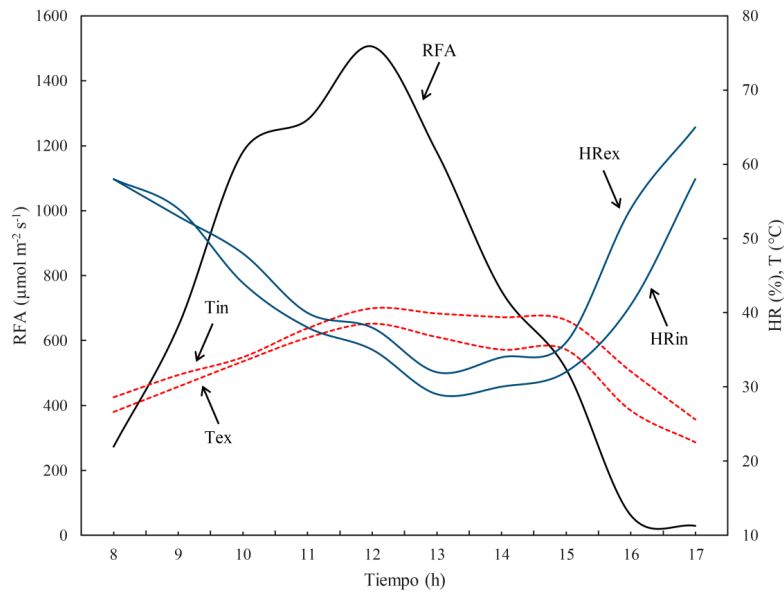
**Figura 2.** Radiación fotosintéticamente activa (RFA), temperatura interna (Tin) y externa (Tex), y humedad relativa interna (HRin) y externa (HRex) en el invernadero durante la realización del experimento.

Photosynthetically active radiation (RFA), internal (Tin) and external (Tex) temperature, and internal (HRin) and external (HRex) relative humidity in greenhouse during the conduction of the experiment.
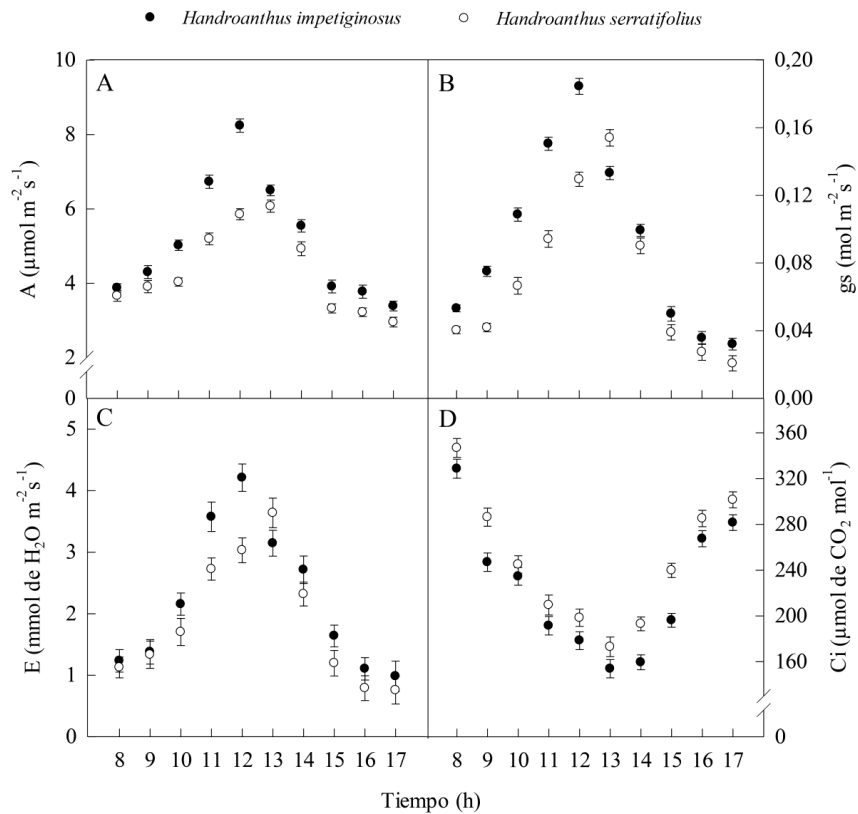


**Figura 3.** Asimilación neta de $CO_2$ (A) (A), conductancia estomática (gs) (B), transpiración (E) (C) y concentración interna de $CO_2$ (Ci) (D) en plantas de *Handroanthus impetiginosus* (●) y *Handroanthus serratifolius* (○) en función de la hora (h) del día.

Net $CO_2$ assimilation (A) (A), stomatal conductance (gs) (B), transpiration (E) (C) and internal $CO_2$ concentration (Ci) (D) in *Handroanthus impetiginosus* (●) and *Handroanthus serratifolius* (○) plants as a function of time (h) of day.

los valores más altos observados a las 11 h y 12 h en *H. impetiginosus* (3,5757 mmol de $H_2O$ $m^{-2}$ $s^{-1}$ y 4,2111 mmol de $H_2O$ $m^{-2}$ $s^{-1}$, respectivamente), y en el período de 12h y 13h en *H. serratifoliius* (3,0306 mmol de $H_2O$ $m^{-2}$ $s^{-1}$ y 3,6384 mmol de $H_2O$ $m^{-2}$ $s^{-1}$, respectivamente), siendo el más bajo observado a las 17 h en ambas especies (figura 3C).

En cuanto a la concentración interna de $CO_2$ (Ci), se observó un comportamiento inverso en relación con las demás variables, registrándose los valores más altos a las 8 h y a las 17 h en las especies estudiadas (328,69 y 281,55 µmol de $CO_2$ $mol^{-1}$ en *H. impetiginosus* y 346,83 y 281,55 µmol de $CO_2$ $mol^{-1}$ en *H. serratifolius*, respectivamente) (figura 3D).

El déficit de presión de vapor (DPV) aumentó gradualmente a lo largo del día, con valores que oscilan entre 1,54 kPa (8h) y 3,21 kPa (12 h) en *H. impetiginosus*, y entre 1,34 kPa (8 h) y 2,84 kPa (12 h) en *H. serratifolius* (figura 4A).

La eficiencia instantánea del uso del agua (EUA), mostró una reducción durante el período entre las 8 h y las 13 h en ambas especies, con una disminución del 34,3 % en *H. impetiginosus* y del 48,9 % en *H. serratifolius*, entre

los valores más altos y los más bajos registrados en este período (figura 4B). Los valores más altos se observaron a las 16 h en *H. serratifolius* y a las 17 h en *H. impetiginosus*, con 4,0850 [(µmol $m^{-2}$ $s^{-1}$) (mmol de $H_2O$ $m^{-2}$ $s^{-1})^{-1}$] y 3,4503 [(µmol $m^{-2}$ $s^{-1}$) (mmol de $H_2O$ $m^{-2}$ $s^{-1})^{-1}$], respectivamente (figura 4B).

En cuanto a la eficiencia intrínseca del uso del agua (EiUA), se observó una tendencia similar a la EUA, donde los valores más altos se obtuvieron a las 16 h y 17 h, y los más bajos entre las 11 h y 13 h, en ambas especies (figura 4C). Los valores oscilaron entre 44,692 [(µmol $m^{-2}$ $s^{-1}$) (mol $m^{-2}$ $s^{-1})^{-1}$] y 105,917 [(µmol $m^{-2}$ $s^{-1}$) (mol $m^{-2}$ $s^{-1})^{-1}$] en *H. impetiginosus*, y entre 39,439 [(µmol $m^{-2}$ $s^{-1}$) (mol $m^{-2}$ $s^{-1})^{-1}$] y 143,136 [(µmol $m^{-2}$ $s^{-1}$) (mol $m^{-2}$ $s^{-1})^{-1}$] en *H. serratifolius* (figura 4C).

La eficiencia instantánea de carboxilación (EiC) mostró un comportamiento similar a la asimilación neta de $CO_2$, aumentando considerablemente a lo largo del día, registrándose valores más altos durante el período de 12 h y 13 h, con 0,0415 [(µmol $m^{-2}$ $s^{-1}$) (µmol de $CO_2$ $mol^{-1})^{-1}$] y 0,0376 [(µmol $m^{-2}$ $s^{-1}$) (µmol de $CO_2$ $mol^{-1})^{-1}$] en *H. impe-*
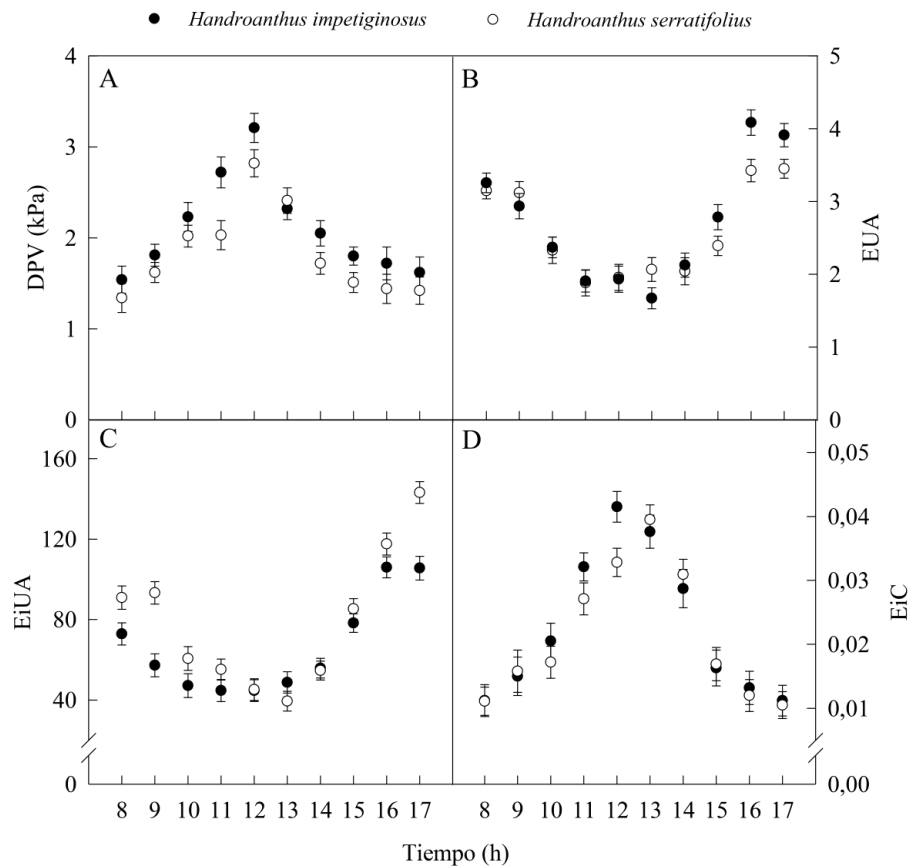


**Figura 4.** Déficit de presión de vapor (DPV) (A), eficiencia instantánea del uso del agua (EUA) (B), eficiencia intrínseca del uso del agua (EiUA) (C) y eficiencia instantánea de carboxilación (EiC) (D) en plantas de *Handroanthus impetiginosus* (●) y *Handroanthus serratifolius* (○) en función de la hora (h) del día.

Vapor pressure deficit (DPV) (A), instantaneous water use efficiency (EUA) (B), intrinsic water use efficiency (EiUA) (C) and instantaneous carboxylation efficiency (EiC) (D) in *Handroanthus impetiginosus* (●) and *Handroanthus serratifolius* (○) plants as a function of time (h) of day.

*tiginosus* , y 0,0328 [(μmol m$^{-2}$ s$^{-1}$) (μmol de CO$_2$ mol$^{-1}$)$^{-1}$] y 0,0395 [(μmol m$^{-2}$ s$^{-1}$) (μmol de CO$_2$ mol$^{-1}$)$^{-1}$] en *H. serratifolius*, respectivamente (figura 4D).

## DISCUSIÓN

Los análisis de la prueba de significación Lambda de Wilks y la correlación canónica (ACC) indican que los grupos están asociados de manera dependiente, lo que evidencia el efecto de las variables meteorológicas en los aspectos ecofisiológicos de *H. impetiginosus* y *H. serratifolius* a lo largo del día. En la ACC, la importancia de las variables de cada grupo (meteorológicas y ecofisiológicas) se asocia al mayor coeficiente canónico (cc), es decir, cuanto mayor es el coeficiente, más importante es la variable.

En cuanto a los datos meteorológicos internos y externos del invernadero, Caron *et al*. (2017) estudiando plantas de *Aleurites fordii* Hemsl., encontraron resultados similares al presente estudio, con valores máximos de radiación fotosintética activa (RFA) registrados en el período entre 11:30 h y 13:30 h y una elevación de la temperatura del aire entre 13:30 h y 15:30 h. La disminución de la humedad relativa del aire a lo largo del día, posiblemente se produce debido al aumento de la RFA y de la temperatura del aire (Dalmago *et al*. 2006). La radiación fotosintéticamente activa, combinada con otros factores meteorológicos, puede regular la capacidad fotosintética de las plantas (Taiz *et al*. 2017).

Entre las 14 y 17 hs, en ambas especies disminuyen A y gs, pero aumentó Ci. Este resultado indica que la disminución en la tasa fotosintética no se debió al cierre estomático, ya que evidentemente el CO$_2$ no fue limitante. En ese caso la disminución en A pudo deberse a una menor concentración de ATP y NADPH, debido a una disminución en la etapa fotoquímica de la fotosíntesis (Šigut *et al*. 2015; Xu *et al*. 2016; Ribeiro *et al*. 2020).

El comportamiento de la transpiración (E) para ambas especies fue similar a la tasa de asimilación neta de CO$_2$ y la conductancia estomática, lo que demuestra que esta variable depende directamente de la apertura y cierre de los estomas, así como su asociación a los mecanismos que regulan la temperatura de las hojas y limitación de la pérdida de agua por las hojas (Simões *et al*. 2015). El aumento de la transpiración en el período de mayor irradiación y temperatura puede haberse producido debido a la mayor eficiencia de las hojas en la asimilación neta del CO$_2$, donde la competencia entre las moléculas de CO$_2$ y H$_2$O posiblemente aumentó la pérdida de agua por los estomas (Lambers y Oliveira 2019). La concentración interna de CO$_2$ disminuyó en el período más caluroso del día, posiblemente debido a la alta tasa de fotosíntesis, lo que indica que el CO$_2$ está siendo fijado por Rubisco (Sun *et al*. 2014). Dalastra *et al*. (2014), a diferencia del presente estudio, destacaron que las plantas sometidas a condiciones ideales, presentan altos valores de concentración interna de CO$_2$ y asimilación neta de CO$_2$, y que la fotosíntesis se ve limitada por la disminución de la concentración de CO$_2$.

El alto déficit de presión de vapor en el período de mayor RFA y temperatura interna y externa puede estar asociada con una mayor apertura de los estomas, de manera que se produzca un mayor flujo de intercambio de gases en las hojas (Souza *et al*. 2016). Los valores más altos de EUA y EiUA encontrados a las 16 y 17 h en ambas especies demuestran que el agua se utilizó de manera más eficiente, lo que indica que hubo una buena absorción de CO$_2$ con una menor pérdida de agua durante este período, además de suponer que el cierre estomático al final de la tarde contribuyó a optimizar el uso del agua por parte de las plantas (Wieser *et al*. 2018).

La eficiencia instantánea de carboxilación (EiC) se mide por la relación entre la tasa de asimilación neta de CO$_2$ (A) y la concentración interna de CO$_2$ (Ci). Aquí, los valores altos encontrados para A y Ci pueden ser indicadores del aumento de la EiC (Silva *et al*. 2015) producido por la disponibilidad de ATP y NADPH y el sustrato utilizado por Rubisco. Así pues, algunos factores influyen en la EiC, como la cantidad de CO$_2$ que se encuentra en el mesófilo foliar, la temperatura, la luminosidad y la actividad enzimática que permite la plena realización de la fotosíntesis (Silva *et al*. 2015).

En general, se pudo observar una alta relación entre las variables ecofisiológicas y los factores meteorológicos analizados en ambas especies. Los aspectos ecofisiológicos de las plantas fueron alterados al ser cuantificados en un ambiente protegido (invernadero), en el cual se satisface la demanda de aire evaporativo y limitando evapotranspiración debido a la disminución de la velocidad del viento y la irradiancia a través de la cubierta plástica del ambiente.

El rendimiento fisiológico de *H. impetiginosus* y *H. serratifolius* presentó oscilaciones según las diferentes condiciones meteorológicas a lo largo del día. Por lo tanto, los aspectos ecofisiológicos de ambas especies dependen en gran medida de las condiciones ambientales.

La menor irradiación y la baja temperatura del aire redujeron el comportamiento fisiológico de las plantas *H. impetiginosus* y *H. serratifolius*.

El momento ideal del día para las evaluaciones de intercambio gaseoso en plantas de *H. impetiginosus* y *H. serratifolius* es entre las 11 a.m. y la 1 p.m.

## AGRADECIMIENTOS

## REFERENCIAS

Alvares CA, JL Stape, PC Sentelhas, JLM Gonçalves, Sparovek G. 2013. Köppen's climate classification map for Brazil.

*Meteorologische Zeitschrift* 22: 711-728. DOI: https://doi.org/10.1127/0941-2948/2013/0507

Beltreschi L, RB Lima, DD Cruz. 2019. Traditional botanical knowledge of medicinal plants in a "quilombola" community in the Atlantic Forest of northeastern Brazil. *Environment, Development and Sustainability* 21: 1185-1203. DOI: https://doi.org/10.1007/s10668-017-0079-6

Benevides DS, FG Carvalho. 2009. Levantamento da flora apícola presente em áreas de caatinga do município de Caraúbas – RN. *Sociedade e Território* 21: 44-54.

Bhatla SC, MA Lal. 2018. Abiotic Stress. *In* Bhatla SC, MA Lal eds. Plant Physiology, Development and Metabolism. Singapore, Malaysia. Springer. p. 969-1028.

Caron BO, JR Schneider, EF Elli, E Eloy, VQ Souza. 2017. Physiological relationships in *Aleurites fordii* Hemsl. seedlings. *Revista Árvore* 41: 2-7. DOI: https://doi.org/10.1590/1806-90882017000100002

CNCFlora. 2020. *Handroanthus* in Flora do Brasil 2020 em construção. Jardim Botânico do Rio de Janeiro. Consultado 26 jun. 2020. Disponible en http://floradobrasil.jbrj.gov.br/reflora/floradobrasil/FB117466

Costa EVS, HPC Brígido, JVS Silva, MR Coelho-Ferreira, GC Brandão, MF Dolabela. 2017. Antileishmanial activity of *Handroanthus serratifolius* (Vahl) S. Grose (Bignoniaceae). *Evidence-Based Complementary and Alternative Medicine* 2017: 1-6. DOI: https://doi.org/10.1155/2017/8074275

Cruces E, R Rautenberger, Y Rojas-Lillo, VM Cubillos, N Arancibia-Miranda, E Ramírez-Kushel, I Gomez. 2017. Physiological acclimation of *Lessonia spicata* to diurnal changing PAR and UV radiation: Differential regulation among down-regulation of photochemistry, ROS scavenging activity and phlorotannins as major photoprotective mechanisms. *Photosynthesis Research* 131: 145-157. DOI: https://doi.org/10.1007/s11120-016-0304-4

Dalastra GM, MM Echer, VF Guimarães, TL Hachmann, AM Inagaki. 2014. Trocas gasosas e produtividade de três cultivares de meloeiro conduzidas com um e dois frutos por planta. *Bragantia* 73: 365-371. DOI: https://doi.org/10.1590/1678-4499.206

Dalmago GA, AB Heldwein, AH Nied, EL Grimm, CR Pivetta. 2006. Maximum evapotranspiration of sweet pepper in plastic greenhouse as a function of solar radiation, temperature, relative humidity and water vapor pressure deficit of the air. *Ciência Rural* 36: 785-792. DOI: https://doi.org/10.1590/S0103-84782006000300010

Dias D, M Pagotto, T Pereira, A Ribeiro. 2017. Estrutura arbórea e sazonalidade da cobertura do dossel em vegetação florestada e aberta no parque nacional serra de Itabaiana, Sergipe, Brasil. *Ciência Florestal* 27: 719-729. DOI: https://doi.org/10.5902/1980509827757

Ferreira DTRG, EP Gonçalves, JS Viana, LN Ralph, JCA Silva, EM Silva. 2020. Temperature and light under the physiological potential of seeds of *Handroanthus impetiginosus*. *Bioscience Journal* 36: 68-77. DOI: https://doi.

org/10.14393/BJ-v36n1a2020-42454

Lambers H, RS Oliveira. 2019. Plant water relations. *In* Lambers H, RS Oliveira eds. Plant Physiological Ecology. New York, USA. Springer. p. 28-48.

Oliveira AR, CL Boechat, SPN Amorim, MEL Souza, LSL Duarte, HF Silva. 2019. Growth and quality of *Handroanthus serratifolius* seedlings in soils incorporating amendments and inorganic residues. *Ceres* 66: 235-242. DOI: https://doi.org/10.1590/0034-737x201966030010

Ribeiro JES, AJS Barbosa, SF Lopes, WE Pereira, MB Albuquerque. 2018. Seasonal variation in gas exchange by plants of *Erythroxylum simonis* Plowman. *Acta Botanica Brasílica* 32: 287-296. DOI: https://doi.org/10.1590/0102-33062017abb0240

Šigut L, P Holišová, K Klem, M Šprtová, C Calfapietra, MV Marek, V Špunda, O Urban. 2015. Does long-term cultivation of saplings under elevated $CO_2$ concentration influence their photosynthetic response to temperature? *Annals of Botany* 116: 929-939. DOI: https://doi.org/10.1093/aob/mcv043

Silva FG, WF Dutra, AF Dutra, IM Oliveira, L Filgueiras, AS Melo. 2015. Gas exchange and chlorophyll fluorescence of eggplant grown under different irrigation depths. *Revista Brasileira de Engenharia Agrícola e Ambiental* 19: 946-952. DOI: https://doi.org/10.1590/1807-1929/agriambi.v19n10p946-952

Simões WL, M Calgaro, DS Coelho, MA Souza, JA Lima. 2015. Respostas de variáveis fisiológicas e tecnológicas da cana-de-açúcar a diferentes sistemas de irrigação. *Revista Ciência Agronómica* 46: 11-20.

Souza ER, ACE Amaro, LS Santos, EO Ono, JD Rodrigues. 2016. Fenologia e trocas gasosas da videira cv. Sweet Sunshine em clima semiárido. *Comunicata Scientiae* 7: 319-333.

Sun Y, L Gu, RE Dickinson, SG Pallardy, J Baker, Y Cao, FM Damatta, X Dong. 2014. Asymmetrical effects of mesophyll conductance on fundamental photosynthetic parameters and their relationships estimated from leaf gas exchange measurements. *Plant, Cell & Environment* 37: 978-994. DOI: https://doi.org/10.1111/pce.12213

Taiz L, E Zeiger, IM Møller, A Murphy. 2017. Fisiologia e desenvolvimento vegetal. Porto Alegre, Brazil. Artmed. 858 p.

Vieira C, O Weber. 2017. Saturação por bases de crescimento e nutrição de mudas de Ipê-Amarelo. *Floresta e Ambiente* 24: 1-10. DOI: https://doi.org/10.1590/2179-8087.001916

Wieser G, W Oberhuber, B Waldboth, A Gruber, R Matyssek, RTW Siegwolf, EE Grams. 2018. Long-term trends in leaf level gas exchange mirror tree-ring derived intrinsic water-use efficiency of *Pinus cembra* at treeline during the last century. *Agricultural and Forest Meteorology* 248: 251-258. DOI: https://doi.org/10.1016/j.agrformet.2017.09.023

Xu Z, Y Jiang, B Jia, G Zhou. 2016. Elevated-$CO_2$ response of stomata and its dependence on environmental factors. *Frontiers in Plant Science* 7: 1-15. DOI: https://doi.org/10.3389/fpls.2016.00657

# Machine learning for carbon stock prediction in a tropical forest in Southeastern Brazil

## Aprendizaje de máquina para la predicción de reservas de carbono en un bosque tropical en el sureste de Brasil

**Daniel Dantas [a]\*, Marcela de Castro Nunes Santos Terra [a],**
**Luis Paulo Baldissera Schorr [a], Natalino Calegario [a]**

\* Corresponding autor: [a] Federal University of Lavras, Departament of Forest Sciences,
Lavras, Minas Gerais, Brazil, tel.: 5538991237493, dantasdaniel12@yahoo.com.br

### SUMMARY

The increasing awareness of global climate change has drawn attention to the role of forests as mitigators of this process as they act as carbon sinks to the atmosphere. Understanding the process of carbon storage in forests and its drivers, as well as presenting consistent models for their estimation, is a current demand. In this sense, the aim of this study was to evaluate the performance of machine learning techniques: support vector machines (SVM) and to propose a new nonlinear model extracted from the training of an artificial neural network (ANN) in the modeling of above ground carbon stock in a secondary semideciduous forest. SVM and ANN construction and training process considered independent variables selected by stepwise: minimum DBH (diameter of breast height - 1.3 m), maximum DBH, mean DBH, total height and number of trees, all by plot. SVM and the model extracted from ANN were applied to the data set intended for validation. Both techniques presented satisfactory performance in modeling carbon stock by plot, with homogeneous distribution and low dispersion of residues and predicted values close to those observed. Analysis criteria indicated superior performance of the model extracted from the artificial neural network, which presented a mean relative error of 6.94 %, while the support vector machine presented 13.52 %, combined with lower bias values and higher correlation between predictions and observations.

*Key words:* artificial intelligence, artificial neural networks, support vector machines, forest biomass.

### RESUMEN

La conciencia de la sociedad en relación a los cambios climáticos globales ha llamado la atención sobre el papel de los bosques como mitigadores de este proceso, ya que actúan como sumideros de carbono en la atmósfera. Comprender el proceso de almacenamiento de carbono en los bosques y sus determinantes, así como presentar modelos consistentes para su estimación es una demanda actual. En este sentido, el objetivo de este estudio fue evaluar el desempeño de las técnicas de máquina de vectores de soporte (SVM) y proponer un nuevo modelo no lineal extraído del entrenamiento de una red neuronal artificial (RNA) para modelar la cantidad de carbono sobre el suelo en un Bosque secundario estacional semidecíduo. El proceso de construcción y entrenamiento de SVM y RNA consideró variables independientes seleccionadas por *stepwise*: DAP mínimo (diámetro de altura del pecho - 1.3 m), DAP máximo, DAP promedio, altura total promedio y número de árboles, todo por unidad de muestreo. La SVM y el modelo extraído de la RNA se aplicaron al conjunto de datos para su validación. Ambas técnicas mostraron un desempeño satisfactorio en la modelación de la cantidad de carbono por unidad de muestreo, con distribución homogénea y baja dispersión de residuos y valores pronosticados cercanos a los observados. Los criterios de análisis utilizados indicaron un desempeño superior del modelo extraído de la red neuronal artificial, que presentó un error relativo promedio de 6.94 %, mientras que la máquina de vectores de soporte presentó 13.52 % junto con valores de sesgo más bajos y una mayor correlación entre predicciones. y observaciones.

*Palabras clave:* inteligencia artificial, redes neuronales artificiales, máquinas de vectores de soporte, biomasa forestal.

## INTRODUCTION

Forests provide numerous ecosystem services, such as regulation of biogeochemical cycles, pollution control and food supply. Among the most acclaimed ecosystem services provided by forests are the atmospheric carbon ($CO_2$)

sequestration and its storage (Canadell and Raupach 2008, Chazdon *et al.* 2016). This service is of strategic importance in mitigating ongoing climate change because it acts directly in controlling global warming (Bonan 2008).

In this context, the quantification of the carbon stock present in the most varied types of forests constitutes

an important tool for monitoring this ecosystem service (Scolforo *et al.* 2015). Many initiatives have been taken to quantify carbon stocks in forests, both by direct means (Dantas *et al.* 2021) and through estimates from related data (indirect methods) (Cordeiro *et al.* 2018).

Carbon stock estimation by indirect methods employs modeling and simulation techniques. Historically, modeling of forest attributes has relied on approaches based on statistical models (*e.g.* Melo *et al.* 2017). These approaches share space today with computational approaches of artificial intelligence/machine learning, such as artificial neural networks, support vector machines, decision trees, among others, which have been gaining space as tools for forest data analyses, modeling, estimation and production prognosis. These tools have provided gains in the quality of estimates and predictions (Vendruscolo *et al.* 2015).

Artificial Neural Network (ANN) is a processor consisting of simple processing units (artificial neurons), based on neurons found in the human brain, that calculate certain functions. These units are layered and connected to each other by weights that store experimental knowledge and weight the inputs of each unit. Thus, the acquired knowledge becomes available for use (Braga *et al.* 2007, Dantas *et al.* 2020a).

The most notable features in ANNs are their ability to learn and to generalize information. In other words, ANNs are able, through a learned example, to generalize assimilated knowledge to an unknown data set. Another interesting feature of ANN is the ability to extract non-explicit features from a set of information provided as examples (Haykin 2001).

Support vector machines (SVM) have also proven to be an interesting alternative for mathematical modeling of complex systems (Heddam and Kisi 2018). They are simple techniques in their conceptual basis and capable of solving extremely complex real problems. SVM is a supervised learning technique that is trained to classify different categories of data from various disciplines (Haykin 2001). These have been used for two-class classification problems and are applicable on both linear and non-linear data classification tasks. SVM creates a hyperplane or multiple hyperplanes in a high-dimensional space, and the best hyperplane in them is the one that optimally divides data into different classes with the largest separation among the classes (Steinwart and Christmann 2008).

Initially, SVM techniques were successfully applied as a data classification methodology (Tong and Koller 2001). They were later extended to regression tasks through the following approaches: support vector regression (SVR) and least-square support vector machines (LS-SVM) (Cherkassky and Mulier 1998, Dantas 2020b).

Compared to ANN, SVM has the advantage of leading to an exact solution, that is, a global optimum (Haykin 2001). However, finding a final SVM model may present computational complexity because it requires solving a quadratic programming model and solving a set of nonlinear equations.

The present study aims at evaluating the performance of the support vector machine and artificial neural network techniques, and at proposing a new nonlinear model to the modeling of above ground biomass (carbon stock), using dendrometric variables as inputs, in a secondary semideciduous seasonal forest. It is proposed, as a hypothesis, that (a) machine learning techniques are suitable in modeling above ground biomass, (b) it is possible to extract accurate above ground biomass equations from the artificial neural network training process.

METHODS

*Study area and data collection.* The study area corresponds to a secondary semideciduous seasonal forest, located in Lavras, Minas Gerais, Brazil, under the coordinates 21° 14' S and 45° 00' W, with average altitude of 900 m (figure 1). The climate is classified as Köppen's Cwb, with dry winters and mild summers (Alvares *et al*. 2013). Mean annual rainfall is around 1,500 mm and mean annual temperature is 19.4 °C (Marques *et al*. 2019). The forest is heterogeneous and presents dominance of tree species of the genus Anadenanthera, popularly known as "angico". Data come from 105 sample plots (10x10 m) launched in the area. In each plot, all trees with diameter at breast height (DBH - 1.3 m from the ground) higher than or equal to 5 cm and their respective heights were measured.

From the data collected in the field, the following variables were obtained by plot: minimum DBH (DBHmin), mean DBH (DBHmed), maximum DBH (DBHmax), minimum total Height (Hmin), mean total Height (Hmed), maximum total Height (Hmax), Mean Square Diameter (Dq) and Number of Trees (N).

Above Ground Biomass (AGB) was estimated by tree individual according to the equation proposed by Chave *et al*. (2014), using DBH and total tree height and average basic wood density of 0.620 g cm$^{-3}$. The estimate was performed using the software R (R Core Team 2018), using the BIOMASS package (Réjou-Méchain *et al*. 2017). The estimate of AGB was converted to carbon stock in Mg ha$^{-1}$, according to Thomas and Martin (2012), a methodology consisting in multiplying AGB by 0.471, which according to the authors corresponds to carbon concentration in tropical forest angiosperms tissues.

*Independent variables selection.* First, a selection of independent variables was performed by the stepwise method, based on the Akaike Information Criterion (AIC). Thus, the combination of variables that make up the model with the lowest AIC is considered the best. subsequently, the selected variables were used as inputs to model carbon stock by plot through machine learning techniques.

*Machine learning algorithms.* For carbon stock modeling, support vector machines (SVM) and artificial neural networks (ANNs) were used. The SVM construction was ba-
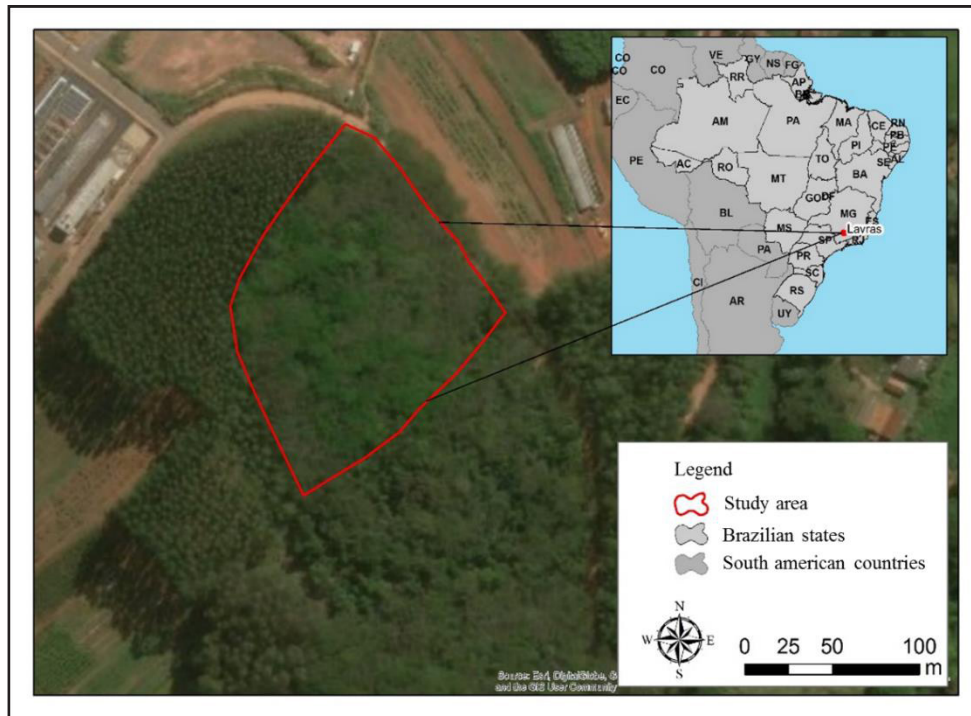
**Figure 1.** Study area. Secondary semideciduous forest path located in Lavras, Minas Gerais, Brazil. (Adapted from Terra *et al.* 2019).
Área de estudio. Bosque semideciduo estacional en Lavras, Minas Gerais, Brasil (Adaptado de Terra *et al.* 2019).

sed on the supervised machine learning process described by Haykin (2001) and Steinwart and Christmann (2008), where there is a set of paired-order n samples (**X**, **Y**), where **X** is a matrix of explanatory variables of the sample and Y is the expected value vector of the sample. Based on this information, taking as input a vector of variables, a chosen function predicts the expected value of the sample. A linear function is given by the form f (**X**) = <**W**, **X**> + b, where **W** is a weight vector.

The type IV error function, also known as *eps-regression*, was used, being the RBF (Radial Basis Function) type Kernel function. Kernel functions offer an alternative solution by designing data in a space with large characteristics to increase the computational power of machine learning, making it possible to represent nonlinear phenomena (Cristianini and Shawe-Taylor 2000). This procedure was performed in software R, version 3.4.1, through the *e1071* package (Meyer *et al.* 2019).

Trained ANNs were Multilayer Perceptron (MLP), composed of an input layer, an intermediate layer and an output layer. The algorithm used was the resilient backpropagation, in which the learning rate was automatically defined by the *neuralnet* package, with values ranging from 0.01 to 1.12.

The choice of the number of neurons in the hidden layer was made using k-fold. This methodology randomly subdivides the database into k subgroups (Ali and Pazzani 1996, Cigizoglu and Kisi 2006). The value of k was

10 subgroups, with a proportion of 90 % for training and 10 % for testing (Diamantopolou 2005), applying cross-validation. Different numbers of neurons, ranging from 1 to 20, were tested.

Logistics (or sigmoidal) was the activation function used, with a range from 0 to 1, which implies limiting the amplitude of the outputs and inputs. Consequently, data were normalized, which consists of transforming the values of each variable to values between 0 and 1. Linear standardization was obtained through equation [1] (Soares *et al.* 2011) and considers the minimum and maximum value of each variable in the transformation of values, maintaining the original distribution of data (Valença 2010).

$$x' = \frac{(x - x_{min}) * (b - a)}{(x_{max} - x_{min})} + a \qquad [1]$$

where: *x'*: normalized value, x: original value, *xmin*: minimum value of the variable, *xmax*: maximum value of the variable, *a*: lower limit of the standardization range, *b*: upper limit of the standardization range.

The stopping criterion for the ANN training process was the maximum number of 100.000 cycles, or the mean square error of less than 1 %, and training was terminated when one of these criteria was met. At the end of training, the best ANN was selected based on the lowest mean square error.

A nonlinear equation for tree biomass prediction was extracted from the artificial neural network. Consequently, we generated a system of equations with coefficients resulting from weights generated by the neurons of ANN. This system was used to predict the carbon stock of the plots that comprised the validation database.

Data were divided into two groups: 70 % for ANN training and SVM construction and 30 % for validation of both techniques. Among the data intended for ANN training, 70 % were used in the training phase and 30 % in the test phase.

*SVM and ANN performance evaluation.* SVM and ANN performances were evaluated in the training and validation phases. Accordingly, the techniques were used to predict the carbon stock in the data set intended for validation, *i.e.* data that had not been used in training. The prediction quality analysis was performed using Mean Relative Error (MRE %) (equation 2), Bias (equation 3), Root Mean Square Error (RMSE %) (equation 4) (Leite and Andrade 2002, Siipilehto 2000), graphs of residuals distribution, graphs of estimated versus observed carbon stocks and the correlation coefficients between estimated and observed values.

$$MRE\ (\%) = \frac{(\hat{Y}\iota - Yi)}{Yi} \times 100 \qquad [2]$$

$$Bias\ (\%) = 100 * \frac{1}{n} * \sum_{i=1}^{n} \left[ \frac{(\hat{Y}\iota - Yi)}{Yi} \right] \qquad [3]$$

$$RMSE\ (\%) = \left[ \sqrt{\sum_{i=1}^{n} \frac{(\hat{Y}\iota - Yi)^2}{n}} / \bar{Y} \right] * 100 \qquad [4]$$

where: $Yi$ represents the observed value, $\hat{Y}\iota$ the estimated value, $n$ the number of observations and $\bar{Y}$ the average of the observed values.

RESULTS

The forest with predominance of *Anadenanthera* sp. contained an average of tree carbon stock (AGC) of 94.25 Mg ha$^{-1}$. Descriptive statistics of the variables used are presented in table 1.

Stepwise method indicated through the Akaike information criterion that the variables minimum DBH, maximum DBH, average DBH, average H and N are those that have a stronger influence on carbon stock variability, and were, therefore, selected for modeling. It should be noted that DBHmed and Hmed represent the main tree growth trends in each plot; DBHmin and DBHmax, the lower and upper limits of diameter growth, respectively; and N represents the density of individuals in each plot. Figure 2 presents the scatter plots between the variables and their respective confidence intervals and the distribution of each variable.

The configurations obtained with the construction of the support vector machine, which resulted in a machine with 44 support vectors, are presented in table 2.

Regarding the approach by artificial neural networks, figure 3 illustrates the architecture and weights obtained

**Table 1.** Descriptive statistics of dendrometric variables of a secondary seasonal semideciduous forest located in Lavras, Minas Gerais, Brazil.

Variables dendrométricas de un bosque semideciduo estacional secundario ubicado en Lavras, Minas Gerais, Brasil.

| Variable | Mean | Minimum | Maximum | Standard deviation | CV( %) |
|---|---|---|---|---|---|
| C | 94.25 | 15.65 | 245.09 | 52.57 | 71.14 |
| DBHmin | 5.84 | 5.00 | 9.07 | 0.90 | 15.34 |
| DBHmax | 29.61 | 12.50 | 55.25 | 8.20 | 29.96 |
| DBHmed | 12.72 | 8.69 | 19.83 | 2.50 | 20.27 |
| Hmin | 6.65 | 5.24 | 11.43 | 1.41 | 21.12 |
| Hmax | 22.00 | 14.86 | 29.00 | 2.39 | 11.05 |
| Hmed | 13.18 | 9.84 | 18.83 | 1.76 | 13.38 |
| N | 14.25 | 3.00 | 30.00 | 4.96 | 34.90 |
| Dq | 14.59 | 9.16 | 22.79 | 3.11 | 22.74 |

Where: C = carbon stock (Mg.ha$^{-1}$), DBHmin = minimum breast height diameter (DBH) of the sample plot (cm), DBHmax = maximum DBH of the sample plot (cm), DBHmed = mean DBH of the sample plot (cm), Hmin = minimum total height of the sample plot (m), Hmax = maximum total height of the sample plot (m), Hmed = mean total height of the sample plot (m), N = number of trees in the sample plot, Dq = mean square diameter of the sample plot (cm).
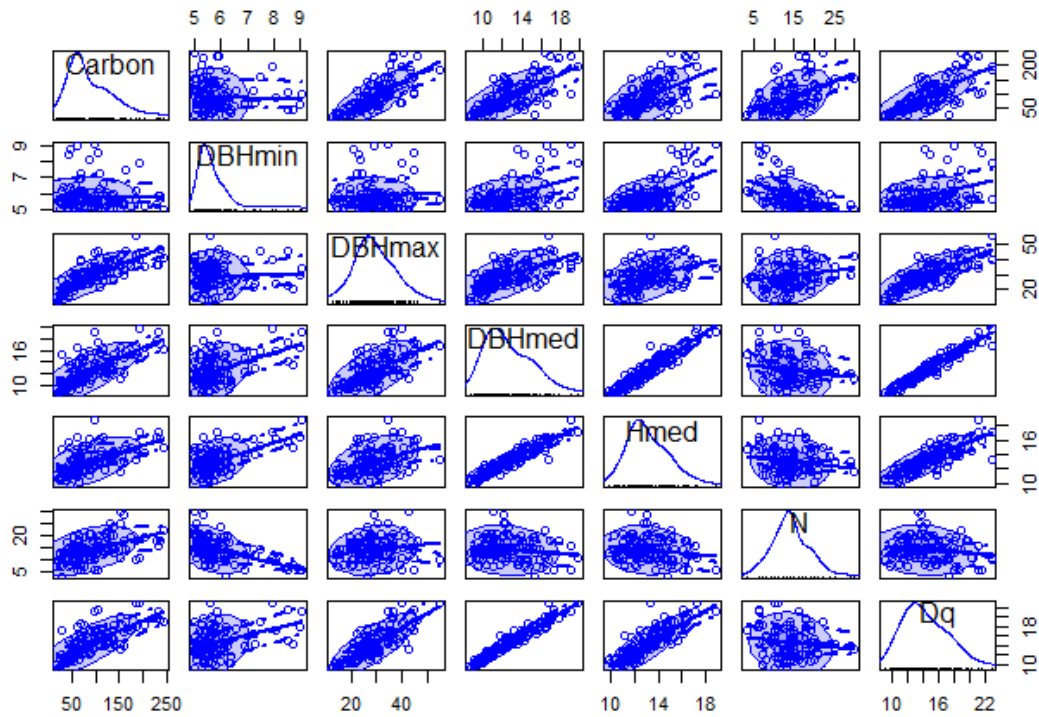
**Figure 2.** Distribution and dispersion of the independent variables selected by stepwise for carbon stock modelling and their respective confidence intervals.

Distribución y dispersión de las variables seleccionadas y sus respectivos intervalos de confianza.

**Table 2.** Support Vector Machine Parameters in the estimation of carbon stock in a secondary semideciduous forest.

Parámetros de máquina de vectores de soporte para estimar las existencias de carbono en un bosque semideciduo estacional secundario.

| SVM | Parameters |
|---|---|
| Type | *eps-regression* |
| Kernel | Radial basis function |
| Cost | 1 |
| Gamma | 0.2 |
| Epsilon | 0.1 |
| Numbers of support vectors | 40 |

from the selected ANN that presented the lowest error among the others evaluated, composed by six neurons in the hidden layer.

From the 5-6-1 architecture artificial neural network, an equation system was extracted to predict carbon stock per plot, with coefficients derived from weights generated by neural network neurons. This system was used to predict the carbon stock of plots that make up the database for validation.

Model [5] expresses the relationship between the hidden layer and the response variable, where β0 is the bias and the other coefficients are weights related to each neuron. Model [6] represents the activation function used in each hidden layer neuron, derived from the logistic model. Finally, model [7] is the result of the relationship between input variables and the respective hidden layer neurons, and a model is generated for each neuron.

$$Carbon' = \beta_0 + \beta_1 * z_1 + \beta_2 * z_2 + \beta_3 * z_3 \\ + \beta_4 * z_4 + \beta_5 * z_5 + \beta_6 * z_6 \quad [5]$$

$$z_n = \left[\frac{1}{1 + e^{-w_i}}\right] \quad [6]$$

$$w_i = \beta_{0.n} + \beta_{1.n} * DBHmin_i' + \beta_{2.n} * DBHmax_i' + \beta_{3.n} \\ * DBHmed_i' + \beta_{4.n} * Hmed_i' + \beta_{4.n} * N_i' \quad [7]$$

where: $\boldsymbol{\beta_0}$: bias, $\boldsymbol{\beta_n}$: model coefficient associated with neuron n, $\boldsymbol{\beta_n}$: model coefficient between input variable k and neuron n, $\boldsymbol{z_n}$: n-th hidden layer neuron response, $\boldsymbol{w_i}$: sum of products between weights and inputs.

The coefficients of the system of equations extracted from the selected artificial neural network are presented in table 3.

The support vector machine and the model extracted from the artificial neural network were applied to the data set intended for validation. The analyzed techniques presented satisfactory performance in the modeling of carbon stock by plot, due to homogeneous distribution and low dispersion of residues and with predicted values close to those observed, as it can be observed in figures 4 and 5, respectively.
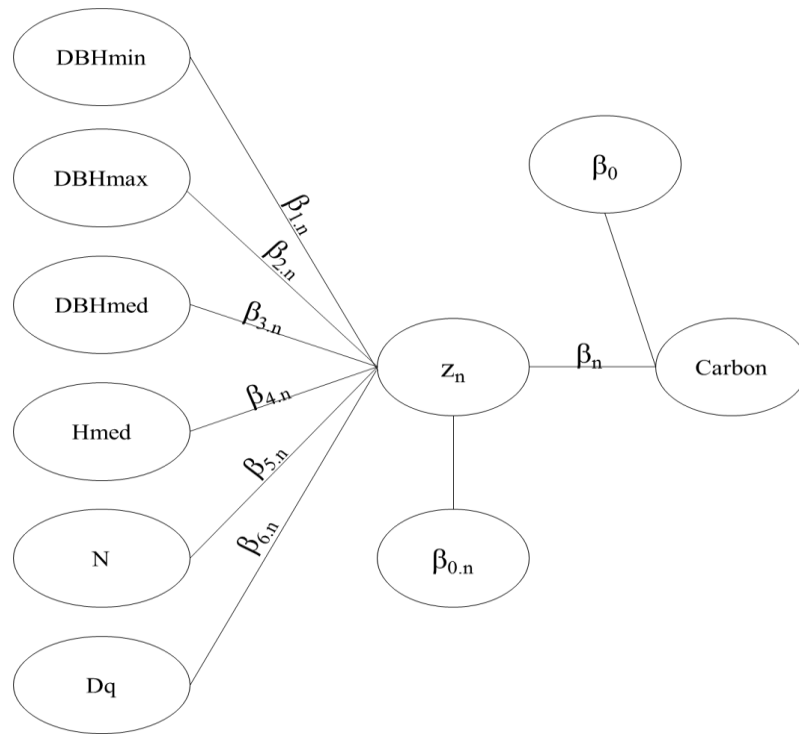


**Figure 3.** Architecture of the selected artificial neural network, composed of six neurons in the hidden layer. Input variables: DBHmin = minimum plot DBH (cm), DBHmax = maximum DBH of the plot (cm), DBHmed = mean DBH of the plot (cm), Hmed = Average total tree height of the plot (m), N = Number of trees in the plot. Output variable: C = carbon stock (Mg.ha$^{-1}$), $\beta_0$: bias; $\beta_n$: coefficient associated with the neuron $n$, $\beta_{k.n}$: coefficient of the model between the input variable $k$ and the neuron $n$, $z_n$: response of n-th hidden layer neuron.

Arquitectura de la red neuronal artificial seleccionada, compuesta por seis neuronas en la capa oculta. Variables de entrada: DAPmin = DAP mínimo de la parcela (cm); DAPmax = DAP máximo de la parcela (cm); DAPmed = DAP medio de la parcela (cm); HTmed = Altura total promedio de los árboles en la parcela (m); N = Número de árboles en la parcela. Variable de salida: C = stock de carbono (Mg.ha$^{-1}$).

**Table 3.** Coefficients (β's) of each neuron (N) of the hidden layer and of the ANN output layer.

Parámetros (β) de la red neuronal artificial. N representa el número de neuronas.

|  | β0 | β1 | β2 | β3 | β4 | β5 | β6 |
|---|---|---|---|---|---|---|---|
| ANN | 0.8609 | -0.7323 | 0.7619 | 0.6785 | -1.7671 | -1.6967 | 1.0353 |
| N1 | -2.3277 | 2.0301 | 0.1250 | 9.7276 | -6.8163 | 6.8954 | - |
| N2 | -1.3559 | 0.6158 | 2.5005 | 2.8092 | -0.3280 | -0.9826 | - |
| N3 | -1.7104 | 2.3549 | 0.9111 | 0.6736 | -2.8348 | 6.2268 | - |
| N4 | -0.1308 | 0.1538 | 0.5098 | -1.6662 | 1.0934 | -0.4838 | - |
| N5 | 0.1174 | -1.2125 | 0.4046 | -1.1707 | 0.2400 | -0.3406 | - |
| N6 | -0.0674 | -2.5130 | 0.6372 | 0.7235 | -0.2786 | 1.3868 | - |
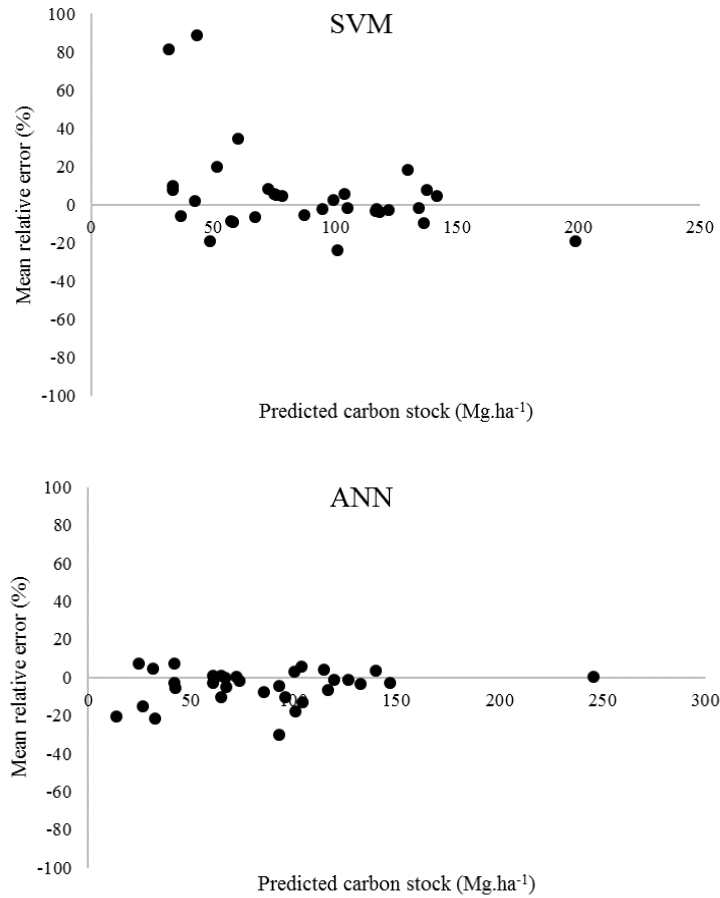
**Figure 4.** Residuals scatter plots of carbon stock modeling in a secondary semideciduous forest using machine learning algorithms.

Dispersión de residuos del modelado de existencias de carbono en un bosque secundario semideciduo mediante algoritmos de aprendizaje automático.
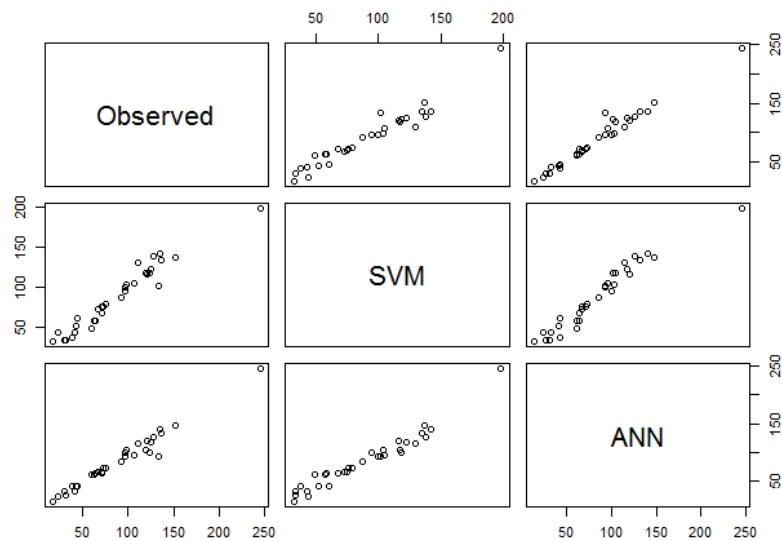


**Figure 5.** Predicted versus observed graphs of the analyzed techniques (artificial neural network and support vector machine) used to estimate carbon stock in a secondary semideciduous forest.

Criterios para evaluar el desempeño de la máquina de vectores de soporte (SVM) y los algoritmos de la red neuronal artificial (ARN) utilizados para estimar las existencias de carbono en un bosque secundario semideciduo.

According to the graphs (figures 4 and 5), there is a slight superiority of ANN, which presented more concentrated residues around zero and predicted values closer to the real ones. SVM presented higher residual dispersion and two relative error values above 80 %, while ANN presented a maximum relative error of 30 %.

The performance evaluation criteria of the analyzed techniques are presented in table 4. The qualities of the estimates made by SVM and by the model extracted from ANN were evaluated on both data used in the training and validation dataset.

The estimates of the analyzed techniques were strongly correlated with the observed values, showing correlation above 0.99 in the training phase and 0.96 in the validation phase. Error magnitudes, represented by RMSE, were below 10 % in the training phase and 15 % in the validation. The lower the RMSE, the higher the accuracy of the estimates, and the optimal situation when it is zero (Mehtätalo *et al.* 2006). Bias indicated slight underestimation trends in the training phase; whereas in validation, there was a tendency of SVM to overestimate carbon stock values (5.6479 %) and of ANN to underestimate them (-4.6217 %). Mean SVM relative error increased from 6.7689 % in the training phase to 13.5185 % in the validation phase; whereas in ANN, this increase went from 4.8035 % to 6.9375 %.

DISCUSSION

The average of tree carbon stock contained in the forest with predominance of *Anadenanthera* sp. (94.25 Mg ha$^{-1}$) is above the average carbon stock for this vegetation type in south-central Minas Gerais (55 Mg ha$^{-1}$, Scolforo *et al.* 2015) and compatible with other local studies in semideciduous seasonal forests in the study region. For instance, Ribeiro *et al.* (2009), quantifying the biomass and tree carbon stock in a mature semideciduous forest in Viçosa, Minas Gerais, Brazil, found 166.67 Mg ha$^{-1}$ and 83.34 Mg ha$^{-1}$ for biomass and carbon stocks, respectively. Likewise, Figueiredo *et al.* (2015) that evaluated the dynamics of the tree carbon stock in a semideciduous

forest in Minas Gerais, Brazil, found an average carbon stock of 71.81 Mg ha$^{-1}$.

Although the average carbon stock was relatively high, its variation among plots (CV%) was also significant. This is mainly due to the fact that the carbon stock variable reflects the variations in other dendrometric variables. Moreover, in natural multiage forests, characteristics such as high ecological complexity, spatial variations in species structure and composition, the presence of clearings and other factors can lead to great variability in biomass/carbon stock values (Soriano-Luna *et al.* 2018) among sample plots.

There is a strong relationship between mean DBH and mean height. Overall, there is a tendency of carbon stock to be positively correlated to the other variables, except for the minimum DBH, in which there was no direct or indirect proportional relationship, which is evidenced by the elliptic shape of the dispersion between these variables. In general, the relationship between carbon and independent variables tended towards linearity. There are, however, some nonlinear behaviors between variables, such as between carbon stock and maximum DBH. In this context, it is worth to emphasize that artificial intelligence/ machine learning has the ability to implicitly detect any nonlinear relationship between the response variable and explanatory variables. In addition to the fact that there are no assumptions regarding input data, such as independence and normality, and its high capacity for learning and generalization.

The main purpose of using these techniques, as in classical regression, is their application to data that were not used in their training. ANN presented better performance in the two analyzed phases, training and validation, which indicates its superiority for modeling the carbon stock per plot in the analyzed data set, when compared to SVM.

ANN was able, with the available variables, to explain almost all the variation in carbon stock in the study area. Several studies have demonstrated the superiority of artificial neural networks when compared to other techniques (Özçelik *et al.* 2013, Vendruscolo *et al.* 2015). This superiority can be explained by the ability of neural networks

**Table 4.** Performance evaluation criteria of the support vector machine (SVM) and artificial neural network (ANN) algorithms used in carbon stock estimation in a secondary semideciduous forest.

Criterios para evaluar el desempeño de la máquina de vectores de soporte (SVM) y la red neuronal artificial (ANN).

| | Train | | Validation | |
|---|---|---|---|---|
| | SVM | ANN | SVM | ANN |
| Mean relative error (%) | 6.7689 | 4.8035 | 13.5185 | 6.9375 |
| Bias (%) | -0.2610 | -1.2371 | 5.6479 | -4.6217 |
| Root mean square error (%) | 7.5858 | 5.4185 | 14.5550 | 10.8191 |
| Coefficient of correlation | 0.9900 | 0.9951 | 0.9690 | 0.9828 |

to detect implicit information and nonlinear relationships between the response variable and explanatory variables provided as examples and to generalize the assimilated knowledge to an unknown data set.

It is worth noting that, although underperforming ANN, SVM was very efficient in estimating carbon stock in the study area. SVM has the advantage over ANN that no evaluation is required after its construction, as it occurs in ANN to select the best network. This is due to the quadratic optimization that occurred during SVM training (Cristianini and Shawe-Taylor 2000) which allows the same result to be obtained for each system configuration whenever applied to the same data set. However, ANNs have more elements to be manipulated; besides, the initialization of neuron parameters occurs at random (Haykin 2001). Thus, each trained network will have slight differences in estimates, even if the same architecture is maintained. These differences highlight the practicality of SVM in relation to ANN as SVM excludes the subjectivity of the operator in choosing the best network to be applied to the database.

Therefore, both approaches were able to explain much of the carbon stock variation in the study area. This is mainly due to the robustness of ANN and SVM. The small part of the carbon stock variation, not explained by the variables in question, is due to the various factors not considered in the present study that are known to affect the variability of carbon stock in forests, such as species diversity, forest size, degree anthropization, among many others and their interactions (McNicol *et al.* 2018)

The results presented in this study provide insights for future assessments of the use of machine learning techniques to obtain carbon stock estimates. Some examples of potential applications are estimates of carbon stock in other forest compartments, such as soil and tree roots, carbon stock estimates through the association between machine learning techniques and remote sensing variables, among others.

## CONCLUSIONS

The present study brings important contributions in the modeling of carbon stocks in forests through the use of machine learning. The machine learning techniques performed satisfactorily, and a new model extracted from an artificial neural network for carbon stock prediction in Mg ha$^{-1}$ is efficient, with potential application in other secondary semideciduous seasonal forests.

Carbon stock modeling using a model extracted from the artificial neural network training presented better performance than that presented by the support vector machine, using the same variables of the analyzed data set.

Determining, modeling and supplying forest carbon stock data are strong scientific and social demands currently, as tree carbon storage is considered a key environmental service in mitigating current climate change by sequestering $CO_2$ from forest atmosphere.

## REFERENCES

Ali KM, MJ Pazzani. 1996. Error reduction through learning multiple descriptions. *Machine Learning* 24(3): 173-202. DOI: 10.1007/BF00058611

Alvares CA, JL Stape, PC Sentelhas, JLM Gonçalves, G Sparovek. 2013. Köppen's climate classification map for Brazil. *Meteorologische Zeitschrift* 22: 711–728. DOI: 10.1127/0941-2948/2013/0507

Bonan GB. 2008. Forests and climate change: forcings, feedbacks, and the climate benefits of forests. *Science* 320(5882): 1444-1449. DOI: 10.1126/science.1155121

Braga AP, APLF Carvalho, TB Ludemir. 2007. Redes Neurais Artificiais: Teoria e Aplicações. Rio de Janeiro, Brasil. Editora LTC. 226 p.

Canadell JG, MR Raupach. 2008. Managing forests for climate change mitigation. *Science* 320(5882): 1456-1457. DOI: 10.1126/science.1155458

Chave J, M Réjou–Méchain, A Búrquez, E Chidumayo, MS Colgan, WBC Delitti, A Duque, T Eid, PM Fearnside, RC Goodman, M Henry, A Martínez–Yrízar, WA Mugasha, HC Muller–Landau, M Mencuccini, BW Nelson, A Ngomanda, EM Nogueira, E Ortiz–Malavassi, R Pélissier, P Ploton, CM Ryan, JG Saldarriaga, G Vieilledent. 2014. Improved allometric models to estimate the aboveground biomass of tropical trees. *Global Change Biology* 20(10): 3177–3190. DOI: 10.1111/gcb.12629

Chazdon RL, EN Broadbent, DMA Rozendaal, F Bongers, AMA Zambrano, TM Aide, P Balvanera, JM Becknell, V Boukili, PHS Brancalion, D Craven, JS Almeida-Cortez, GAL Cabral, BD Jong, JS Denslow, DH Dent, SJ Dewalt, JM Dupuy, SM Durán, MM Espírito-Santo, MC Fandino, RG César, JS Hall, JL Hernández-Stefanoni, CC Jakovac, AB Junqueira, D Kennard, SG Letcher, M Lohbeck, M Martínez-Ramos, P Massoca, JA Meave, R Mesquita, F Mora, R Muñoz, R Muscarella, YRF Nunes, S Ochoa-Gaona, E Orihuela-Belmonte, M Peña-Claros, EA Pérez-García, D Piotto, JS Powers, J Rodríguez-Velazquez, IE Romero-Pérez, J Ruíz, JG Saldarriaga, A Sanchez-Azofeifa, NB Schwartz, MK Steininger, NG Swenson, M Uriarte, MV Breugel, HVD Wal, MDM Veloso, H Vester, ICG Vieira, TV Bentos, GB Williamson, L Poorter. 2016. Carbon sequestration potential of second-growth forest regeneration in the Latin American tropics. *Science Advances* 2(5):e1501639. DOI: 10.1126/sciadv.1501639

Cherkassky V, F Mulier. 1998. Learning from data: Concepts, theory, and methods. New York, United States. Wiley. 560 p.

Cigizoglu HK, Ö Kisi. 2006. Methods to improve the neural network performance in suspended sediment estimation. *Journal of Hydrology* 317(3): 221-238. DOI: 10.1016/j.jhydrol.2005.05.019

Cristianini N, J Shawe-Taylor. 2000. An introduction to support vector machines: and other kernel-based learning methods.

New York, United States. Cambridge University Press. 204 p.

Cordeiro NG, KMG Pereira, MCNS Terra, JM Mello. 2018. Variação temporal do estoque de carbono e volume de madeira em um fragmento de cerrado *sensu stricto*. *Enciclopédia Biosfera* 15(28): 931-942. DOI: [10.18677/EnciBio_2018B76](10.18677/EnciBio_2018B76)

Dantas D, LOR Pinto, MCNS Terra, N Calegario, MLR Oliveira. 2020a. Reduction of sampling intensity in forest inventories to estimate the total height of eucalyptus trees. *Bosque* 41(3): 353-364. DOI: [10.4067/S0717-92002020000300353](10.4067/S0717-92002020000300353)

Dantas D, N Calegario, FW Acerbi Júnior, SPC Carvalho, MAI Júnior, EA Melo. 2020b. Multilevel nonlinear mixed-effects model and machine learning for predicting the volume of *Eucalyptus* spp. trees. *Cerne* 26(1): 48-57. DOI: [10.1590/01047760202026012668](10.1590/01047760202026012668)

Dantas D, MCNS Terra, LOR Pinto, N Calegario, SM Maciel. 2021. Above and belowground carbon stock in a tropical forest in Brazil. *Acta Scientiarum. Agronomy* 43:e48276. DOI: [10.4025/actasciagron.v43i1.48276](10.4025/actasciagron.v43i1.48276)

Diamantopoulou MJ. 2005. Artificial neural networks as an alternative tool in pine bark volume estimation. *Computers and Electronics in Agriculture* 48(3): 235-244. DOI: [10.1016/j.compag.2005.04.002](10.1016/j.compag.2005.04.002)

Figueiredo LTM, CPB Soares, AL Sousa, HG Leite, GF Silva. 2015. Dinâmica do Estoque de Carbono em Fuste de Árvores de uma Floresta Estacional Semidecidual. *Cerne* 21(1): 161–167. DOI: [10.1590/01047760201521011529](10.1590/01047760201521011529)

Haykin, S. 2001. Redes neurais: princípios e prática. 2.ed. Porto Alegre, Brasil. Bookman. 900 p.

Heddam S, O Kisi. 2018. Modelling daily dissolved oxygen concentration using least square support vector machine, multivariate adaptive regression splines and M5 model tree. *Journal of Hydrology* 559: 499-509. DOI: [10.1016/j.jhydrol.2018.02.061](10.1016/j.jhydrol.2018.02.061)

Leite HG, VCL Andrade. 2002. Um método para condução de inventários florestais sem o uso de equações volumétricas. *Revista Árvore* 26(3): 321-328. DOI: [10.1590/S0100-67622002000300007](10.1590/S0100-67622002000300007)

Marques RFPV, MCNS Terra, VA Mantovani, AF Rodrigues, GA Pereira, RA Silva, CR Mello. 2019. Rainfall Water Quality Under Different Forest Stands. *Cerne* 25(1): 8–17. DOI: [10.1590/01047760201925012581](10.1590/01047760201925012581)

Mcnicol IM, CM Ryan, KG Dexter, SMJ Ball, M Williams. 2018. Aboveground carbon storage and its links to stand structure, tree diversity and floristic composition in south-eastern Tanzania. *Ecosystems* 21(4): 740-754. DOI: [10.1007/s10021-017-0180-6](10.1007/s10021-017-0180-6)

Mehtätalo L, M Maltamo, A Kangas. 2006. The use of quantile trees in the prediction of the diameter distribution of a stand. *Silva Fennica* 40(3):id333. DOI: [10.14214/sf.333](10.14214/sf.333)

Melo EA, N Calegario, AR Medonça, EL Possato, JA Alves, MAI Júnior. 2017. Modelagem não Linear da Relação Hipsométrica e do Crescimento das Árvores Dominantes e Codominantes de *Eucalyptus* sp. *Ciência Florestal* 27(4): 1325–1338. DOI: [10.5902/1980509829895](10.5902/1980509829895)

Meyer D. 2019. e1071: Misc Functions of the Department of Statistics, Probability Theory Group (Formerly: E1071), TU Wien. R package version 1.7-1. Consultado 24 aug. 2019. Disponible en [https://CRAN.R-project.org/package=e1071](https://CRAN.R-project.org/package=e1071)

Özçelik R, MJ Diamantopolou, F Crecente-Campo, U Eler. 2013. Estimating Crimean juniper tree height using nonlinear regression and artificial neural network models. *Forest Ecology and Management* 306: 52–60. DOI: [10.1016/j.foreco.2013.06.009](10.1016/j.foreco.2013.06.009)

R Development Core Team. 2018. R: a language and environment for statistical computing. ViennaR Foundation for Statistical Computing, 2018. Consultado 24 aug. 2019. Disponible en [https://www.r-project.org/](https://www.r-project.org/)

Réjou-Méchain M, A Tanguy, C Piponiot, J Chave, B Hérault. 2017. biomass: an r package for estimating above-ground biomass and its uncertainty in tropical forests. *Methods in Ecology and Evolution* 8(9): 1163–1167. DOI: [doi.org/10.1111/2041-210X.12753](doi.org/10.1111/2041-210X.12753)

Ribeiro SC, LAG Jacovine, CPB Soares, SV Martins, AL Souza, AMB Nardelli. 2009. Quantificação de biomassa e estimativa de estoque de carbono em uma floresta madura no município de viçosa, Minas Gerais. *Revista Árvore* 33(5): 917-926, 2009. DOI: [10.1590/S0100-67622009000500014](10.1590/S0100-67622009000500014).

Scolforo HF, JRS Scolforo, CR Mello, JM Mello, ACF Filho. 2015. Spatial distribution of aboveground carbon stock of the arboreal vegetation in Brazilian Biomes of Savanna, Atlantic Forest and Semi-arid woodland. *PLoS ONE* 10(6): 1-20. DOI: [10.1371/journal.pone.0128781](10.1371/journal.pone.0128781)

Siipilehto J. 2000. A comparison of two parameter prediction methods for stand structure in Finland. *Silva Fennica* 34: 331-349. DOI: [http://dx.doi.org/10.14214/sf.617](http://dx.doi.org/10.14214/sf.617)

Soares FAAMN, EL Flores, CD Cabacinha, GA Carrijo, ACP Veiga. 2011. Recursive diameter prediction and volume calculation of eucalyptus trees using Multilayer Perceptron Networks. *Computers and Electronics in Agriculture* 78(1): 19-27. DOI: [10.1016/j.compag.2011.05.008](10.1016/j.compag.2011.05.008)

Soriano-Luna MLA, et al. 2018. Determinants of above-ground biomass and its spatial variability in a temperate forest managed for timber production. *Forests* 9(8): 1–20. DOI: [10.3390/f9080490](10.3390/f9080490)

Steinwart I, A Christmann. 2008. Support vector machines. Berlin, Germany. Springer. 601 p.

Terra MCNS, D Dantas, LOR Pinto, N Calegario, SM Maciel. 2019. Estimativa do estoque de carbono em floresta semidecidual: uma comparação entre regressão e redes neurais artificiais. In Oliveira AC ed. Fontes de Biomassa e Potenciais de Uso. Ponta Grossa, Brasil. Editora Atena. p. 24-35.

Thomas SC, AR Martin. 2012. Carbon content of tree tissues: A synthesis. *Forests* 3(2):332-352. DOI: [10.3390/f3020332](10.3390/f3020332)

Tong S, D Koller. 2001. Support vector machine active learning with applications to text classification. *Journal of Machine Learning Research* 2: 45-66. DOI: [10.1162/153244302760185243](10.1162/153244302760185243)

Valença M. 2010. Fundamentos das redes neurais: exemplos em Java, ver. ampli. 2 ed. Olinda, Brasil. Livro Rápido. 386 p.

Vendruscolo DGS, R Drescher, HS Souza, JPVM Moura, FMD Mamoré, TAS Siqueira. 2015. Estimativa da altura de eucalipto por meio de regressão não linear e redes neurais artificiais. *Revista Brasileira de Biometria* 33(4): 556–569, 2015. DOI: [10.13140/RG.2.1.1742.5684](10.13140/RG.2.1.1742.5684)

# Growth dynamics of *Geoffroea decorticans* and *Parkinsonia praecox* and their response to climate in arid and semiarid environments in Argentina

## Dinámica de crecimiento y relación con el clima de *Geoffroea decorticans* y *Parkinsonia praecox* en ambientes áridos y semiáridos de Argentina

**Maria Alicia Cendoya [a]\*, Marcia Micca [b], Stella Marys Bogino [b]**

\*Autor de correspondencia: [a] Instituto Nacional de Tecnología Agropecuaria, EEA San Luis, Villa Mercedes, San Luis, Argentina, tel.: +54 2657204863, malicia.cendoya@gmail.com

[b] Universidad Nacional de San Luis, Departamento de Ciencias Agropecuarias, Villa Mercedes, San Luis, Argentina.

SUMMARY

Arid and semiarid environments dominate the Earth's surface and are very vulnerable to global change. Chañar (*Geoffroea decorticans*) and brea (*Parkinsonia praecox*) are two ubiquitous woody species of these environments. They grow in degraded forests, strongly modified areas and as a main component of secondary forests. Despite the value of both species, little is known about their growth dynamics and their relationship with climate. The objective of this research was to determine their dendrochronological potential and the connection between growth and climate variables. Anatomical and standard dendrochronological methods were applied. First of all, we stated the anatomical characteristics that allowed us to detect tree-ring boundaries (terminal parenchyma and variation in the shape of vessels). Further, after dating and measurement of tree rings we determined significant correlation between series, which means a common growth signal among trees as a result of environmental variable effects. Trees were not older than 40 years. Mean annual radial growth was 3.37 mm (SD±0.71) and 2.16 mm (SD±0.61) for chañar and brea, respectively. Finally, chañar and brea had a negative growth-mean temperature association. Rainfall affected chañar and brea growth in summer previous to the growing season. Southern Oscillation Index (SOI) had an inverse association with growth of brea. This means, in the case of brea, a significant association with local (temperature and rainfall) and global (SOI) climate variables. These results evidenced the growth dynamics of both species and their value for dendroclimatological studies for the first time.

*Key words:* dendrochronology, dendroclimatology, wood anatomy, espinal, monte.


RESUMEN

Los ambientes áridos y semiáridos dominan la superficie terrestre y son muy vulnerables en el contexto actual del cambio global. El chañar (*Geoffroea decorticans*) y la brea (*Parkinsonia praecox*) son especies que crecen en estos ambientes en bosques degradados, en áreas severamente transformadas o bien como componentes secundarios de los bosques maduros. A pesar de la importancia de ambas especies poco se conoce sobre su dinámica de crecimiento y su relación con el clima. El objetivo de este trabajo fue: determinar el potencial dendrocronológico y el vínculo entre el crecimiento y las variables climáticas de ambas especies. Se aplicaron métodos anatómicos y dendrocronológicos estándares. En primer lugar, establecimos las características anatómicas que nos permitieron detectar los límites de los anillos de crecimiento de los árboles. En segundo lugar, determinamos una correlación significativa entre las series, lo que significa una señal de crecimiento común entre los árboles como resultado de los efectos de las variables ambientales. Las series medidas en ambas especies permitieron estimar correlaciones significativas que demuestran una señal común de crecimiento ambiental. El crecimiento radial medio para ambas especies fue de 3,37 (DS±0,71) y 2,16 (DS±0,61) respectivamente. La longevidad no superó los 40 años. Por último, el crecimiento de chañar y brea tuvieron una asociación inversa con la temperatura media. La precipitación afectó los crecimientos de chañar en el verano y de la brea en la estación previa al crecimiento. El IOS (Índice de Oscillation Sur) tuvo una asociación inversa con el crecimiento de la brea. Esto implica, en el caso de la brea, una asociación significativa con variables climáticas locales (temperatura y lluvia) y globales (IOS). Estos resultados señalaron por primera vez la dinámica de crecimiento de ambas especies y su valor para estudios dendroclimatológicos.

*Palabras clave:* dendrocronología, dendroclimatología, anatomía del leño, monte, espinal.

INTRODUCTION

Arid and semiarid environments occupy more than sixty percent of Argentina's landscape. The driest area of Argentina's pampas region is covered by forests dominated by *Prosopis* species (Oyarzabal *et al.* 2018). Chañar (*Geoffroea decorticans* (Gill. ex Hook. *et* Arn.) Burkart) (*Fabaceae*, *Papilionoideae*) and brea (*Parkinsonia praecox* (Ruiz *et* Pav.) Hawkins) (*Fabaceae*, *Caesalpinioideae*) are two woody species that grow in these environments. They are pioneers with individuals recruiting massively after disturbances in severely transformed areas or degraded forests (Anderson *et al.* 1970).

*Geoffroea decorticans* is an antagonistic species from the anthropic point of view. On the one hand, it is considered an invasive woody shrub of the adjacent psammophilous grasslands that belong to the pampean grassland steppe dominated by C4 photosynthesis species of the genus *Aristida*, *Bothriochloa*, *Chloris*, *Elionurus*, *Eragrostis*, *Poa*, *Schizachyrium*, *Sorghastrum*, *Sporobolus* and *Stipa* (Anderson 1976). On the other hand, in the forests of Chaco, Monte and Espinal, it is a main component of the secondary forests (Giménez and Moglia 2003). *Parkinsonia praecox* grows in places known as *peladales,* which are highly degraded areas previously affected by fire and overgrazing, where it forms homogeneous forests or *breales* (Martínez Carretero 1986, Paez and Marco 2000).

Both species are the first to be established after severe disturbance, especially fire (Medina *et al.* 2000, Dussart *et al.* 2011). Considering that disturbance, including fires, is an essential component of forest systems (Oliver and Larson 1996) and that both species react in a similar way after its occurrence, it is essential to know how its temporal growth dynamic is. However, there is no information about it. Furthermore, in this context of global change, the value of forests as providers of ecosystem services has been reconsidered and the quantification of biomass for estimating the capacity to fix carbon is one of the most interesting variables in the world (Bar-on *et al*. 2018). Therefore, being able to estimate the growth rate of woody species makes it possible to accurately quantify this variable.

Two useful tools are available to evaluate the dynamics of forest systems over time: repeated measurements in permanent plots or an analysis applying dendrochronological techniques. Dendrochronology is the science that studies environmental events recorded in the growth rings of woody species. In this way, it is possible to annually analyze the relationship between individuals and the environment (Speer 2010). One of the most relevant applications of a growth-ring analysis is its use to establish the relationship between annual growth and climatic variables and, consequently, the reconstruction of past climatic conditions. Previous dendrochronological studies in the arid and semi-arid environments of Argentina had analyzed the most long-lived species with the highest timber value with special emphasis on the genus *Prosopis* (Morales *et al.* 2005, Villagra *et al.*

2005, Dussart *et al.* 2011, Bogino *et al.* 2015). Therefore, knowing about the growth dynamics of pioneer species will complement these studies and establish the interconnection between main species and those that are codominant or intermediate in a secondary forest (Gorzelak *et al.* 2015).

Despite the fact that *G. decorticans* is a widely distributed species in arid and semi-arid areas of Argentina, Bolivia, Chile, Uruguay and Peru (figure 1AB), there are no previous dendrochronological studies. To date, the approach has been limited to describe its anatomy and growth-ring width (Giménez *et al.* 2013). *P. praecox* has a wider geographic distribution area than that of *G. decorticans*: from the Sonoran Desert in Mexico 32° N to the south of the Argentine Chaco 35° S and from sea level to 2000 m asl (Schuch and Kelly 2008) (figure 1AC).

Before establishing the dendrochronological potential of any species, it is necessary to determine whether its growth rings are identifiable. Previous studies on the anatomy of *G. decorticans* are contradictory: on the one hand, according to Tortorelli (1956), differentiating tree rings is uncertain due to its diffuse semi-circular porosity, although on the other hand, further studies indicate that chañar is one of the few species from the Argentine Chaco that presents well-defined tree rings (Giménez 2009). A 33-year-old *G. decorticans* forms rings with an average thickness of 4.7 mm which implies that chañar is a species with the highest annual growth in the Semi-arid Chaco (Gimenez 2009). Regarding *P. praecox*, growth rings can be differentiated due to their semi-circular porosity (Tortorelli 1956). Previous studies in the Guajira of Colombia pointed out its association with regional and local climate variables (Ramirez and del Valle 2011) consequently, there is a need of complementing these previous studies to establish a common pattern of the species response to climate variables.

Considering that there are no studies on both species that determine their growth dynamics and relationship with environmental variables at their southern distribution area, our research questions are: Is it possible to successfully date the growth rings and analyze the temporal growth dynamics in relation to climate for both species? May climate-growth association determine the dynamics of both species? Therefore, the working hypothesis is: both species are possible to be dated as previous studies encourage us to think of the possibility of detecting tree ring boundaries and that their ubiquity responds to a scarce relationship with climatic variables. The objectives of this research are: a) to determine the anatomical characteristics of both species for their possible dating and b) from the feasibility of this fact, to reconstruct the growth dynamics and the relationship with climate.

METHODS

*Sampling sites.* The study site for *Geoffroea decorticans* was in the so-called sandy pampas (natural area #9 of the province of Cordoba; 33°32'11.4"S, 65°00'01.3"W) (figure 2A). The topography of the area is undulating or gently
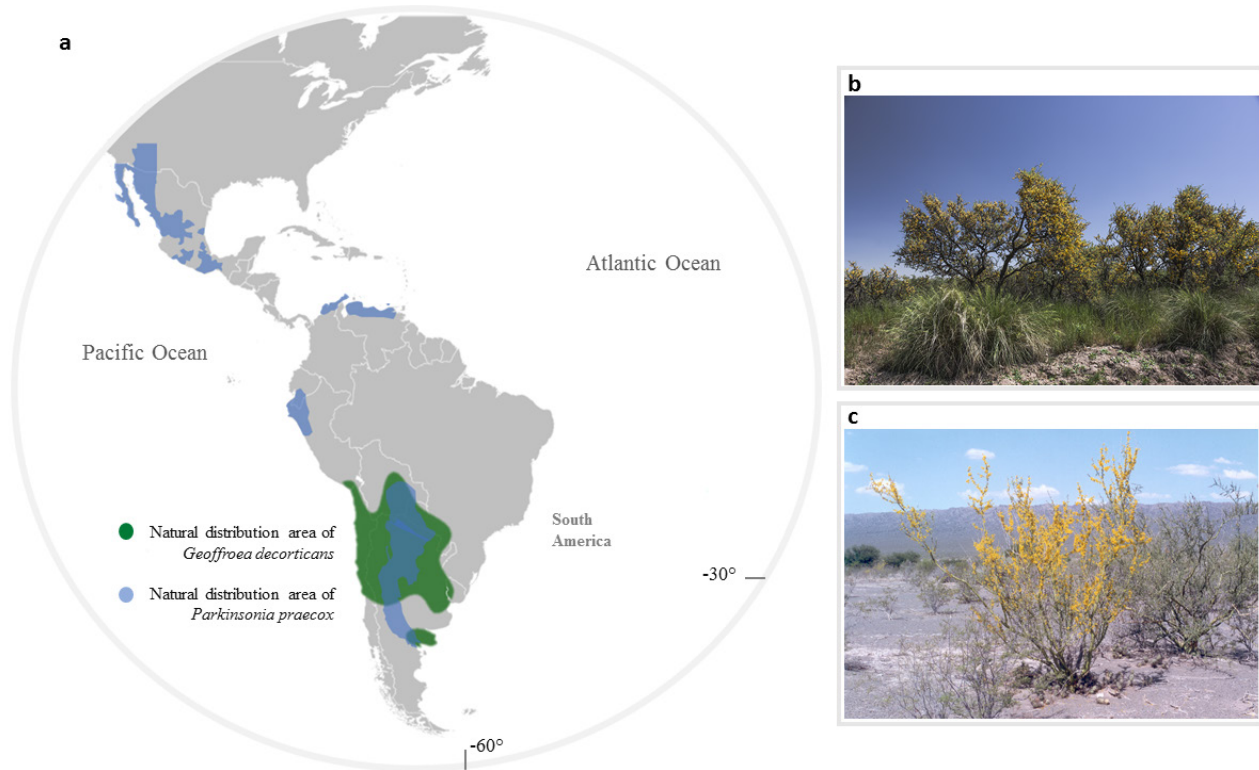
**Figure 1.** Distribution area of chañar (*Geoffroea decorticans*) and brea (*Parkinsonia praecox*) (A). Photographs of chañar (B) and brea (C).

Área de distribución de chañar (*Geoffroea decorticans*) y de brea (*Parkinsonia praecox*) (a). Fotografías de chañar (b) y brea (c).



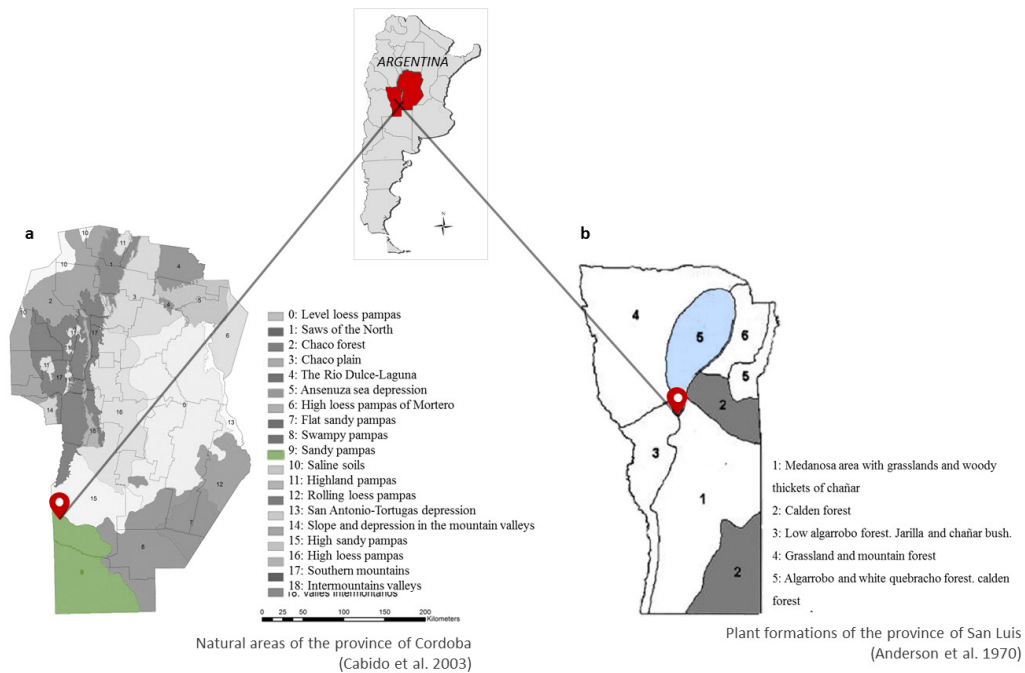**Figure 2.** Sampling sites for chañar (*Geoffroea decorticans*) (A) and brea (*Parkinsonia praecox*) (B) according to the phytogeographic distribution in the center of Argentina.

Sitios de muestreo de chañar (*Geoffroea decorticans*) (a) y de brea (*Parkinsonia praecox*) (b) de acuerdo con la distribución fitogeográfica correspondiente para el centro de Argentina.

143

undulating due to the presence of dunes of different ages. The predominant soils are Entisols (with the dominance of the typical Ustipsaments). Soils are sandy, shallow, with little differentiation of horizons, excessively drained, without aggregation and with low content of organic matter (Cabido *et al*. 2003). Climate is temperate (Köppen 1931) with a wide range of thermal oscillation (absolute maximums of 44 ºC and minimums of –11 ºC). Annual rainfall reaches 600 mm and is mainly distributed between October and March (Cabido *et al*. 2003). Altitude is of approximately 500 m a.s.l. This region is part of Espinal Phytogeographic Province (Cabrera 1976). Probably, in the past, vegetation was calden (*Prosopis caldenia* Burkart) forests and grasslands. However, the interpretation of the predominant landscape until the settlement of the Spanish conquerors in the 16th century is difficult due to practically non-existent written testimonies. Nowadays, the area is affected by wind erosion due to land use changes and agricultural activities. In this context of disturbance, *G. decorticans* colonizes the ridges of dunes formed by wind erosion.

The *Parkinsonia praecox* sampling site was located in the southern extreme part of arid Chaco within the area of grasslands and mountain forests (plant formation #5 of the province of San Luis (33º28'43.81"S, 66º26'16.63"W) (Anderson *et al*. 1970) (figure 2B). The area presents a physiography of arid foothills. Entisols are the predominant soils with low content of organic matter and high susceptibility to wind and water erosion (Peña Zubiate *et al*. 1998). Annual rainfall is between 400 and 500 mm and it is characterized by strong seasonal, annual and multi-year variability (Karlin *et al*. 2013). Average annual temperature is 17.8 ºC and the average temperature of the warmest (January) and coldest (July) months is 25 and 9 ºC, respectively. Altitude varies between 450 and 500 m asl. Vegetation is characterized as a disetaneous secondary forest mostly dominated by *Aspidosperma quebracho blanco* Griseb. and *Prosopis* species (15-18 m high) accompanied by a shrubby layer (Anderson *et al*. 1970).

For anatomical studies, stem cross sections were cut with a chainsaw at 20 cm high from three individuals of each species. Light microscopic sections of 15µm thickness were obtained from transversal sections using a sliding microtome Leica, Hn 40 Model. Afterwards, the samples were whitened with sodium hypochlorite and dehydrated with xylol. Finally, they were colored using Safranin (1%), fast green and 80° alcohol and sealed using Entellán (D'Ambrogio de Argüeso 1986). For wood description, the terminology of the List for the identification of hardwoods was used (IAWA Committee 1989).

For dendrochronological studies, cross sections at the tree base were taken using a chainsaw. In July 2016, 14 dominant individuals of *G. decorticans* (10 alive and 4 dead) and in January 2011, 15 living dominant trees of *P. praecox* were sampled. The basal cross-sections were polished using sandpaper with increasingly fine grain size to try to visualize tree rings (40-600 sieves in$^{-2}$). The rings were visualized

and demarcated with the help of an Olympus SZ61 magnifying glass (0.9 to 4X). Two different radii per cross section were determined. For the correct assignment of the calendar year to each ring, the convention of Schulman (1956) for the southern hemisphere was applied. The rings were measured with a Unislide TA 4020H1-S6 Velmex equipment (0.01 mm precision). The validity of the dating was verified with the COFECHA program that compared the variability of the width of the rings to correctly establish the calendar year of each ring and to determine false or missing rings (Grissino-Mayer 2001, Fritts 2001). Mean correlation between series and mean sensitivity (growth variability between two consecutive years) were determined. The age of trees must be determined with an annual or absolute level of precision, which is essential for any dendrochronological study, since the correct and precise estimation of the calendar year in which each growth ring was formed is a fundamental condition for dating (Speer 2010). Furthermore, the date of establishment of each individual can be stated.

After obtaining the chronologies of the ring-width index of both species, the series were standardized to maximize high frequency variability possibly associated with climate. The standardization applied was first of all a negative exponential and, after, a 40-year spline that generated three chronologies of average indices for each species (row, standardized and residual). The residual chronology of each species was compared with the climatic variables. To establish the validity of chronologies, three indicators were used: signal-to-noise ratio (SNR), Expressed Signal of the Population (EPS) and variance of the first vector. The climatic data used were: monthly precipitation and monthly mean temperature of INTA Villa Mercedes (33°39'07.3"S, 65°25'11.2"W) and San Luis (33°15'36.0"S, 66°14'24.0"W) meteorological stations. Monthly SOI (Southern oscillation index) were obtained from the Climatic Research Unit of the University of East Anglia. SOI is a standardized index of water sea level pressure oscillation between Tahiti and Darwin (Australia) that determines El Niño and La Niña events (Ropelewski and Jones 1987). The DENDROCLIM 2002 program (Biondi and Waikul 2004) was applied to analyze the relationship between climatic variables and ring width indices. Statistical analyses in both species were performed with the Infostat version 12 package (Di Rienzo *et al*. 2012).

## RESULTS

*Anatomical analysis. Geoffroea decorticans* has a semicircular porosity. The vessels are circular or oval, solitary, multiple short vessels (2-3) and occasionally have multiple long radials (4-5 vessels). In latewood, the few vessels are grouped in clusters, sometimes in ulmoid to semi-ulmoid positions and parallel to the rays. Many pores are occluded by tylosis and xylochromatic substances. The parenchyma is confluent. Normally, at the limit of each growth ring there is a band of 2-5 cells of terminal parenchyma that

allows the delimitation of the border (figure 3A). The radii are linear. *Parkinsonia praecox* has semicircular porosity, solitary or multiple short vessels (2-6) where some of them are grouped. Vessels are circular or oval with linear rays and irregularly distributed. The axial parenchyma is confluent or paratracheal (figure 3B).

*Dendrochronological analysis.* The dating of *Geoffroea decorticans* and *Parkinsonia praecox* was possible (figure 4A and 4B) and consequently the first chronologies for both species were constructed since the sampled indivi-

duals could be correctly dated. The establishment date was estimated for the four dead specimens of G. decorticans, which died by both natural and anthropic causes. On the other hand, it was possible to co-date the time series of both species to obtain a master chronology. The statistics that characterize both chronologies are adequate to continue with a dendroclimatic study (table 1).

The mean radial growth of the 14 individuals of *G. decorticans* was 3.37 mm (SD ± 0.71 mm) and the extreme values ranged between 1.99 mm and 5.57 mm year^{-1} for trees between 16 and 29 years old (figure 5A and 5B). The
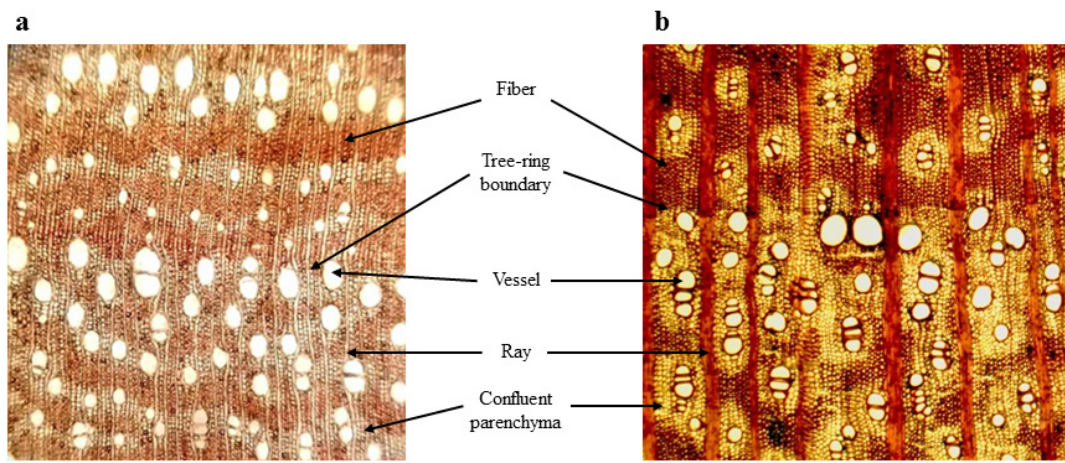


**Figure 3**. Wood anatomy of chañar (*Geoffroea decorticans*) (A) and brea (*Parkinsonia praecox*) (B) in transversal sections. Magnifying glass (4X).

Anatomía de la madera de chañar (*Geoffroea decorticans*) (a) y de brea (*Parkinsonia praecox*) (b) donde se visualizan elementos que conforman el leño y los distintos anillos de crecimiento (Zoom 4X).
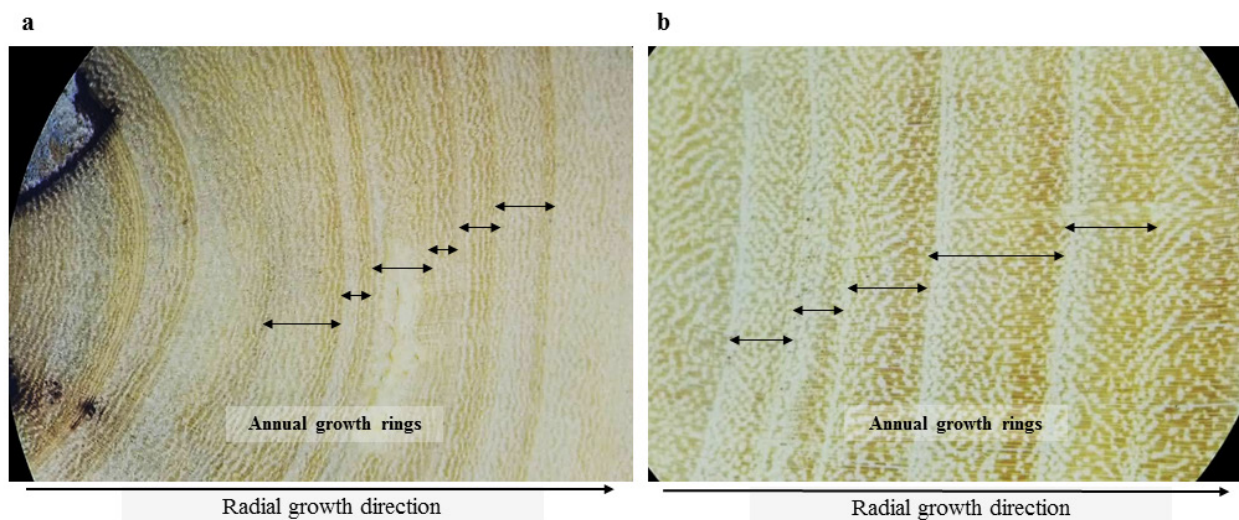


**Figure 4.** Demarcation of chañar (*Geoffroea decorticans*) (A) and brea's (*Parkinsonia praecox*) (B) growth rings for dating using Olympus SZ61 magnifying glass (0.9 to 4X).

Demarcación de los anillos de crecimiento de chañar (*Geoffroea decorticans*) (a) y de brea (*Parkinsonia praecox*) (b) para datación mediante lupa Olympus SZ61 (0,9 a 4X).

145

**Table 1**. Statistical values that characterize the chronologies of chañar (*Geoffroea decorticans*) and brea (*Parkinsonia praecox*).

Valores estadísticos para las cronologías de ancho de anillo de chañar (*Geoffroea decorticans*) y de brea (*Parkinsonia praecox*).

| | *Geoffroea decorticans* | *Parkinsonia praecox* |
|---|---|---|
| Number of trees | 14 | 15 |
| Number of series | 27 | 30 |
| Master series | 1987-2015 | 1971-2009 |
| Mean annual radial growth (mm) | 3.37 (SD±0.71) | 2.16 (SD±0.61) |
| Mean sensitivity | 0.32 | 0.4 |
| Correlation between series | 0.52 | 0.38 |
| SNR (residual) | 2.03 | 7.87 |
| EPS | 0.67 | 0.88 |
| Variance of the first vector (%) | 31.34 | 42.28 |

Mean sensitivity: tree-ring width variability between two subsequent years, SNR: signal to noise radio, EPS: Expressed population signal.
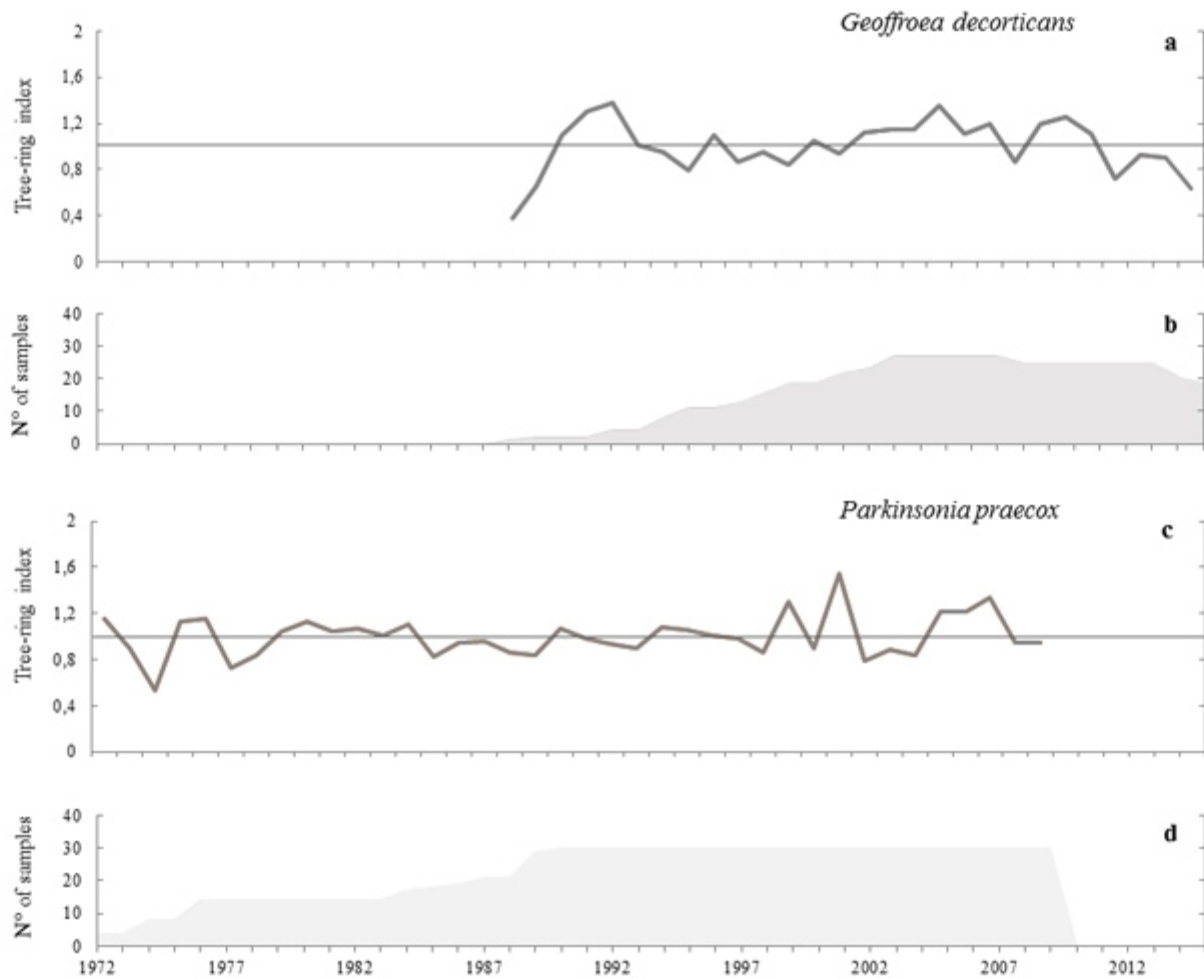


**Figure 5.** Standardized chronologies of chañar (*Geoffroea decorticans*) and brea (*Parkinsonia praecox*) for arid and semi-arid environments of Argentina. Indexed growth rate for each species over time (A and C) and number of samples used in each chronology (B and D).

Cronologías estandarizadas de chañar (*Geoffroea decorticans*) y de (*Parkinsonia praecox*) para ambientes áridos y semiáridos de Argentina. Índice de crecimiento para cada especie a lo largo del tiempo (a y c) y número de muestras utilizadas en cada cronología (b y d).

mean radial growth of the 15 individuals of *P. praecox* was 2.16 mm (SD ± 0.61 mm) and the extreme values ranged between 1.15 and 3.07 mm year[1] for trees between 23 and 39 years old (figure 5C and 5D).

*Dendroclimatic analysis.* The analysis of the relationship between the residual chronology of tree-ring widths and the climatic variables determined that: *G. decorticans* had an inverse and significant relationship with the temperatures of May (autumn) and July (winter) prior to the growing season, and with May at the end of the growing season

(figure 6). *P. praecox* showed an inversely significant relationship with temperature throughout the growing season. In relation to rainfall, *G. decorticans* showed an inverse association in summer (December) and *P. praecox* an inverse association previous to the growing season (May and July) and a positive association in summer (January). Unlike *G. decorticans, P. praecox* had an inverse relationship with global weather patterns such as SOI during May prior to the growing season and at the end of it (from May to September) (figure 6).
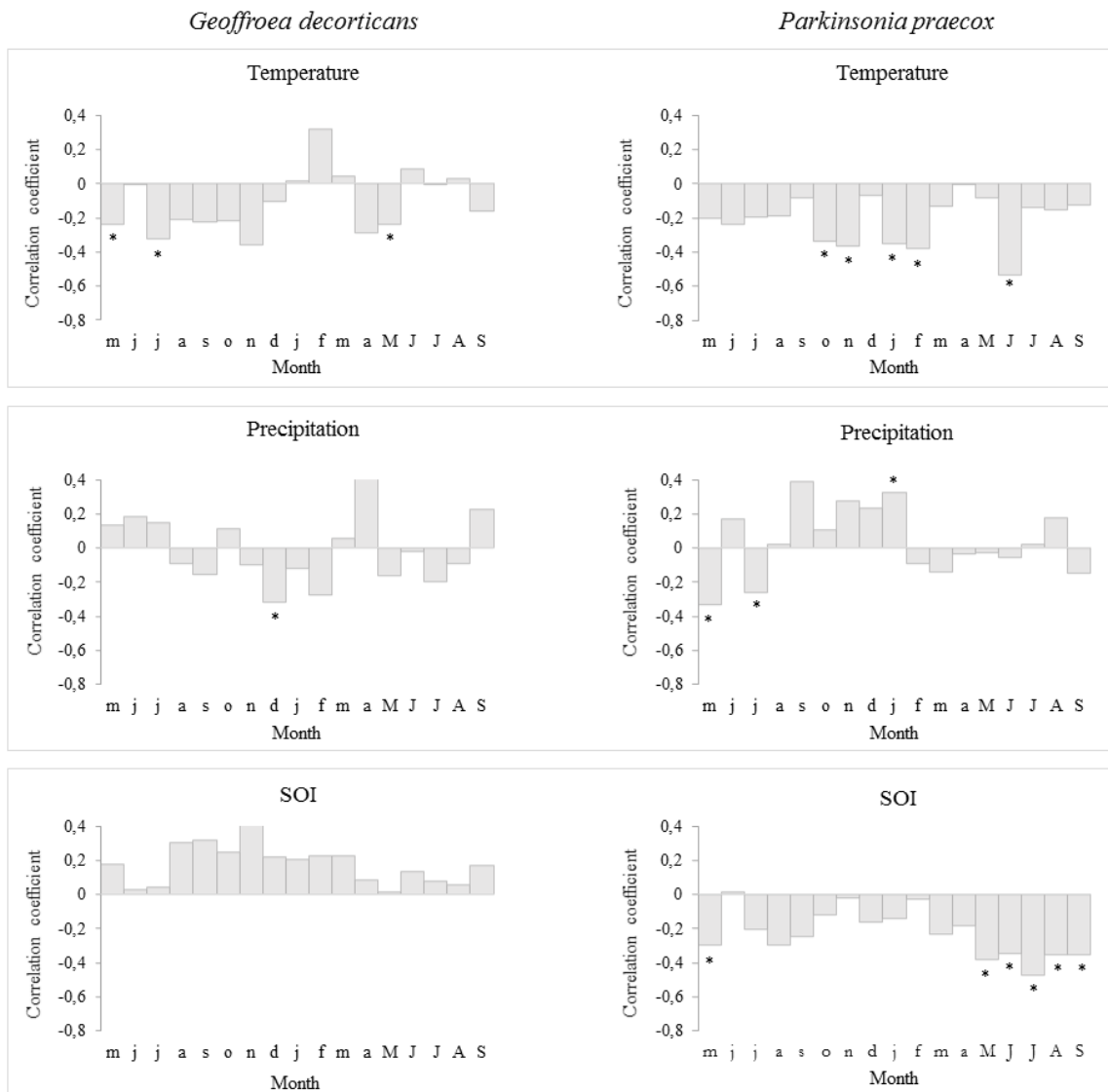


**Figure 6.** Pearson's correlation coefficients (bars) that indicate the effect of local and global climatic variables chañar (*Geoffroea decorticans*) and brea's (*Parkinsonia praecox*) growth at both sites during the 1972-2015 period. The analyzed period covered from May before growth to September of the current growing year (\*P < 0.05).

Coeficientes de correlación de Pearson (barras) entre las cronologías residuales de chañar (*Geoffroea decorticans*) y de brea (*Parkinsonia praecox*) y las variables climáticas locales (temperatura media mensual y precipitación mensual) y globales (Índice de Oscilación del Sur) para ambos sitios durante el período 1972-2015. El período analizado va desde el mes de mayo del año previo al crecimiento y se extiende hasta septiembre donde finaliza el período anual de crecimiento (\* = P < 0,05 R).

## DISCUSSION

Anatomical observations, mainly the presence of terminal parenchyma, made it possible to establish the feasibility of dating both species. The results obtained through the analysis of the growth rings of *Geoffroea decorticans* and *Parkinsonia praecox* allowed the reconstruction of the first chronology for both species in Argentina. The dendrochronological potential of both species was proven and supported by the statistics that characterize both chronologies in spite of contradictions regarding the possibility of dating *G. decorticans* (Tortorelli 1956, Giménez *et al.* 2013). Both species showed a significant correlation between series, 0.49 and 0.39, respectively, which may imply a strong association between growth and environment, possibly connected to climatic conditions.

The mean radial growth of *G. decorticans* (3.95 mm year$^{-1}$) is similar to that of *Prosopis caldenia* (2.69 - 5.12 mm year$^{-1}$) growing in the same area (Bogino and Villalba 2008) or in the province of La Pampa (2.2 - 4.52 mm year$^{-1}$) (Bogino *et al.* 2015, Velasco *et al.* 2018). These results pointed out that woody species have similar growing rates even though they are dominant (*P. caldenia*), or codominant or intermediate (*G. decorticans*) species. Furthermore, their growth rates are similar to the records of *Pinus elliottii* Engelm, an exotic species widely recommended for forestry purposes (Bogino *et al.* 2005), which is considered a worldwide invader nowadays. These annualized growth rates are highly valuable for further quantification of biomass and the estimation of the carbon fixing capacity of these systems.

The association between residual tree ring chronologies and climate showed, for both species, a significant inverse relationship with temperature. This variable controls other species growth in these environments such as *P. caldenia* (Bogino and Jobbágy 2011). Results clearly demonstrate that in a context of increased average temperature, both species would have growth limitations, which reinforces the idea of the vulnerability of arid and semi-arid systems to global warming (Pachauri *et al.* 2014). Concerning chañar, rainfall has a negative impact on summer growth. Considering that this species forms thickened groups of individuals favored by asexual reproduction and that all of them belong to the same tree, a more humid environment in summer may favor the growth of the younger individuals and limit it, in the case of the dominant trees sampled in this research. Regarding brea, rainfall previous to the growing season limited growth, showing a positive effect in summer (January). Further physiological studies are needed to understand why this humidity previous to the growing season can limit growth. Both species are vulnerable to local climatic factors (temperature and rainfall) although brea is also vulnerable to global forces (SOI), which is among the most important climatic variables regulating the planet's climate, meaning that the higher the SOI values, the lesser the growth rate. Since *P. praecox* was also vulnerable to SOI in the Guajira (Colombia), present results may contribute to consider a similar pattern of growth response of *P. praecox* to global drivers (Ramírez and Del Valle 2011).

Asexual reproduction by gemipherous roots is the most common way for the establishment of *G. decorticans*. Chañar forms thickened groups of trees known as small islands (islets), which makes it almost a unique species regarding this dynamic. These trees with the same genetic background growing together may be a factor that determines its limited response to climate in comparison with brea. In some cases, it is considered a native species expanding within the encroachment process (Rauber *et al* 2020), which may be the result of its climatic independence.

We concluded that starting from a general objective that proposes to reconstruct the temporal growth dynamics from the growth rings of *G. decorticans* and *P. praecox* and their association with climate, the construction of the first chronology of ring width was feasible for both species as well as the quantification of the annual growth rate. Dating both species was possible despite previous references questioning the feasibility of this process for *G. decorticans*. When interpreting the population and growth dynamics of both species based on environmental variables, a difference was found in this relationship according to the species. *G. decorticans* showed a connection with regional variables (temperature) while *P. praecox* is related to regional variables (temperature and rainfall) and global (SOI) ones. On the other hand, results reveal the capacity of pioneer species for carbon fixation and the adaptive climate response they possess with respect to main components of the forest (*P. caldenia*) and exotic components (*Pinus elliottii* Engelm.). These results also highlight the importance of an individual analysis of each of the components of forest systems since it is possible to assume a different environmental response in this context of global change. Therefore, the analysis of the system as a whole is relevant, emphasizing the impact of each intervening variables.

## ACKNOWLEDGMENT

## REFERENCES

Anderson DL, JA Del Águila, AE Bernardón. 1970. Las formaciones vegetales en la provincia de San Luis. *Revista de Investigaciones Agropecuarias, INTA* 7(3): 153-158.

Anderson D. 1976. Invasión del chañar (*Geoffroea decorticans*) en los pastizales de la Pcia de San Luis. *RIA* (7): 153-172.

Bar-On YM, R Phillips, R Milo. 2018. The biomass distribution on Earth. *Proceedings of the National Academy of Sciences* 115(25): 6506-6511. doi: 10.1073/pnas.1711842115.

Biondi F, K Waikul. 2004. Dendroclim 2002: a C ++ program for statistical calibration of climate signals in tree-ring chronologies. *Comp Geoscience* 30: 303–311. DOI: 10.1016/j. cageo.2003.11.004.

Bogino S, R Villalba. 2008. Radial growth and biological rotation age of *Prosopis caldenia* Burkart in Central Argentina. *Journal of Arid Environments* 72: 16-23. doi: 10.1016/j. jaridenv.2007.04.008.

Bogino S, E Jobbágy. 2011. Climate and groundwater effects on the establishment, growth and death of *Prosopis caldenia* trees in the pampas (Argentina). *Forest Ecology and Management* 262: 1766-1774. doi: 10.1016/j.foreco.2011.07.032.

Bogino S, M Gómez, A Avila, Z Furlán, S Escudero, A Corral, R Luna, R, J Martín García. 2005. Crecimiento de *Pinus elliottii* Engelm en el área serrana de la provincia de San Luis, Argentina. *Revista Yvyraretá* 13: 31-35.

Bogino S, C Roa Giménez, AT Velasco Sastre, ML Cangiano, L Risio, V Rozas. 2015. Synergistic effects of fire, grazing, climate, and management history on *Prosopis caldenia* recruitment in the Argentinean pampas. *Journal of Arid Environments* 117: 59-66. doi: 10.1016/j.jaridenv.2015.02.014.

Cabido D, MR Cabido, SM Garré, JA Gorgas, RA Miatello, AC Ravelo, L Argüello. 2003. Regiones naturales de la provincia de Córdoba. Córdoba, Argentina. Agencia Córdoba DACyT. 103p.

Cabrera AL.1976. Regiones fitogeográficas argentinas. Buenos Aires, Argentina. ACME. 85p.

Climatic research Unit, University of East Anglia. Accessed June 26, 2017. Available at https://crudata.uea.ac.uk/cru/data/soi/.

D'Ambrogio de Argüeso. 1986. Manual de Técnicas en Histología Vegetal. Buenos Aires, Argentina. Hemisferio Sur. 83p.

Di Rienzo J, M Balzarini, F Casanoves, L González, E Tablada, C Robledo. 2012. Infostat Software Estadístico versión 12. (on-line statistical software). Grupo infoStat, FCA, Universidad Nacional de Córdoba, Argentina. Last access 18 February 2020. Available at https://www.infostat.com.ar.

Dussart E G, C C Chirino, E Morici, R Peinetti. 2011. Reconstrucción del paisaje del caldenal pampeano en los últimos 250 años. *Quebracho* 19(1-2): 54-65.

Fritts HC. 2001. Tree rings and climate. Caldwell, USA. Blackburn Press. 567 p.

Giménez AM, JG Moglia. 2003. Árboles del Chaco Argentino. Guía para el reconocimiento dendrológico. Ed. Secretaria de Ambiente y Desarrollo Sustentable. Ministerio de Desarrollo Social Facultad de Ciencias Forestales. Santiago del Estero, Argentina. Universidad Nacional de Santiago del Estero. 307 p.

Giménez AM 2009. Anatomía de madera, corteza y anillos de crecimiento de *Geoffroea decorticans* (Gill., Ex Hook. *et* Arn.) Burk. *Quebracho* 17(1,2): 16-30.

Giménez AM, P Hernández, N Ríos, F Calatayu. 2013. Crecimiento de árboles individuales de *Geoffroea decorticans*, en un bosque del Chaco semiárido, Argentina. *Madera y Bosques* 19(1): 37-51.

Gorzelak MA, AK Asay, BJ Pickles, SW Simard. 2015. Interplant communication through mycorrhizal networks mediates complex adaptive behaviour in plant communities. *AoB Plants* 7. doi: 10.1093/aobpla/plv050.

Grissino-Mayer HD. 2001. Evaluating crossdating accuracy: a manual and tutorial for the computer program COFECHA. *Tree-Ring Research* 57: 205-221.

Iawa Committee. 1989. IAWA list of microscopic features for hardwood identification. *IAWA Bulletin* 10(3): 219-332.

Karlin MS, UO Karlin, RO Coirini, GJ Reati, RM Zapata. 2013. El Chaco Árido. Córdoba, Argentina. Universidad Nacional de Córdoba. 420 p.

Köppen W. 1931. Grundriss der klimakunde. Berlin, Deutschland. De Gruyter. 388p.

Martínez Carretero E. 1986. Ecología, Fitogeografía y Variación Intraespecífica de *Cercidium praecox* (Ruiz *et* Pavon) Harms. (Leguminosae) en Argentina. *Documents Phytosociologiques* 10(2): 319-329.

Medina A, E Dussart , D Estelrich, E Morici. 2000. Reconstrucción de la historia del fuego en un bosque de Prosopis caldenia (Burk.) de Arizona, sur de la provincia de San Luis. *Multequina* 9: 91-98.

Morales MS, R Villalba, JA Boninsegna. 2005. Climate, land-use and Prosopis ferox recruitment in the Quebrada de Humahuaca, Jujuy, Argentina. *Dendrochronologia* 22: 169–174. doi: 10.1016/j.dendro.2005.05.004.

Oliver CD, BC Larson. 1996. Forest Stand Dynamics (update edition). New York, USA. John Wiley. 544 p.

Oyarzabal M, JR Clavijo, LJ Oakley, F Biganzoli, PM Tognetti, IM Barberis, M Oesterheld. 2018. Unidades de vegetación de la Argentina. *Ecología Austral* 28: 40-63.

Pachauri RK, MR Allen, VR Barros, J Broome, W Cramer, R Christ, NK Dubash. 2014. Climate change 2014: synthesis report. Contribution of Working Groups I, II and III to the fifth assessment report of the Intergovernmental Panel on Climate Change (IPCC).151p.

Paez SA, DE Marco. 2000. Seedling habitat structure in dry Chaco forest (Argentina). *Journal of Arid Environment* 46: 57-68.

Peña Zubiate CA, DL Anderson, MA Demmi, JL Sáenz, A D'Hiriart. 1998. Carta de suelos y vegetación de la provincia de San Luis. San Luis, Argentina. Payne Publishing. 115p.

Ramírez J, I Del Valle. 2011. Local and global climate signals from tree rings of *Parkinsonia praecox* in La Guajira, Colombia. *International Journal of Climatology* 32: 1077-1088. doi: 10.1002/joc.2335.

Rauber RB, MR Demaría, D Arroyo, PA Cipriotti. 2020. Characterization of the herbaceous layer in woody thickets of Geoffroea decorticans in central Pampean grasslands. *Phytocoenologia*: 297-311. doi: 10.1127/phyto/2020/0357.

Ropelewski CF, PD Jones. 1987. An extension of the Tahiti–Darwin southern oscillation index. *Monthly Weather Review* 115(9): 2161-2165.

Schuch UK, JJ Kelly. 2008. Palo verde trees for the urban landscape. *Aridus* 20: 1-8.

Schulman E. 1956. Dendroclimatic changes in semiarid America. Arizona, EUA. University of Arizona Press. 142p.

Speer J. 2010. Fundamentals of tree-ring research. Tucson, USA. The University of Arizona Press. 333 p.

Tortorelli LA. 1956. Maderas y bosques argentinos. Buenos Aires, Argentina. ACME. 910p.

Velasco Sastre T, M Vergarechea, A Tapia, E Dussart, J Leporati, S Bogino. 2018. Growth dynamics and disturbances along the last four centuries in the *Prosopis caldenia* woodlands of the Argentinean pampas. *Dendrochronologia* 47: 58-66. doi: 10.1016/j.dendro.2017.12.005.

Villagra PE, JA Boninsegna, JA Alvarez, M Cony, E Cesca, R Villalba. 2005. Dendroecology of *Prosopis flexuosa* woodlands in the Monte desert: Implications for their management. *Dendrochronologia* 22: 209-213. doi: 10.1016/j.dendro.2005.05.005.

# Instrucciones para los autores de la revista Bosque, proceso de publicación y políticas para los árbitros

## Instrucciones para los autores

Bosque es una revista científica que publica trabajos originales relacionados con el manejo y producción de recursos forestales, ciencias y tecnología de la madera, silvicultura, ecología forestal, conservación de recursos naturales y desarrollo rural asociados con los ecosistemas forestales. Las fechas de publicación son en abril, agosto y diciembre de cada año. Las contribuciones podrán ser en las modalidades de artículos, revisiones, notas u opiniones, en castellano o inglés.

- *Artículos.* Informan acerca de investigaciones inéditas de carácter científico que proyectan el conocimiento actualizado en un campo particular contemplado en los ámbitos de la revista y están sustentados en datos procedimentales propios o generados a partir de otros estudios publicados. La extensión máxima de los manuscritos será de 8.000 palabras, considerando todo su contenido (incluye todos los archivos del manuscrito con sus contenidos completos).
- *Revisiones.* Síntesis y discusión de la información científica más actual con respecto a un tema relevante en el ámbito de la revista. La extensión máxima de los manuscritos será de 8.000 palabras, considerando todo su contenido.
- *Opiniones.* Analizan, desde un punto de vista personal o con apoyo bibliográfico, un tema de actualidad relacionado con el carácter de la revista. La extensión máxima de los manuscritos será de 3.000 palabras, considerando todo su contenido.
- *Notas.* Describen metodologías o técnicas nuevas en el ámbito de la revista, o bien informan acerca de investigaciones en desarrollo, con resultados preliminares. La extensión máxima de los manuscritos será de 3.000 palabras, considerando todo su contenido.

*Estructura de los manuscritos*

La organización de artículos y notas debe seguir la siguiente estructura:

- *Título.* El título debe ser preciso y conciso. Elegir con mucho cuidado todas las palabras del título; su asociación con otras palabras debería ser cuidadosamente revisada. Debido al acceso internacional de la revista, se recomienda incluir en el título información relevante sobre la localización geográfica del estudio cuando corresponda.

- *Autores.* Indicar el nombre y apellido de todos los autores con letras minúsculas, con las letras iniciales en mayúscula. Separar los autores con coma. Ordene cada dirección mencionando los datos necesarios, primero la institución matriz (por ejemplo, la universidad) y luego las dependencias dentro de aquella en orden decreciente (por ejemplo, facultad, departamento, laboratorio); a continuación indique la ciudad y el país de residencia del autor. Aplique el formato del siguiente ejemplo:

Nombre1 Apellido1 [a], Nombre2 Apellido2 [b]*, Nombre3 Apellido3 [a,b]

[a] Universidad Uuu, Facultad Ffff, Departamento de Dddd, Ciudad, País.

*Autor de correspondencia: [b] Instituto de Iiiii, Departamento de Dddddd, Nombre de calle y número, Ciudad, País, tel.: 56-63-2221056, correo@electronico.cl

- *Resumen.* Debe contener el planteamiento del problema, el objetivo, fundamentos metodológicos, resultados y conclusiones más relevantes, con un máximo de 250 palabras. Evite descripciones largas de métodos y no incluya citas bibliográficas ni los niveles de significancia estadística.
- *Palabras clave.* Como máximo cinco palabras (puede incluir una o dos frases breves de un máximo de tres palabras) que identifiquen claramente el tema del trabajo. Se sugiere usar nuevas palabras no incluidas en el título del manuscrito.
- *Introducción.* Comprende planteamiento del problema, importancia del tema, hipótesis si compete, objetivos, alcances del trabajo y limitaciones para su desarrollo, si es que las hubo. En este capítulo se realizará una síntesis e interpretación de la literatura relacionada directamente con el título y objetivos del trabajo.
- *Métodos.* Proveerá información suficiente y concisa de manera que el problema o experimento pueda ser reproducido o fácilmente entendido por especialistas en la materia. Deberán señalarse claramente las especificaciones técnicas y procedencia de los materiales usados, sin describir materiales triviales. Los organismos bióticos deberán ser convenientemente identificados de acuerdo con las normas internacionales que correspondan. En los métodos empleados se deberá señalar claramente el procedimiento experimental o de captación de datos y los métodos estadísticos, así

como los programas computacionales. Si el método no fuese original, se indicará bibliográficamente; si fuera original o modificado se describirá convenientemente. En cualquier caso, la presentación de varios métodos será cronológica.

- *Resultados*. Incluye la presentación sintética, ordenada y elaborada de la información obtenida. Entrega resultados en forma de texto escrito con apoyo de cuadros y figuras, si corresponde, conjuntamente con análisis e interpretación de los datos. Se deberá evitar tanto la repetición de detalles dados en otros capítulos como la descripción de aquello que sea evidente al examinar los cuadros o figuras que se presenten.

- *Discusión*. Incluye la interpretación integrada de los resultados y, cuando corresponda, la comparación de ellos con los de publicaciones previas. Es un análisis crítico de los resultados de acuerdo con los objetivos y la hipótesis, si fuera el caso. Debe comentarse el significado y la validez de los resultados, de acuerdo con los alcances definidos para el trabajo y los métodos aplicados. En este capítulo no deberán repetirse los resultados obtenidos.

- *Conclusiones*. Podrán ser incluidas en un capítulo único de conclusiones o bien integradas en la discusión. En caso de presentarlas como un capítulo, se incluirán allí en forma precisa y concisa aquellas ideas más relevantes que se deriven directamente de lo aportado por el trabajo. Deben dar respuesta a las hipótesis o a los objetivos planteados en la introducción. Deben redactarse en forma clara y objetiva sin incluir citas bibliográficas. Pueden incluir recomendaciones para trabajos futuros.

- *Agradecimientos*. En este acápite se deberán mencionar brevemente a personas e instituciones que contribuyeron con financiamiento u otro tipo de colaboración para la realización del trabajo.

- *Referencias*. Se indicarán las referencias de todas las citas bibliográficas señaladas en el texto, ordenadas alfabéticamente. La precisión y la veracidad de los datos entregados en las referencias bibliográficas son responsabilidad del o los autores de las contribuciones y deben corresponder a publicaciones originales. El número máximo de referencias será de 25 para artículos, notas y opiniones, y de 40 para revisiones. Utilice literatura moderna, relevante y directamente relacionada con su trabajo. Por lo menos 2/3 de las referencias deberán corresponder a revistas científicas de corriente principal.

Para las modalidades de revisión y opinión no se exige seguir la estructura indicada anteriormente. En todo caso, deben contener las secciones de título, autores, resumen, palabras clave, introducción, el desarrollo del trabajo adecuadamente dividido en capítulos, agradecimientos y referencias.

*Estilo y formato*

En general, el resumen, métodos y resultados del manuscrito deberán estar redactados en tiempo pasado, y la introducción, discusión y conclusiones en tiempo presente. Use tiempo presente cuando se refiera a resultados publicados previamente, esto ayuda a diferenciar entre los hallazgos de su estudio (tiempo pasado) y los hallazgos de otros estudios. En el texto no utilice acrónimos ni abreviaturas, escriba el nombre completo de las cosas; las excepciones que se pueden utilizar son aquellas de dominio global como, por ejemplo, ADN, pH, $CO_2$ y muy pocas otras. Tampoco utilice en el texto los símbolos de los elementos químicos. Acate las reglas gramaticales en todo el manuscrito, incluidos cuadros y figuras.

El trabajo debe estar escrito en hojas tamaño carta (279 x 216 mm), con márgenes de 2 cm por lado, interlineado a espacio y medio, letra Times New Roman, tamaño 12 puntos, con numeración de página en el extremo inferior derecho y número de línea correlativo para todo el trabajo, a la izquierda. Separar los párrafos a renglón seguido y con sangría de ocho caracteres a la izquierda de la primera línea. Debe presentarse en archivos electrónicos con procesador de texto Word o formato RTF.

El título principal se escribirá con letras minúsculas y negritas, centrado. En él deberá omitirse la mención de los autores de nombres científicos, los que, sin embargo, se presentarán la primera vez que se mencionen en el texto a partir de la introducción. En el encabezado superior derecho de cada página debe incluirse un título abreviado con un máximo de 60 caracteres y espacios.

Las ecuaciones se numerarán en el margen derecho con paréntesis cuadrados "[ ]"; en el texto se mencionarán de acuerdo con esta numeración.

Las unidades de medidas deberán circunscribirse al Sistema Internacional de unidades (SI). En la notación numérica, los decimales deberán ser separados por coma (,) y las unidades de miles por punto (.). En los textos en inglés, los decimales separados por punto y las unidades de miles por coma. Usar cero al comienzo de números menores a una unidad, incluyendo valores de probabilidad (por ejemplo, $P < 0,001$).

La descripción de los resultados de cada prueba estadística en el texto debe incluir el valor exacto de probabilidad asociado $P$. Para valores de $P$ menores que 0,001, indique como $P < 0,001$. En cuadros y figuras usar asteriscos para señalar el nivel de significancia de las pruebas estadísticas: $* = P < 0,05$; $** = P < 0,01$; $*** = P < 0,001$; ns = no significativo.

Debe indicarse el nombre científico de todos los organismos biológicos que aparezcan en el texto, de acuerdo con la nomenclatura internacional respectiva. Si un nombre común es usado para una especie, la primera vez que cite en el texto, a partir de la introducción, se debe dar a continuación su nombre científico en cursiva entre paréntesis, por ejemplo, coihue (*Nothofagus dombeyi* (Mirb.)

Oerst.). Citas posteriores pueden aparecer con el nombre del género abreviado seguido del adjetivo del nombre científico (por ejemplo, *N. dombeyi*), siempre y cuando no produzca confusiones con otras especies citadas en el manuscrito. Al iniciar una oración con el nombre de una especie, escriba su género completo y no lo abrevie con su inicial. En el resumen y en el título no mencione los autores de nombres científicos.

En los cuadros se deben incluir los datos alfanuméricos ordenados en filas y columnas, escritos con fuente Times New Roman de 12 puntos (mínimo 9 puntos de tamaño), sin negritas. Sólo los encabezamientos de las columnas y los títulos generales se separan con líneas horizontales; las columnas de datos deben separarse por espacios y no por líneas verticales. En las figuras se incluyen otras formas de presentación de datos o información, como gráficos, dibujos, fotografías y mapas. En cuadros y figuras se deben incluir los títulos auto explicativos en castellano e inglés numerados en forma consecutiva (cuadro 1., cuadro 2., …; figura 1., figura 2., …). Las figuras llevan el título en el margen inferior y los cuadros en el margen superior. Los cuadros y figuras deben tener una resolución tal que permitan ser reducidos sin perder legibilidad. Sólo se trabaja en blanco, negro y tonos de grises. Sin embargo, podrán usarse colores en las figuras si ello es imprescindible para su comprensión. La inclusión de figuras con colores deberá acordarse previamente con el editor. El espacio que ocupen cuadros y figuras en el trabajo deberá ser menor al 50 % del total del impreso. Incluya en el archivo de texto principal los cuadros con sus respectivos títulos, ubicándolos lo más próximo posible después de haberlos citado por primera vez en el texto. Los cuadros deben estar en el formato de tablas (editables, no como imágenes). Las figuras deben ser entregadas en un archivo aparte, con un formato editable; su ubicación en el texto principal debe ser informada, incluyendo su título, al igual que los cuadros.

En las figuras todos los rótulos y leyendas deben estar escritos con letra Times New Roman de tamaño 9 a 12 puntos, sin negrita y respetando la gramática y normas de escritura de la revista. Las figuras pequeñas deberán estar diseñadas con un ancho máximo de 8 cm (una columna en la revista) y las grandes con un máximo de 16 cm de ancho (dos columnas en la revista). Excepcionalmente, una figura podrá tener 23 cm de ancho (y máximo 14 cm de alto) para presentarla en formato apaisado. Organice las figuras reuniendo en una sola aquellos objetos afines (por ejemplo, gráficos de un mismo tipo de información) e identifíquelos con una letra mayúscula (A, B, C…), la que se explicará en el título de la figura.

Los manuscritos en castellano deben incluir en un archivo separado las respectivas traducciones al inglés de:

- Título del manuscrito.
- Summary: debe ser equivalente en contenido al resumen en castellano.

- Key words: equivalentes a las palabras clave en castellano.
- Títulos de cuadros y de figuras.

En el caso de manuscritos en inglés, se debe incluir el respectivo texto en castellano.

*Citas y referencias*

Las citas bibliográficas se indicarán en el texto por el apellido del o los autores, seguido del año de publicación. Algunos ejemplos de citas bibliográficas más frecuentes son:

- Citas bibliográficas de uno y dos autores:

Santamaría (2010) constata que el crecimiento...
... están influidos por el sitio en cuestión (Santamaría 2010, López y Castro 2011).

- Citas bibliográficas de más de dos autores:

Barría *et al*. (2009) señalan como factor más importante...
... entre otros, el diámetro y la altura (Barría *et al.* 2009, Morán *et al.* 2010).

- Citas bibliográficas de un mismo autor, publicadas en un mismo año:

Rodríguez (2009abd) observa que en cada unidad de muestreo...
... lo que es coincidente con estudios anteriores (Rodríguez 2009ab, Morán *et al.* 2010acd).

- Citas de más de una publicación a la vez, se ordenan cronológicamente:

Cerón (2007), García y Villanueva (2009) y Suárez *et al.* (2010) analizan los componentes edafoclimáticos...

En el capítulo de referencias, las referencias bibliográficas deben incluir apellido paterno e inicial del o los nombres de todos los autores, el año de publicación, el título y la información complementaria que permita localizar la fuente del documento en cuestión; si cuentan con DOI, debe agregarlo al final de la respectiva referencia. Algunos ejemplos de los formatos de las referencias bibliográficas más frecuentes son:

- Referencias de artículos en revistas periódicas (escriba con cursiva los nombres completos de las revistas, sin abreviar):

Guddants S. 2008. Replicating sawmill sawing with top-saw using CT images of a full-length hardwood log. *Forest Products Journal* 48(1): 72-75.

Kogan M, C Alister. 2010. Glyphosate use in forest plantations. *Chilean Journal of Agricultural Research* 70(4):652-666. DOI: 10.4067/S0718-58392010000400017.

Karzulovic JT, MI Dinator, J Morales, V Gaete, A Barrios. 2009. Determinación del diámetro del cilindro central defectuoso en trozas podadas de pino radiata (*Pinus radiata*) mediante atenuación de radiación gamma. *Bosque* 26(1):109-122.

- Referencias de libros como un todo:

Morales EH. 2005. Diseño experimental a través del análisis de varianza y modelo de regresión lineal. Santiago, Chile. Andros. 248 p.

CONAF (Corporación Nacional Forestal, CL). 2007. Estadísticas de visitantes e ingresos propios de áreas silvestres protegidas de la Décima Región de Los Lagos. 52 p. (InformeEstadístico Nº 47).

- Referencias a partes o capítulos de libros:

Gutiérrez B, R Ipinza. 2010. Evaluación de parámetros genéticos en *Nothofagus*. *In* Ipinza R, B Gutiérrez, V Emhart eds. Domesticación y mejora genética de raulí y roble. Valdivia, Chile. Exion. p. 371-390.

- Referencias a memorias, tesis, seminarios de titulación o trabajos de titulación:

Emhart V. 2006. Diseño y establecimiento de un huerto semillero clonal de *Eucalyptus nitens* (Deane *et* Maiden) con fines de producción, investigación y docencia. Tesis Ingeniero Forestal. Valdivia, Chile. Facultad de Ciencias Forestales, Universidad Austral de Chile. 79 p.

Aparicio J. 2008. Rendimiento y biomasa de *Eucalyptus nitens* con alternativas nutricionales para una silvicultura sustentable en suelo rojo arcilloso. Tesis Magíster en Ciencias. Valdivia, Chile. Facultad de Ciencias Forestales, Universidad Austral de Chile. 234 p.

- Referencias a documentos en internet:

De Angelis JD. 2009. European pine shoot moth. Oregon State University Extension (Urban Entomology Notes). Consultado 10 jul. 2009. Disponible en http://www.ent.orst.edu/urban/home.html.

Para mayor información respecto de otros casos específicos relacionados con las citas bibliográficas y referencias bibliográficas, se pueden consultar los documentos que a continuación se señalan. No obstante, el orden y la tipografía de los elementos constituyentes de las citas y referencias bibliográficas deberán ajustarse a la reglamentación de la revista Bosque.

Biblioteca Conmemorativa Orton (IICA/CATIE). 2011. Normas para citar referencias bibliográficas en artículos científicos 4 ed. Consultado13 abr.2011. Disponible en http://biblioteca.catie.ac.cr/index.php?option=com_content&task=view&id=18&Itemid=50

The Council of Biology Editors (CBE). 1994. Scientific style and format: The CBE manual for authors, editors, and publishers. 6 ed. Cambridge, New York. Cambridge University Press. 704 p.

*Carta de envío*

Los autores deberán acompañar su manuscrito con una carta de envío que indique que el trabajo es original, no ha sido publicado previamente y no está siendo considerado para publicación en otro medio de difusión. También deberán declarar cualquier posible conflicto de intereses que pudiesen tener. Se deberá señalar el tipo de contribución del manuscrito (artículo, revisión, opinión, nota). La carta deberá ser firmada al menos por el autor líder del manuscrito.

*Envío de documentos*

Los archivos deberán ser nombrados según el tipo de información contenida en el archivo. Por ejemplo, los archivos digitales del manuscrito se etiquetarán de la siguiente forma:

Texto.doc: texto principal del trabajo (incluye cuadros).
Figuras.doc: figuras con sus títulos en castellano.
Ingles.doc: textos en inglés con el siguiente orden: título del trabajo, summary, key words, títulos de cuadros y de figuras.
Carta: carta de presentación y envío del manuscrito.

Los archivos digitales del manuscrito deben ser remitidos por correo electrónico a revistabosque@uach.cl. El autor de correspondencia recibirá una carta de acuse de recibo del Editor.

**Proceso de publicación**

El cabal cumplimiento de las instrucciones para los autores se refleja en menores tiempos del proceso editorial. El comité editor revisa el manuscrito para verificar la pertenencia al ámbito de la revista y el cumplimiento de las instrucciones para los autores. Cuando no se cumplen tales condiciones, el manuscrito es devuelto al autor de correspondencia, informándole su situación. Cuando se ha verificado el cumplimiento de dichas condiciones, se registra esa fecha como recepción del manuscrito y el comité editor envía el manuscrito a un mínimo de dos árbitros o revisores externos, en un sistema de doble ciego. A los árbitros se les solicita declinar la revisión de un manuscrito cuando sientan que presentan conflictos de interés o que no podrán realizar una revisión justa y objetiva. Los

árbitros evalúan el manuscrito de acuerdo con la pauta que proporciona la revista. Si los árbitros o el comité editor lo estiman pertinente, podrán solicitar a los autores, a través del editor, información adicional sobre el manuscrito (datos, procedimientos, etc.) para su mejor evaluación. La respuesta de los árbitros puede ser: publicar con modificaciones menores, publicar con modificaciones mayores o no publicar. Las observaciones de los árbitros son evaluadas por el comité editor, el cual informa por escrito al autor de correspondencia la decisión de continuar o no en el proceso de publicación y si su manuscrito deberá ser nuevamente evaluado por árbitros. Cuando el manuscrito es aceptado, el comité editor envía al autor de correspondencia una carta de aceptación de su manuscrito, indicando el tipo de modificación necesaria. En no más de ocho semanas el autor de correspondencia debe devolver una versión modificada a la revista, para que el comité editor analice el manuscrito corregido. El comité editor decide el orden en que aparecerán los trabajos publicados en cada número. Una contribución puede ser rechazada por el comité editor en cualquiera de las instancias del proceso de publicación, ya sea por cuestiones de fondo o de forma que no cumplan con las instrucciones para los autores. Ante sospecha de conducta poco ética o deshonesta por parte de los autores que han sometido su manuscrito al proceso de edición, el editor se reserva el derecho de informar a las instituciones patrocinadoras u otras autoridades pertinentes para que realicen la investigación que corresponda.

Los trabajos publicados en Bosque están bajo licencia Creative Commons Chile 2.0.

Ante cualquier duda se sugiere contactarse con el editor (revistabosque@uach.cl) o revisar la información adicional de nuestra página web www.revistabosque.cl

La versión electrónica de libre acceso de los trabajos completos publicados por Bosque se encuentran en: http://mingaonline.uach.cl/scielo.php, http://www.scielo.cl, y http://redalyc.uaemex.mx/.

**Políticas para los árbitros**

Los árbitros o revisores de los manuscritos son integrantes clave del proceso editorial de la revista. Tienen la misión de contribuir a que la ciencia avance a través de su aporte en garantizar la alta calidad de los trabajos antes que estos se publiquen. Su trabajo es altruista y anónimo con respecto a los autores de los manuscritos.

El editor envía cada manuscrito a por lo menos dos árbitros que considera idóneos para el tema y así el comité editor puede considerar diversas opiniones de especialistas para decidir sobre el proceso editorial.

La responsabilidad de los árbitros es la de evaluar rigurosamente los manuscritos dentro del plazo propuesto por la revista.

Los árbitros deberán declinar la revisión del manuscrito cuando sientan que presentan conflictos de interés o que no podrán realizar una revisión justa y objetiva, los árbitros deberán declinar la revisión del manuscrito. Un arbitraje apropiado incluye virtudes y debilidades del manuscrito, sugerencias para su mejoramiento, preguntas precisas para que los autores puedan responderlas y orientaciones para que el trabajo sea de mejor calidad y mayor aceptación por los futuros lectores. Los árbitros deben mantener la confidencialidad de los manuscritos que reciben para revisión y nunca utilizar o difundir datos o información de ellos; el hacerlo es una conducta reñida con la ética. Los árbitros deberán abstenerse de solicitar la inclusión de aspectos que el manuscrito no busca responder, como también de insinuar que sean citados sus propios trabajos.

Frente a la revista, los árbitros deberán velar por la calidad y rapidez de sus revisiones y evitar los conflictos de intereses. Los árbitros deben cumplir los plazos y formatos solicitados por la revista. Cuando ello no sea posible, deberán declinar oportunamente el arbitraje. Cuando requieran de un tiempo adicional para la revisión de un manuscrito, deberán informar al editor. Si un árbitro presenta conflicto de intereses con respecto a un manuscrito, deberá abstenerse de realizar la revisión, informando al editor. Cuando un árbitro propone no publicar un manuscrito o hacerlo sólo después de cambios mayores, podrá recibir una nueva versión corregida por los autores que haya acogido las sugerencias de mejoramiento. El arbitraje es una herramienta eficaz para mejorar la calidad de los trabajos.

El editor podrá difundir informes de arbitrajes entre los revisores (conservando el anonimato) para promover el buen desempeño, resolver controversias y mejorar el proceso de edición.

Los árbitros serán informados del destino del manuscrito que revisaron. Como una forma de retribuir sus valiosos aportes, el editor les enviará una carta de agradecimiento por cada arbitraje y publicará sus nombres a inicios del año siguiente a su colaboración.

## Árbitros que colaboraron con revista Bosque el año 2020

| Árbitro | Institución |
| --- | --- |
| Manuel Acevedo | Instituto Forestal - INFOR, Chile |
| Fabio Achinelli | Universidad Nacional de La Plata, Argentina |
| Julio Arce | Universidade Federal do Paraná, Brasil |
| Óscar Aguirre | Universidad Autónoma de Nuevo León, México |
| Ünal Akkemik | Istanbul University-Cerrahpasa, Turquía |
| Karla Mayara Almada Gomes | Universidade Federal do Oeste do Pará, Brasil |
| Susana Alvarado | Red de Ecología Funcional, Instituto de Ecología, México |
| Ernesto Andenmatten | Instituto Nacional de Tecnología Agropecuaria, Bariloche, Argentina |
| Camila Andrzejewski | Universidade Federal de Santa Maria, Brasil |
| Armando Aparicio | Universidad Veracruzana, México |
| José Carlos Arthur | Universidade Federal Rural do Rio de Janeiro, Brasil |
| Marcelo Arturi | Universidad Nacional de La Plata, Argentina |
| Andrea Ávila | Universidad Austral de Chile |
| Marcelo Barrera | Universidad Nacional de La Plata, Argentina |
| Carolina Barroetaveña | CONICET-CIEFAP, Chubut, Argentina |
| Alicia Basilio | Universidad de Buenos Aires, Argentina |
| Pablo Becerra | Pontificia Universidad Católica de Chile |
| Marcelo Beltrán | Instituto de suelos del INTA, Argentina |
| Antonio Bento Gonçalves | Universidade do Minho, Portugal |
| Pete Bettinger | University of Georgia, USA |
| Claudia Bonomelli | Pontificia Universidad Católica de Chile |
| Eduardo Borges | Universidade Federal de Viçosa, Brasil |
| Sharon Bywater-Reyes | University of Northern Colorado, USA |
| Antonio Cabrera | Universidad Católica del Maule, Chile |
| Orlando Sílvio Caires Neves | Universidad Federal de Bahía, Brasil |
| Pedro Calaza | Universidad de Santiago de Compostela, España |
| Juan Caldentey | Universidad de Chile |
| Julieta Carilla | CONICET, Tucumán, Argentina |
| María Eugenia Casanueva | Universidad de Concepción, Chile |
| Miguel Castillo | Universidad de Chile |
| Sergio Castro | Universidad de Santiago de Chile |
| Juan Manuel Cellini | Universidad Nacional de La Plata, Argentina |
| Víctor Manuel Cetina Alcalá | Colegio de Posgraduados, México |
| Luis Chauchard | Universidad Nacional del Comahue, Argentina |
| Carlos Chávez | Universidad de Talca, Chile |
| María Verónica Chillo | Universidad Nacional de Río Negro, Argentina |
| Alper Hüseyin Çolak | İstanbul Üniversitesi, Turquía |
| Elena Corral | Universidad del País Vasco |
| Alejandro Costantini | Universidad de Buenos Aires, Argentina |

| | |
|---|---|
| Dylan Craven | Universidad Mayor, Chile |
| Patricia Delgado Valerio | Universidad Michoacana de San Nicolás de Hidalgo, México |
| Tuğba Deniz | Istanbul University-Cerrahpasa, Turquía |
| Maura Díaz | Universidad Nacional de Asunción, Paraguay |
| Ignacio Díaz-Maroto H. | Universidad de Santiago de Compostela, España |
| Pablo Donoso | Universidad Austral de Chile |
| Sergio Donoso Calderón | Universidad de Chile |
| Fernando Droppelmann | Universidad austral de Chile |
| Beatriz Eibl | Universidad Nacional de Misiones, Argentina |
| Mehmet Eker | Isparta University of Applied Sciences, Turquía |
| Seyed Eshagh Ebadi | Islamic Azad University of Chalous Branch, Irán |
| Carlos Esse | Universidad Autónoma de Chile |
| Bruno Estevez | Instituto Politécnico de Viseu, Portugal |
| Javier Figueroa Ortiz | Universidad Central, Chile |
| Arão Raimundo Finiasse | Instituto Superior Politécnico de Gaza, Mozambique |
| Ane Fortes | Instituto Federal de Educação, Ciência e Tecnologia da Paraíba, Brasil |
| Andrés Fuentes | Universidad de La Frontera, Temuco, Chile |
| Ignacio García González | Universidad de Santiago de Compostela, España |
| Enrique García de la Riva | Consejo Superior de Investigaciones Científicas, España |
| Rodrigo García | Federal University of Paraiba, Brasil |
| Natalia Gavilán | Pesquisadora EmergeAgro, Brasil |
| Víctor Gerding | Universidad Austral de Chile |
| Eugenia Mabel Giamminola | Universidad Nacional de Salta, Argentina |
| Miriam Gobbi | Universidad Nacional del Comahue, Bariloche, Argentina |
| Ferhat Gokbulak | Istanbul University-Cerrahpasa, Turkey |
| Carlos González Benecke | Oregon State University, USA |
| Álvaro González | Universidad Mayor, Chile |
| Eric Bastos Görgens | Universidade Federal dos Vales do Jequitinhonha e Mucuri, Brasil |
| Corina Graciano | Universidad Nacional de La Plata, Argentina |
| Alkan Günlü | Çankırı Karatekin University, Turquía |
| Ivon Gutiérrez | Pontificia Universidad Católica de Chile |
| Javier Gyenge | INTA Tandil, Buenos Aires, Argentina |
| Francisco Hernández | Instituto Tecnológico de El Salto, México |
| Jaime Hernández | Universidad de Chile |
| Pedro Higuchi | Universidade do Estado de Santa Catarina, Brasil |
| Andrés Hirigoyen | Instituto Nacional de Investigación Agropecuaria (INIA), Uruguay |
| Bora İmal | Çankırı Karatekin University, Turquía |
| Roberto Ipinza | Instituto Forestal-INFOR, Chile |
| Andrés Iroumé | Universidad Austral de Chile |
| Rodolfo Iturraspe | Universidad Nacional de Tierra del Fuego, Argentina |
| Constanza Jana | INIA INTIHUASI, La Serena, Chile |
| Uzay Karahalil | Karadeniz Technical University, Turquía |

| | |
|---|---|
| Dagma Kratz | Universidade Federal do Paraná, Brasil |
| Marilia Lazarotto | Universidad Federal de Rio Grande do Sul, Brasil |
| Maurecilne Lemes Carvalho | State University of Mato Grosso, Brasil |
| Pedro León | INIA La Platina, Chile |
| Federico Letourneau | Instituto Nacional de Tecnología Agropecuaria (INTA), Argentina |
| Christian Little | Instituto Forestal- INFOR, Chile |
| Paulina Lobos | Universidad Austral de chile |
| Verónica Loewe | Instituto Forestal-INFOR, Chile |
| María Josefa Lombardero Díaz | Universidad de Santiago de Compostela, España |
| Javier López Upton | Colegio de Postgraduados, México |
| Miguel Ángel López | Colegio de Postgraduados, México |
| Federico Luebert | Universidad de Chile |
| Mario Luna Cavazos | Colegio de Postgraduados, México |
| Maria Chiara Manetti | Research Centre for Forestry (Arezzo) (CRA-SEL), Italy |
| César Marín | Universidad de O'Higgins, Chile |
| Luciana Martínez | INTA-Santiago del Estero-, Argentina |
| Cibele Chalita Martins | FCAV - UNESP Jaboticabal, Brasil |
| Francisco Matus | Universidad de La Frontera, Temuco, Chile |
| Natan Medeiros Guerra | Universidade Federal Rural do Semi-Árido, Brasil |
| César Medina | Universidad Nacional de San Agustín de Arequipa, Perú |
| Diego Meloni | Universidad Nacional de Santiago del Estero, Argentina |
| Mario Meneses | Universidad austral de Chile |
| Sandro Menezes | Universidade Federal da Grande Dourado, Brasil |
| Francisco Mesén | Centro Agronómico Tropical de Investigación y Enseñanza, Costa Rica |
| Juana Graciela Moglia | Universidad Nacional de Santiago del Estero, Argentina |
| Juan Ramón Molina | Universidad de Córdoba, España |
| Leonardo Monteiro Ribeiro | Universidade Estadual de Montes Claros, Brasil |
| Cristian Montes | University of Georgia, USA |
| Ernesto Morici | Universidad Nacional de la Pampa, Argentina |
| Roger Moya | Instituto Tecnológico de Costa Rica, Costa Rica |
| Rodrigo Mujica | Instituto Forestal-INFOR, Chile |
| Gastón Muñoz | Universidad San Sebastián, Chile |
| Maka Murvanidze | Agricultural University of Georgia |
| Guiomar Nates Parra | Universidad Nacional de Colombia |
| Celso Navarro | Universidad Católica de Temuco, Chile |
| Rafael Navarro Cerrillos | Universidad de Córdoba, España |
| Marcio Navroski | Universidade Estadual de Santa Catarina, Brasil |
| Patricia Negreros Castillo | Universidad Veracruzana, México |
| Mario Niklitschek | Universidad Austral de Chile |
| Murata Norio | National Institute for Basic Biology, Okazaki, Japan |
| Taner Okan | Istanbul University, Turquía |
| Gisele Cristina de Oliveira Menino | Instituto Federal de Educação Ciência e Tecnologia Goiano, Brasil |

| | |
|---|---|
| Víctor Manuel Ordaz Chaparro | Colegio de Posgraduados, México |
| Alicia Ortega | Universidad austral de Chile |
| Juan Ovalle | Universidad de Chile |
| Marcelo Rodrigo Pace | Universidad Nacional Autónoma de México |
| Juarez Benigno Paes | Universidad Federal Espírito Santo, Brasil |
| Alessandro Paletto | CREA-MPF, Italia |
| Gabriela Paranhos Barbora | Instituto Federal de Minas Gerais, Brasil |
| Mario Juan Pastorino | IFAB (INTA – CONICET), Bariloche, Argentina |
| Raúl Peinetti | Universidad Nacional de la Pampa, Argentina |
| Gustavo Pereira Valani | Universidade de São Paulo, Brasil |
| Magali Pérez Flores | Universidad Nacional de La Plata, Argentina |
| Patricia Perissi | Universidad Nacional de Córdoba, Argentina |
| Mariel Perreta | Universidad Nacional del Litoral, Argentina |
| Julio Amílcar Pineda-Insuasti | Centro Ecuatoriano de Biotecnología del Ambiente |
| Juan Carlos Pinilla | Instituto Forestal-INFOR, Chile |
| Daniel Piotto | Universidade Federal do Sul da Bahia, Brasil |
| Sergio Piraino | Universidad Nacional de Cuyo, Argentina |
| Patricia Pires | Universidade Federal de Goias, Brasil |
| Marín Pompa García | Universidad Juárez del Estado de Durango, México |
| Kenia de Quadros Tronco | Fundação Universidade de Rondônia, Brasil |
| Gerónimo Quiñonez Barraza | Instituto Nacional de Investigaciones Agrícolas, Pecuarias y Forestales, México |
| Kishore S Rajput | The Maharaja Sayajirao University of Baroda, India |
| C.P. Reghu | Rubber Research Institute of India |
| René reyes | Instituto Forestal-INFOR, Chile |
| Román Carlos Ríos | Universidade Federal do Paraná, Brasil |
| Juan Manuel Ríos | Universidad Intercultural del Estado de Guerrero, México |
| Carlos Rivas | Universidad de Manabí, Ecuador |
| Vinicius Rodrigues | Universidad Federal de Viçosa, Brasil |
| Luis Enrique Rodriguez de Francisco | Instituto Tecnológico de Santo Domingo, República Dominicana |
| Dante Arturo Rodríguez | Universidad Autónoma Chapingo, México |
| Roque Rodríguez | Universidad de Santiago de Compostela, España |
| Yasna Rojas | Instituto Forestal-INFOR, Chile |
| Aldo Rolleri | Universidad austral de Chile |
| María Cristina Romero | Universidad Nacional de Asunción, Paraguay |
| Ana Paula Rovedder | Universidad Federal de Santa María, Brasil |
| Adriana Rovere | Instituto de Investigaciones en Biodiversidad y Medioambiente (INIBIOMA), Argentina |
| Martín Rubí Arriaga | Universidad Autónoma del Estado de México |
| Verónica Rusch | INTA Bariloche, Argentina |
| Christian Salas | Universidad Mayor, Chile |
| Raúl Salas | Instituto Politécnico de Coimbra, Portugal |
| Seir Antonio Salazar | Universidad Francisco de Paula Santander, Colombia |
| Jaime Salinas | Instituto Forestal - INFOR, Chile |

| | |
|---|---|
| Carlos Sanquetta | Universidade Federal do Paraná |
| Wenceslao Santiago García | Universidad de la Sierra Juárez, México |
| Robson Silva de Medeiros | Universidad Estadual Paulista, Brasil |
| José Augusto Silva Santana | Universidad Federal do Rio Grande do Norte, Brasil |
| Rosina Soler | Centro Austral de Investigaciones Científicas, Argentina |
| Julia Sonsin | Universidade de Brasília, Brasil |
| Daniel Soto | Universidad de Aysén, Chile |
| Caian Souza Gerolamo | Universidade de São Paulo, Brasil |
| Sergio Soza Amigo | Universidad Austral de Chile |
| Flavio César Speranza | Estación Experimental Agropecuaria Yuto, Argentina |
| José Tarragó | Instituto de Botánica del Nordeste, Argentina |
| İbrahim Turna | Karadeniz Technical University, Turquía |
| Mario Tuzine | Instituto Superior Politécnico de Gaza (ISPG Lionde) |
| Daniel Uteau | University of Kassel, Alemania |
| José René Valdez Lazalde | Colegio de Postgraduados, México |
| José Valero | Universidad Autónoma de Ciudad Juárez, México |
| Rodrigo Vargas | Universidad de La Frontera, Temuco, Chile |
| William Vargas | Instituto de Investigación de Recursos Biológicos Alexander von Humboldt, Colombia |
| Marcos Vinicius Winckler | Federal University of Espírito Santo, Brasil |
| George N. Zaimes | Technological Educational Institute of Kavala |
| Hugo Zerda | Universidad Nacional de Santiago del Estero, Argentina |
| Qi Zhang | North Dakota State University, USA |